

**Print ISSN : 2395-1990**

**Online ISSN : 2394-4099**

[www.ijsrset.com](http://www.ijsrset.com)



**National Conference on  
'Advanced Analytical Tools for  
Materials Characterization'  
(AATMC-2018)**

**Organised by  
Department of Chemistry,  
Birla College, Kalyan, Maharashtra, India**

**VOLUME 5, ISSUE 4, JANUARY-FEBRUARY-2018**

**INTERNATIONAL JOURNAL OF SCIENTIFIC  
RESEARCH IN SCIENCE,  
ENGINEERING AND TECHNOLOGY**

UGC Approved Journal [ Journal No : 47147 ]

Email : [editor@ijsrset.com](mailto:editor@ijsrset.com) Website : <http://ijsrset.com>



**Kalyan Citizens' Education Society's  
Birla College of Arts, Science and Commerce, IJSRSET  
Kalyan**



**National Conference  
on  
'Advanced Analytical Tools for Materials  
Characterization' (AATMC-2018)  
(Supported by the DBT- Star Status & Century Rayon,  
Shahad)**

'College of Excellence' Status by UGC (2015-2020)  
Reaccredited by NAAC with 'A' Grade (CGPA – 3.58) -2014  
'Performance Excellence Trophy – 2011 in Education by IMC RBNQA  
Trust

'Best College Award' by University of Mumbai (2009)

ISO 9001:2008 Certified

DBT - 'Star Status'

(Department of Botany, Chemistry, Physics, Microbiology and Zoology )  
28th February, 2018

**in**

**In Association with**

**International Journal of Scientific Research in Science, Engineering  
and Technology**

Print ISSN : 2395-1990 Online ISSN : 2394-4099

**Volume 5, Issue 4, January-February-2018**

**Organized By**

**Department of Chemistry, Birla College, Kalyan, Maharashtra, India**

Website: [www.birlacollegekalyan.com](http://www.birlacollegekalyan.com)

**Published By**

**Technoscience Academy**

(The International Open Access Publisher)

[ [www.technoscienceacademy.com](http://www.technoscienceacademy.com) ]

## **National Advisory Committee**

Prof. D.B. Shinde: Vice Chancellor, Shivaji University, Kolhapur  
and Acting Vice Chancellor, University of Mumbai  
Prof. G.D. Yadav: Vice Chancellor, ICT, Mumbai  
Prof. V.G. Gaikar: Vice Chancellor, BATU, Lonere  
Prof. A.K. Tyagi: Scientist, BARC, Mumbai  
Prof. Sundar Manoharan: Former Vice Chancellor, K.I. Technology and Sciences,  
Coimbatore, Tamilnadu  
Prof. D.C. Kothari: Ex. I/C Director CNSNT, University of Mumbai  
Prof. Jayesh Bellare: IIT, Mumbai  
Prof. P.S. Kalsi: Former Dean at PTU, Jalandhar  
Prof. R.B. Mathur: National Physical Laboratory, Delhi

## **Local Organizing Committee**

Dr. Naresh Chandra, Principal (Chairman)  
Mr. Kamod Dongare (Convener)  
Dr. Sandesh Jaybhaye (Organizing Secretary)  
Mr. Balasaheb Pathare (Treasurer)  
Dr. Jossy Varghese  
Dr. Geetha Unnikrishnan  
Dr. Avinash Patil  
Dr. Madhavi Thakurdesai  
Dr. Maninder Dhaliwal  
Dr. Mahendra Khandpekar  
Dr. Seema Manchanda  
Dr. Archana Singh  
Dr. Pranjali Maskar  
Mr. Nagesh Pawar  
Dr. Khemraj Barhate  
Dr. Vijay Jadhav  
Dr. Harish Dubey  
Dr. Datta Kshirsagar  
Mr. Sachin Golhe  
Ms. Snehal Pednekar  
Mrs. Amrita Singh  
Mr. Brijesh Gaud  
Mr. Sandip Wakchaure

## **Editorial Board**

Dr. Debdatta Ratna, Scientist, NMRL, Ambarnath

Dr. Sandesh Jaybhaye, Department of Chemistry, Birla College, Kalyan

Dr. Mahendra Khandpekar, Department of Physics, Birla College, Kalyan

Dr. Vilas Kahiarnar, Department of Chemistry, Birla College, Kalyan

डॉ. मनोरंजन पत्री  
निदेशक

**Dr. M. Patri**  
**Director**



कार्यालय / Off. : 0251-2623037  
फैक्स / Fax : 0251-2623004  
ई - मेल / E-mail : director@nmri.drdo.in  
भारत सरकार, रक्षा मंत्रालय  
रक्षा अनुसंधान तथा विकास संगठन  
नौसेना सामग्री अनुसंधान प्रयोगशाला  
शील बदलापुर रोड, अति. अंबरनाथ, महाराष्ट्र  
पिन - 421 506  
Govt. of India, Ministry of Defence  
Defence Research & Development Organisation  
NAVAL MATERIALS RESEARCH LABORATORY  
Shil Badlapur Road, Addl. Ambarnath (E), Maharashtra  
Pin - 421 506



## *Message*

It gives me great pleasure to know that Birla College of Arts, Science & Commerce, Kalyan is organizing National Conference on "Advanced Analytical tools for materials characterization: (AATMC-2018) on 28<sup>th</sup> Feb 2018.

Development of newer materials is rapidly progressing for structural, functional and strategic requirement both in civil as well as defence sector. Detailed characterization of materials using various analytical tools is essential to find their physical and chemical properties. These properties in turn will assist the designer to predict the environment stability and service life of the products made out of materials.

I am certain that the conference will provide an ideal platform for interaction of delegates and specialists from different field of materials and can catalyse exchange of information and sharing of experience for characterisation of materials. I wish AATMC-2018 a grand success.

22 February 18

(Dr Manoranjan Patri)

**Dr. Naresh Chandra**

M.Sc., M. Phil., Ph.D., F.B.S.

**Principal**

Former Pro-Vice- Chancellor,  
University of Mumbai



**Birla College of Arts, Science & Commerce,**

Kalyan (W)- 421304 (M.S.) India

Email: birlapincipal1972@gmail.com

Web: www.birlacollege.org

P : (0251) 2232930 (O); 2231029 (F); 2230373 (R)



**Message**

Birla College of Arts, Science and Commerce, Kalyan, a premier institution of higher education, has a vibrant work culture and a holistic approach to education is encouraged. The College was established in 1972, by Kalyan Citizens' Education Society with the blessings of Syt. B. K. Birla ji and Late Smt. Sarala ji Birla. We believe, research is an integral part of teaching.

We are glad to know that Department of Chemistry, Birla College is organizing one day National Conference on '*Advanced Analytical Tools for Material Characterization*' (AATMC-2018) to be held on Wednesday the 28<sup>th</sup> February 2018. It is an opportunity for us to organize the National conference on the eve of National Science Day, which is celebrated to mark the discovery of Raman effect by Indian physicist Sir C. V. Raman. Every year this day is celebrated to widely spread a message about the importance of Science used in the daily life of the people, to display all the activities, efforts and achievements in the field of Science and Technology.

It gives me immense pleasure to extend hearty welcome to the distinguished guests, invitees and all the delegates attending this Conference.

This conference will make an attempt to promote research in various fields of Chemistry, Physics and Biological Sciences. The main aim of the conference is to provide a forum for teaching fraternity in higher education, industry personnel and students all over the nation to participate and discuss the advanced analytical tools used in scientific community.

I am sure that the Conference will provide an opportunity to young researchers to present their research work, to get interdisciplinary exposure and to interact with the eminent Scientists.

We sincerely thank the esteemed Management for their constant support, guidance and motivation. I appreciate the efforts of Mr. Kamod Dongare, Head, Dept. of Chemistry (Convener), Dr. Sandesh Jaybhaye (Organizing Secretary) and other colleagues for organizing this event.

I once again extend a hearty welcome to the participants and convey my best wishes for the success of Conference.

(Dr. Naresh Chandra)

**Mr. Kamod Dongare**

Head, Dept. of Chemistry

(Convener)

**AATMC-2018**



### **Message**

It is a matter of great pleasure for us at the Department of Chemistry, Birla College of Arts, Science and Commerce, Kalyan welcome you all to the 'National Conference on Advance Analytical Tools for Material Characterization (AATMC-2018),' We are especially privileged to receive distinguished guests, speakers and invitees on this occasion.

We are in the era where every day new material is synthesized to cater the need of mankind. The contribution of chemical and other sciences are amazing and stunning. There is need to upgrade the knowledge & analytical skills for characterization of novel materials to meet the future challenges.

At the national level, we need to realize that we can no longer afford to treat chemistry as a compartmentalized subject. It will necessarily have to be interdisciplinary, if we sincerely wish to focus on our own national needs in order to deliver sustainable and useful technologies for mass consumption. The scientific community faces yet another challenge in the form of clean synthetic routes to create new materials and processes. There is need of quality interdisciplinary research which will be competitive and of international standards. PG Diploma in Bio-nanotechnology is unique, innovative and interdisciplinary course which will be helpful in chemical research and other allied areas.

In this conference, we have invited talks which would focus on materials characterization techniques with oral and poster presentations. We believe that deliberations in the conference would expose the participants to the excitement and challenges in key research areas of Chemistry.

I take this opportunity to thank Birla College, Kalyan and Century Rayon, Shahad for their generous financial support towards hosting this conference. I wish all the participants a pleasant stay at this sprawling and beautiful campus with a confidence that you will carry rewarding memories of AATMC-2018.

**Dr. Sandesh Jaybhaye**

Organizing Secretary

AATMC-2018



### **Message**

It gives me immense pleasure to welcome you all invitees and delegates to One Day National Conference 'Advance Analytical Tools for Material Characterisation' AATMC-2018 supported by 'DBT Star Status and Century Rayon Ltd. Shahad. I would like to thank Principal Dr. Naresh Chandra Birla College and College Management, Century Rayon, DBT Star status and administrative staff for their motivation, support and guidance to successful organization of National Conference AATMC- 2018.

Being Organizing Secretary for One Day National Conference certainly has given me a different view of the depth and breadth of the Chemistry and Analytical Tools for material Characterisation. This Conference will make an attempt to promote research in various fields of Chemistry, Physics, and Biological Sciences. The researchers need a platform to express their research ideas and interaction with subject experts.

The National Conference will mainly aim to provide a common platform for interchange of ideas between the scholars and subject experts.

It will also be a boost to young researchers as they will get endorsement from senior researchers and the right analytical tool to be used for the cost-efficient problem solving and characterization of novel materials.

Such a gathering is thus interdisciplinary in a way that is far beyond what we would normally even conceive.

I am so honored to be the Organizing Secretary for the one day National Conference and welcome you all to our college to have a great time and interaction.



## BIRLA COLLEGE OF ARTS, SCIENCE AND COMMERCE, KALYAN

### Profile

*Birla College of Arts, Science and Commerce, Kalyan*, a multi faculty premier institution of higher learning, with an enrolment of more than 9,500 students (6,000 for UG, PG and Research Programmes) is affiliated to the University of Mumbai. The College was established in 1972, by Kalyan Citizens' Education Society with the blessings of Syt. B. K. Birla ji and Late Smt. Sarala ji Birla.

*Birla College* offers several Under Graduate and Post Graduate Programmes in Arts, Science and Commerce and Ph. D. in Botany, Biotechnology, Physics, Microbiology, Chemistry, Zoology, Hindi, History and Economics. The College also conducts PG Diploma in Bio - nanotechnology and PGDMLT programme. The College has started a *Community College for Diploma in Accounting and Taxation* (sanctioned by UGC) from 2015 - 16.

The College is spread over an area of 20 acres of land (including Birla School) in the prime location of Kalyan city and developed as an eco-friendly campus.

The College has been re-accredited (3<sup>rd</sup> Cycle) by NAAC and awarded 'A' Grade with CGPA - 3.58 in 2014. The College has been awarded the "*Best College Award*" (in the Urban category) by the University of Mumbai (2009) and also awarded the '*IMC - RBNQ Performance Excellence Trophy - 2011*' in Education. The College has been certified with the ISO 9001: 2008.

The College has been sanctioned funds under the FIST Programme of DST to strengthen Teaching and Research Facilities in all Science Departments. It also has UGC sponsored Gandhian Studies Centre, Women's Study Centre, Centre for Yoga and Philosophy, Centre for Epigraphy and Centre for Foreign Languages.

The College has been awarded '*College of Excellence*' status by UGC (2015 - 2020).

The departments of Botany, Chemistry, Microbiology, Physics and Zoology have been awarded '*Star Status*' by the Department of Biotechnology (DBT), Govt. of India, New Delhi in 2017. Recently, the departments of Mathematics, Information Technology and Computer Science have been selected for support under strengthening component of Star College Scheme by DBT, Govt. of India, New Delhi.

*Birla College* has a vibrant work-culture. A holistic approach to education is encouraged. The teaching - learning process is supported by the use of ICT, interactive exercises, projects, assignments, etc. in addition to chalk and talk method. The results have always been higher than the University's average results. In extra-curricular activities including NCC, NSS and Sports, etc., the performance of students is excellent. Every year few students of Birla College figure in the University merit list.

Research is an integral part of teaching. 22 of our faculty members are Ph.D. Guides. Many are working on major / minor research projects and have published a number of research papers in national and international journals.

The College has an International Linkages Committee. The College has signed MoU with a few Universities abroad, namely in USA, Italy and China for faculty exchange and collaborative research. Since 2015, a student exchange has also been initiated.

We, at Birla College, stand committed to the cause of higher education, catering to the diverse needs of the students and enabling them to develop as intellectually alive and socially - responsible citizens ready for continuous and professional growth.

### **PROFILE OF DEPARTMENT OF CHEMISTRY**

Department of Chemistry, Birla College, Kalyan is recognized as **Highly Rated Department** by UGC and awarded Star Status by DBT. Department is conducting **UG , PG, Ph.D.** programs, Career Oriented UGC sponsored Add-on Course in **Industrial Chemistry** (Certificate and Diploma) and coordinating multidisciplinary PG Diploma programme in **Bionano Sciences**. It is actively involved in research activities and has well established Nanotechnology Research Lab with required equipments and facilities. Department has signed MoU with University of Genoa, Italy for Ph.D. and Post Doctoral research. Department provides consultancy to nearby Industries. Department has successfully organized Research Scholars Meet - 2004, Workshop on Characterization and Analysis Techniques-2005, National Conference of ICC-2006, Science Exhibition as a part of celebration of IYC-2011, National conferences RTNS-2011, RAAT-2012 and RTBN-2017.

Department has organized one day workshop on S. Y. B. Sc revised syllabus jointly with Board of Studies, University of Mumbai, Mumbai. Department has also organized Department has also organized one day Symposium BFP- 2016, Science Exhibitions – GST- Dec. 2014, STD- Jan. 2016, IIST- Dec.2016 and GE –Dec. 2017.

### **ABOUT PG DIPLOMA IN BIONANOTECHNOLOGY**

PG Diploma in Bio-nanotechnology is sanctioned by UGC under the innovative programme. It is one year full time course and sanctioned seats for this course are 20.

The eligibility for this diploma course is M. Sc. in any subject from Biological Sciences/ Biochemistry / Chemistry with any one subject of Biological Sciences up to second year level from any recognized University. The admission process is as per the guidelines of the University of Mumbai.

The unique features of this course are: Innovative course supported by UGC, well equipped Nanotechnology laboratory and eminent scientists from IIT, BARC, TIFR, Center of Nanoscience & Nanotechnology and University of Mumbai are the visiting faculties.

## **Themes of the Conference**

- 1) Analytical tools and techniques for material analysis
- 2) Synthesis, characterization and applications of novel
- 3) materials
- 4) Chromatography and separation techniques
- 5) Different Spectroscopic techniques
- 6) Hyphenated techniques
- 7) Nanomaterials and Bio-nanomaterials
- 8) Material science and allied areas
- 9) Microscopic technique

## **Aims and Objectives**

The right analytical tool must be used for the costefficient problem solving and characterization of novel materials, (i.e., one that has the correct measurement capabilities and characteristics). The aim of this conference is to provide timely forum for the exchange & dissemination of new ideas & techniques among the researchers in the field of manufacture and analysis of novel materials. There is need to upgrade the knowledge & analytical skills for characterization of these novel materials to meet the future challenges. This Conference will make an attempt to promote research in various fields of Chemistry, Physics, and Biological Sciences. The researchers need a platform to express their research ideas and interaction with subject experts. This conference provides opportunities for the delegates to exchange new ideas face-to-face, to establish business or research relations as well as to find partners for future collaborations. We hope that the conference results will lead to significant contributions to the knowledge in these up-to-date scientific fields. The focus of the conference is to establish an effective platform for institutions and industries to share ideas and to present the works of scientists, engineers, educators and students from all over the India.

## CONTENTS

Sr. No	Article/Paper	Page No
1	<b>Environmentally Friendly Synthesis and Antimicrobial Activity of ZnONPs</b> Amrita Singh, Brijesh Gaud, Sandesh Jaybhaye	01-05
2	<b>Ambient Air Quality Monitoring in Vasai Virar City Municipal Corporation Region (Maharashtra, India)</b> B. S. Pansare, G. R. Bhagure	06-09
3	<b>Synthesis of Carbon Fibers and Its Surface Area Mesurments</b> Brijesh Gaud, Amrita Singh, Sandesh Jaybhaye	10-14
4	<b>Production and characterization of the biosurfactant obtained by Bacillus subtilis</b> Dhiraj B Shekhawat, Pradnya A. Josh, Maninder Dhaliwal, Raghunath Patil	15-19
5	<b>Accumulation of organophosphate estimated by Gas liquid chromatography in fresh water sponges (S.lacustris)</b> D. N. Shinde	20-22
6	<b>Studies on effect of Copper Oxide nanoparticles on Chickpea Cicer arietinum seed germination and root elongation</b> Dinesh Wanule, Simran Modgekar, Sandesh Jaybhaye, Kantilal Nagare	23-25
7	<b>Analysis of oxidative rancidity of different oil samples collected from Kalyan Taluka</b> Kantilal Nagare, SoniYadav, Manasi Dhupal, Vina Yashwantrao, Manali Kolkur, Khushboo Singh, Rachna Mishra, Dinesh Wanule	26-29
8	<b>Characterization and Comparative Study of Fly ash from Various Sources for its Sustainable Utilization</b> Gauravi Patil, Ajitha Rani R	30-36
9	<b>Study of Antibacterial activity of Mulethi and Amla against gram negative bacteria Escherichia coli</b> H A Padwal, N B Kamble, C P Thomas, A J Rathore, V S Narayane	37-42
10	<b>Copper Oxide Nanoparticles : Synthesis and Characterization</b> Himanshu Narayan, Hailemicheal Alemu, Lineo F. Maxakaza , Sandesh Jaybhaye	43-47
11	<b>Inhibition of Mild Steel Corrosion Caused by Sulphate Reducing Bacteria by Using 2-Methylimidazole</b> Jitendra D. Girase , R. S. Dubey	48-53
12	<b>Study of Glassy Carbon Films Synthesized Using Natural Precursor</b> Dattatray E. Kshirsagar, Harish K. Dubey. K. D. Barhate, Maheshwar Sharon	54-57
13	<b>Effect of Euphorbia Tirucalli L. Extracts on Brain and Muscle Proteins of Fish</b>	58-64

	Kranti Ozarkar, Mayur Rao, Geetha Unnikrishnan	
14	<b>EPR Study of Nickel Doped Mn-Zn Ferrite Nanoparticles</b> L. N. Singh, F. A. Ahmed	65-68
15	<b>Synthesis &amp; Thermal, Optical &amp; Dielectric characteristics of Gadolinium doped EuF<sub>3</sub> nanoparticles in presence of <math>\alpha</math> – glycine</b> Manoj P Mahajan, M. M. Khandpekar	69-71
16	<b>Study of Antibacterial Properties of Azadirachta indica and Trachyspermum ammi A Commonly Used Plant Material That Aids Digestion</b> Nutan. B. Kamble, Roothmary. S. Nadar, Greeshma. R. Bale, Vinod. S. Narayane	72-79
17	<b>Protease Production Using Solid State Fermentation</b> Dhaliwal MK, Patil RN, Sambare S	80-88
18	<b>LC-MS analysis of dye extracted from Butea monosperma (Lamk.) Taub. flowers</b> Pooja Gupta, Naresh Chandra	89-94
19	<b>Study of 1,2,4-Triazole As Effective Corrosion Inhibitor For Mild Steel Used In Oil And Gas Industries In 1M HCl</b> Pratap Kamble , R. S. Dubey	95-102
20	<b>Inhibitive effect of 8-hydroxy Quinoline on the corrosion of mild steel in 1M HCl</b> R. S. Dubey, Pratap Kamble	103-107
21	<b>Study of Ground Water Pollution in Roha, District Raigad, Maharashtra, India</b> Ranjana A. Kularni , G. R. Bhagure	108-111
22	<b>Applications of Hyphenated Analytical Techniques to Pharmaceutical Drug Analysis : A Review</b> Ratnakar Hole, Vinod Lohakane, Sandesh Jaybhaye, Rajesh Dwivedi, Achyut Munde	112-121
23	<b>Growth, Structural and Optical Studies of Semi Organic Mixed Amino-Nitrate (GSA) Crystal</b> S S Dongare, S B Patil, M M Khandpekar	122-126
24	<b>Synthesis of Carbon Nano Sheet by Using Cobalt Nano Catalyst and Its Analysis</b> Sandip V. Wakchaure, Vilas R. Khairnar	127-132
25	<b>Green synthesis of silver nanoparticles from plant sources and evaluation of their antimicrobial activity</b> Sapna G. Yadav, Sudeep H Patil, Pratima Patel, Vineetha Nair , Shahida Khan, Shivani Kakkar ,Annika Durve Gupta	133-139
26	<b>Loading of Anti Cancer Drug on Carbon Nanotubes</b> Seema Manchanda, Madhuri Sharon, Maheshwar Sharon	140-145
27	<b>GC-MS Analysis of Luffa Cylindrica (L.) M.Roem. Vegetable Peel</b> Shivani Kakkar , Annika Durve Gupta, Meeta Bhot	146-150

28	<b>Structural, Vibrational and Thermal Analysis of L-arginine Potassium Sulphate (LAKS) Crystal Having NLO Response</b> Smita S. Patil, Mahendra M. Khandpekar	151-154
29	<b>A Comparative study of Heavy Metals in Leachate and Groundwater near Solid Waste Dumpsite in Kalyan (MS)</b> Sonal Tawde	155-161
30	<b>Application of Spectroscopic Techniques for analysis of interaction between Thermophiles and metal ions</b> Sonali Zankar Patil, Geetha Unnikrishnan	162-168
31	<b>Cauliflower Leaves, an Agro waste: Characterization and its Application for the Biosorption of Copper, Chromium, Lead and Zinc from aqueous solutions</b> Vandana Gupta, Sandesh Jaybhaye, Naresh Chandra	169-174
32	<b>Comparative Analysis of Antibacterial Properties of Clove and Ginger Extracts Using Gram Negative Bacteria E.coli</b> Vinod S. Narayane, Rahat R. Khan, Sumaiya R. Majeed, Nutan B. Kamble	175-180
33	<b>Bio-Electricity Generation Using Kitchen Waste And Molasses Powered MFC</b> Yash Manjerkar, Shivani Kakkar, Annika Durve Gupta	181-187
34	<b>Ferroelectric SbSI-Crystals Exhibiting Dual Electrical Nature</b> Harish K. Dubey, Dattatray E. Kshirsagar, K. D. Barhate, Maheshwar Sharon	188-192
35	<b>Surface Area measurement of Carbon Nanomaterials obtained from Castor oil</b> Vinod Lohakane Ratnakar Hole, Sandesh Jaybhaye, Achyut Munde	193-196
36	<b>Effluent Treatment by Multi Walled Carbon Nano Tubes</b> Archana Singh, Sandesh Jaybhaye, Harish K. Dubey, Siddhesh Kalambe, Brijesh Gaud	197-200

# Environmentally Friendly Synthesis and Antimicrobial Activity of ZnONPs

Amrita Singh, Brijesh Gaud, Sandesh Jaybhaye

Nanotech Research Lab, Department of Chemistry, Birla College, Kalyan, Maharashtra, India

## ABSTRACT

The use of nanotechnology in the textile industry has increased rapidly. This is mainly due to the conventional methods used to impart different properties to fabrics often do not lead to permanent effects, and will lose their functions after laundering or wearing. Nanoparticles can provide high durability for treated fabrics, with respect to conventional materials, because they possess large surface area and high surface energy that ensure better affinity for fabrics and lead to an increase in durability of the textile function. Various methods have been employed to improve the size and property of the Zinc Oxide Nano Particles (ZnONPs) so as to enhance the performance of ZnONPs based material. Biological methods for nanoparticle synthesis using microorganisms, enzymes, and plants or plant extracts have been suggested as possible eco-friendly alternatives to chemical and physical methods. In this work, ZnONPs have been synthesized by reduction of Zinc Nitrate in plant extract and study the antimicrobial activity of synthesized ZnONPs. FT-IR spectra peak at  $483\text{ cm}^{-1}$  indicated characteristic absorption bands OF ZnO nanoparticles. UV-Vis absorption spectrum showed a typical spectrum for ZnO nanoparticles. The SEM and AFM image shows that ZnONPs prepared in this study are spherical in shape with smooth surface have size of minimum 16nm to maximum 36 nm and it also shows excellent inhibition to gram positive and gram negative bacteria.

**Keywords:** ZnONPs, FT-IR Spectroscopy, Environmental friendly method, Zinc Nitrate, Gram positive and Gram negative

## I. INTRODUCTION

Nanotechnology is the study of nanoparticles, and by definition, a nanoparticle is any material measuring less than 100 nanometers in at least one dimension. Nano sized materials have unique optical, thermal, electrical and/or magnetic properties and have been used in cosmetics and paints.

Nanotechnology concerns with the development of experimental processes for the synthesis of nanoparticles of different sizes, shapes and controlled disparity. This provides an efficient control over many of the physical and chemical

properties with various potential applications including pharmaceuticals and medicine. Most of the chemical methods used for the synthesis of nanoparticles are too expensive and are found to be responsible for various biological risks. But, synthesis of nanoparticles using plant extracts is the most adopted method as green, eco-friendly production of nanoparticles and also has a special advantage in such a way, that the plants are widely distributed, easily available, much safer to handle and act as a source of several metabolites rich in pharmacological constituents. Hence a novel approach for synthesizing ZnONPs using plants extracts. With the advent of nanoscience and technology, a new area has developed in the area of

textile finishing called Nano finishing. Growing awareness of health and hygiene has increased the demand for bioactive or antimicrobial. Nanoparticles have selective toxicity to bacteria but exhibit minimal effects on human cells. Several studies have reported the broad-spectrum antimicrobial activity for including antibacterial, antiviral, antifungal, and antimalarial activities.

In this work, ZnONPs have been synthesized by reduction of Zinc Nitrate in plant extract and study the antimicrobial activity of synthesized ZnONPs. FT-IR spectra peak at  $483\text{ cm}^{-1}$  indicated characteristic absorption bands of ZnO nanoparticles. UV-Vis absorption spectrum showed a typical spectrum for ZnO nanoparticles. The SEM image and AFM shows that ZnONPs prepared in this study are spherical in shape with smooth surface.

## II. METHODS AND MATERIAL

The Hibiscus rosa-sinensis (HRS) Leaves were washed with sterile double distilled water to remove the surface contamination and dried in oven to remove water for 60 Minutes. The dried plant material was cut into in small pieces. 10 g of plant material was taken and mixed with 100 ml of sterile double distilled water and kept in water bath for reflux at  $100^{\circ}\text{C}$  for 1 hours. The obtained reflux solution is then filtered by Whatman No. 1 filter paper. The filtered extract was stored in refrigerator at  $20^{\circ}\text{C}$  for further studies.

The solution of plant extract having pH 5 was mixed with 10mm concentration of Zinc Nitrate, time for sonication and temperature maintained 30 minutes and  $80^{\circ}\text{C}$  respectively.

The bio-reduction of the Zinc ions in the solution was monitored periodically by measuring the UV-Vis spectroscopy (200–800 nm) of the solutions. The formation of a yellowish brown-colored solution indicated the formation of the ZnONPs. The ZnONPs obtained was centrifuge and then obtain

ZnONPs were purified by sterile deionized water three times to remove the water-soluble biomolecules such as proteins and secondary metabolites. After that dried ZnONPs were used to characterize the structure and composition.

## III. CHARACTERIZATIONS

### 1. FT-IR Analysis:

Two milligram of ZnO NPs was mixed with 200 mg of potassium bromide (FTIR grade) and pressed into a pellet. The sample pellet was placed into the sample holder and FTIR spectra were recorded in FTIR spectroscopy. To validate again the nature of the synthesized nanoparticles and their purity Fourier Transform Infrared spectroscopy (FTIR) (Jasco) studies were performed. A reports the typical FTIR spectrum of the pressed powder in the spectral range of  $200\text{--}4000\text{ cm}^{-1}$ . The IR transmission is plotted so to single out the major absorptions observed at lower wave numbers.

An IR spectrum of synthesized zinc oxide shows the characteristic bands corresponding to M-O (Zn-O) stretching at  $483\text{ cm}^{-1}$ . Peaks at  $3404\text{ cm}^{-1}$  and  $1651\text{ cm}^{-1}$  may be due to presence of moisture and carbon dioxide present in atmosphere. The presents of diagnostic bands at  $1384$  and  $1107\text{ cm}^{-1}$ , related to the symmetrical and asymmetrical stretching modes of the carboxylate groups of plant extract. The IR spectrum of the ZnONPs powder collected after washing with water treatment of the original ZnONPs shows a slight shift and a decrease in the intensity of the characteristic bands shows in figure 1.

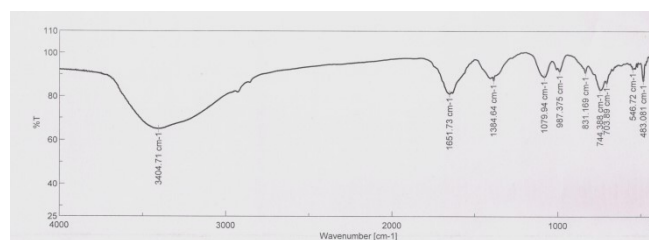


Figure 1. FT-IR spectra of ZnONPs



## 2. XRD Analysis:

X-ray diffraction (XRD) analysis (MiniFlex) with Cu-K $\alpha$  radiation ( $k = 1.54178 \text{ \AA}$ ) with 40 kV, 15 mA was used to examine the crystalline structure of the products. Fig. 2 XRD patterns of all prepared powders. All of the diffraction peaks are well matched with the standard hexagonal structure of ZnO (JCPDS card No. 00-079-0207). Both samples show wurtzite crystal structure of ZnO, For three curves, the average crystalline sizes were calculated using the Debby–Scherer equation ( $d = k\lambda / \beta \cos\theta$ ), where  $d$  is the mean crystalline size of the powder,  $k$  is the wavelength of Cu-K $\alpha$  ( $k = 1.54178 \text{ \AA}$ ),  $B$  is the full width at half maximum (FWHM) intensity of the peak in radian, the Bragg's diffraction angle and  $k$  is a constant usually equal to  $\sim 0.9$ ). The average crystallite size of samples I and II were determined to be about 16, 18 and 36 nm, respectively. Diffraction peaks corresponding to the impurity were not found in the XRD patterns, confirming the high purity of the synthesized products.

The X-Ray diffraction (XRD) pattern reveals the formation of ZnO NPs, which attributes to the crystalline nature of nanoparticle (Fig 2). XRD spectra showed strong diffraction peaks at 31, 34, 36, 47, 56, 62, 66, 67 and 68 degrees of  $2\theta$  which corresponds to (100), (002), (101), (102), (110), (103), (200), (112) and (201) crystal planes, which were in significant agreement with the JCPDS file 361451 ( $a = b = 3.249 \text{ \AA}$ ,  $c = 5.206 \text{ \AA}$ ) and indexed as the hexagonal wurtzite structure of ZnO NPs. This indicates the crystalline nature of synthesized nanoparticle.

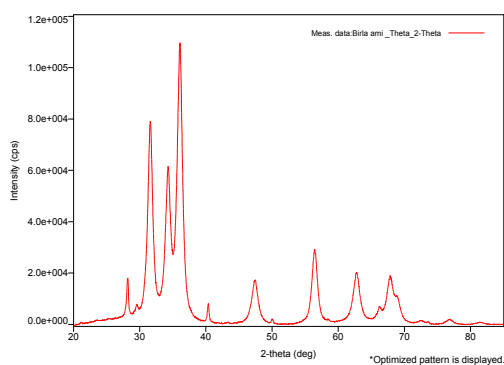


Figure 2. XRD spectra of ZnONPs

## 3. UV-Vis Spectroscopy analysis:

Initially, the solution turned yellow, characteristic of the spherical particles, but over 30 hours the solution turned Yellowish brown. We observed a decrease in intensity of the characteristic surface plasmon band in the ultraviolet-visible (UV-Vis) spectroscopy for the spherical particles at  $\lambda_{\text{max}}$  358–372 nm appeared. The absorption band is observed at 280 nm and a small but sharp peak at 380 nm for spherical ZnO nanostructure. In this case, the first and second band gaps were calculated 4.43 and 3.27 eV, respectively. It has been concluded that both morphologies have nearly similar band gaps, which may be due to having similar particle sizes.

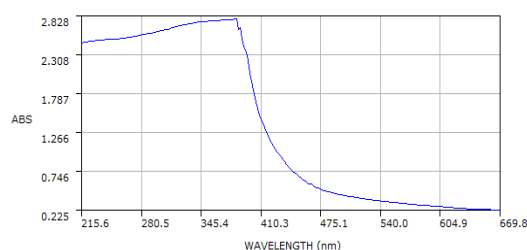


Figure 3. UV-visible spectra of ZnONPs

## 4. SEM Analysis :

The SEM image was taken at X 25,000 magnification. The image shows ZnO particles are spherical in shape with smooth surface and the size of the particles around 16–36 nm.

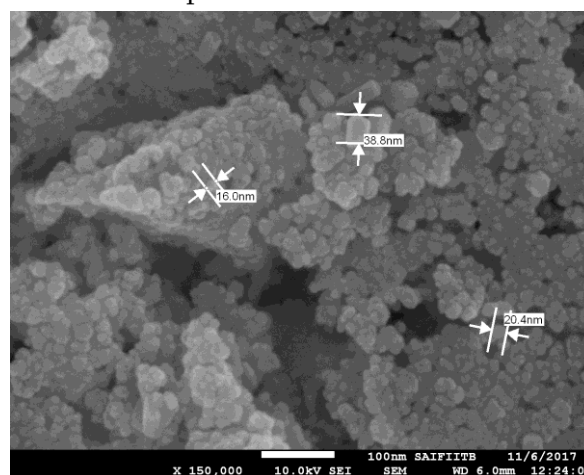


Figure 4. SEM Image of ZnONPs

## 5. AFM Analysis:

Size and shape of the nanoparticles which obtained directly from tip-corrected AFM measurements, and the shape of the nanoparticles is estimated on the

basis of AFM images and line scans. The ZnONPs obtained using green method gave size in the range of 20–36 nm and elongated in shape.

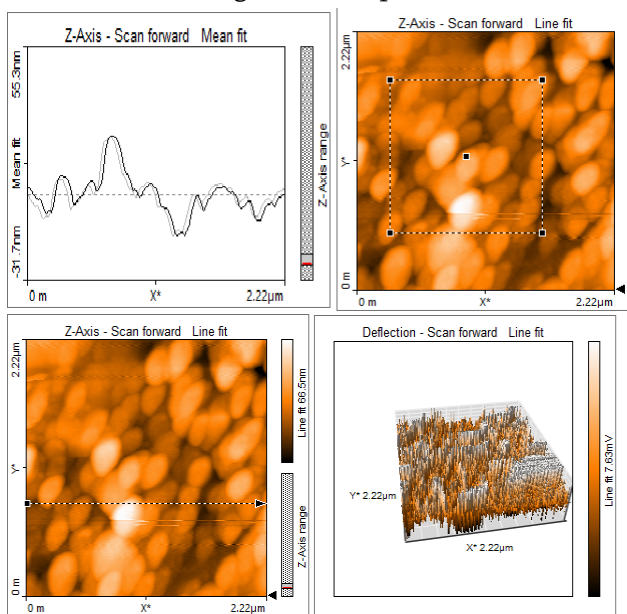


Figure 5. AFM Image of ZnONPs

#### 6. Antimicrobial properties:

The antibacterial activities of ZnONPs were measured by Agar well diffusion method. The test was done against Gram positive and negative bacteria. It was proved that this ZnONPs has excellent antibacterial activity and could be used as anti-microbial agents.

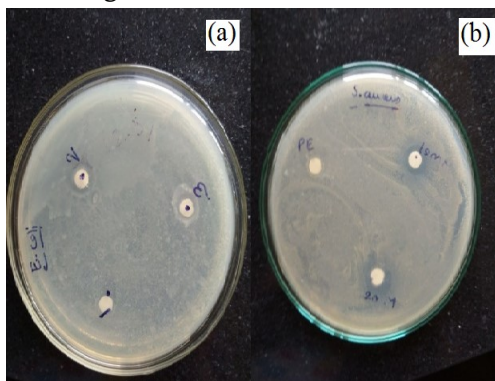


Figure 6. (a) Antibacterial activity against *E. coli*  
(b) Antibacterial activity against *S. aureus*

### IV. RESULTS AND DISCUSSION

Several approaches have been employed to obtain a better synthesis of ZnONPs such as chemical and biological methods. Recently, synthesis of ZnONPs using plant extracts getting more popular. The development of easy, reliable and eco-friendly methods helps to increase interest in the synthesis.

The present work addresses the synthesis and characterization of ZnO nanoparticles obtained through a homogeneous phase reaction between zinc nitrate and plant extract Solution having pH = 5 at 10mm in concentration with constant sonication time and temperature. The particles were then characterized, by evaluating their chemical composition through FTIR spectroscopy; their crystallinity through X-ray diffractometry and particle size by AFM and SEM Analysis.

### V. CONCLUSION

The present work shows rapid biological synthesis of ZnONPs using Plant extract which provides an environmental friendly, simple and efficient route for synthesis of nanoparticles and characterization of ZnONPs obtained through a homogeneous phase reaction between zinc nitrate and plant extract Solution having pH 5 at change in concentration with constant sonication time and temperature.

FTIR shows that peak at  $533\text{ cm}^{-1}$  is the characteristic absorption of zinc oxide bond which confirms formation of zinc oxide nanoparticles.

X-ray diffraction confirms the formation of a hexagonal wurtzite phase which is the most stable form of zinc oxide at ambient conditions. The average crystalline sizes were calculated using the Debye–Scherrer equation to be about 16 nm.

AFM measured nanoparticles 20–36 nm and spherical in shape.

SEM image showed that most of the nanoparticles are spherical in shape formed within diameter range of 10–40 nm ZnO NPs have been economically synthesized by Bio-Reduction of Zinc nitrate using plant extract.

### VI. REFERENCES

1. Megan J. Osmond, & Maxine J. McCall, Zinc oxide nanoparticles in modern sunscreens: An analysis of potential exposure and hazard, *Nanotoxicology*, 4(1): March 2010; 15–41.

2. Sandesh Jaybhaye Anti-microbial activity of AgNPs synthesized from waste vegetable fibers, *Int. J. Materials Today: Proceedings*, 2015, Vol. 2(9) Part A, pp 4323-4327.
3. Sandesh Jaybhaye, Eco-friendly Synthesis of Silver Nanoparticles using Caster Leaves, *Int. Journal of Contemporary Research in India* (2014), 58-60 (ISSN 2231-2137).
4. Vishal Saxena, Niraj Kumar, Vinod. Kumar Saxena, A comprehensive review on combustion and stability aspects of metal nanoparticles and its additive effect on diesel and biodiesel fuelled C.I. engine, *Renewable and Sustainable Energy Reviews* 70 (2017) 563-588
5. P. Rajiv, Sivaraj Rajeshwari, Rajendran Venckatesh, Bio-Fabrication of zinc oxide nanoparticles using leaf extract of *Parthenium hysterophorus* L. and its size-dependent antifungal activity against plant fungal pathogens, *Spectrochimica Acta Part A: Molecular and Biomolecular Spectroscopy* 2013, 112, 384-387.
6. Amir Kajbafvala, Hamed Ghorbani, Asieh Paravar, Joshua P. Samberg, Ehsan Kajbafvala, S.K. Sadrnezhad, Effects of morphology on photocatalytic performance of Zinc oxide nanostructures synthesized by rapid microwave irradiation methods, *Superlattices and Microstructures* 51, (2012), 512-522
7. Jiao Qu, Xing Yuan, Xinhong Wang, Peng Shao, Zinc accumulation and synthesis of ZnO nanoparticles using *Physalis alkekengi* L, *Environmental Pollution* 159, (2011), 1783-1788
8. Michał Moritz, Małgorzata Geszke-Moritz, The newest achievements in synthesis, immobilization and practical applications of antibacterial nanoparticles, *Chemical Engineering Journal* 228, (2013), 596-613
9. Mehrez El-naggar, Tharwat I. Shaheen, Saad Zaghoul, Mohamed Hussein El-Rafie, and Ali Ali Hebeish, Antibacterial activities and UV-protection of the in-situ synthesized titanium oxide nanoparticles on cotton fabrics, *Ind. Eng. Chem. Res.*, February 24, (2016)
10. Milica Milosevic, Ana Krkobabic, Marija Radoicic, Zoran Saponjic, Vesna Lazic, Milovan Stoiljkovic and Maja Radetic, Antibacterial And Uv Protective Properties Of Polyamide Fabric Impregnated With TiO<sub>2</sub>/Ag Nanoparticles, *J. Serb. Chem. Soc.* 80(5) (2015), 705-715.
11. Maryam Ahmadzadeh Tofighy, Toraj Mohammadi, Application Of Taguchi Experimental Design In Optimization Of Desalination Using Purified Carbon Nanotubes As Adsorbent, *Materials Research Bulletin* 47, (2012), 2389-2395.
12. R. Dastjerdi and M. Montazer; A review on the application of inorganic nano-structured materials in the modification of textiles: Focus on anti-microbial properties; *Colloids Surf. B: Biointerfaces* 79, (2010), 5-18.
13. M. Milosevic, A. Krkobabic, M. Radoicic, Z. Saponjic, V. Lazic, M. Stoiljkovic and M. Radetic; Antibacterial and UV protective properties of polyamide fabric impregnated with TiO<sub>2</sub>/Ag nanoparticles; *J. Serb. Chem. Soc.* 80 (5), (2015), 705-715.
14. M.J. Osmond and M.J. McCall; Zinc oxide nanoparticles in modern sunscreens: An analysis of potential exposure and hazard; *Nanotoxicology* 4 (1), (2010), 15-41.
15. R.Y. Hong, J.H. Li, L.L. Chen, D.Q. Liu, H.Z. Li, Y. Zheng and J. Ding; Synthesis, surface modification and photocatalytic property of ZnO nanoparticles; *Powder Technol.* 189, (2009), 426-432.
16. C.-L. Kuo, C.-L. Wang, H.-H. Ko, W.-S. Hwang, K.-m. Chang, W.-L. Li, H.-H. Huang, Y.-H. Chang and M.-C. Wang; Synthesis of zinc oxide nanocrystalline powders for cosmetic applications; *Ceramics Int.* 36, (2010), 693-698.
17. G.J. Nohynek, E.K. Dufour and M.S. Roberts; Nanotechnology, cosmetics and the skin: Is there a health risk?; *Skin Pharmacol. Physiol.* 21, (2008), 136-149.
18. L.M. Katz, K. Dewan and R.L. Bronaugh; Nanotechnology in cosmetics; *Food Chem. Toxicology*, 85, (2015), 127-137. doi: 10.1016/j.fct.2015.06.020.
19. R. Silpa, J. Shoma, U.S. Sumod and M. Sabitha; Nanotechnology in cosmetics: Opportunities and challenges; *J. Pharmacy Bioallied Sci.* 4 (3) (2012), 186-194.
20. G. Sangeetha, S. Rajeshwari and R. Venckatesh; Green synthesis of zinc oxide nanoparticles by aloe barbadensis miller leaf extract: Structure and optical properties; *Mater. Res. Bull.* 46, (2011), 2560-2566
21. Rinkesh Kurkure, Sandesh Jaybhaye, Abhijeet Sangale, Synthesis of copper/copper oxide nanoparticles in ecofriendly and nontoxic manner from floral extract of *Caesalpinia pulcherrima* *Int. J. on Recent and Innovation Trends in Computing and Communication (IJRITCC)* Vol. 4 (4), (2016), pp 363-366 ISSN: 2321-8169.

# Ambient Air Quality Monitoring in Vasai Virar City Municipal Corporation Region (Maharashtra, India)

B. S. Pansare, G. R. Bhagure\*

Department of Chemistry, Satish Pradhan Dnyansadhana College, Thane, Maharashtra, India

## ABSTRACT

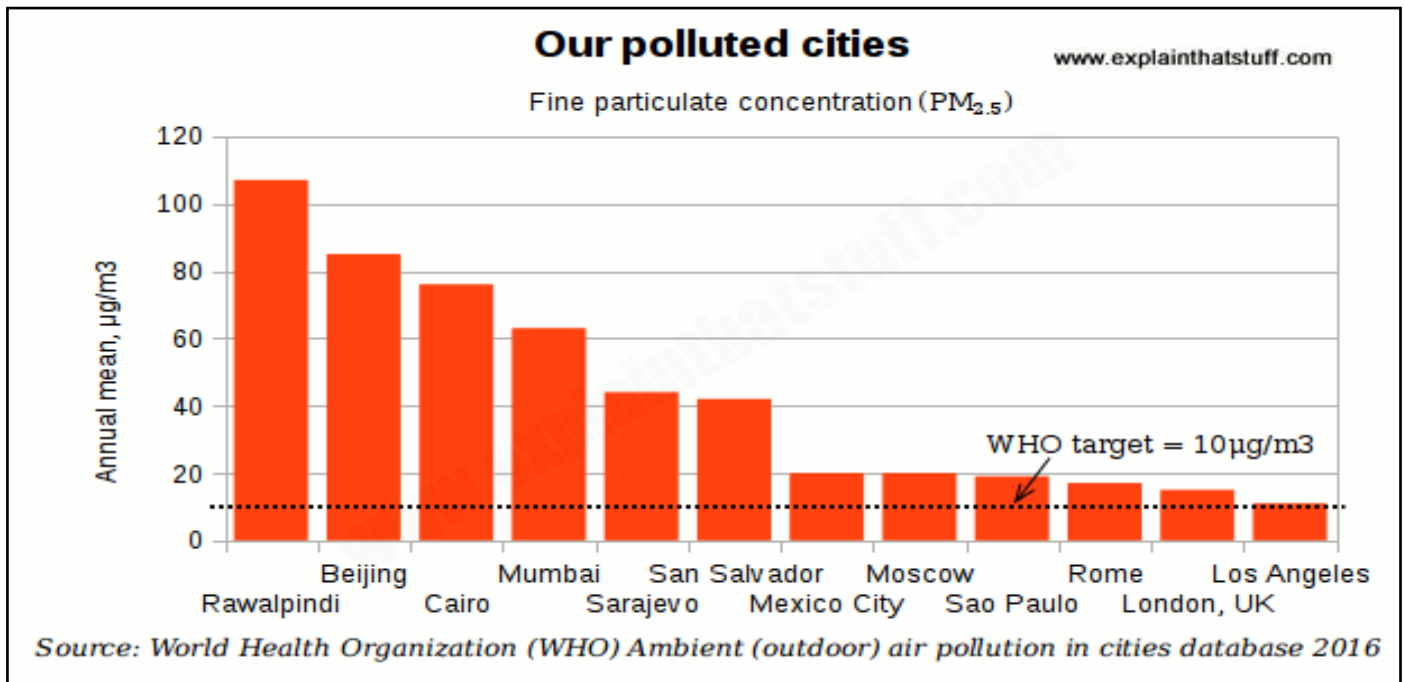
Ambient air quality criteria or standards are concentrations of pollutants in the air (usually outdoor air but sometimes indoor air) specified for a variety of reasons including for the protection of human health, buildings, crops, vegetation, ecosystems, as well as for planning and other purposes. Ambient air quality in Vasai Virar City Municipal Corporation Region was monitored during the June 2014 to May 2015. Concentrations of Oxides of nitrogen ( $\text{NO}_x$ ), oxides of sulphur ( $\text{SO}_x$ ), suspended particulate matter (SPM) and Ammonia ( $\text{NH}_3$ ) were collected over successive periods of about 8 hour in a day. Twenty representative sites were selected over the whole stretch of the region for the study. Characteristics of the sites are mainly comprising of the residential, commercial, public places. High volume air sampler was used to measure the concentration of oxides of nitrogen ( $\text{NO}_x$ ), oxides of sulphur ( $\text{SO}_x$ ), suspended particulate matter (SPM) and Ammonia ( $\text{NH}_3$ ). Vasai Virar city municipal corporation region is fast urbanizing city in Maharashtra, India, thereby increasing population in exponential rates. Increasing population lead to burden on the administration of the region and thereby on various services provided by the administration namely transportation, water supply, solid waste disposal, sewage disposal etc. Method used for sampling and analysis of the pollutant are standard IS methods. Results, outcome of the analysis of the collected pollutants are compared to limits as prescribed by National Ambient Air Quality Standards (NAAQS), 2009. Criteria pollutants SPM,  $\text{SO}_2$  and  $\text{NO}_2$  measured are found to have either crossed or on the average of crossing the limits or in the permissible limits of NAAQS. Reasons responsible for the pollutants were observed mainly vehicular pollution and dust suspended in the air due to heavy traffic, transport. While transport related emissions are the major sources of air contamination, increasing building construction, civil infrastructure development activities also contribute to particulates. The exponential rise in volume of vehicles, inappropriate and unplanned traffic flow pattern and human interceptions deserve due attention. The value of SPM was crossing the permissible limit at number of monitoring locations and was exceeding the National Ambient Air Quality Standard (NAAQS). The concentration of  $\text{SO}_2$ ,  $\text{NO}_2$  and  $\text{NH}_3$  was within of National Ambient Air Quality Standard (NAAQS) at all the locations. SPM, dust concentrations are responsible for various lung diseases, respirable illness, and heart related diseases in the children as well as adult. Present study necessitating the immediate actions for controlling and efficient management of traffic in the region which is major source of dust and pollution in the region. Plantation of the trees along and sides of the road, Installation of a continuous air monitoring stations at different location in the city will be helpful to tackle pollution issue in the region.

**Keywords** - Ambient Air Quality, Vehicular Pollution, Pollutant, Urbanization, Construction Activities.

## I. INTRODUCTION

Clean or pollution free air is need of every human and living being. However, human development and

smaller than 2.5 microns and believed to be most closely linked with adverse health effects. Above chart drawn using data from Ambient air pollution in



resources used for human development causes contamination of the natural resources especially air. Air pollution is nothing but contamination of the air, atmosphere with the solid, liquid, gaseous products, by products which can endanger human health and welfare of the plants and animals. Air pollution levels in cities of the developed countries is degrading continuously. These air pollutants can be mix with the air, atmosphere either through natural processes or even through anthropogenic sources. As urban air quality declines, the risk of stroke, heart disease, lung cancer, and chronic and acute respiratory diseases, including asthma, increases for the people who live in them [1]. Most of the world's major cities routinely exceed World Health Organization (WHO) air pollution guidelines. Following chart compares annual mean PM<sub>2.5</sub> levels in 12 representative cities around the world with the WHO guideline value of 10µg per cubic meter (dotted line). PM<sub>2.5</sub> particulates are those

cities database 2016 courtesy of World Health Organization [2]. India's rapidly worsening air pollution is causing about 1.1 million people to die prematurely each year and is now surpassing China's as the deadliest in the world [3].

### A. Adverse health Hazard of the Air Pollution:

Continuous exposure to ambient air pollution leads to adverse effects on health from affecting the functioning of the respiratory system, cardiovascular system to psychological instability and even can lead to premature death. Risk of adverse effects on health is high in young children, aged people and even pregnant females and their foetus etc. Health related issues due to pollution is seems to be more common in the developing countries than developed countries [4]. Many recent studies have shown associated relationship between significant exposure to air pollution and adverse effects on health including

mortality and morbidity [5]. Oxides of sulphur in the air may harm human lungs, respiratory system and even may lead to acid rain. Particulate matter suspended in the atmosphere are responsible for respiratory diseases and gastric cancer etc. Continuous exposure to this may lead to breathing problem, cough, and lung diseases. Coughing and wheezing are the most common complication of nitrogen oxides toxicity, but the eyes, nose or throat irritations, headache, dyspnea, chest pain, diaphoresis, fever, bronchospasm, and pulmonary edema may also occur [6]. Exposure to high concentrations of ammonia in air causes immediate burning of the nose, throat and respiratory tract. This can cause bronchiolar and alveolar edema, and airway destruction resulting in respiratory distress or failure [7].

#### **The Study Area:**

Vasai Virar City Municipal Corporation is formed 8 years back on 3<sup>rd</sup> July 2009. VVCMC is formed by merging of the Vasai, Virar, Navghar, Manikpur and Nalasopara municipalities and 53 villages of the surrounding area. VVCMC has total area of 311 sq. km and is fifth largest city in Maharashtra as per 2011 Census. Population of the VVCMC is 1.3 million as per 2011 Census. VVCMC area is bounded by Vaitarna River on the north, Vasai creek on south, Arab Sea on west and Tungar ranges on the west. Various historical monuments from B.C. 540 to 19<sup>th</sup> Century like Buddha Stupa, Portuguese forts along with religious places like Jivdani Mata Temple thereby contributing to tourism in the area. Stations which are selected for air quality survey are mainly characterized by public places, residential area, commercial as well as industrial area. Brief characteristics of the locations are as follows,

1. Vasai Railway Station: Vasai railway station is administered by Western Railway of Indian Railways. It is one of the busiest railway stations on Western Railway. Surrounding area is consists of mainly commercial as well as residential like hotels, clinics, retail shops etc.
2. Nalasopara Bus Stand: Located on the very outside of Nalasopara railway station on west side. Hundreds of buses travel through the bus stand daily. More than usual traffic on surrounding road.
3. Vitthal Rukmini Temple, Valiv: Located on Nalasopara East. Densely populated residential area. Station is mostly surrounded by chowli system.
4. Pelhar Tehasildar office: It is taluka administrative office. Station is surrounded by roads with heavy traffic. Number of vehicles, people travel daily.
5. Aamchi Shala, Zilha Parishad: Surrounded by ZP school and residential area. There is usual traffic over road. Traffic is higher in the morning and evening.
6. Vatar Village Road: Located nearby sea shore/ Navapur beach. Location is surrounded by tree cover. Traffic is usual. Location is characterized by high speed sea shore winds.
7. Sativali MIDC: Location is surrounded by the MIDC industrial area. Variety of medium and small-scale industries are located in the surrounding area. Residential area is also located nearby.
8. Gokhivare Road: Location is characterized by mix zone area i.e. residential, commercial, public service area etc. and high traffic.
9. BSNL Office, Vasai: Very densely populated residential area with usual traffic on road. Location is surrounded by residential apartments, offices, hospitals. Municipal public garden is also located nearby location.
10. Nalasopara Railway station: Busy railway station on Western Railway. Location is surrounded by heavy traffic area, roads Nalasopara bus stand is located nearby.
11. VVCMC office, Virar: Very much outside of Virar railway station. Heavy traffic is on both side of the virar railway station.
12. Hanuman Temple, Agashi: Location is mainly surrounded by Residential area. Lake is located on north east side of monitoring location.
13. Global City, Virar: Huge residential Complex with usual traffic over road. Minimum or no tree/forest cover over surrounding open area.
14. Navghar: Surrounding area of the location is densely populated. Location is surrounded by offices, retail shops, residential apt. etc.

15. Achole Road: Heavy traffic road area surrounded by residential buildings, banking offices etc.
16. Vasai Station Road, Manikpur: Location is densely populated with residential buildings, apartments etc. Traffic is usual on road surrounded by schools etc.
17. Viva Super Market, Virar: Location is nearby East side of virar railway station. Heavy traffic, traffic jams are observed on the road.
18. Arnala Beach: Located nearby sea shore/beach. Location is surrounded by tree cover. Traffic is usual. Location is characterized by high speed sea shore winds.
19. Ambadi Municipal Park: Location is surrounded by roads having heavy traffic. Park is located on the east of the monitoring location. Area is mainly surrounded by residential area.
20. Navghar Bus stand, Vasai: Location is mainly surrounded by residential area. Usual traffic on road.

## II. METHODS AND MATERIAL

SPM (suspended particulate matter) concentrations were measured by finding the sample air volume ( $m^3$ ) through an orifice meter and the mass ( $\mu g$ ) of particulate matter collected in a Watt man grade 1 fiberglass filter paper. Concentrations of  $SO_2$  and  $NO_2$  ( $\mu g/m^3$  or PPM) were calorimetrically determined using a spectrophotometer. 5 to 20 ml of reagent (sodium tetra chloro mercurate for West and Geake method to find  $SO_2$  and sodium hydroxide for  $NO_2$ ) filled in a train of impingers of the high-volume sampler trap specific contaminant in air. Air flows to the impingers were determined using rota meters.

### Sampling of Suspended Particulate Matter (SPM):

High volume air sampler was used for the monitoring of particulates. Before sampling, the whatman filter GFA (20.3cm  $\times$  25.4cm) of the high-volume sampler was kept at 15-34  $^{\circ}C$ , 50% relative humidity for 8 hours and then weighed. The filter paper was placed into the filter holder of the high-volume sampler and air was drawn filter at the flow rate of 1.80  $m^3/min$ . The filter was removed after sampling. The mass concentration of suspended

particulates in ambient air, expressed in micrograms per cubic meter, was calculated by measuring the mass of particulates collected and the volume of air sampled.

### Sampling of Nitrogen Oxides (NOx):

Ambient air was continuously drawn in 30 ml of absorbing reagent. Absorbing reagent is prepared by dissolving 4.0 gm of Sodium Hydroxide with 1.0 gm of Sodium Arsenite in 1000 ml of distilled water. Air was drawn for 8 hours at the sampling rate of 0.8 Lit/min. The nitrite ion thus formed is reacted with sulfanilamide and N-(1-naphthyl) ethylenediamine (NEDA) in phosphoric acid to form the highly colored azo dye. The absorbance of the highly colored azo-dye is measured on a spectrophotometer at a wavelength of 540 nm.

### Sampling of Sulphur Oxides (SOx):

Ambient air was drawn at the in 30 ml of absorbing reagent. Absorbing reagent was prepared by dissolving 10.86 g, mercuric chloride, 0.066 g EDTA, and 6.0 g potassium chloride in distilled water. Air suction is done at the rate of 1.5 Lit/min for continuous 8 hours. Air sample is collected using high volume sampler in impinger containing absorbing solution. The amount of  $SO_2$  is then estimated by the color produced when para – rosaniline hydrochloride and formaldehyde is added to the solution. The red-violet color is shown strong absorbance at 560nm.

### Sampling of Ammonia (NH<sub>3</sub>):

Sampling for Ammonia is done using high volume sampler in impinge box containing 10 ml of absorbing solution. Absorbing solution is prepared by diluting 3.0ml of concentrated  $H_2SO_4$  (18M) to 1 litre with water to obtain 0.1N  $H_2SO_4$ . Ammonia in the atmosphere is collected by bubbling a measured volume of air through a dilute solution of sulphuric acid to form ammonium sulphate. The ammonium sulphate formed in the sample is analyzed colorimetrically by reaction with phenol and alkaline sodium hypochlorite to produce indophenol. The reaction is accelerated by the addition of Sodium Nitroprusside as catalyst.

### III. RESULTS AND DISCUSSION

It is observed from the outcomes of the study of pollutants level at 20 sites, there is remarkable correlation between activities at site and pollutant concentration observed. Locations characterized by heavy traffic of vehicles etc is observed with high concentrations of the pollutants. SPM concentration level is crossed the standard limit (200 µg/m<sup>3</sup>) at number of locations and is on the verge of crossing standard limit at almost all locations. Concentration of other pollutants i.e. SO<sub>2</sub>, NO<sub>x</sub>, NH<sub>3</sub> is within the standard limit at all locations. There is also seasonable variation of the pollutant level at the locations. Concentration of the pollutants in Pre-Monsoon season is observed to be higher than in other seasons.

Table 1

Sr. No.	Pollutant	Standard Limit
1.	Suspended Particulate matter	200 µg/m <sup>3</sup>
2.	Oxide of Sulphur	80 µg/m <sup>3</sup>
3.	Oxides of Nitrogen	80 µg/m <sup>3</sup>
4.	Ammonia	400 µg/m <sup>3</sup>

Source: National Ambient Air Quality Standards<sup>[9]</sup>

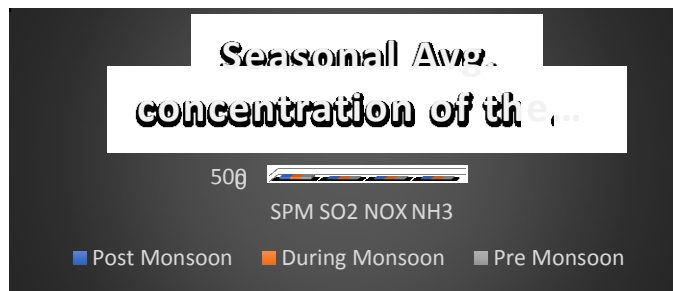


Figure 1. Seasonal Average Concentration of the pollutants

### IV. CONCLUSION

Season wise average of the SPM is seeming to be crossing the standard limit for that parameter. Higher level of the SPM concentration at location is alarming and this situation may further get worsen in coming years. Main contributors to the increasing level of the SPM and other pollutants is mainly addition of the 2,3,4- wheelers on the roads of the urban city.

Regular study of the pollutants in the city/town will help to understand the range pollutant level, cause effects, correlations, trend, pattern evaluations, preventive as well as strategic remedies to tackle the worsening air quality etc. Proper road management, better traffic regulations, controlling emission features of vehicles, proper synchronization of the office, school timings, tree plantation around the roads, creating green zones by planning gardens, encouraging citizens for use of public transport, continuously arranging awareness programmes for citizens etc. are some of the immediate remedies for upward pollution. Safety measures against poor ambient air quality should be analysed and implemented. More emphasis should be given on public places like bus stand, railway station, road junctions etc. Equal contribution of the local authorities, public administration along with active participation of the citizens is needed.

### V. REFERENCES

- [1] World Health Organization database, 2016.
- [2] Woodford, Chris. (2010/2017) Air pollution. Retrieved from <http://www.explainthatstuff.com/air-pollution-introduction.html>. [Accessed 01/02/2018]
- [3] India's Air Pollution Now Rivals China's as Deadliest in the World, Feb 14, 2017, The New York Times
- [4] Indoor air pollution in developing countries: a major environmental and public health challenge by Nigel Bruce, Rogelio Perez-Padilla & Rachel Albalak, Department of Public Health, University of Liverpool
- [5] Air pollution and population health: a global challenge by Bingheng Cheng and Haidong Kan, Department of Environmental Health, School of Public Health, Fudan University
- [6] Chen TM, Gokhale J, Shofer S, Kuschner WG. Outdoor air pollution: Nitrogen dioxide, sulfur dioxide, and carbon monoxide health effects. *Am J Med Sci.* 2007;333:249–56
- [7] Facts about Ammonia, Department of Health, New York State
- [8] Guidelines for measurement of ambient air pollutants (Volume 1) by Central Pollution Control Board
- [9] Gazette notification number B 29016/20/90/PCI-I by Central Pollution Control Board, dated 18<sup>th</sup> November 2009



# Synthesis of Carbon Fibers and Its Surface Area Measurements

Brijesh Gaud, Amrita Singh, Sandesh Jaybhaye

Nanotech Research Lab, Department of Chemistry, B.K.Birla College, Kalyan, Maharashtra, India

## ABSTRACT

Carbon fibre (CFs) are fibre about 5–10 Micrometres in diameter and composed mostly of carbon atoms. Carbon based materials such as graphenes, carbon black, carbon fibers (CFs), CNFs, carbon nanotubes (CNTs), carbon nanocoils, and carbon onions have attracted growing interest because of their low weight, small thickness, and high flexibility. Among various carbonaceous materials, CFs and their composites have been found to be fascinating candidates owing to their excellent mechanical and electrical properties, low cost, and wide availability as compared to CNTs and graphenes. Carbon fibres have several advantages including high stiffness, high tensile strength, low weight, high chemical resistance, high-temperature tolerance and low thermal expansion. In the present work, CFs is synthesized by using organic waste precursor obtained from plant fibre at 600°C in inert atmosphere of Argon. The surface area analysis has done using Surface area analyzer instrument. Characterisation study of CFs was done with the help of SEM, FT-IR and XRD. The size observed in SEM for CFs is in the range of 1-2  $\mu\text{m}$ .

**Keywords:** Carbon fibres, Plant Fibre precursor, Scanning Electron Microscope, FT-IR, XRD.

## I. INTRODUCTION

The first known use of carbon fiber filaments is attributed to Thomas Edison in 1879 during his work on the incandescent light bulb through the baking of cotton threads or bamboo strips.

Over the past few years there have been very major improvements in the range of properties available in carbon fibres. Carbon fiber is increasingly being utilized as a reinforcing material due to its high strength and high modulus, which is imparted into the properties of the final composite. This is a result of advances in carbon-fibre technology.

Short discontinuous fibers are widely used to improve the tensile and bending performance of breakable materials, such as concrete and textile fibres.

Currently, PAN serves as the principal precursor (~96% of the carbon fiber market) material for carbon fiber production, although other precursors such as pitch and Rayon are also utilized.

Carbon fiber is a unique material to the extent that the material properties span a wide range of thermo-

physical properties as well as series of outstanding properties of high strength, high modulus, high temperature resistance, corrosion resistance, fatigue resistance, creep resistance, light weight, and electric conduction that can be tailored to the desired application, allowing for a vast range of material properties.

Carbon fiber composites are currently utilized in the aerospace, athletics, automotive, construction, marine, and wind energy sectors, among others.

Carbon fibers in particular have garnered much attention. Compared to the unreinforced materials, material composites containing carbon fibers with lengths on the order of millimeters to one micro meter have shown superior tensile strength, flexural strength and flexural toughness.

As part of the continued push for improvements in specific strength and modulus, low-density electrical conductivity, and thermal conductivity, carbon fibers are being developed which possess a hollow structure. By increasing the final heat treatment temperature of carbon fibers, increases in tensile modulus, electrical

conductivity, and thermal conductivity can be achieved. This is due to the increasing structural order in the fiber as the carbonization temperature is increased.

Xie *et al.* also reported that the longer fibers in the non-conductive matrix were more effective to conduct electricity than shorter ones. Thus, the dosage of fibers could be minimized to achieve a certain conductivity value.

Chung compared the effectiveness of various electrically conductive components, including steel fibers, steel dust, carbon fibers, carbon nanofiber, coke powder and graphite, on the electrical conductivity of cement-based materials. It was found that steel fiber with 8  $\mu\text{m}$  diameter was the most effective conductive filler for lowering the electrical resistivity.

In respect to carbon-based materials, carbon fiber with 15  $\mu\text{m}$  diameter was more effective than carbon nanofiber, coke powder or graphite powder in improving the electrical conductivity. In the present work CFs is synthesized by using organic waste precursor obtained from plant fibre and its characterisation study was done with the help of SEM, FT-IR, XRD and surface area analysis.

## II. METHODS AND MATERIAL

Synthesis of CFs by using organic waste precursor i.e Corn Hair was collected from market of kalyan. Then sample of Corn Hair 1<sup>st</sup> wash with distilled water to remove water soluble impurity like dust and other ingredient and pesticide. Then sample was dried in oven at 120<sup>o</sup>C to remove the water and sample shocked in 10% KOH solution for 6 Hours. After 6 Hours sample was washed with distilled water till neutral pH and again dried in oven at 120<sup>o</sup>C to remove the water. Finally sample was calcinated / pyrolysis at 600<sup>o</sup>C at inert atmosphere for 2h in CVD furnace.

Synthesized black particle i.e. CFs was collected and dipped into 1:1 HCl to remove the organic physical impurity and metal present in Corn hair after that sample was sonicated in 1:1 HCl solution for 30 minutes residue was filter through what man paper of No. 41 and dry in air. Dried sample wash with distilled water and again dried in Oven at 120<sup>o</sup>C.

## III. CHARACTERIZATIONS

### 1. FT-IR Analysis:

2 milligram of CFs was mixed with 200 mg of potassium bromide (KBr) (FTIR grade) and pressed into a pellet. The sample pellet was placed into the sample holder and FTIR spectra were recorded in FTIR spectroscopy. To validate again the nature of the synthesized CFs and their purity Fourier Transform Infrared spectroscopy (FTIR) (Jasco) studies were performed. Reports the typical FTIR spectrum of the pressed powder in the spectral range of 400-4000  $\text{cm}^{-1}$  are shown in figure 1.

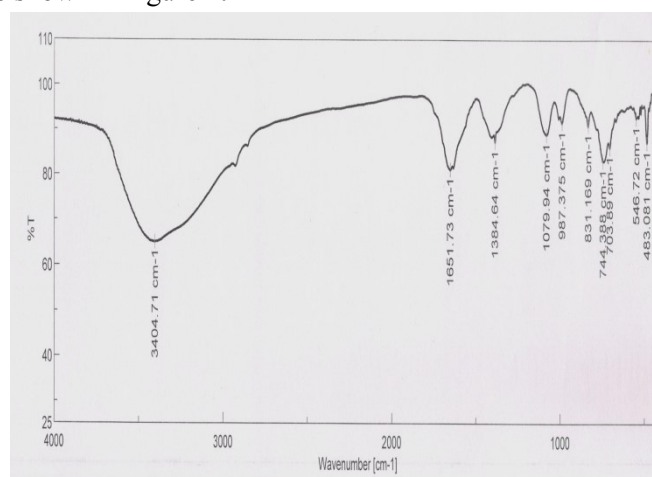


Figure 1. FT-IR Spectra of CFs

### 2. XRD Analysis:

X-ray diffraction (XRD) analysis (MiniFlex) with Cu-K $\alpha$  radiation ( $k = 1.54178 \text{ \AA}$ ) with 40 kV, 15 mA and Scan speed of Duration time 04.00 deg./minutes was used to examine the crystalline structure of the products. Fig.2 XRD patterns of prepared CFs powders.

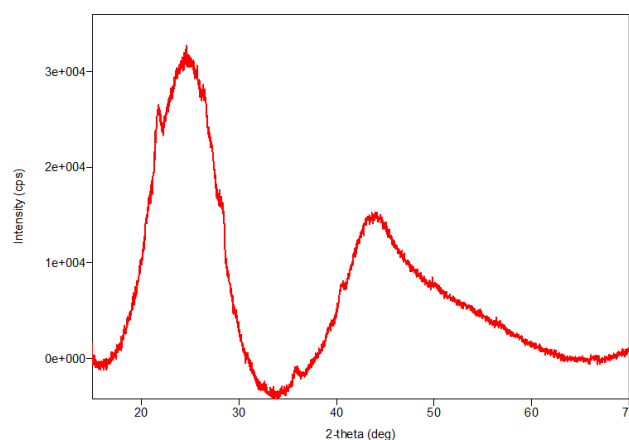
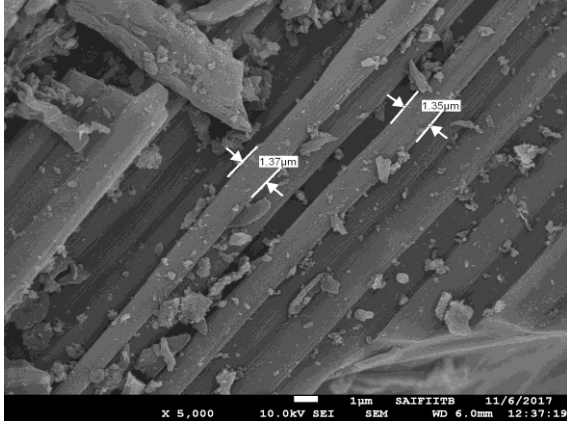


Figure 2. XRD Spectra of CFs

### 3. SEM Analysis :

Fig. 3 shows the SEM image of CFs. The SEM image was taken at X 25,000 magnification. These

pictures confirm the formation of CFs having diameter of 1-2  $\mu\text{m}$ .



**Figure 3.** SEM image of CFs

#### 4. Surface area analyser:

Sample exposed to Nitrogen gas at liquid Nitrogen temperature adsorbs Nitrogen and forms a single molecular layer of Nitrogen on the surface of the powder. Surface area can be calculated by measuring the volume of Nitrogen adsorbed using a modified single point BET equation based on theory by Brunauer, Emmet and Teller and using formula:

$$\text{Surface Area} = \frac{4.38 \times 273 \times 1 - \frac{P}{P_0}}{273 + \text{Room Temp.}} \times \frac{\text{Desorption Count}}{\text{Injection Count}} \times \frac{\text{Injection Volume}}{\text{Sample Weight}}$$

Sample is first regenerated to remove the adsorbed gases & moisture from the surface. Mixture of Helium gas (70%) and Nitrogen gas (30%) is passed over the sample in the tube. Sample is then dipped in liquid Nitrogen. Sample powder adsorbs Nitrogen on the surface at liquid Nitrogen temperature. After confirming that adsorption is over, sample tube is dipped in the water. This leads to desorption of adsorbed Nitrogen from sample, which is quantitatively determined using a Thermal Conductivity Detector coupled with an in-built Electronic Integrator and surface area was found to be  $48.69 \text{ m}^2\text{gm}^{-1}$ .

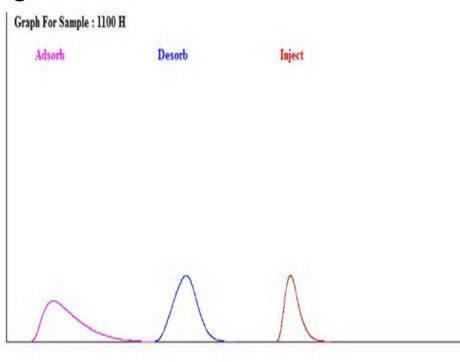


**Figure 4.** adsorption and desorption graph of CFs

#### IV. RESULTS AND DISCUSSION

Several approaches have been employed to obtain a uniform size synthesis of CFs Such as chemical and thermal methods. The development of easy, reliable and eco-friendly methods helps to increase interest in the synthesis. In this work CFs was synthesized using

corn hair at  $600^\circ\text{C}$  in argon atmosphere. FT-IR analysis show that synthesized CFs have C-C and C=C stretching which was indicated by peak at  $1651$  and  $1384 \text{ cm}^{-1}$ ,  $703, 831, 987 \text{ cm}^{-1}$  also indicate the C-C binding stretching in finger print region and peak at  $3404 \text{ cm}^{-1}$  indicate that presence of amine ( $\text{NH}_2$ ) group on the smooth surface of CFs. In XRD Spectra peaks at  $25.6^\circ$  belong to carbon crystallographic structure of the carbon fibers.

SEM analysis show that The average diameters of the CFs were measured and found to be approximately in between  $1-2 \mu\text{m}$  having smooth surface on fibre was observed.

#### V. CONCLUSION

In conclusion, Carbon fibers were prepared From organic waste precursor i.e. Corn hair by optimizing the temperature of pyrolysis to carbonisation of organic content at inert atmosphere to obtain uniform size of CFs. The average diameters of the CFs were measured and found to be approximately in between  $1-2 \mu\text{m}$ . it also show that matrix residue of the surface of CFs was completely removed, and a smooth fiber surface was observed. Synthesised CFs has high-temperature tolerance and low thermal expansion because of that it can be used in athletics, automotive, construction industries.

## VI. REFERENCES

- [1] Vilas R. Khairnar, Sandesh V. Jaybhaye and Maheshwar Sharon, "The capacitive performance of spring like carbon nanotubes for electric double layer capacitor", in *Int. Journal of Chemistry*, Vol. 3(4), PP. (Dec. 2014) 376-380.
- [2] Vinod lohakane and Sandesh Jaybhaye, Carbon nanotubes obtained from plant based oils (*Nigela Sativa*) and its Hydrogen storage capacity, *Int. Journal of Science and Research (IJSR)* 2015 pp 2440-42.
- [3] Sandesh Jaybhaye, Pandurang Satpute and Mandar Medhi, Carboxylation of Multi-walled Carbon Nanotubes by Ultra sonication, *Int. Journal of Chemistry*, Vol 3 (2) (2014) pp 224 – 228.
- [4] S. Jaybhaye, M. Sharon, L. Singh, A. Ansaldo, D. Ricci, E. Di Zitti, "Taguchi Methodology to Grow Single-Walled Carbon Nanotubes on Silicon Wafer", *Int. Journal, IEEE- Xplore Digital Library* (2009) 838-841.
- [5] Ansaldo, D. Ricci, M. Chiarolini, E. Di Zitti, S. Jaybhaye, "Improving Quality of Single-Walled Carbon Nanotube Networks", *Int. Journal, IEEE- Xplore Digital Library* (2009). 827-830.
- [6] Jidong Dong, Chuyuan Jia, Mingqiang Wang, Xiaojiao Fang, Huawei Wei, Huaquan Xie, Tong Zhang, Jinmei He, Zaixing Jiang, Yudong Huang "Improved mechanical properties of carbon fiber-reinforced epoxy composites by growing carbon black on carbon fiber surface", *j.compscitech* 06 (2017) 30666-30668.
- [7] DOI: 0.1016/j.compscitech.2017.06.002
- [8] Xiang Shu, Ryan K. Graham, Baoshan Huang , Edwin G. Burdette "Hybrid effects of carbon fibers on mechanical properties of Portland cement mortar" , *Materials and Design* 65 (2015)1222–1228.
- [9] DOI: <https://doi.org/10.1016/j.matdes.2014.10.015>
- [10] Binneng Chen , Bo Li , Yan Gao , Tung-Chai Ling , Zeyu Lu , Zongjin Li "Investigation on electrically conductive aggregates produced by incorporating carbon fiber and carbon black" , *Construction and Building Materials* 144 (2017) 106–114.
- [11] DOI:<https://doi.org/10.1016/j.conbuildmat.2017.03.168>
- [12] Wang Chuanga, Jiao Geng-shengb , Li Bing-lianga , Peng Leia , Feng Yinga , Gao Nia , Li Ke-zhi "Dispersion of carbon fibers and conductivity of carbon fiber-reinforced cement-based composites", *Ceramics International* 43 (2017) 15122–15132.
- [13] DOI:<https://doi.org/10.1016/j.ceramint.2017.08.041>
- [14] P. Xie, P. Gu, J.J. Beaudoin, "Electrical percolation phenomena in cement composites containing conductive fibres", *J. Mater. Sci.* 31 (15) (1996) 4093– 4097.
- [15] D.D.L. Chung, "Electrically conductive cement-based materials", *Adv. Cem. Res.* 16 (4) (2004) 167–176.
- [16] Yunxia Huang, Yan Wang, Zhimin Li, Zi Yang, Chunhao Shen, and Chuangchuang He. "Effect of Pore Morphology on the Dielectric Properties of Porous Carbons for Microwave Absorption Applications". *J. Phys. Chem. C* (2014), 1-18, 26027–26032
- [17] Honglin Luo , Guangyao Xiong, Zhiwei Yang , Qiuping Li , Chunying Ma , Deying , Li , Xiaobing Wu , Zheren Wang , Yizao Wan , "Facile preparation and extraordinary microwave absorption properties of carbon fibers coated with nanostructured crystalline SnO<sub>2</sub>" , *j. materresbull* 02,007 (2014).
- [18] Wei Xie , Hai-Feng Cheng, Zeng-Yong Chu , Yong-Jiang Zhou, Hai-Tao Liu, Zhao-Hui Chen. "Effect of FSS on microwave absorbing properties of hollow-porous carbon fiber composites". Elsevier Ltd 2008,12-01.
- [19] Xiaosi Qi, Yu Deng, Wei Zhong, Yi Yang, Chuan Qin, Chaktong Au, and Youwei Du "Controllable and Large-Scale Synthesis of Carbon Nanofibers, Bamboo-Like Nanotubes, and Chains of Nanospheres over Fe/SnO<sub>2</sub> and Their Microwave-Absorption Properties". *J. Phys. Chem. C*, 114 (2010), 808–814
- [20] Ting Zhanga, Daqing Huangb, Ying Yang, Feiyu Kanga, Jialin Gub, "Fe<sub>3</sub>O<sub>4</sub>/carbon composite

- nanofiber absorber with enhanced microwave absorption performance” *J. Mater. Sci. B*, 10(2012).
- [21] Lei Liu, Kechao Zhou, Pingge He, Tengfei Chen. “Synthesis, Microwave absorption properties of carbon-coil-carbon, fiber hybrid materials”, *Materials Letters* 110(2013)76–79.
- [22] Caifeng Wang, Jun Li, Shaofan Sun, Xiaoyu Li, Guangshun Wu, Yuwei Wang, Fei Xie and Yudong Huang, “Controlled growth of silver nanoparticles on carbon fibers for reinforcement of both tensile and interfacial strength”, *RSC Adv.*, 6, (2016), 14016–14026.

# Production and characterization of the biosurfactant obtained by *Bacillus subtilis*

Dhiraj B Shekhawat\*, Pradnya A. Josh, Maninder Dhaliwal, Raghunath Patil  
Birla College of Arts, Science & Commerce, Kalyan, Maharashtra, India

## ABSTRACT

Biosurfactants are surface active amphiphilic compounds with effective surface-active and biological properties applicable to several industries and processes. In this study, isolation and identification of biosurfactant producing strain were assessed. Soil samples from petrol pumps in Kalyan and Ulhasnagar area was collected and 38 strains were isolated. To confirm the ability of isolates to produce biosurfactant, emulsification assay, E<sub>24</sub> test and surface tension measurement tests were performed. *Bacillus subtilis* isolated from petrol pump station, was used to produce biosurfactant using a modified mineral salt medium with 2% diesel as sole source of carbon. The chemical composition of the biosurfactant was qualitatively analyzed by thin layer chromatography. The FT-IR analysis revealed the lipopeptide nature of the biosurfactant. The surface tension measurement using Kruss processor tensiometer showed the CMC of 140 mgL<sup>-1</sup>. The biosurfactant was found to be quite stable under varying conditions of temperature and pH.

**Keywords:** Biosurfactants, FT-IR, CMC and *Bacillus subtilis*

## I. INTRODUCTION

Biosurfactants are the biologically synthesised surface-active agents (Nitschke and Pastore, 2006). They are amphiphilic compounds consisting of hydrophilic and hydrophobic domains. The hydrophilic domain can be carbohydrate, amino acid, phosphate group or some other compounds whereas the hydrophobic domain usually is a long chain fatty acid (Lang, 2002). The majority of known biosurfactants are synthesized by microorganisms grown on water immiscible hydrocarbons, but some have been produced on water soluble substrate such as glucose, glycerol and ethanol (Abu-Ruwaida et al., 1991). Microorganisms have been reported to produce several classes of biosurfactants such as glycolipids, lipopeptides, phospholipids, neutral lipids or fatty acids and polymeric biosurfactants (Franzetti et al., 2010; Banat et al., 2010). Chemically synthesized surfactants have been used in the oil

industry to aid clean up of oil spills as well as to enhance oil recovery from oil reservoirs. These compounds are not biodegradable and can be toxic to environment. Biosurfactants have special advantage over their commercially manufactured chemical surfactants because of their lower toxicity, biodegradable nature and effectiveness at extreme temperature, pH, salinity and ease of synthesis (Ilori and Amund, 2001; Ilori et al., 2005). This study describes the screening and isolation of a potent biosurfactant producing microorganism, the biochemical characterization and emulsification ability of the biosurfactant.

## II. MATERIALS AND METHODS

### Screening of biosurfactant producing bacteria

Biosurfactant producing bacteria were isolated by successive enrichment culture technique from the petroleum contaminated soil using Minimal Salt

medium containing diesel oil (2%) as a sole source of carbon. The minimal salt media used consist of (g/L<sup>-1</sup>):MgSO<sub>4</sub>:0.2, CaCl<sub>2</sub>:0.02, KH<sub>2</sub>PO<sub>4</sub>:1, K<sub>2</sub>HPO<sub>4</sub>:1, NH<sub>4</sub>NO<sub>3</sub>:1, FeCl<sub>3</sub>.6H<sub>2</sub>O:0.05 pH adjusted to 7.0 (Patel and Desai, 1997).The isolation was done on solidified minimal salt medium where diesel oil was introduced in vapour phase transfer technique as described by Raymond et al.,(1976). Incubation was carried out at room temperature for 5 days.

**Emulsification Index (E<sub>24</sub>%)** - Emulsification index of cell free broth was determined by adding 2 ml of fuel oil to 2 ml cell free broth, mixing with a vortex for 2 min, and leaving it undisturbed for 24 h. The E<sub>24</sub> index is given as percentage of height of emulsified layer (mm) divided by total height of the liquid column (mm) (Cooper and Goldenberg, 1987).

**Identification of biosurfactant producer**-The biosurfactant producers were identified on the basis of their morphological, cultural and biochemical characteristics as described by Holt et al., (1994).

**Selection of best biosurfactant producer**- The best biosurfactant producer was selected based upon the emulsification activity, biomass and biosurfactant yield and by measuring reduction in surface tension of the culture media.

**Emulsification activity assay**- 2.0 ml cell free broth sample obtained from each of the isolate were added in a tube containing 15 ml of 0.2 M Tris buffer pH 8.0 and 0.2 ml of fuel oil. The mixture was then vortexed for 10 min, allowed to rest for 1 min. Then extinction was read at 540 nm against blank containing buffer and fuel oil (Banat et al.,1990).

**Biomass determination**-The culture media was centrifuged at 10,000 rpm for 30 min to obtain pellet. Six volume of a mixture of petroleum ether and acetone (1:3 ratio) was mixed thoroughly with the pellet and centrifuged at 3000 rpm for 20 min. This was repeated till all the unutilised oil sample was removed leaving the solvent layer clear. Such cell mass free of oil settled down even at low speed centrifugation. The upper solvent layer was removed

and cell mass was further treated with acetone. The cell mass was then washed with distilled water and dried at 60°C overnight in a preweighed crucible. The dry mass of cells was determined.

**Extraction of biosurfactant**-The pH of the cell free supernatant was adjusted to pH 2 using 6 N HCl and kept at 4°C for 24 hr. The cell free supernatant and chilled mixture of chloroform and methanol (2:1) in equal volume was added and mixed vigorously to obtain the biosurfactant within the organic layer. This layer was separated using a separating funnel and dried at 40°C for 4-5 hours to obtain dry mass. The yield as g/L was recorded (Desai and Banat, 1997).

**Surface tension**-The surface tension of the cellfree broth was measured by Kruss Processor Tensiometer K-12 (Wilhelmy plate) method as described by (Singh et al., 1989, Tuleva et al., 2005).

**Analysis of component of biosurfactant by Thin layer Chromatography**-The crude extract was separated by TLC using aluminium sheets silica gel plates with chloroform:methanol:acetic acid and water (25:15:4:2). Ninhydrin reagent was used to detect free amino groups. The lipid components were detected as brown spots after spraying the plate with chromosulphuric acid. The carbohydrate compound were detected as red spots after spraying the plates with α-naphthol in concentrated sulphuric acid.

**Fourier transform infra red spectroscopy (FT-IR)**- 2.0 mg of the biosurfactant was mechanically blended with KBr in the ratio of 1:100 and pressed to form a pellet. Infra-red absorption spectra were recorded on a FT-IR in the 4000-400 1/cm range with a 16-scan speed at a resolution 2 cm<sup>-1</sup>. KBr pellet was used as the background reference.

**CMC determination**-In this method, different concentration of biosurfactant was prepared (40 mgL<sup>-1</sup>- 200 mgL<sup>-1</sup>) in distilled water. Surface tension of these biosurfactant solutions were determined

using Kruss K-12 tensiometer and the concentration at which the surface tension reduction remains stable i.e. no further reduction in the surface tension is seen is considered as CMC. The CMC was determined by plotting the surface tension versus concentration of bisurfactant in the solution.

**Stability study-** For determining the stability of the emulsion, the biosurfactant solution and oil mixture were incubated under varying conditions of temperature from 4°C to 100°C and pH from 2.0 to 12.0 one hour and then the emulsification activity was recorded at 540 nm. The percent residual emulsification activity was recorded after 24 hr by oil emulsification assay (Banat et al., 1990) and emulsion stability was expressed in percentage.

### III. RESULT AND DISCUSSION

**Screening of biosurfactant producing bacteria-** From petrol pump soil samples of Kalyan and Ulhasnagar area 38 isolates were obtained. 29 isolates showed emulsification index ranging from 10% to 30% and 9 isolates showing emulsification index of more than 30% were selected. Isolate B17 Kalyan petrol pump gave maximum emulsification index of 40%. These 9 isolates exhibited good emulsification activity as shown in Table 1.1.

**Table 2.** Emulsification index of the isolates

Isolates	Emulsification index (E24%)
U1	30
K1	32
K2	34
K4	34
<b>B17</b>	<b>40</b>

**Table 3.** Selection of best biosurfactant producer based on emulsification activity, surface tension, biomass and biosurfactant yield

Isolates	Biomass (gL <sup>-1</sup> )	E.A(O.D-540nm)	Biosurfactant (gL <sup>-1</sup> )	Surface tension(mN/m)
U1	0.85	0.12	0.10	40.3
K1	0.81	0.16	0.06	42.0
K2	0.76	0.15	0.12	42.6
K4	1.3	0.35	0.43	39.2
B17	1.85	0.58	0.69	37.0
B3	0.92	0.18	0.25	40.8
G6	0.95	0.27	0.25	39.9

B3	36
G6	32
G4	35
B4	38

**Identification of biosurfactant producer-**The biosurfactant producers were identified on the basis of their morphological, cultural and biochemical characteristics as described by Holt et al., (1994). Among these 9 isolates 5 isolates were Gram positive and 4 were Gram negative. The gram negative isolates belonged to Pseudomonas, Serratia and Azotobacter sp. and among the gram positive isolates Bacillus sp were predominant (Table 1.2)

**Table 2.** The isolates were identified as follows-

Isolate	Name of the organism
U1	Bacillus megaterium
K1	Bacillus coagulans
K2	Serratia
K4	Bacillus polymyxa
B17	Bacillus subtilis
B3	Pseudomonas aeruginosa
G6	Bacillus licheniformis
G4	Pseudomonas sp
B4	Arthrobacter

**Selection of best biosurfactant producer-** The isolates gave a biomass yield ranging from 0.74 g/L to 1.85 g/L and the biosurfactant yield from 0.06 g/L to 0.69 g/L. All the isolates lowered the surface tension of the media from 65 mN/m to 42 mN/m and below (Table 1.3).



G4	0.74	0.17	0.12	42
B4	0.81	0.19	0.14	40.4

**Thin layer Chromatography of biosurfactant-** The biosurfactant showed purple colour spot when sprayed with ninhydrin, indicating the presence of free amino groups. The lipid components were observed as brown spots when sprayed with chromosulphuric acid.

**FT IR analysis of biosurfactant-** A broad absorbance peak around  $3433\text{ cm}^{-1}$  was observed as a result of C-H stretching vibrations and N-H stretching vibrations. Sharp absorbance peaks are observed at  $1463\text{ cm}^{-1}$ ,  $1379\text{ cm}^{-1}$ ,  $2955\text{ cm}^{-1}$  and  $2854\text{ cm}^{-1}$  indicative of aliphatic chains. These peaks reflect the presence of alkyl chains in the compound. Carbonyl groups were indicated by bands at  $1741\text{ cm}^{-1}$ ,  $1726\text{ cm}^{-1}$  (fig 1).

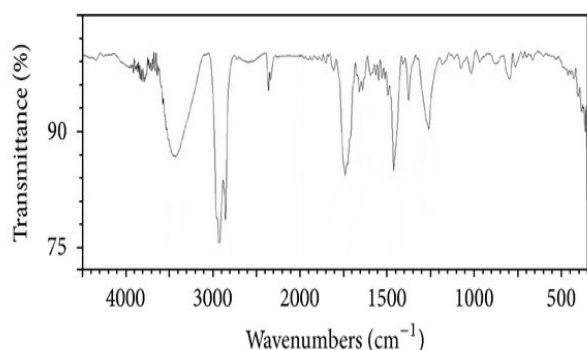


**Figure 1.** FT-IR spectrum of biosurfactant

**CMC determination-** The CMC of  $140\text{ mgL}^{-1}$  obtained with *Bacillus subtilis* B17 is very significant, as most of the literature reviewed showed that biosurfactant achieved surface tension 25 to 39 mN/m at higher CMC values. This CMC was much lower when compared with some chemical surfactant, for instance, sodium dodecyl sulphate (SDS) had a CMC value of  $2100\text{ mgL}^{-1}$  (Chen et al., 2006) (fig 2).

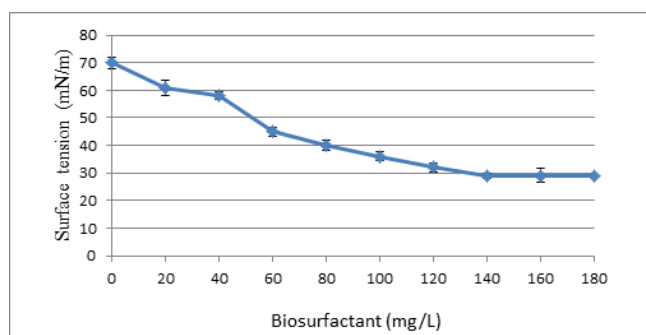


**Figure 2.** CMC of biosurfactant

**Stability studies-** Biosurfactant was found quite stable over a temperature range of  $4^{\circ}\text{C}$  to  $100^{\circ}\text{C}$ . A slight decrease in the biosurfactant activity was noticed at high temperature. However, biosurfactant was found to retain more than 60% of emulsion activity even at extreme temperatures of  $4^{\circ}\text{C}$  and  $100^{\circ}\text{C}$  (fig 3). Similarly, at the acidic pH of 2 and 4 the emulsification activity and the stability was found to be lowest. This loss of activity at pH 2.0 and pH 4.0 may be due to precipitation of the biosurfactant at low pH which hinders the emulsion formation. Increase in pH has a positive effect on emulsification activity and emulsion stability (fig 4).

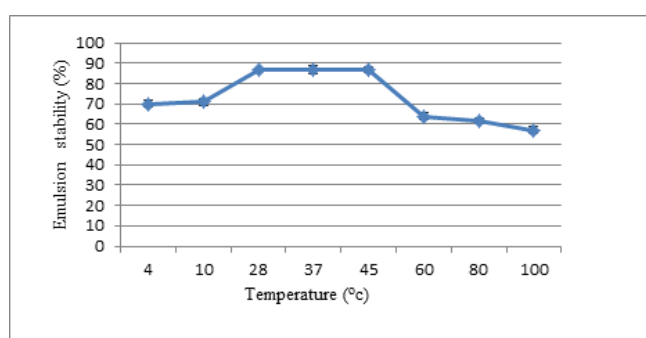


**Figure 2.** Effect of temperature on stability of emulsion

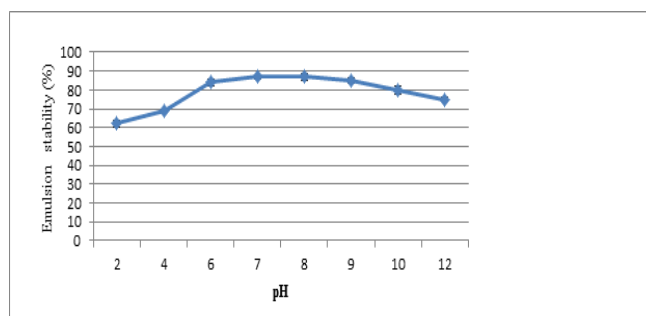


**Figure 3.** Effect of pH on stability of biosurfactant

#### IV. CONCLUSION

In the present study, biosurfactant producing organisms were enriched and isolated from petroleum contaminated sites. The potent biosurfactant producer *Bacillus subtilis* B17 was selected as it showed strong emulsification ability and low CMC. These studies suggest that the biosurfactant obtained from *Bacillus* sp. can be efficiently used in environmental remediation remediation strategies.

#### V. REFERENCES

- 1) Abu-Ruwaida, A.S, Banat, M., Haditirto, Salem, S., Kadri, A. (1991). Isolation of biosurfactant producing bacteria product characterization and evaluation. *Acta Biotech*, 11(4):315-24
- 2) Banat, I. M. (1990). Biosurfactant production and use in oil tank clean up. *World J. of Microbiol. Biotechnol*, 7:80-88
- 3) Banat, I.M., Franzetti, A., Gandolfi, I., Bestetti, G., Martinotti, M.G., Fracchia, L., Smyth, T.J. and Marchant, R. (2010). Microbial biosurfactants production, applications and future potential. *Appl. Microbiol. Biotechnol*. 87: 427–444.
- 4) Cooper, D.G. and B.G. Goldenberg (1987). Surface active agents from two bacillus species. *Appl. Environ. Microbiol.* 53:224-229
- 5) Desai, J. D. and Banat, I. M. (1997). Microbial production of surfactants and their commercial potential. *Microbiol and Mole Bio. Rev.*, 61:47-56
- 6) Franzetti, A., Tamburini, E., Banat, I.M., (2010). Application of biological surface active compounds in remediation technologies. In: Sen, R. (Ed.), *Biosurfactants: Advances in experimental medicine and biology*. Springer-Verlag, Berlin Heidelberg. 672: 121–134.
- 7) Holt, J.G., Krieg, N. R., Sneath, P.H.A., Stanley, J.T., William, S.T. (1994). *Bergey's Manual of Determinative Bacteriology*. William and Wilkins, Baltimore Cirigliano MC, 1994. P.111.
- 8) Ilori, M. O. and Amund, O. O. (2001). Production of a peptidoglycolipid bioemulsifier by *Pseudomonas aeruginosa* grown on hydrocarbon. *Z. Naturforsch*, 56C:547-552
- 9) Ilori, M.O., Amobi, C.J., Odocha, A.C. (2005). Factors affecting biosurfactant production by oil degrading *Aeromonas* sp. isolated from a tropical environment. *Chemosphere*, 61:985-992
- 10) Lang, S. (2002). Biological amphiphiles (microbial biosurfactants). *Curr. Opin. Colloid. Interface. Sc.* 7:12-20
- 11) Nitschke, M. and Pastore, G. M. (2006). Production and properties of a surfactant obtained from *Bacillus subtilis* grown on cassava waste flour. *Biores. Technol.*, 97:336-341
- 12) Patel, R.M. and Desai, A.J. (1997). Surface active properties of rhamnolipids from *Pseudomonas aeruginosa* GS3. *J. Basic. Microbiol.* 37:281-286
- 13) Raymond, R. L., Hudson, J. O. and Jamison, V. W. (1976). Oil degradation in soil. *Appl. Environ. Microbiol.*, 31:522-535
- 14) Singh, M. and Desai, J. D. (1989). Hydrocarbon emulsification by *Candida tropicalis* and *Debaromyces polymorphus*. *Ind. J. of Exp. Biol.*, 27: 224-226
- 15) Tuleva, B., Christova, N. and Jordanov, B. (2005). Naphthalene degradation and biosurfactant activity by *Bacillus cereus* 28BN. *Z Naturforsch (c)*, 60 (7-8): 577-582
- 16) Chen, J., Wang, X.J., Hu, J.D. and Tao, S. (2006). Effect of surfactants on biodegradation of PAHs by white-rot fungi. *Environment Science*, 27:154-9

# Accumulation of organophosphate estimated by Gas liquid chromatography in fresh water sponges (*S.lacustris*)

D.N. Shinde

Department of Chemistry, BNN College, Bhiwandi, Thane, Maharashtra, India

## ABSTRACT

Accumulation of the pesticides varies as per the target tissue in the victim. The amount of pesticidal residue accumulated by an organism via oral or other routes of entry. In the present study the accumulation of organophosphate (dimethoate) exposed to fresh water sponge at sub-lethal concentrations. As sponges have a canal system for incurrent and excurrent. Accumulation of dimethoate was estimated by gas liquid chromatography with standard concentration of pesticide and experimental *S.lacustris*. The GLC results showed that accumulation of dimethoate in the fresh water sponge (*S.lacustris*).

**Keywords :** *S.Lacustris*, Phylum Porifera, Organophosphate, Accumulation, GLC.

## I. INTRODUCTION

One of the prime factors for the degradation of the biosphere is a synthetic organic chemical, which includes pesticide, polychlorobiphenyls, and polyaromatic hydrocarbon. The use of pesticides in agriculture and other areas is not recent but prior to 1940s. The insecticides like lime, sulphur, nicotine, pyrethrum, kerosene and rotenone were extensively used. In the progress of time with increasing population the demand of the food has increased, as a result the use of chemicals in the agriculture sector has increased for maximum food production.

The amount of pesticidal residue accumulated by an organism via oral or other route of entry, results in increased concentration of pesticide in the specific body tissues [1]. The pesticide level can be determined by uptake or elimination, which in terms of the concept, translocation, accumulation, and behaviour of pesticide residues among the biological system [2]. Accumulation occurs whenever the

amount of uptake is larger than elimination [3]. Some reports about the concentration of organochlorine compounds in different species of fishes [4]. At least 25% of the insecticide used for agricultural and pest vector control are expected to reach water reservoirs [5].

In the present study, accumulation of organophosphate in *S.lacustris* exposed to sub-lethal concentration was studied. *Spongilla* is a group of filter-feeding organisms and considered as an excellent for bio-monitoring purpose [6]. Fresh water sponges can tolerate a minor amount of pollution [7]. Keeping the perspectives in mind, the *Spongilla lacustris* were selected as an experimental organism and the pesticide organophosphate (dimethoate) was used.

Study area—*S.lacustris* were brought from Latipada Dam, at Pimpalner, Tal, Sakri, Dist. Dhule (M.S.). Dam is located at the latitude 20°55'N and longitude at 74°5'30"E at 532 MSL.

## II. METHODS AND MATERIAL [ Page Layout ]

The test organism *S.lacustris* was brought in the laboratory for acclimatization then it was subjected to sub lethal concentration of dimethoate for thirty days. The method used for estimation of pesticide by GLC for pesticidal analysis [8]. A stock solution of dimethoate 5ppm were prepared with chloroform and used as a standard. After thirty days adoption *S.lacustris* were brought to about one gm of weight and homogenized in pestle and mortar with 10 cm<sup>3</sup> of chloroform and filtered by watmann no.1 filter paper. The pesticide residues were extracted by chloroform followed by the method [9]. The extract was evaporated about 1cm<sup>3</sup> and further analysis by gas liquid chromatography (GLC). Operating conditions for estimation as below,

GLC model--- Nucon-5700

Column-----1/8 inches,packing OV-17

Carrier-----Nitrogen@30ml/min.

Oxidant-----Oxygen@300ml/min

Fuel-----Hydrogen@30ml/min

Sample concentration-----5ppm

Injected volume-----5.00ul

Injector temp.-----260°C

Detector temp.-----260°C

Oven initial temp.-----180°C

Oven final temp.-----250°C

Detector-----FID.

## III. RESULTS AND DISCUSSION

The results estimated by GLC indicate that the accumulation of dimethoate was 87.68% than the standard concentration of dimethoate. Few reports are available to state the bio-monitoring role of sponges for heavy metals [10]. In fresh water sponges *E.fluviatilis*, *E.muelleri* and *S.lacustris* accumulates the pollutants [11]. Some reports [6] were showed that *S.lacustris* is the excellent species for monitoring chlorinated hydrocarbon pesticides. Similar studies on toxicity have shown the accumulation in the tissues of aquatic organisms. [12]

The pesticide residues are known to bio-accumulate in the lipid tissues of the fish and via food chain to the human bodies [13].

In the present study the lipid content present in the tissues of *S.lacustris* developed by secreted cells in the form of droplets. The accumulation of dimethoate in the tissues observed in the gemmules, ameobocytes, loaded vesicles etc. were disrupted to certain extent.

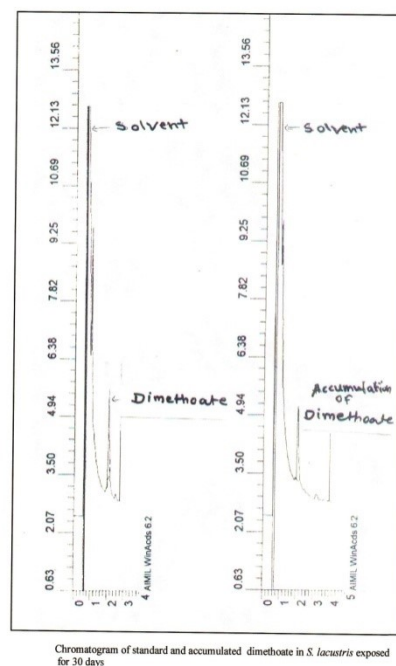


Figure 1

## IV. CONCLUSION

Pesticides are added in the aquatic environment mainly through agricultural activities affects on fresh water sponges. The accumulation of pesticides was observed in the tissues estimated by GLC technique. Preservation and conservation of sponges is important due to their environmental value. Sponges are able to tolerate wide range of pollutants. Hence a group of sponges can be considered as a pollution indicator.

## V. REFERENCES

1. Kenaga, E. E.: Factors related to bioconcentrations of pesticides *In* : Matsumura; (Ed. G. M. Bousch and T. Misato), Environmental Toxicology of pesticides. Academic Press. New York , (1972 a),193-328.
2. David B. V., C. Tamil Selvan and S. Manick Avasagam: Bioaccumulation of pesticides in the environment An overview, Differences of accumulation factors by fishes. *Chemosphere* 9, 359-364 (1978).
5. ]Rand G. M. and S. R. Petrocelli: (Ed) Fundamentals of Aquatic Toxicology. Distributed by McGraw-Hill International Bond company (1985).
6. Sarkka, J.: Mercury and chlorinated hydrocarbon in zoobenthos of Lake Paijanne, finland. *Environ. Contam. Toxicol.* 8, 161-173 (1979).
7. Robert P.W.: Fresh water Invertebrates of United states, The Ronald Press Comp.N.Y.77-97 (1953).
8. Luke, M.A., Froberg, J.E., Doose,G.M. and Masumoto, H.T: Improved multi residue Gas chromatographic determination of organophosphorus, organonitrogen and organochlorine pesticides in produce, using flame photometric and electrolytic ,conductivity. Detectors. *J.A.O.A.C.* 64 : 1187-1195 (1981).
9. Jain, H. H., S. Y. Pandey, N. P., Agnihotry and R. S. Dewan : Rapid estimation of *In*: Pesticides; Their Ecological Impact in Developing countries (Ed. G. S. Dhaliwal and Balwinder Singh), Common wealth publishers, Delhi 51 (1993).
3. Frazier, J. M.: Bioaccumulation of cadmium in marine organisms, *Environmental Health Perspectives* 28, 75-79 (1979).
4. Sugiura, K.,T. Washino, M. Hottori, E. Sato and Goto: Accumulation of organochlorine compounds in fishes. organophosphate insecticide. *Indian. J.Ent.*, 36: 145 - 148 (1974).
10. Potts, E. : Contribution towards a synopsis of the American forms of freshwater sponges with descriptions of those named by other authores and from all parts of the world, *Proc. Acad. Natur.Sci. Philadelphia* 39: 158 - 279 (1887).
11. Richelle, E., Degudene, Y., Dejonghe L, Van-de-Vyver, G.; Expermental and field studies on the effect of selected heavy metals on three Freshwater spong species : Ephydatia fluviatilis, Ephydatia muelleri and Spongilla lacustris, *Arch.hydrobiol.* 135 (2): 209 - 231 (1995).
12. Tripathi, G.: Relative toxicity of aldrin, fenvalerate, captan and diazinon to the freshwater fod fish, *Clarias batrachus. Biomed. Environ. Sci.*, 5, 33-38 (1992).
13. Tilak, K. S, K. Veeraiah, T. Anita susan and K. Yacobu: Toxicity and residue studies of fenvalerate to some selected freshwater fishes. *J Environ. Biol.* 22(3), 17-180 (2001 ).

# Studies on effect of Copper Oxide nanoparticles on Chickpea *Cicer arietinum* seed germination and root elongation

Dinesh Wanule<sup>1\*</sup>, Simran Modgekar<sup>1</sup>, Sandesh Jaybhaye<sup>2</sup> and Kantilal Nagare<sup>1</sup>

<sup>1</sup>Department of Zoology, B.K. Birla College of Arts, Science and Commerce, Kalyan, Maharashtra, India

<sup>2</sup>Department of Chemistry, B.K. Birla College of Arts, Science and Commerce, Kalyan, Maharashtra, India

## ABSTRACT

Nanotechnology is an emerging branch of science. Nanoparticles have unique physical and chemical properties and thus used in diverse applications. In present study copper oxide nanoparticles were used to determine their effect on seed germination and root elongation. 5ppm and 10ppm concentrations of CuO NP prepared in distilled water. 20 seeds were treated with 5ppm and 10ppm concentration respectively for 30 min. 10 treated seeds were transferred aseptically per sterilized petriplates containing moist filter paper and labeled respectively. Similar experiment was carried out using distilled water as control. The experiment was carried out in duplicate. The plates were kept in dark for 7 days. 5ppm, 10ppm as well as distilled water treated seeds showed 100 % germination. The highest mean root length 16.93 cm was observed in 5ppm CuO NP treated seeds followed by 13.69 cm in 10ppm CuO NP treated seeds. While in control the root length was found to be 11.93cm. The current experiment revealed that these concentrations of CuO NP does not affect the germination but enhance the root elongation mechanism.

**Keywords:** Copper Oxide Nanoparticles, *Cicer arietinum*, Seed germination .

## I. INTRODUCTION

Nanoparticles occur naturally as well as synthesized artificially having at least any one dimensions between 1-100 nm. Nanoparticles possess unique properties like high surface area to volume ratio, high reactive distinct properties [1-2]. Since nanoparticles have distinct properties are used in many industries for production of energy, transportation, pharmaceutical, antimicrobial, cosmetics and agriculture [3-5]. Nanoparticles of Gold(Au), Copper (Cu), Aluminum (Al), Silica(Si), Zinc(Zn), Zinc Oxide(ZnO), Titanium (Ti), Magnesium Oxide (MgO) have found applications in agriculture [6]. Nanoparticles are used in agriculture for enhancing crop production, protection, improvement in fertilizers and irrigation management. Copper is one

of the essential micronutrient for the proper growth of plants. Copper deficiency in plant is expressed as curled leaves, petioles bend downwards and high chlorosis with permanent turgor loss in leaves, while the higher doses of Copper can cause toxicity, growth inhibition, photosynthesis interference, oxidative stress in plants [7-9]. The purpose of this study was to analyze the effect of CuO NP (synthesized using green technology) on germination and growth of *Cicer arietinum*. The *Cicer arietinum* is the Worlds' most consume pulses since it is rich in protein. It is believed that it was reached to Mediterranean region by 4000 BC and 2000 BC in India [10]. India produced 64% of the world total of chickpeas in 2016 [11].

## II. METHODS AND MATERIAL

Seeds of Chickpeas (*Cicer arietinum*) were collected from a local farmer from Koravle village, Taluka Murbad, District Thane, Maharashtra India. CuO NP's were synthesized in laboratory of size the between range of 30-50 nm and used for the study. 5ppm and 10 ppm concentrations of Copper Oxide nanoparticles were prepared in sterilized distilled water. The seeds were transferred aseptically into these concentration solutions and rotated thoroughly and allowed to stand for 30 minutes. The seed germination and root elongation was studied using modified Top of paper method [12] The seeds were transferred aseptically in sterilized petriplates containing moist Whatman filter paper no. 1 and labelled respectively. The experiment was carried out in duplicate. Control was also maintained using seeds treated with distilled water. The plates were allowed to incubate at room temperature for 7 days. The seeds were observed daily. The results were recorded after 7 days.

## III. RESULTS AND DISCUSSION

Results of the study were depicted in table no 1 and shown in fig no. 1. In current study findings showed 100% germination in 5ppm , 10 ppm CuO NP treated seeds as well as distilled water treated seeds also. The 100 percent seeds germination may be because of seeds were disease free and well preserved and stored which helps to maintain its germination quality. The highest mean root length 16 cm.93 was observed in 5ppm CuO NP treated seeds. In 10 ppm CuO NP treated seeds showed moderate root length i.e. 13.69 cm but found more mean root length than of distilled water treated seeds. This clearly indicate that CuO NP played an important role in seed growth. Khodakoyaskaya *et. al.* 2012 reported that nanoparticles have tendency to replicate plant seed coats and enhance seed germination and growth [13]. CuO NPs possess property to enhance water imbibition process. Ajey Singh *et. al.* 2017 reported reduced trend of plumule length, radicle length of

*Vigna radiate* (L.) with increase in Nanoparticle concentrations [6]. The results of present study showed the same pattern but the root length of experimental seeds were found to be higher than root length of control seeds. This indicates that both CuO NPs concentrations were non-toxic to the seeds and root length promoting.

**Table 1.** Effect of CuO NP on *Cicer arietinum* seeds germination and root elongation

Test	DW	5ppm Cuo NPs	10ppm Cuo NPs
Mean seed germination	100%	100%	100%
Mean root elongation in cm	11.93	16.93	13.69

## IV.CONCLUSION

The current experiment revealed that 5ppm and 10ppm concentrations of CuO NP prepared in distilled water did not show any adverse effect on seeds germination. When root elongation parameter was considered, 5 ppm CuO NP treated seeds found more effective than 10 ppm CuO NP treated seeds.



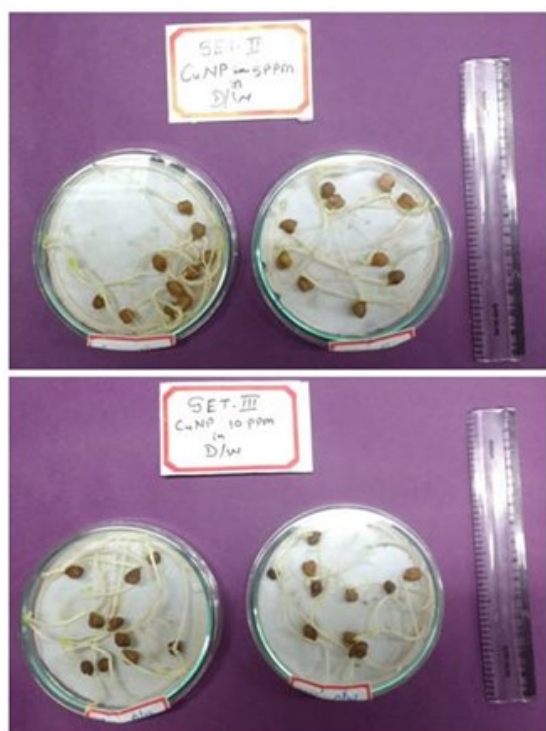


**Figure 1.** Effect of CuO NP on *Cicer arietinum* seeds germination and root elongation .

#### V. REFERENCES

G .Singhal , B. Riju, K. Kasariya, R. A. Sharma and R.P. Singh (2011) "Biosynthesis of silver nanoparticles using *Ocimum santacum*(tulsi) leaf extract and screening its antimicrobial activity". *Journal of Nanoparticles Research* 13:2981-2988

- [1] [https://www.epa.gov/sites/production/files/2014-03/documents/ffrrofactsheet\\_emergingcontaminant\\_nanomaterials\\_jan2014\\_final.pdf](https://www.epa.gov/sites/production/files/2014-03/documents/ffrrofactsheet_emergingcontaminant_nanomaterials_jan2014_final.pdf)
- [2] P. Kuppusamy, M. M. Yusoff, G. P. Maniam and N. Govindan, 2016, "Biosynthesis of metallic nanoparticles using plant derivatives and their new avenues in pharmacological applications – An updated report" *Saudi Pharmaceutical Journal* Volume 24, Issue 4, Pages 473-484
- [3] J. Hong1, J. R. Peralta-Videa1, J. L. Gardea-Torresdey 2013, "Nanomaterials in Agricultural Production: Benefits and Possible Threats?" *Sustainable Nanotechnology and the Environment: Advances and Achievements* Chapter 5, pp 73–90 DOI: 10.1021/bk-2013-1124.ch005

- [4] S. Griffin , M. I. Masood, J. N. Muhammad, S. Muhammad , P. E. Azubuikie, S. Karl-Herbert 3, M. K. Cornelia and J. Claus 2018, " Review Natural Nanoparticles: A Particular Matter Inspired by Nature" *Antioxidants* 7, 3 doi:10.3390/antiox7010003
- [5] A. Singh, N. Singh, B. Hussain Z, Singh H and Yadav V. "Synthesis and charecharization of copper Oxide nanoparticles and its impact on germination of *vigna radiata*(L.) R.Welczek", *Tropical plant research* 4 (2):246-253,2017.
- [6] Lijie Zhang and T. J. Webster , 2008 "Nanotechnology and nano materials: Promises for improved tissue regeneration", *Nano today*.2009;4 (1) : 66-80. doi:10.1016..j.nantod.2008.10.014
- [7] Z. Yruela.(2005), "Copper in plants", *Brazilian journal of plant physiology* 17(1)145-156.
- [8] A. Manceau, K. L. Nagy, M. A. Marcus, M. Lanson, N. Geoffroy, T. Jacquet and T. Kirpichtchikova 2008 " Formation of metallic copper nanoparticles at the soil-root interface", *Brazilian Journal of Plant Physiology*, 17(1) 1;42(5):1766-72. <http://dx.doi.org/10.1590/S1677-04202005000100012>
- [9] [eol.org/pages/685208/overview](http://eol.org/pages/685208/overview) Accessed on 27-02-2018
- [10] [croppgenebank.sgrp.cgiar.org](http://croppgenebank.sgrp.cgiar.org) Accessed on 27-02-2018
- [11] M. V. Khadakovskaya, K. de Silva, A.S. Biris, G. Denvishi and H .Villagarcia. 2012, "Carbon nano tubes induce growth enhancement of tobacco" *Cely. A C S Nanoletters* 6(3)2128-2135
- [12] V. Kathiravan, S. Ravi, S.A. Kumar, S. Velmurugan, K. Elumalai. and C.P. Khativvada , 2015, "Green synthesis of silver nanoparticles. Using croton sparciflorces morong leaf extract and their antibacterial and antifungal activities", *Spectrochimica Acts Part A:Molecular and Biomolecular spectroscopy* 139.200-205.



# Analysis of oxidative rancidity of different oil samples collected from Kalyan Taluka

Kantilal Nagare\*, SoniYadav, Manasi Dhumal, Vina Yashwantrao, Manali Kolkur, Khushboo Singh, Rachna Mishra, Dinesh Wanule

Department of Zoology, B.K. Birla College of Arts, Science & Commerce, Kalyan, Maharashtra, India

## ABSTRACT

Rancidity is the process which causes a substance to have unpleasant smell or taste. It is a biochemical reaction between fats and oxygen which causes oxidation of fats turning the substance rancid. There are three types of rancidity namely oxidative, ketonic, and hydrolytic rancidity. Consuming rancid substances may be slightly toxic and the harmful free radicals may cause cellular damage and digestive distress. In this analysis 30 samples were collected from different stores of KalyanTaluka and studied for oxidative rancidity using method prescribed by International Fragrance Association IFRA. The result showed oxidative rancidity values for 30 oil samples were between 0.11 to 1.66 mEq/Kg range which is considered under the lower oxidative rancidity range i.e.<10mEq/Kg. Mustard oil showed highest mean peroxide value i.e. 1.028 mEq/Kg followed by sunflower oil with 0.636 mEq/Kg. where as palm oil and Castor oil showed least peroxide values which was 0.13 mEq/ Kg. This study concluded that all oil samples collected from KalyanTaluka were less rancid and within permissible limit.

**Keywords:**Rancidity, oil, toxic, oxidation, fats

## I. INTRODUCTION

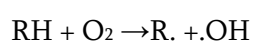
The term “lipid” has been frequently used as any of a group of organic compounds that are insoluble in water but soluble in organic solvents [1] Lipid is known as the collective name for fats, oils, waxes and fat-like molecules (such as steroids) found in the body [2]. It is found in the tissues of plants and animals and is broadly classified as: a) fats, b) phospholipids, c) sphingomyelins, d) waxes, and e) sterols. [3] Lipids are versatile biomolecules in living organisms performing various important functions like structural - element of biological membrane, hydrophobic anchor for proteins, “chaperones” to assist membrane folding ; chemical – cofactor for enzymes, electron carriers, light absorbing pigment; physical – amphipathic ,

hydrophobic barrier; chemical messenger – hormones and steroids[4],[5] . It also plays an important role in transport of biomolecules and delivering drugs and toxins across the biological membrane[6-8].Kauzelet. al. reported GlycosphingolipidGSLs Receptors from human colon epithelial cell lines Caco-2 and HCT-8 and ,determined the Shiga toxins (released by Stx-producing Escherichia coli) mediated cellular damage of Caco-2 and HCT-8 [9]. It is also an energy rich biomolecule. As per ICMR guidelines *Fats* are a concentrated source of energy providing 9 *Kcal/g*. [10]According to the Report of the Expert Group of the Indian Council of Medical Research recommend dietary allowances (RDA) of fat for Indian is between 15-30 %E [11].

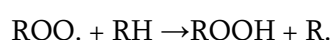
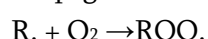
Report of Commodity Profile of Edible Oil for October – 2017 mentioned that production of edible oils in 2016-17 is 10.97 MT which is more than the actual production last year in 2015 -16 (i.e. 9.18 MT) while total import of edible oil is 12.63 MT [12] The global vegetable oil production for 2016/17 was 185.75 million metric tons [13].

Oils or fats are an important part of the diet of people across the world hence its quality is an important parameter and need to assess regularly. Factor which may affect the quality of oils or fats are impurities, oxidation during processing and storage via autoxidation and photosensitized oxidation, contamination with various microorganism, adulteration etc. [14-15] The oil may spoil because of rancidity. Rancidity is the process which causes a substance to have unpleasant smell or taste. The oxidation is responsible for decrease in nutritional and sensory quality of lipids like vegetable oils, animal fats, or even meat product etc. [16]. The degradation and reduction in shelf life of lipid are subjected to auto-oxidation, insufficient or improper storage [17]. There are three types of rancidity namely oxidative, ketonic, and hydrolytic rancidity. Oxidative rancidity involves oxygen attack of glycerides and subdued by careful choice and maintenance of oil [18]. When the unsaturated fats and oils breakdown it is because of their chemical structure and the reaction which takes place is called free radical chain reaction that abstracts the hydrogen from the fatty acid chain which is followed by reaction with oxygen causing rearrangements and cleavages and the end product being rancid oil or fat [18].

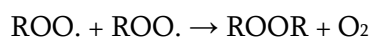
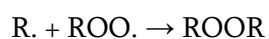
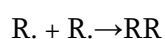
#### Initiation



Propagation



Termination



There are many chemical and physical methods that have been developed to determine the oxidative change in oils and fats [19]. The two most popular methods of indicating the quality of fats and oils are peroxide and thiobarbituric (TBA) value determination. The peroxide value of <2meq/kg considered to be low for fats and oils [20]. In India packed and unpacked oils and fats are sold in markets with predominance of sale of unpacked oils among the people below poverty line. Unpacked oils and fats may undergo rapid oxidation and the way it is handled, stored and hygienic practises also a matter of concern in many part of India.

The present study was carried out to check the peroxide rancidity of various edible and non-edible oils of Kalyan Taluka as it has a combination (loose and packed) of buyers for oils or fats.

## II. METHODS AND MATERIAL

30 packed and loose samples of fats and oils were collected randomly from various shops of Kalyan Taluka. Oxidative rancidity of fats and oils was determined as per the analytical modified method prescribed by International Fragrance Association (IFRA)[21]. 1g of sample oil or fat was taken into a clean dry 100ml beaker. To this sample 1g of powdered potassium iodide and 20 ml solvent mixture (2Glacial acetic acid: 1chloroform) was added. Beaker was placed in boiling water bath and allowed it to boil vigorously for 30 sec. The content was transferred quickly to a conical flask containing 20ml of 5%KI solution. 2-3 drops of starch indicator was added to the flask and titrated against N/500 sodium thiosulphate till blue colour disappears. The experiment was carried out in triplicate and mean reading was recorded.

### III. RESULTS AND DISCUSSION

The results for the mean peroxide value of various oils and fats was showed in table no. 1. Mustard oil showed highest mean peroxide value i.e. 1.028 mEq/Kg followed by sunflower oil with 0.636 mEq/Kg. where as palm oil and Castor oil showed least peroxide values which was 0.13 mEq/ Kg. The peroxide values for non-edible hair oil was 0.885mEq/Kg which was also high. This experiment showed oxidative rancidity values for 30 oil samples were between 0.11 to 1.66 mEq/Kg. The mean peroxide value for all 30 samples was 0.426 mEq/Kg. The reason behind highest peroxide value for mustard oil because it was stored for longer time and less consumption since it is not used frequently in daily food preparation. The palm oil showed less rancidity because it is preferably used among poor community in this area and hence shelf storage of palm oil is shorter in as compared to mustard oil.

**Table 1.** Showing results for peroxide value of various oils/fats samples

Name of oil/ fat	Number of samples	Mean Peroxide Value mEq/Kg
Mustard	10	1.028
Sunflower	5	0.636
Soybean	4	0.475
Peanut	2	0.385
Ayurvedic hair oil	2	0.885
Almond	1	0.13
Castor	1	0.13
Coconut	1	0.22
Ghee	1	0.44
Palm	1	0.13
Sesame	1	0.22
Mixed oil	1	0.44
Total oil samples	30	Mean peroxide value =0.426

Figure showing results for peroxide value of various oils/fats samples

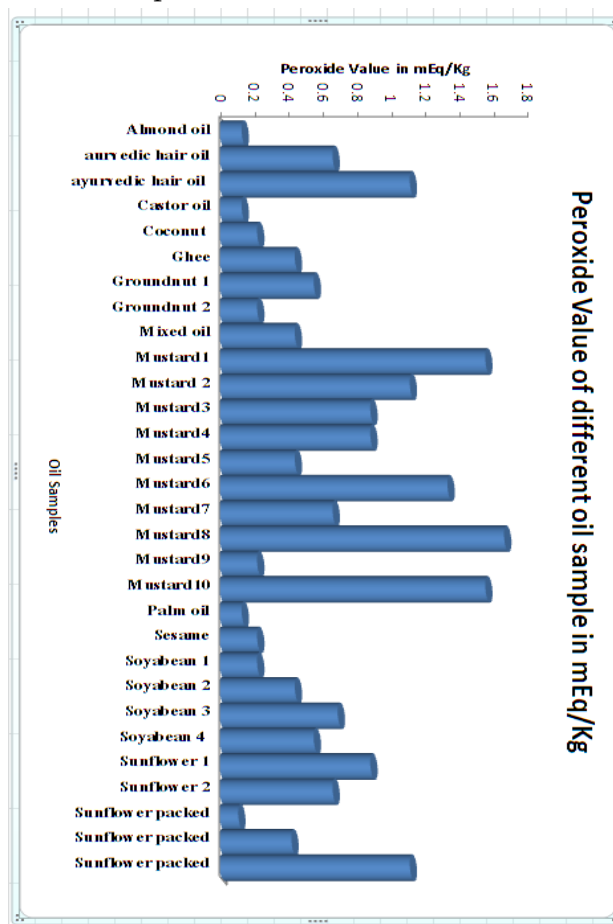


**Figure 1**

Rancid oil creates harmful free radicals in body which are associated with diabetes, Alzheimer's disease, Atherosclerosis and obesity. These free radicals are known to cause cellular damage. The rancidity of oil or fat reduces taste and odour, along with increased toxic levels of aldehydes, epoxides and hydroperoxides in body [22]. According to Dr. Andrew Weil rancidity can also cause damage to DNA, accelerate aging, promoting tissue degradation, and foster cancer development [23].

### IV. CONCLUSION

In this study all samples were found to be rancid as it has some peroxide value. The peroxide values for all samples remain in low range of peroxide value i.e. <10 mEq/ Kg. The study strongly recommends further

investigations on long term effect of use of less rancid oils on human health.

## V. ACKNOWLEDGEMENT

Authors are thankful to the DBT, Ministry of Science and Technology, Govt. of India for providing funds under Star Status. The authors also thankful to the Dr. Naresh Chandra, Principal, B.K. Birla College of Arts, Science and Commerce, Kalyan for providing laboratory and library facilities.

## VI. REFERENCES

1. Eoin Fahy, Dawn Cotter, Manish Sud, and Shankar Subramaniam (2014) "Lipid classification, structures and tools" *Biochim Biophys Acta* 1811(11):637–647 doi:10.1016/j.bbaliip.2011.06.009.
2. <http://www.rsc.org/Education/Teachers/Resources/cfb/lipids.htm> accessed on 20-03-2018
3. <http://www.fao.org/docrep/x5738e/x5738e05.htm> accessed on 20-03-2018.
4. B. Alberts, A. Johnson, J. Lewis, M. Raff, K. Roberts, P. Walter, 2002 "Molecular Biology of The Cell" 4 edition, CBS Publishers & Distributors, PP 1616
5. D. L. Nelson and M. M. Cox, 2006 "Principles of Biochemistry" 4th edition, W.H. Freeman and Company, New York, pp 1216
6. C.W. Pouton. 2006 Formulation of poorly water – soluble drugs for oral administration: physicochemical and physiological issues and the lipid formulation classification system. *Eur J Pharm Sci.*, 29, 278–287.
7. N. Tejeswari, H. Chowdary.V, N. Hyndavi, T. Jyotsna Y. Gowri Y. Prasanna Raju 2014 "Lipid based drug delivery system for enhancing oral bioavailability – a contemporary review" *Journal of Global Trends in Pharmaceutical Sciences*, 5(4)- 2074–2082
8. H. Shrestha, R. Bala, and S. Arora, 2014 "Lipid-Based Drug Delivery Systems", *Journal of Pharmaceutics* Volume 2014 <http://dx.doi.org/10.1155/2014/801820>
9. I. U. Kouzel, G. Pohlentz, J. S. Schmitz, D. Steil, H. Humpf, H. Karch and J. Müthing 2017 "Shiga Toxin Glycosphingolipid Receptors in Human Caco-2 and HCT-8 Colon Epithelial Cell Lines", *Toxins* 2017, 9, 338; doi:10.3390/toxins9110338
10. <http://ninindia.org/DietaryGuidelinesforNINwebsite.pdf>
11. Indian Council of Medical Research.
12. Nutrient requirements and recommended dietary allowances for Indians. Report of the Expert Group of the Indian Council of Medical Research. Hyderabad: National Institute of Nutrition; 2010
13. <http://agricoop.gov.in/sites/default/files/Edible%20oil%20Profile%2016-10-2017.pdf>
14. <https://www.statista.com/statistics/263978/global-vegetable-oil-production-since-2000-2001/>
15. Eunok Choe and David B. Min 2006, "Comprehensive Food Science and Food Safety", *Comprehensive Reviews In Food Science And Food Safety* Vol. 5, pp 169-186 doi/pdf/10.1111/j.1541-4337.2006.00009.x
16. [http://www.ifrj.upm.edu.my/19%20\(01\)%202011/\(36\)IFRJ-2011-142%20Sheila.pdf](http://www.ifrj.upm.edu.my/19%20(01)%202011/(36)IFRJ-2011-142%20Sheila.pdf)
17. Hradkova I., Merkl R., Smidrkal J., Kyselkaj., Filip V. (2013). Anti oxidant effect of mono and dihydroxy phenol in sunflower oils with different level of naturally present tocopherol. *European journal of lipid science and technology*, 115; 747-755.
18. Milanez K.D.T.M., Pontez M.J.C (2014); Classification of edible vegetable oil using digital image and pattern recognized techniques. *Microchemical Journal* 113:10-16.
19. [www.sserc.org.uk](http://www.sserc.org.uk)
20. Gray J.I. (1978) Measurement of lipid oxidation: A review *J. Am. oil chemist's Soc.*, 55:539-546.
21. A. Kumar and B.S. Bector (1985). A comparative study on the determination of oxidative rancidity in ghee by different methods. *Arian j. Dairy Res.*, 4(1):23-28. [www.ifra.org](http://www.ifra.org)
22. S.G. Morris (1954). Recent studies on the mechanism of fat oxidation in its relation to rancidity. *Journal of Agricultural and Food Chemistry.*, 126-132
23. [www.australianolives.com.au](http://www.australianolives.com.au)

# Characterization and Comparative Study of Fly ash from Various Sources for its Sustainable Utilization

Gauravi Patil<sup>1</sup>, Ajitha Rani R<sup>\*2</sup>

<sup>1,\*2</sup>Guru Nanak Institute for Research and Development, G.N.Khalsa college, Mumbai, Maharashtra, India

## ABSTRACT

Fly ash is a waste product generated from various sources in very large quantities around the globe. Effective utilization of fly ash which not only reduces disposal problems but also leads to sustainable development. In this study, characterization of five different fly ash samples was performed using Brunauer–Emmett–Teller (BET), X-Ray Fluorescence (XRF), Scanning Electron Microscopy (SEM), Fourier Transform Infrared Spectroscopy (FTIR) and Thermo-gravimetric Analysis (TGA) techniques. The presence of SiO<sub>2</sub>, Al<sub>2</sub>O<sub>3</sub> and CaO as the major constituents and irregular surfaces of fly ash support adsorption process. The comparative study of fly ash samples showed various characteristics depending on the source of the sample and environmental conditions. Sample collected from sugar factory was found to have comparatively more surface area and good adsorption property. Hence it can further be utilized for the pre-clean up treatment of samples having diverse nature.

**Keywords:** Fly ash, Sustainable development, Characterization, Adsorption

## I. INTRODUCTION

Coal is the major source of energy in India and nearly hundred million metric tons of fly ash is generated annually by burning of coal from factories and several thermal power plants. Hence, the disposal of such a huge quantity of fly ash is the major environmental concern. Ash produced from such factories and thermal power plants is dumped in landfills and ash ponds. Due to the shortage of landfill sites, increasing costs of the land and strict environmental regulations, the disposal of fly ash has become a major issue. This also creates many environmental hazards if not managed well and causes soil pollution and ground water pollution [1]. In the recent few years, many studies have investigated effective ways to utilize fly ash for valuable applications such as manufacturing of bricks and building blocks, sintered aggregates, pozzolana cement, concrete, filler material for reclamation of low lying waste lands, filling of mines, improvement

of foundation soils, asphalt concrete, as a stabilizer of sub-grade and sub-bases in pavement construction and zeolite synthesis for waste water treatment [2,3]. Fly ash has potential use in waste water treatment as it fulfils the physical properties of adsorption like porosity, surface area and particle size distribution. The presence of major chemical components like silica, alumina, calcium oxide, magnesium oxide and carbon also contribute towards its use as a good adsorbent [4]. Now a days sustainable development and natural resources preservation have gained significant importance. Hence, utilization of fly ash not only alleviates the disposal problem but also converts a waste material into a marketable commodity [5,6]. Characterization of fly ash in terms of composition and surface chemistry is of fundamental importance in the development of various applications of fly ash related to its adsorption property [7]. A comparative analysis of characteristics of fly ash collected from different sources could generate more information

regarding its utilization in areas other than its regular applications. This paper describes a comprehensive study of five different samples of fly ash, with the intention of elucidating their chemical and physical properties as an incentive to their sustainable utilization of adsorption property.

## II. METHODS AND MATERIAL

### A. Fly ash collection and adsorbent preparation:

1) Samples:

1. Sugar Factory Sample 1 (SF1)
2. Sugar Factory Sample 2 (SF2)
3. Thermal Power Plant (TPP)
4. Wood Ash (WA)
5. Foundry (FOU)

All the fly ash samples were sieved through ASTM 45 mesh, treated with distilled water to remove all adhering dust particles and organic matter, dried in an oven at 110°C and were stored in labelled polyethylene terephthalate (PET) bottles at room temperature.

### B. Characterization of Fly ash:

Proximate analysis which includes pH test (DBK Digital pH meter), specific gravity (Using Pycnometer), Bulk density, Moisture content, Loss on Ignition (LOI) were performed.

In order to characterize and compare the utility of the fly ash samples they were subjected to Scanning Electron Microscopy (SEM) (FEI QUANTA 200), to study the morphological features and characteristics, Brunauer–Emmett–Teller (BET) (Smart Sorb 92/93), for specific surface area calculations, X-Ray Fluorescence (XRF) (Shimadzu, EDX 7000), for knowing the composition, Fourier Transform Infrared Spectroscopy (FTIR) (Shimadzu IRAffinity-1), for functional group study and Thermo-gravimetric Analysis (TGA) (METTLER STAR<sup>0</sup>SW 12.10) to check the thermal stability of the samples.

### C. Batch adsorption study:

To analyse adsorption property and effectiveness of fly ash, a representative batch adsorption study was performed by considering Indigo carmine dye (supplied by Molychem) as an adsorbate. The parameters such as dye concentration, amount of adsorbent, pH, temperature and contact time, were optimized by varying all the conditions within a defined range using the One-Factor-At-A-Time approach. Known amount of adsorbents with 25 cm<sup>3</sup> of known concentration of dye solution was taken in 50 cm<sup>3</sup> of Erlenmeyer flasks. These flasks were agitated in orbital shaker. (Pooja lab equipments orbital shaker cum incubator OSI-200) The pH of the solution was adjusted by 0.1 N NaOH or HCl. Once the equilibrium was established, supernatant liquid was filtered off using Whatman filter paper no. 41 and the filtrates were analyzed for the residual (unadsorbed) dye, spectrophotometrically. (Shimadzu UV-1650 PC) Calibration curve was plotted of absorbance Vs. concentration of standard dye solutions.

The amount of dye adsorbed at time t,  $q_e$  (mg/g), was obtained by calculating the difference between the initial and the final dye concentration as shown in equation 1:

$$q_e = (C_0 - C_e) \times V / W \quad (1)$$

Where  $q_e$  is the amount of dye adsorbed (mg/g) and  $C_0$  is the initial dye concentration (mg/L), while  $C_e$  is the concentration of dye in solution at equilibrium (mg/L),  $V$  is the volume (L), and  $W$  is the weight of adsorbent (g).

The percentage removal of the dye was computed using the following equation

$$\text{Percentage of removal (\%)} = (C_0 - C_e) \times 100 / C_0 \quad (2)$$

Where  $C_0$  and  $C_e$  are the initial and equilibrium concentration of dye (mg/L) in solution [8].

### III. RESULTS AND DISCUSSION

**A. Proximate analysis:** The results of proximate analysis are mentioned in Table 1. The specific surface area and LOI of SF1 was high when compared with the other samples. The presence of unburned carbon in fly ash changes its color to black and appears to be responsible for the adsorption process [9]. The specific gravity values for fly ash range between 1.70 and 2.43. In general, the bulk density, pH and moisture content values recorded did not show significant variations.

**Table 1.** Proximate analysis of Fly ash samples

Samples	SF1	SF2	TPP	WA	FOU
Color	Tan	Grey	Grey	Grey	Brown
Bulk density ( $\text{gcm}^{-3}$ )	1.224	1.213	1.308	1.021	1.332
Specific gravity ( $\text{gcm}^{-3}$ )	1.804	2.285	1.706	2.290	2.430
Moisture content (%)	0.027	0.004	0.001	0.009	0.004
pH	8.6	9.2	7.5	10.9	8.6
LOI (%)	1.039	0.231	0.079	1.199	0.466
BET ( $\text{m}^2\text{g}^{-1}$ )	51.96	10.94	2.04	29.15	2.77

**B. Scanning Electron Microscopy (SEM):** In the present study, majority of particles were found to be of irregularly shaped. The surface tends to be more rough and uneven, which is favours/beneficial for adsorption (Fig 1) [10].

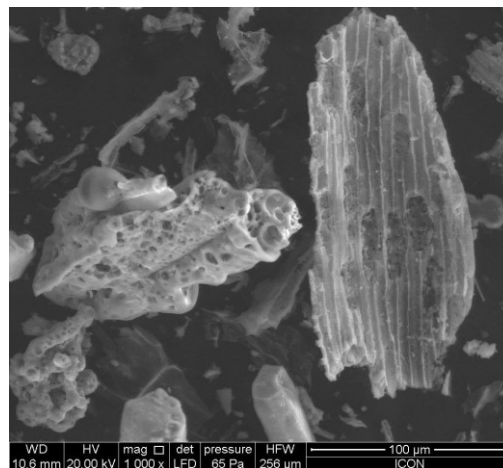


**Figure 1.** Representative SEM image.

**C. X-Ray Fluorescence (XRF):** The details of the chemical constituents in the samples determined by XRF are provided in Table 2. It shows the presence of major constituents as  $\text{SiO}_2$ ,  $\text{Al}_2\text{O}_3$ ,  $\text{Fe}_2\text{O}_3$ ,  $\text{MgO}$ ,  $\text{CaO}$  and  $\text{K}_2\text{O}$ . Similar constituents of fly ash were obtained by others [4,8].

**Table 2.** XRF Analysis

Analyte	SF1(%)	SF2(%)	TPP(%)	WA(%)	FOU(%)
$\text{SiO}_2$	75.821	81.518	61.230	23.805	54.892
$\text{Al}_2\text{O}_3$	0.538	0.578	26.088	1.500	19.031
$\text{MgO}$	2.399	3.207	0.711	7.434	2.659
$\text{SO}_3$	2.030	0.222	0.088	1.723	4.237
$\text{CaO}$	4.829	3.867	1.412	28.262	6.272
$\text{Fe}_2\text{O}_3$	1.734	1.172	6.553	2.852	7.982
$\text{TiO}_2$	0.259	0.163	2.113	0.404	1.923
$\text{K}_2\text{O}$	6.766	6.162	1.280	25.175	1.172
$\text{CuO}$	0.035	0.012	----	0.046	0.787
$\text{ZnO}$	0.017	0.026	0.010	0.069	0.348
$\text{MnO}$	0.080	0.076	0.076	0.139	0.176
$\text{PbO}$	----	----	----	----	0.111
$\text{V}_2\text{O}_5$	0.015	----	0.069	----	0.096
$\text{ZrO}_2$	0.003	0.002	0.065	----	0.066
$\text{SnO}_2$	----	----	----	----	0.058
$\text{Cr}_2\text{O}_3$	0.012	0.009	0.024	0.297	0.056

SrO	0.026	0.021	0.037	0.080	0.056
P <sub>2</sub> O <sub>5</sub>	2.258	2.963	0.239	3.663	0.051
NiO	----	----	----	----	0.026
NbO	----	----	0.004	----	----
Cl	3.181	----	----	4.552	----

**D. Fourier Transform Infrared Spectroscopy (FTIR):** The FTIR technique is an important tool to identify some characteristic functional groups. By comparing the observed frequencies with available literature, following interpretation could be drawn. A strong peak in the region 1200-900 cm<sup>-1</sup> is typical of the glassy phase in fly ash which is the main provider of Si and Al sources. This vibration band in this region varies with different Si to Al ratios and Ca content. The presence of Si-O-Si stretching vibration in this region was observed in all the samples. The peaks between 794-777 cm<sup>-1</sup> in SF1, SF2 and TPP samples could be assigned to the presence of quartz with Si-O symmetrical stretching vibrations. The peaks in WA sample at around 711 cm<sup>-1</sup> and 873 cm<sup>-1</sup> could be assigned to carbonate group (C-O bending) of calcite. The midinfrared region (1500-1400 cm<sup>-1</sup>) of the spectra of WA sample is dominated by the vibrational modes of carbonate ions (C-O stretching) (Figure 2) [11,12].

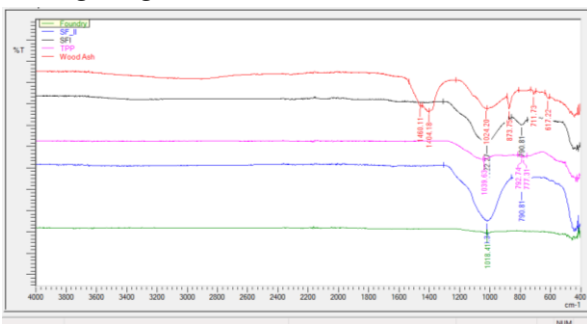


Figure 2. FTIR Spectra

**E. Thermogravimetric Analysis (TGA):** The initial loss in all the samples is related to the loss of adsorbed moisture. The weight loss between 550°C to 650°C in WA and FOU samples could be due to the thermal decomposition of Acetate.

There is a presence of broad peak between 750°C to 950°C in the WA sample and that could be of CaCO<sub>3</sub> [13]. Rest all other samples did not show any major loss (Figure 3).

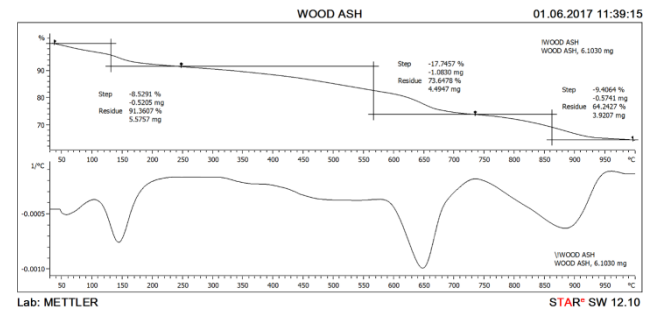


Figure 3. Representative TGA

**F. Sorption study:**

1) Effect of contact time:

Various contact times ranging from 20 to 60 minutes were considered to study the effect of contact time. The amount of dye adsorbed on to the sample was calculated at each time interval and it was found that as the contact time increases the amount of dye adsorbed increased up to 30 minutes. The optimal contact time to attain equilibrium was experimentally found to be 30 minutes. Beyond that, saturation of active sites was observed which do not allow further adsorption (Figure 4) [8].

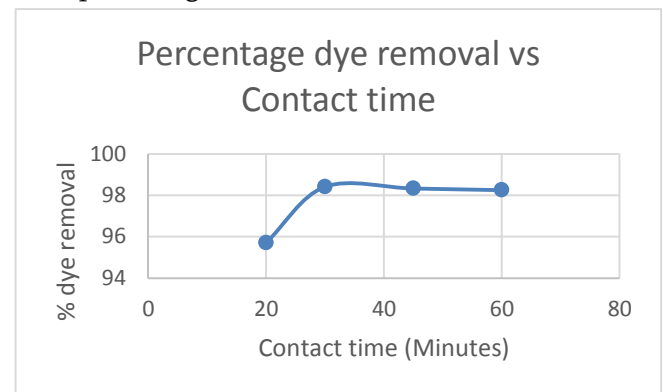
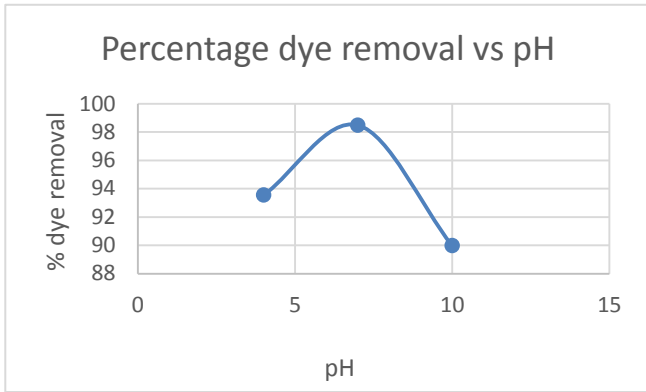


Figure 4. Effect of contact time

2) Effect of pH:

A range of 3.0 to 10.0 was selected for the optimization of pH and it was adjusted using 0.1 N HCl or 0.1N NaOH. The dye removal efficiency was found to be maximum at pH 7 (Fig 5) [14].





**Figure 5.** Effect of pH

**3) Effect of adsorbent dosage:**

Adsorbent dose is the important parameter in the adsorption studies which determines the capacity of an adsorbent for a given initial concentration of the adsorbate [10]. To investigate the effect of mass of adsorbent on the adsorption of dye, a series of different adsorbent dosage ranging from 0.2 to 2.5g for 25mL was taken. An increase in the percentage removal efficiency up to 1.0g for 25mL of dye dosage is observed, beyond which it attains saturation/ shows less efficient removal of dye (Figure 6).

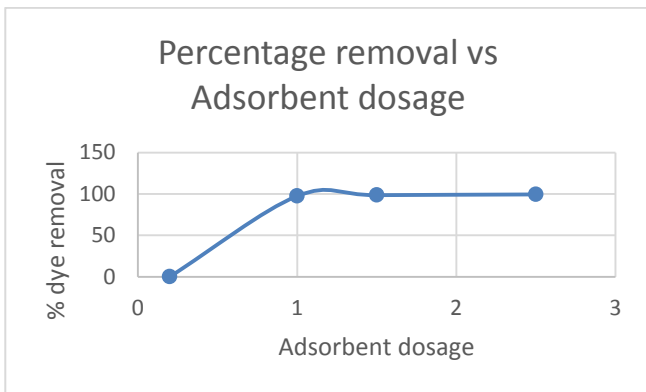


**Figure 6.** Effect of Adsorbent dosage

**4) Effect of concentration of dye:**

Concentrations ranging from 50 to 250 mgL<sup>-1</sup> were selected and it was observed that with the increase in concentration, there is a decrease in the percent removal of the dye [15]. However, 100 mgL<sup>-1</sup> was chosen as the optimized concentration of the dye for the further analysis as the amount of dye adsorbed on to the adsorbent

from the initial dye concentration was found to be maximum with the selected concentration (Fig 7).

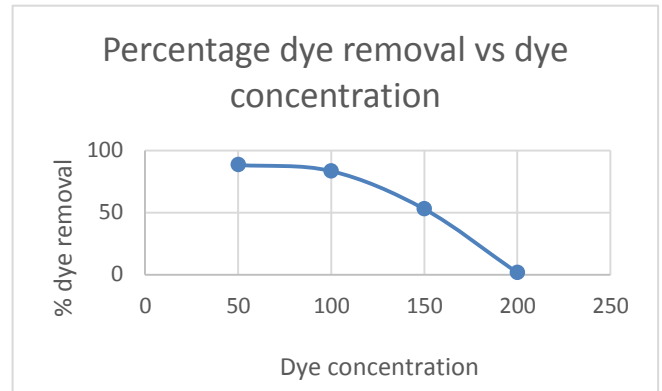


**Figure 7.** Effect of Dye concentration

**5) Effect of temperature:**

The temperature range of 25°C to 60°C was investigated for all the samples. A very high temperature i.e beyond 45°C was not found to be favourable for the adsorption process. This may be due to the weakening of adsorptive forces between the active sites of the adsorbent and adsorbate with the temperature condition as mentioned above [8]. The ideal temperature of 45°C was selected for the further study (Figure 8).

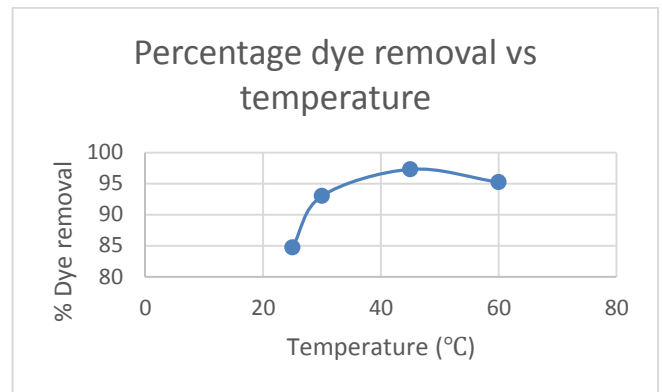


**Figure 8.** Effect of Temperature

**G. Optimized Parameters:**

**Table 3.** Optimized parameters

Sr.No	Parameters studied	Optimized Parameters
1	Contact time	30 minutes
2	pH	7
3	Adsorbent dosage	1g
4	Dye concentration	100mgL <sup>-1</sup>
5	Temperature	45°C

#### H. Possible use of adsorption property of fly ash for sustainable development:

The bulk utilization of fly ash in adsorption process is highlighted to achieve sustainable solution. The role of fly ash samples as good adsorbents, generated from the experimental data signifies the utility of these samples for a sustainable method development. Fly ashes, considered as major industrial waste materials, with its good adsorption properties could find enormous applications in reducing the issues specially in the areas of environmental pollution to a large extent. Apart from the known applications of fly ash, the current work has given a scope to identify the applications for the pre-treatment of samples having diverse nature which can further be analysed using techniques like HPTLC, HPLC etc. Samples can have many interfering agents which interfere in the analysis and hamper the performance of results. Most of the times activated charcoal is used for the removal of such interfering components but now-a-days focus has been shifted towards developing a low-cost adsorbent. The utilization of fly ash will create new revenues as well as business opportunities while protecting the environment.

#### IV. CONCLUSION

In the characterization study, the morphology of the samples indicates that the surface is rough and irregular which supports adsorption. BET surface area was observed in the range of SF1>WA>SF2>FOU>TPP. WA and SF1 showed comparatively high LOI value which could be the result of unburnt carbon present in the sample. Carbon helps in the adsorption process. XRF analysis depicts the presence of SiO<sub>2</sub> in all the samples as a major component which is a known adsorbent. SF1 showed comparatively high specific surface area, LOI and presence of SiO<sub>2</sub>

which helps in the process of adsorption hence amongst all five samples SF1 showed maximum dye removal from aqueous solution after the optimization of all the parameters. Percentage dye removal from aqueous solution using SF1 was found to be 97.82%. Fly ash is a potent adsorbent which can be used for the treatment of samples having many interfering agents. Hence, such new technologies will extend and enhance the usefulness of fly ash as renewable resource for value added products and for ways of making industrial process more sustainable. There is a good scope of research to extend the applications of various fly ash as an effective adsorbent for sustainable development.

#### V. ACKNOWLEDGEMENT

The authors express their sincere gratitude to Prof. Ravindra Deore (G.N.Khalsa college) for his kind help in collecting the samples. The authors appreciate the help from Dr. Purav Badani from University of Mumbai (Kalina) for his constructive comments on interpretation of TGA analysis and also thanks to Mr. Sachin Arote and Ms. Sampada Khopkar from Shimadzu Analytical Pvt.Ltd for their help in FTIR and XRF analysis. The authors appreciate the assistance received from Ms. Suvarna Singh and Mr. Virendra Gupta for performing B.E.T Surface area analysis.

#### VI. REFERENCES

- [1] R Sherly and S Shantha Kumar. 1970. Journal of Industrial Pollution Control. (Jan 1970), ISSN (0970-2083)
- [2] Y Benjelloun, A Lahrichi, S Boumchita, M Idrissi, Y Miyah, Kh Anis, V Nenov, and F Zerrouq. 2017. Journal of Materials and Environmental Science. (Oct 2016), ISSN: 2028-2508
- [3] P Hałas, D Kołodyńska, A Płaza, M Gęca, and Z Hubicki. 2017. Adsorption Science &

- Technology. (April 2017), DOI: 10.1177/0263617417700420
- [4] DS Yücel. 2017. *Karaelmas Fen ve Mühendislik Dergisi*. (April 2017), DOI: <http://dx.doi.org/10.7212%2Fzkufbd.v1i1.288>
- [5] J Wang, Y Zhao, P Zhang, L Yang, H Xu, and G Xi. 2017. *Chinese Journal of Chemical Engineering*. (April 2017), DOI: 10.1016/j.cjche.2017.04.011
- [6] M Ahmaruzzaman. 2010. *Progress in Energy and Combustion Science*. (June 2010), DOI: 10.1016/j.pecs.2009.11.003
- [7] R Kumar, S Kumar and S P Mehrotra. 2007. *Resources, Conservation and Recycling*. (Dec 2017), DOI: <https://doi.org/10.1016/j.resconrec.2007.06.007>
- [8] MK Dwivedi, N Jain, P Sharma, and C Alawa. 2015. *IOSR Journal of Applied Chemistry (IOSR-JAC)*. (April 2015), e-ISSN: 2278-5736
- [9] M Mohebbi, F Rajabipour, and BE Scheetz. 2015. In *World of Coal Ash Conference (WOCA)*, Nashville, TN.(May 2015), ([www.worldofcoalah.org](http://www.worldofcoalah.org)).
- [10] V Chandane, and VK Singh. 2016. *Desalination and Water Treatment*. (Feb 2016), DOI: <https://doi.org/10.1080/19443994.2014.991758>
- [11] P Chindapasirt, C Jaturapitakkul, W Chalee, and U Rattanasak. 2009. *Waste Management*. (Feb 2009), DOI: <https://doi.org/10.1016/j.wasman.2008.06.023>
- [12] J Clara Jeyageetha, SP Kumar. 2016. *International Journal of Science and Research(IJSR)*. (July 2016), ISSN (Online): 2319-7064
- [13] M Mladenov, and Y Pelovski. 2014. *Comptes rendus de l'Académie bulgare des Sciences*. (Jan 2014)
- [14] UR Lakshmi, VS Srivastava, ID Mall, and DH Lataye. 2009. *Journal of Environmental Management*. (Feb 2009), DOI: <https://doi.org/10.1016/j.jenvman.2008.01.002>
- [15] V Vimonses, S Lei, B Jin, CWK Chow, and C Saint. 2009. *Chemical Engineering Journal*. (May 2009), DOI: <https://doi.org/10.1016/j.cej.2008.09.009>

# Study of Antibacterial activity of Mulethi and Amla against gram negative bacteria *Escherichia coli*

H A Padwal, N B Kamble, C P Thomas, A J Rathore, V S Narayane

Department of Zoology, Birla College, Kalyan, Maharashtra, India

## ABSTRACT

Present investigation is performed on comparative study of antibacterial potential of two plants viz., *Glycyrrhiza glabra* and *Embllica officinalis* commonly known as Mulethi and Amla respectively, against the gram negative bacteria *Escherichia coli*. *E. coli* is a well-known and a commonly used bacterium which is a useful tool for genetic research because of its relatively small size, easy availability and ability to grow rapidly under conducive situations. *Glycyrrhiza glabra* is commonly used as condiment in sweets, teas, soft drinks and tobacco products. It not only acts as a good flavouring agent but is also widely used home remedy because of its medicinal properties. This medicinal herb has wide reaching health benefits in naturally treating sore throat, chest congestion, rheumatoid arthritis, strengthening of bones and muscles, kidney problems, mouth ulcers, etc. According to Ayurveda, *Embllica officinalis* balances all the three fundamental bio-elements of the body (viz., pitta, vatta and kapha). Apart from its ability to soothe digestion, Amla may be used as a rejuvenating agent, anti-inflammatory agent, and anti-diabetic agent, helps to reduce fever, stimulate hair growth and enhance intellect. Aqueous and crude extracts of these plants were prepared to find their antibacterial efficacy. The crude extracts of Mulethi and Amla exhibited greater antibacterial properties against the bacteria, as confirmed with the help of antibacterial assays. The growth inhibition of bacteria was studied using growth curve assay at 660 nm using Elico CL63 photometer. Well diffusion assay was performed for 1%, 10% and 100% crude extracts for either plant materials and it was found that 100% extract had maximum antibacterial effect.

**Keywords:** *E. coli*, *Glycyrrhiza glabra*, *Embllica officinalis*, antibacterial assay, growth curve, well diffusion, crude extract, Photometer.

## I. INTRODUCTION

Indian subcontinent and India in particular is known for its rich wealth of medicinal plants, spices, ornamental plants as well as the plants of agricultural importance. In the vastness of dense Indian forests many tropical medicinal herbs are hidden some with known ethnic uses and some, yet to be explored.

'Green medicines' obtained from these plants has high curative ability and gaining the importance around the globe as they are considered as very

good alternatives with lesser known side effects over the synthetic drugs.

*Glycyrrhiza glabra* also called liquorice is known for many medicinal uses. It is also known for its other uses as confectionary and in preparation of tobacco. Studies over the past 50 years have yielded information about pharmacological and physiological effects of liquorice on the intact adrenal gland. Earlier studies suggested that *G. glabra* is useful in treatment of Addison's disease due to the presence of chemicals which mimic corticosteroids secreted by healthy adrenal gland;

however, wide information is available about its role in treating diabetes as its inherent sweetness is thought to reflect its medicinal use to treat high sugar levels. *G.glabra* is sweet in taste due to the presence of a sugar glycyrrhizine (a demulcent starch) in its roots<sup>1</sup>. It has also been reported to have various pharmacological applications like Anti-tussive & expectorant, Antioxidant, Skin lightening and skin tightening, Anti-bacterial, Anti-malarial, Anti-inflammatory, Anti hyperglycaemic, Immunostimulatory effects<sup>2</sup>

*Emblica officinalis* also known as Amla or Indian gooseberry is native to India and is believed to have the capacity to increase the defence against diseases. It has its curable and beneficial role in treating cancer, diabetes, heart trouble, ulcer, anaemia and various other diseases. It shows a variety of applications as antioxidant, immunomodulatory, antipyretic, analgesic, cytoprotective, antitussive and gastroprotective. Additionally, it is useful in enhancing memory, curative on ophthalmic disorders and effective in lowering cholesterol level<sup>3</sup>. Previous studies have shown that these plants had been of great medicinal use. Stems and roots of GG are used in the treatment inflammation, ulcers and allergies as it contains certain active components which are said to be responsible for anti-ulcer, anti-inflammatory, anti-diuretic, anti-allergic and antioxidant properties<sup>4</sup>. EO plays a major role in the treatment of Diabetes mellitus, hepatomegaly, leucorrhoea, inflammations, skin diseases, greying of hair and also has an antisenescence activity<sup>5,6</sup>. Studies have shown different properties of GG and EO. Both of these herbs are well known for its anti-microbial and anti-bacterial property. Present investigation is based on the antibacterial property of both *G.glabra* and *E.officinalis*.

## II. METHODS AND MATERIAL

### Collection of Sample:

Fruits of *E.officinalis* and stems of *G.glabra* were collected from the local market.

### Preparation of Extracts:

The cleaned and cut samples were oven dried over 37°C for 2 days. The dried samples were powdered

using clean grinder and were stored in sterile containers at room temperature before extraction. Soxhlet Apparatus was used for extraction of Mulethi and Amla. Extract was stored at room temperature in sterile containers. For crude aqueous extraction, decoction process was done by boiling dried powder of the plant with sterile water in 1:1 proportion.

### Preparation of bacterial suspension:

Pure isolated colonies of *E.coli* were obtained from the Department of Microbiology, Birla College, Kalyan. *E.coli* was sub-cultured by growing the colonies on nutrient agar slants and preserved in refrigerator.

### Preparation of nutrient broth:

25ml of sterile nutrient broth was prepared using distilled water, and stored at 4°C

### Preparation of nutrient agar plates:

20ml of sterile nutrient agar was poured on sterile plates.

### ANTIMICROBIAL ASSAY: GROWTH CURVE:

24ml of sterile autoclaved nutrient broth was inoculated with 1ml of soxhleted mulethi stem extract and 1ml of *E.coli* culture in triplicate. It was then inoculated in Remi Orbital shaking inoculator at 37°C for 24h, growth was determined at regular intervals of 1hr using Elico CL 63 Photometer at 660 nm. Similar methods were followed for dry and wet Amla extract. Experimental control group was also studied for comparison.

### ANTIMICROBIAL ASSAY: WELL DIFFUSION METHOD:

Sterile Agar plates were used as medium for screening antibacterial activity. About 15 to 20 ml of agar was poured in the sterile petridishes which were allowed to solidify. Wells of 1cm were dug out using a sterile cork borer in solidified agar medium. 1ml of 24hr old cultures of *E.coli* was inoculated evenly using a sterile spreader. Dilutions were made from the crude extract that was used for inoculation. Dilutions of 1%, 10% and crude extract that is 100% of solutions were used. The plates were incubated at

37°C for 24hrs and observed for inhibition zone of growth around the wells<sup>7</sup>.

### III. RESULTS AND DISCUSSION

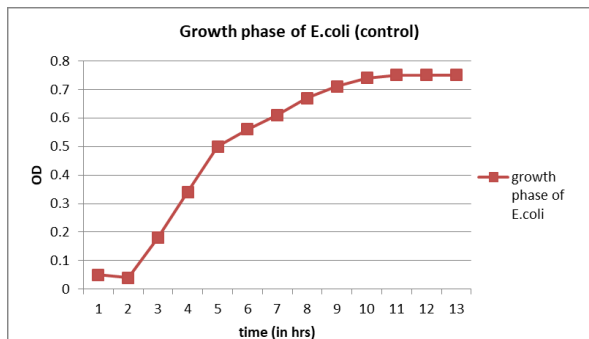


Figure 1. Growth curves of E.coli for Control.

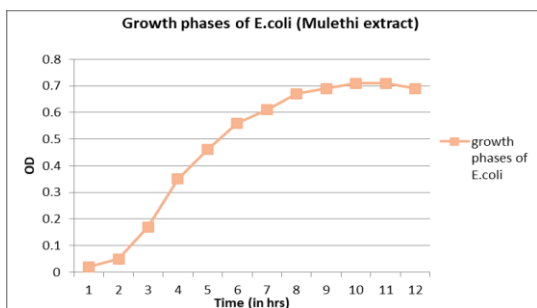


Figure 2. Growth curves of E.coli for Mulethi aqueous extract.

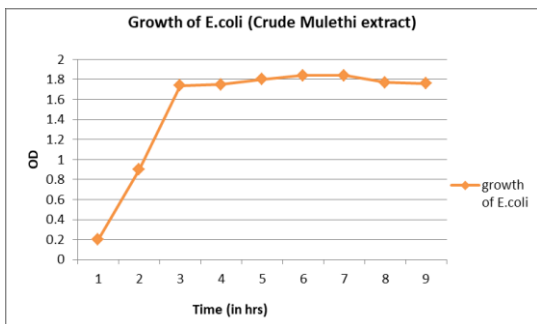


Figure 3. Growth curves of E.coli for Mulethi crude extract.

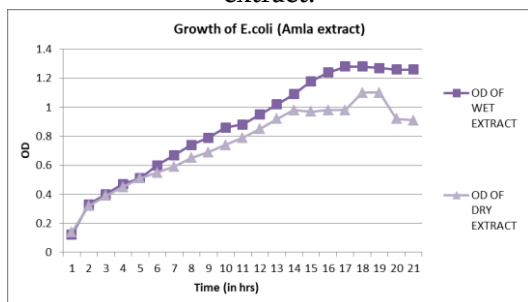


Figure 4. Growth curves of E.coli for Amla aqueous extract.

extract.

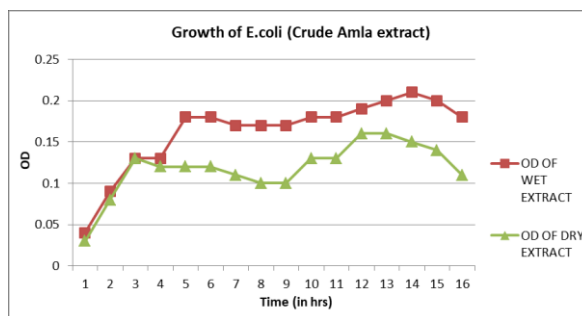


Figure 5. Growth curves of E.coli for Amla crude extract.

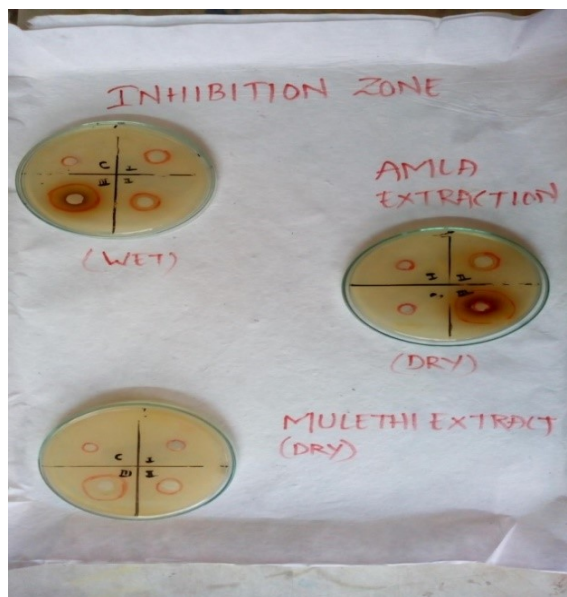


Figure 6. Inhibition zones (mm) for the wet extract of Amla, dry extract of Amla and dry extract of Mulethi obtained by a well diffusion method

**Table. 1.** Inhibition Zones (Mm) For The Wet Extract Of Amla Obtained By A Well Diffusion Method

Extract used	Control	Dry extract of Mulethi			Dry extract of Amla			Wet extract of Amla		
% Dilution	100%	1%	10%	100%	1%	10%	100%	1%	10%	100%
Average Diameter of Zone of Inhibition in mm	0	1	6	14	2	8	17	7	9	15

Comparison of control bacterial culture with that of Soxhlet aqueous extract (Pure extract) yielded expected outcome. Although very little difference was seen in the growth curve, it is noticeable that the stationary phase arrived slightly earlier in case of pure extract “Fig.2” than that of the control “fig1” on the other hand it can be commented from the growth curve prepared after using crude extract “Fig.3” that the stationary phase arrived much earlier than control as well as pure samples. Time taken by the culture to arrive at stationary phase in case of crude sample is nearly half to its other counter parts.

Results produced by well diffusion method are in corroboration with those shown by growth curve as it can be seen from the “Fig.6” and table.1 that the zone of inhibition is much larger when crude extract is incorporated in nutrient agar.

Two separate samples of Amla were prepared as given in the methodology where one sample was prepared using wet Amla and the other using dry Amla. In both cases a general comment can be made that the stationary phase arrived much latter than their control counter parts. When compared among them it can be commented that the extract made out of dry Amla was less effective than the wet amla as again the arrival of growth curve was slower in former than the latter “Fig.4 and 5”.

Growth curve obtained using crude extract showed contradictory results as it was found that extracts made using wet sample were more effective than the one made out of dry sample confirmed as the

stationary phase appeared late in the former than the latter.

Results obtained from well diffusion “Fig.6” assay showed nearly similar results and hence on that basis it is difficult to comment which sample is more effective.

Plants have formed the basis for traditional medicine system and natural product make an excellent and wide way out for any new drug development<sup>8</sup>. Approximately 80% of the world’s population rely on the natural remedies as their primary health care system<sup>9</sup>. The World Health Organization (WHO) is encouraging, promoting and facilitating programs based on herbal medicines and their uses<sup>10</sup>. Bacteria have the genetic ability to transmit and acquire resistance against the drugs which are utilised as the therapeutic agents.<sup>11</sup>

*Glycyrrhiza glabra* (GG) (licorice, Fabaceae/Papilionaceae) is a plant with a rich ethnobotanical history<sup>12</sup>.The active components are triterpene saponins, glycyrrhizin and glycyrrhetic acid, which makes this plant more effective in treating many diseases and thus becoming one the best home remedy due to its antioxidant property which also helps to fight against low blood pressure<sup>13</sup>. Studies on GG extracts have been shown to possess antidepressant-like, memory-enhancing activities and produce antithrombotic effects. On the other hand, the root extracts are reported to exhibit anti androgenic and antitumor activities and radio-protective effects. Besides that, the extracts from GG roots viz. glabridin (an isoflavan) and isoliquiritigenin (a flavonoid), are known to be

pharmacologically active compounds<sup>2</sup>. Glabridin is reported to be a potent antioxidant towards LDL oxidation, whereas isoliquiritigenin is known to exert anti-platelet, anti-viral, estrogenic activities and has the protective potential against cerebral injury.<sup>14</sup>

Inhibition zone for Methanolic extract of GG was found to be 9mm, 11mm and 25mm<sup>15</sup> when compared with the results after investigation it can be clearly seen that the zone of inhibition with crude aqueous extract arrived much earlier (Table.1). Therefore, crude aqueous extract of GG shows more potency against E.coli than the methanolic extract.

*Emblica officinalis* (EO) is a good source of polyphenols, flavones, and tannins and other bioactive compounds<sup>16</sup>. It contains many alkaloids like phyllantine, phyllembin, phyllantidine, flavonoids like kaempferol, quercetin, citric acid, and phenolic compounds like gallic acid, methyl gallate, ellagic acid & trigallayl glucose as its active components and Chebulagic acid, Emblicanin-A, Gallic acid, Emblicanin-B, Punigluconin, Pedunculagin as its few chemical compounds<sup>3</sup>.(3). The major components like tanins, citric acid, phyllembin; pectin smoothens the digestion and also helps in other digestion related problems. EO is one of the important ingredients of Chyavanprash and a constituent of Triphala powder<sup>17</sup>. It is reported to be one of the important constituent in many of the ayurvedic tonics, as the active compounds helps in reducing nausea, excessive salivation, giddiness, regurgitation, and spermatorrhea. EO also helps in maintaining the body homeostasis and menstrual cycle in women.<sup>18, 19</sup>.

Earlier studies showed that the inhibition zone for both methanolic extract and aqueous extract were found to be more or less similar<sup>20</sup>. However, when compared with results it was found to be similar, but, significant differences can be seen for the crude extract of Dry and Wet Amla“Fig.6”.

#### IV. CONCLUSION

The present study concludes that the crude extract is more effective than that of pure aqueous extract

prepared using Soxhlet in both cases such as Mulethi as well as Amla. When compared among them it can be said that Mulethi is more potent as antimicrobial agent than Amla.

#### V. REFERENCES

- [1] Elizabeth A. Davis ' and David J. Morris (1991): Review: Medicinal uses of licorice through the millennia: the good and plenty of it, Molecular and Cellular Endocrinology, Elsevier Scientific Publishers Ireland, Ltd.78:1-6
- [2] Monica Damle (2014):Glycyrrhiza glabra (Liquorice) - a potent medicinal herb, International Journal of Herbal Medicine; 2(2): 132-136
- [3] K.H. Khan (2009): Roles of *Emblica officinalis* in Medicine - A Review, Botany Research International 2 (4): 218-228
- [4] Asha Roshan, Navneet Kumar Verma, Chaudhari Sunil Kumar, Vikas Chandra, Devendra Pratap Singh, Manoj Kumar Panday(2012) : Phytochemical Constituent,Pharmacological Activities and Medicinal Uses through the Millenia of *Glycyrrhiza glabra* Linn: A Review, IJRP,ISSN 2230-8407,3(8)
- [5] Liu, X., et al(2012): Immunomodulatory and anticancer activities of phenolics from *emblica* fruit (*Phyllanthus emblica* L.), Food Chem. **131**, 685-690
- [6] Jamwal, K.S., et al.( 1959): Pharmacological investigations on the fruits of *Emblicaofficinalis*, J. Indus. Res. **18c**, 180-181
- [7] John Thomas and Veda B : Screening of ten Indian Medicinal Plants for their Antibacterial Activity against *Shigella* species and *Escherichia coli* ., Afr.J.Infect Diseases.1(1): 36-41
- [8] Newmann DJ, Cragg GM, Snadder KM,(2000): The Influence of natural product on drug discovery, Natural product res.; 17, 215-234



- [9] Cragg GM, Boyd MR, Khanna R, Kneller R, Mays TD, Mazan TD, Newmann DJ, Sausville EA (1999): International collaboration in drug discovery and development, the NCT experience. *Pure Appl. Chemistry*; 71,1619-1633.
- [10] Gupta Priya, Nain Parminder, Sidana Jaspreet (2012): Antimicrobial and Antioxidant activity on *Emblica officinalis* seed extract., *IJRAP* 3(4)
- [11] Cohen ML (2002): Changing patterns of Infection diseases, *Nature*; 406, 762-767
- [12] Kataria R, Hemraj, Singh G, Gupta A, Jalhan S, Jindal A (2013): Pharmacological activities on *Glycyrrhiza glabra*—a review, *Asian J Pharm Clin Res*; 6(1):5-7.
- [13] Hai Zhong Huo, Bing Wang, Yong Kang Liang, Yong Yang Bao and Yan Gu. Hepatoprotective and antioxidant effects of licorice extract against ccl4-induced oxidative damage in rats. *Int. J. Mol. Sci.* 2011; 12; 6529-6543.
- [14] Lakshmi T, Geetha R.V (2011): *Glycyrrhiza glabra* Linn Commonly known as Licorice: A Therapeutic Review, *International Journal of Pharmacy and Pharmaceutical Sciences*, ISSN- 0975-1491 Vol 3, Issue 4.
- [15] P.K.P. Gaitry Chopra\* , Binda D. Sarafa, Farhin Inama and Sujata S. Deoa (2013): Antimicrobial and Antioxidant Activities of Methanol Extract Roots of *Glycyrrhiza Glabra* and HPLC Analysis, *International Journal of Pharmacy and Pharmaceutical Sciences* ISSN- 0975-1491 Vol 5, Suppl 2
- [16] . Zhang, L.Z., et al. (2003) Studies on chemical constituents in fruits of Tibetan medicine *Phyllanthus emblica*, *Zhongguo Zhong Yao Za Zhi.* 28, 940-943
- [17] Ghosala S, Tripathi, Chouhan S (1996): Active constituents of *Emblica officinalis*: part I The Chemistry and Antioxidative effect of two new hydrolysable tannins, *Emblicanin A and B.*, *Indian J. of Chem.* 35B; 941-948
- [18] Treadway, Linda (1994): *Amla Traditional food and Medicinal Herbal Gram.*, *The Journal of American Botanical Council*, 31:26
- [19] Jayaweera DMA (1980): *Medicinal Plants used in Ceylon Part -2*, National Science Council of Sri Lanka, Colombo.
- [20] Ankita Gautam and Sangeeta Shukla (2017): *Journal of Pharmacognosy and Phytochemistry*, 6(2): 233-236

# Copper Oxide Nanoparticles : Synthesis and Characterization

Himanshu Narayan<sup>1\*</sup>, Hailemicheal Alemu<sup>2</sup>, Lineo F. Maxakaza<sup>2</sup>, Sandesh Jaybhaye<sup>3</sup>

<sup>1</sup> Department of Physics & Electronics, National University of Lesotho, Roma, Lesotho

<sup>2</sup> Department of Chemistry & Chemical Technology, National University of Lesotho, Roma, Lesotho

<sup>3</sup> Nanotech Research Lab, Department of Chemistry, Birla College, Kalyan, India

## ABSTRACT

We report the synthesis of copper oxide (CuO) nanoparticles from  $\text{Cu}(\text{NO}_3)_2$  through wet chemical precipitation method. Characterization was done by X-ray diffraction (XRD) analysis, scanning electron microscopy (SEM), particle size analyzer and Fourier transform infra-red spectroscopy (FTIR). Two most prominent peaks in XRD profile, around  $2\theta = 35.9^\circ$  and  $39.2^\circ$ , which are combinations of double-reflections  $\{(002) \text{ and } (-111)\}$  and  $\{(111) \text{ and } (200)\}$ , respectively, are characteristics of monoclinic CuO. Unit cell parameters determined through Reitveld analysis of XRD data under FullProf Software Suite were:  $a = 4.6927$ ,  $b = 3.4283$  and  $c = 5.137 \text{ \AA}$ , with  $\alpha = \gamma = 90^\circ$  and  $\beta = 99.546^\circ$  for monoclinic Cc space group. Moreover, crystallite size estimation from XRD data using Debye-Scherrer formula produced average size of 34 nm for the nanoparticles. However, the particle size analyzer measured the average grain-size as 86 nm. Therefore, it was concluded that each grain of the nano-sized CuO seemed to be made up of roughly 16 crystallites. SEM pictures showed uniform distribution of ice-glass like crystalline particles, which are agglomeration of smaller particles. FTIR results showed expected peaks corresponding to Cu-O stretching. As a potential application as carbon paste electrode (CPE) modifier, the electrocatalytic efficiencies of CuO nanoparticles are being investigated.

**Keywords:** Copper oxide; Nanoparticles; Wet chemical precipitation; X-ray diffraction

## I. INTRODUCTION

In the past few decades, nanoparticles of a variety of shapes, sizes and compositions, have been discovered. Many of them are with excellent conductivity and fascinating catalytic properties that make them suitable for constructing novel electrochemical sensors. Nanostructured transition metal oxides have attracted considerable attention from researchers in the recent years. Copper (II) oxide, CuO, also known as cupric oxide is a p-type semiconductor with a bandgap of 1.2 – 1.9 eV. It is a black transition metal oxide with monoclinic crystal structure and many interesting characteristics, e.g., high thermal

conductivity, photovoltaic properties, high stability and antimicrobial activity. Because of such useful properties, CuO has been investigated extensively for its wide range of potential applications, such as, in electrochemical cell, gas sensors, magnetic storage devices, field emitters and in catalysis [1]. Nanocomposites are known for significantly improving the electrocatalytic properties of substrates, decrease the overpotential, increase the reaction rate and improve reproducibility of the electrode response in the area of electroanalysis [2,3,4].

In this report we present the synthesis of CuO nanoparticles using wet chemical precipitation (WCP)

method, using  $\text{Cu}(\text{NO}_3)_2$  and 1,10-phenanthroline as precursors, and ethanol/water mixture and NaOH as a reducing agents. Characterization of the synthesized CuO nanoparticles have been done by X-ray diffraction (XRD), Fourier Transform Infra-Red spectroscopy (FTIR), thermogravimetric analysis (TGA) and particle-size analysis.

## II. METHODS AND MATERIAL

### Synthesis of CuO nanoparticles:

NaOH was obtained from ACE (South Africa), 1,10-phenanthroline from Saarchem (South Africa), ethanol from Laboratory & Analytical Suppliers Co. (Pty) Ltd (South Africa). All reagents were used as received and ultra-pure water was used throughout. Phosphate buffer of pH 7 (supporting electrolyte was prepared from stock solution of 0.1 M disodium hydrogen phosphate and 0.1 M HCl.  $\text{Cu}(\text{NO}_3)_2$  3 mM and 1,10-phenanthroline 6 mM were prepared in 1:1 ethanol/water mixture. 2 M NaOH aqueous solution was then added to the solution under magnetic stirring and heating. The alkaline solution was transferred into an autoclave. The autoclave was then sealed and maintained at 160 °C for 24 h. The solution was then cooled to room temperature; the black precipitates were filtered, washed with water and absolute ethanol for several times and then dried in an oven at 50 °C.

Figure 1 shows the synthesis route and reactions for the preparation of CuO nanoparticles. In reaction R1, water displaces the nitro group because it is a stronger ligand, resulting in a blue complex of  $\text{Cu}(\text{H}_2\text{O})_6^{2+}$ . The same is true for reaction R2 [7]. 1, 10-phenanthroline is an organic compound that enhances formation of individual nanowires, a flower of nanowires agglomerated together would otherwise result if it was not used. It does not take part in the chemical synthesis of the reaction.

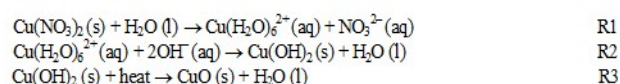
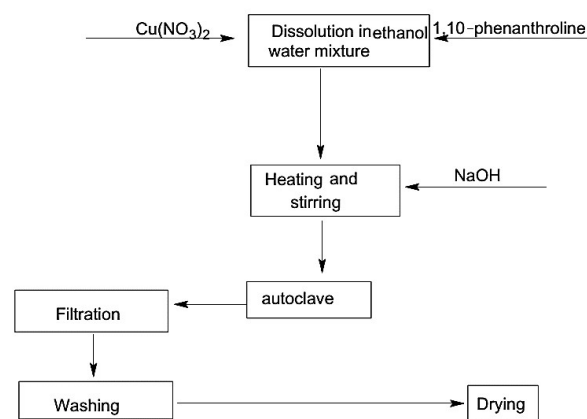


**Figure 1.** Synthesis route of CuO nanoparticles and chemical reactions.

### Characterization and measurements:

X-ray diffraction measurements were executed with a Shimadzu D6000 Diffractometer (from Shimadzu, Japan) using Cu  $K_{\alpha}$  radiation ( $\lambda = 1.5406 \text{ \AA}$ ) in the  $2\theta$  range from  $20^{\circ}$  to  $60^{\circ}$ . Scanning electron microscopy (SEM) was carried out on a Zeiss crossbeam series with Gemini FESEM unit. Fourier transform infra-red (FTIR) spectroscopy was carried out with Shimadzu FTIR, run from  $400 \text{ cm}^{-1}$  to  $4000 \text{ cm}^{-1}$  using diffuse reflection method, and KBr pellet was used for background measurement. Thermogravimetric analysis (TGA) was carried out with SDT 2960 Simultaneous DSC-TGA, TA Instruments from  $24^{\circ}\text{C}$  to  $700^{\circ}\text{C}$  at a ramp of  $10^{\circ}\text{C}/\text{min}$ . Particle size analysis was performed using Microtrac/Nanotracer TM150, which employs optical light scattering of particles suspended in water.

## III. RESULTS AND DISCUSSION

### X-ray diffraction analysis of CuO nanopowder:

X-ray diffraction pattern of nano-sized CuO is shown in Figure 2. A detailed Reitveld analysis of XRD data to determine the crystal structure was also performed using FullProf Software Suite [4]. The two most prominent peaks around  $2\theta = 35.9^{\circ}$  and  $39.2^{\circ}$ , which

were identified as combinations of double-reflections  $\{(002) \text{ and } (-111)\}$  and  $\{(111) \text{ and } (200)\}$ , respectively, are characteristics of CuO. Further the acceptable FullProf solution after several trails produced monoclinic unit-cell with Cc space group and cell parameters:  $a = 4.6927 \text{ \AA}$ ,  $b = 3.4283 \text{ \AA}$ ,  $c = 5.137 \text{ \AA}$ ,  $\alpha = 90^\circ$ ,  $\beta = 99.546^\circ$  and  $\gamma = 90^\circ$ . These results are in very good agreement with the already reported single crystal data for CuO [5]. It is also noteworthy that the actual peaks recorded for the CuO nanopowder are apparently shifted approximately by  $+0.3^\circ$  of  $2\theta$  value, which may be tentatively attributed to the strains within the crystallites.

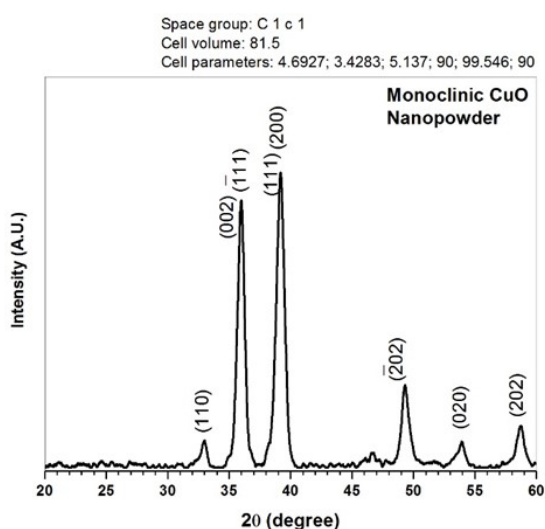


**Figure 2.** X-Ray Diffraction spectrum of CuO nanopowder.

#### Particles size analysis:

Average crystallite size of 34 nm for the CuO nanoparticles was estimated using Debye-Scherrer method. FWHM of the Gaussian best-fit to prominent peaks in the XRD data was used in the formula. Though this method has its own limitations, it immediately gives a rough estimation of the size without much effort. Since the X-rays penetrate through the surface of the particles, what is measured here is the size of small crystallites within the grains that diffract X-rays coherently [8].

On the other hand, the grain-size was measured on a particle size analyzer. A solution of copper oxide was

prepared with pure water and agitated in an ultrasonic bath to obtain an evenly dispersed solution. Instrument was set to zero using the solvent (water) then the CuO solution was filled in the cell and measured. Distribution of grain-size obtained is shown in Figure 3. The mean grain size of CuO nanoparticles was determined to be 86 nm by the particle size analyzer, which measures the average diameter of the grains using light as a probe. Obviously, light cannot penetrate through the surface and therefore, this method gives the size of individual grains that could possibly be made up of several crystallites.

A comparison of volumes created by the two sizes reveals that apparently each grain consists of approximately 16 crystallites, on an average.

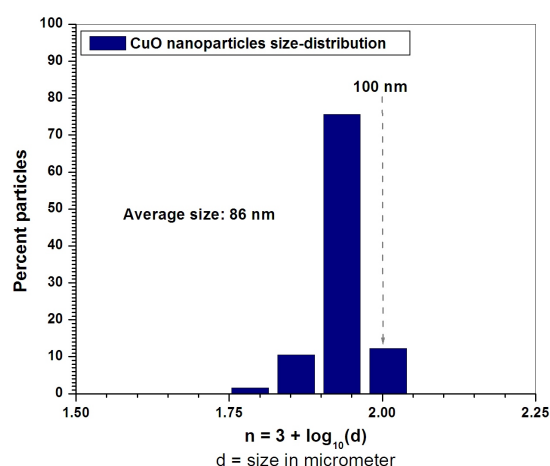


**Figure 3.** Particle size distribution of CuO nanoparticles.

#### Scanning electron microscopy:

SEM pictures at two different magnifications are shown in Figure 4. Highly crystalline, broken glass like structures are clearly visible in the pictures. The observed white spots in the SEM pictures are presumably traces of 1,10-phenanthroline left after washing. Moreover, the energy dispersive X-ray spectroscopy (EDX) carried out on the same machine established the composition of the nanoparticles as CuO.

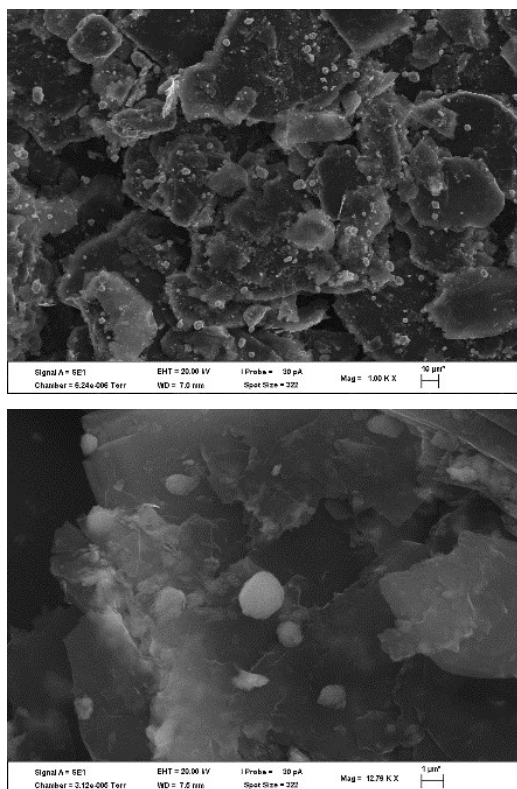


Figure 4. SEM pictures of CuO nano-particles.

#### FTIR and TGA:

FTIR spectrum of CuO nanoparticles is shown in Figure 5. Characteristic peaks of CuO range from around  $400\text{ cm}^{-1}$  to  $1000\text{ cm}^{-1}$ . Peaks around  $420\text{ cm}^{-1}$ ,  $500\text{ cm}^{-1}$  and  $610\text{ cm}^{-1}$  can be assigned to Cu–O stretching along  $[-202]$  Cu–O direction. Small sharp peak around  $450\text{ cm}^{-1}$  is attributed to Cu–O stretching along  $[202]$  direction. The peak around  $2300\text{ cm}^{-1}$  can be assigned to  $\text{CO}_2$  stretching, which could have been entrapped in the sample holder during packing. The broad peak around  $3500\text{ cm}^{-1}$  is due to O–H stretch and bending from adsorbed water.

Thermogravimetric analysis of 8.4 mg of CuO nanoparticles was run from  $24\text{ }^\circ\text{C}$  to  $700\text{ }^\circ\text{C}$  at a ramp of  $10\text{ }^\circ\text{C}/\text{min}$  (picture not shown). It shows that in the temperatures range of  $80 - 140\text{ }^\circ\text{C}$ , the percentage weight loss with temperature is about 1.0 %. This can be attributed to loss of adsorbed water and ethanol, 2.0 % weight loss around  $260 - 340\text{ }^\circ\text{C}$  with is attributed to loss of hydroxyl ions. Weight percentage remains fairly constant above  $500\text{ }^\circ\text{C}$ , thus most impurities were lost at this temperature. The total

weight loss is about 3 %. It can therefore be concluded that CuO nanoparticles are stable at elevated temperatures.

As a potential application, electrochemical responses of carbon-paste electrodes modified with CuO nanoparticles are being investigated for the detection of ascorbic acid, atenolol, diclofenac, dopamine, hydrazine and glucose using the method of cyclic voltammeter. The results will be published elsewhere.

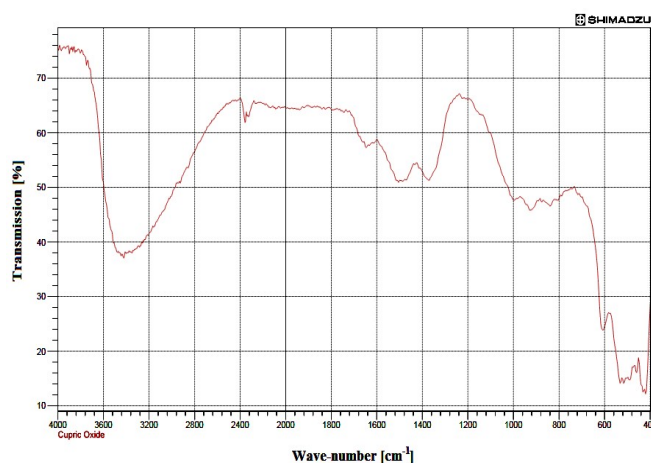


Figure 5. IR spectrum of CuO nanoparticles.

#### IV. CONCLUSION

Synthesis and characterization of nano-sized copper oxide (CuO) powder has been reported. Prominent XRD peaks around  $2\theta = 35.9^\circ$  and  $39.2^\circ$ , which are combinations of double-reflections  $\{(002)\text{ and }(-111)\}$  and  $\{(111)\text{ and } (200)\}$ , respectively, have been identified as the characteristics of monoclinic CuO, with unit-cell parameters estimated as:  $a = 4.6927$ ,  $b = 3.4283$  and  $c = 5.137\text{ \AA}$ ;  $\alpha = \gamma = 90^\circ$ ,  $\beta = 99.546^\circ$ . Moreover, the crystallite size calculated from XRD data through Debye-Scherrer method produced average size of 34 nm for the nanoparticles. The average grain-size measured on particle size analyzer however 86 nm was. Therefore it was concluded that each grain of the nano-sized CuO was apparently made up of nearly 16 crystallites. Uniform distribution of ice-glass like crystalline particles was visible in SEM pictures, which were agglomerations of smaller

particles. FTIR results showed stretching of Cu-O bonds as expected.

Electrochemical properties of CuO nanoparticles as carbon paste electrode modifier are being investigated against electrochemical oxidation of ascorbic acid, atenolol, diclofenac, dopamine, hydrazine and glucose using cyclic voltammetry. The initial results seem to be very promising.

## V. REFERENCES

1. Y. Aparna, K.V. Enkateswara Rao and P. Srinivasa Subbarao; Synthesis and characterization of CuO nano particles by novel sol-gel method; 2012 2nd International Conference on Environment Science and Biotechnology IPCBEE vol. 48 (2012) IACSIT Press, Singapore 156-160. DOI: 10.7763/PCBEE.2012. V48. 30
2. Hadi Beitollahi, Susan Ghofrani Ivvari and Masoud Torkezadeh-Mahani; Voltammetric determination of 6-thioguanine and folic acid using a carbon paste electrode modified with ZnO-CuO nanoplates and modifier; Mater. Sci. Engineering C **69** 2016 128–133.
3. Rinkesh Kurkure, Sandesh Jaybhaye; Synthesis of Copper / Copper Oxide nanoparticles in eco-friendly and non-toxic manner from floral extract of Hibiscus rosa-sinensis; J. Bio-Nano Frontier **9** (2) 2016 105-10.
4. Rinkesh Kurkure, Sandesh Jaybhaye, Abhijeet Sangale; Synthesis of copper/copper oxide nanoparticles in ecofriendly and nontoxic manner from floral extract of Caesalpinia pulcherrima; Int. J. Recent Innovation Trends Computing Commun. (IJRITCC) **4** (4) 2016 363-366. ISSN: 2321-8169.
5. J.D. Lee; Concise Inorganic Chemistry; 5th Ed, Blackwell Science, UK 1996 pp. 827-831. <https://doi.org/10.1063/1.3610496.9>.
6. Himanshu Narayan, Hailemichael Alemu, Pusetso F. Nketsa, Toka J. Manatha and Madhavi Thakurdesai; Synthesis and structure of some nano-sized rare-earth metal ions doped potassium hexacyanoferrates; Physica E **69** 2015 127-132.
7. S. Asbrink and A. Waskowska; CuO: x-ray single-crystal structure determination at 196 K and room temperature; J. Phys.: Cond. Matter **3** 1991 8173-8180.
8. Himanshu Narayan, Hailemichael Alemu, Lebohang Macheli, Madhavi Thakurdesai and T.K. Gundu Rao; Synthesis and characterization of Y<sup>3+</sup>-doped TiO<sub>2</sub> nanocomposites for photocatalytic applications; Nanotechnology **20** 2009 255601 (8pp).

# Inhibition of Mild Steel Corrosion Caused by Sulphate Reducing Bacteria by Using 2-Methylimidazole

Jitendra D. Girase , R. S. Dubey

Department of Chemistry, R.J.College of Arts, Science and Commerce, Ghatkopar (W), Mumbai, Maharashtra, India

## ABSTRACT

In this study, the inhibitive performance of 2-methylimidazole derivative as a corrosion inhibitor of mild steel was examined in Barr's medium inoculated with sulphate reducing bacteria (*Desulfovibrio desulfuricans*). The coupons were exposed with different concentrations of 2-methylimidazole in Barr's medium inoculated with sulphate reducing bacteria. The corrosion behaviour of mild steel was measured by weight loss, corrosion potential and polarization techniques. The surface analysis has been performed by scanning electron microscopy (SEM). The inhibitor exhibits their best performance at 500 ppm solution. The inhibitor obeys the Langmuir adsorption isotherm phenomenon since it obtained a straight line graph.

**Keywords :** SRB, Mild Steel, SEM.

## I. INTRODUCTION

Though the serious consequence of corrosion can be controlled to a great extent by selection of highly corrosion resistant materials, the phenomenon of corrosion remains a major concern to industries around the world. Microbiologically Influenced Corrosion (MIC) is a major problem in many industries such as oil and gas, as well as water utilities. Sulphate Reducing Bacteria (SRB) is often found to be the cause of MIC [1-8].

Microbiologically influenced corrosion (MIC) has been estimated to account for 20% of annual corrosion damage of metallic materials, of which sulphate-reducing bacteria (SRB) are commonly considered to be the principal culprits among the causative organisms of corrosion [9-11]. SRB are strict anaerobes that gain their biochemical energy for growth by oxidizing certain organic

compounds or hydrogen ( $H_2$ ) with sulphate or other sulphur compounds such as sulphite, thiosulphate or sulphur as terminal electron acceptors and reducing these compounds to sulphides ( $H_2S$  and  $HS^-$ ) [12-15].

The purpose of this paper is to study inhibition performance of 2-methylimidazole as corrosion inhibitor for mild steel in Barr's medium inoculated with sulphate reducing bacteria. It has been studied through different corrosion monitoring methods and surface analytic techniques. In addition, adsorption performance and mechanism at mild steel surfaces are also discussed. The study confirms that the imidazole derivative protect mild steel from microbiological influenced corrosion due to its antimicrobial properties and by adsorption on metal surface.

## II. EXPERIMENTAL DETAILS

### 2.1. Metals and Alloys

Mild Steel coupons having composition (C – 0.16%, Si – 0.10%, Mn – 0.40%, P - 0.013%, S - 0.02% and remaining as iron) have been used as working electrode in the present study.

### 2.2. Chemicals

Chemicals used in corrosion test solutions and corrosion inhibitors were obtained from Merck (India), Loba chemie (India). All these chemicals were of AR grade and were used without any further purification.

### 2.3. Bacteria

The bacteria used in the present study were obtained from National collection of Industrial Micro-organisms (NCIM), Biochemical Science Division, National Chemical Laboratory, Pune-411088, Maharashtra.

The bacteria used in the present study were *Desulfovibrio desulfuricans*. Composition of the culture medium is given below,

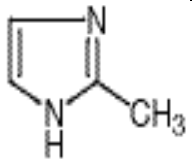
Table 1

Name of the Organism	NCI M No.	Medium used
<i>Desulfovibrio desulfuricans</i> .	2047	Barr's medium (sulfur bacteria) K <sub>2</sub> HPO <sub>4</sub> 0.05g, NH <sub>4</sub> Cl 0.19, CaSO <sub>4</sub> 0.29, Sodium Lactate 0.79, MgSO <sub>4</sub> .7H <sub>2</sub> O 0.29, Ferrous Ammonium Sulfate 0.05g, Distilled Water 100 cm <sup>3</sup> (medium is sterilized for three consecutive days at 121°C for 20 min and the final pH is adjusted to 7.0-7.5).

### 2.4. Biocide:-

The biocide 2-methylimidazole is added in to the test solution. The chemical structure of 2-methylimidazole is as follows,

Table 2

Inhibitor	Molecular Structure.
2-methylimidazole	

### 2.5. Sample Preparation:

For weight loss experiments, rectangular shaped coupons (1 cm X 3 cm) were sheared from sheets of mild steel and flag shaped specimens with 1 cm<sup>2</sup> working area were used for electrochemical experiments. The surface of specimens was prepared by sequential polishing with 1/0, 2/0, 3/0, 4/0 grade emery papers, it was polished with the next higher grade in a right angle to the first. During the polishing of mild steel surface, the emery paper was impregnated with a dilute solution of paraffin wax in kerosene oil. All specimens were washed with triple distilled water and degreased with 95% ethyl alcohol. Specimens were dried and stored over silica gel in vacuum desiccators.

### 2.6. Immersion Test

Specimens were weighed on an electronic balance (Shimadzu Type BL220H, least count 0.001g) before and after immersion tests. After removing the specimens from the test solution the corrosion products were removed from the surface with the help of brush. Generally duplicate experiments were performed in each case and the mean value of the weight loss was recorded.

### 2.7. Electrochemical Measurements

The variation of corrosion potential of mild steel was measured against saturated calomel electrode in absence and presence of various concentrations of inhibitors. The time dependence of OCP for different experiments was recorded for one hour



exposure period. Then same sample was used for potentiodynamic polarization (PD) experiments. Different electrochemical results obtained from potentiodynamic polarization are reported. The polarization studies were carried out in unstirred solutions. For electrochemical polarization studies (corrosion potential and potentiodynamic polarization) flag shaped specimens with sufficiently long tail were cut from the mild steel sheet. These samples were polished as described earlier leaving a working area of 1 cm<sup>2</sup> on one side of the flag and a small portion at the tip for providing electrical contact. Rest of the surface was coated with enamel lacquer including side edges. The test specimen was connected to the working electrode holder through the tip of the tail. About 50 ml of the corrosive medium was taken in a mini corrosion testing electrochemical cell.

Electrochemical measurement system, DC 105, containing software of DC corrosion techniques from M/S Gamry Instruments Inc., (No. 23-25), Louis Drive, Warminster, PA- 18974, USA has been used for performing corrosion potential and polarization experiments. The electrochemical studies were performed in a three electrodes Pyrex glass vessel with mild steel coupons as working electrode, saturated calomel electrode as reference electrode and spectroscopic grade graphite rod as counter electrode.

### 2.8. Scanning Electron Microscopic Analysis

The composition and surface morphology of corrosion product on mild steel sample after 240 hours (10 days) immersion in the Barr's medium in the absence and presence of 2-methylimidazole was studied by a scanning electron microscopy (SEM).

## III. RESULTS AND DISCUSSION

### 3.1. Weight Loss Measurement-

Weight loss data of mild steel in Barr's medium inoculated with *Desulfovibrio desulfuricans* in

the absence and presence of various concentrations of inhibitor were obtained and are given in Table-1. Inhibition efficiencies (IE %) were calculated by formula as:

$$(IE \%) = [W_0 - W] / W_0 \times 100$$

Where W and W<sub>0</sub> are the weight loss of mild steel in the presence and absence of inhibitor, respectively. The results show that the inhibition efficiencies increase with increasing inhibitor concentration. The results obtained from the weight loss measurements are in good agreement with those obtained from the electrochemical methods.

**Table 3.** Weight loss data for inhibition of corrosion of mild steel exposed to Barr's medium inoculated with *Desulfovibrio Desulfuricans* with different concentration of 2-methylimidazole.

Inhibitor	Conc. (ppm)	Weight Loss (mg)	Surface Coverage (θ)	Inhibition Efficiency (IE %)
Blank (Barr's medium inoculated with <i>Desulfovibrio Desulfuricans</i> )	-----	210	----- -	-----
2-methylimidazole	100	138	0.34	34%
	300	96	0.54	54%
	500	42	0.80	80%

### 3.2. Open Circuit Potential Measurement (OCP)

The electrochemical behavior of mild steel in 1M HCl was studied by monitoring change in corrosion potential (E<sub>corr</sub>) with time. The change in open circuit potential of mild steel in absence and presence of various concentrations of inhibitor 2-methylimidazole in Barr's medium is shown in figure 3.

The change in open circuit potential of mild steel in absence and presence of inhibitors were measured after 10 days exposure in Barr's medium inoculated with *Desulfovibrio Desulfuricans* for period of 1h with sample period of one data per second. The potential attains steady state after exposure of 0.5h. The steady state potential is an equilibrium state at which  $I_{ox}$  is equal to  $I_{red}$ . In the presence of various concentrations of inhibitors the steady state potential of mild steel shifts more towards positive value. This is due to adsorption of inhibitors on metal surface resulting in passivation of metal.

The influence of various concentration (100, 300, and 500 ppm) of 2-methylimidazole on open circuit potential of mild steel in Barr's medium is given in fig .3 . It is obvious from figure that, it exhibit good inhibition performance at 100 ppm and above. Inhibition efficiency increases with increase in concentration of 2-methylimidazole.

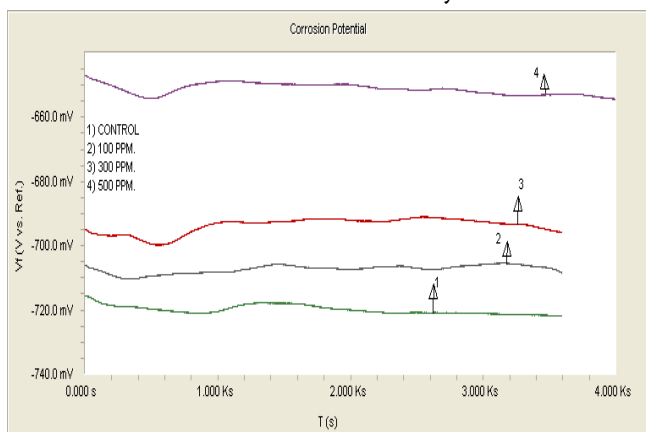


**Figure 1.** Corrosion potential of mild steel exposed to the solution of Barr's medium with different concentrations of 2-methylimidazole.

### 3.3. Potentiodynamic Polarization Measurement

Figure 4 depicts typical potentiodynamic polarization curves for mild steel in Barr's medium solution in the absence and presence of different concentrations of 2-methylimidazole at 30°C.

It could be observed that extent of damage to mild steel surface is very less, the rate of corrosion was reduced considerably in the presence of inhibitors, it revealed that there was a good protective film adsorbed on metal surface, which acted as a barrier and was responsible for the inhibition of corrosion.

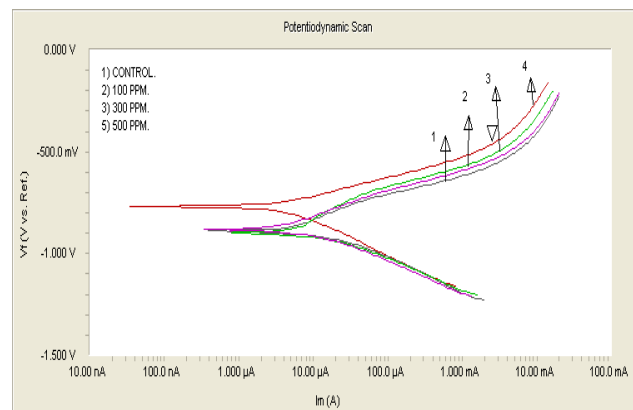


**Figure 2.** Potentiodynamic polarization curve of mild steel exposed to Barr's medium inoculated with *Desulfovibrio Desulfuricans* with different concentrations of 2-methylimidazole.

**Table 4.** Electrochemical Parameters for Inhibition of corrosion of mild steel exposed to 1M HCl with different concentration of 2-methylimidazole.

Conc. (ppm)	$\beta_a$ (V/dec.) $e^{-3}$	$\beta_c$ (V/dec.) $e^{-3}$	$I_{corr}$ ( $\mu A.cm^2$ )	$E_{corr}$ (mV)	%IE
Contro	231.4	113.0	15.10	-897.0	-
<b>2-methylimidazole.</b>					
100	160.7	128.7	8.52	-881.0	43.57
300	106.0	176.6	5.45	-768.0	63.90
500	104.3	175.2	3.12	-765.0	79.33

### 3.4. Adsorption Isotherm

The surface coverage values,  $\theta$ , (defined as  $\theta = \text{IE} \% / 100$ ), increases with increasing inhibitor concentration as a result of adsorption of more inhibitor. The corrosion inhibition efficiency was calculated by using the following equation: Inhibition efficiency (IE %) =  $\frac{100(i_0 - i)}{i_0}$ , Where  $i_0$  and  $i$  are the corrosion current densities in the absence and presence of inhibitor in the solution, respectively.

**Table 5.** Adsorption parameters of 2-methylimidazole.

C (PPM)	$\theta$	IE%
100	0.4357	43.57
300	0.6390	63.90
500	0.7933	79.33

It is observed that the adsorption behavior of 2-methylimidazole obeys the Langmuir's adsorption isotherm as it gives straight line when graph of  $C \text{ (ppm)} / \theta$  is plotted against  $C \text{ (ppm)}$  as shown in Fig 1. It was proposed that adsorption of 2-methylimidazole occurs by physisorption and chemisorptions. Thus the surface of inhibitor layer formation on the mild steel is the combination of both, physisorption and chemisorptions.

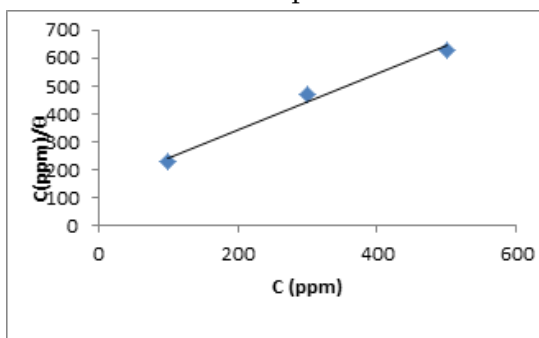


**Figure 3.** Adsorption Isotherm of 2-methylimidazole.

### 3.5. Scanning Electron Microscopic (SEM) Analysis

SEM micrographs obtained from unexposed and exposed specimen coupons in Barr's medium inoculated with *Desulfovibrio Desulfuricans* for 240 hours in the absence and presence of 500 ppm 2-methylimidazole which are shown in Fig. 2, respectively. The accelerating voltage for SEM scanning was 10KV. The results obtained from weight loss and electrochemical measurements were further supported by SEM analysis.

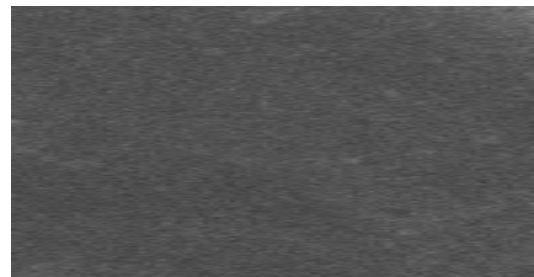


**Figure 4.** SEM of mild steel: a) Polished and without inhibitor.

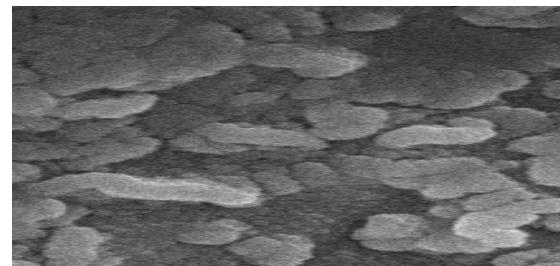


**Figure 4.b)** After immersion in Barr's medium inoculated with *Desulfovibrio desulfuricans* without inhibitor.

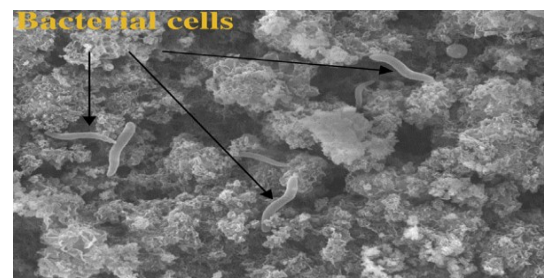


**Figure 4. c).** After immersion in Barr's medium inoculated with *Desulfovibrio desulfuricans* with 500 ppm of inhibitor.

#### IV. CONCLUSION

On the basis of above results following conclusions are obtained:

- 1] The result obtained by gravimetric analysis, hold good agreement with the result obtained by electrochemical studies; revealed that 2-methylimidazole is acting as a very good corrosion inhibitor of mild steel in Barr's medium.
- 2] The inhibition efficiency increases with the increasing concentration of inhibitor.
- 3] In the present investigation, 500 ppm solution of 2-methylimidazole shows nearly 80% inhibition.
- 4] 2-methylimidazole is mixed type of inhibitor.
- 5] The SEM examination shows the formation of protective surface film of inhibitor molecules on the surface of mild steel and obeys the Langmuir adsorption isotherm.

#### V. REFERENCES

- [1] Hamilton WA. Sulfate-reducing bacteria and anaerobic corrosion. *Annu Rev Microbiol* 1985;39:195–217.
- [2] Rueter P, Rabus R, Wilkest H, Aeckersberg F, Rainey FA, Jannasch HW, et al. Anaerobic oxidation of hydrocarbons in crude oil by new types of sulphate reducing bacteria. *Nature* 1994;372:455–8.
- [3] Miranda E, Bethencourt M, Botana F, Cano M. Biocorrosion of carbon steel alloys by an hydrogenotrophic sulfate-reducing bacterium *Desulfovibrio Capillatus* isolated from a Mexican oil field separator. *Corros Sci* 2006;48:2417–31.
- [4] AlAbbas FM, Williamson C, Bhola SM, Spear JR, Olson DL, Mishra B, et al. Influence of sulfate reducing bacterial biofilm on corrosion behavior of lowalloy,high-strength steel (API-5L X80). *Int Biodeter Biodegr* 2013;78:34–42.
- [5] Guamet PS, Gomez de Saravia SG. Laboratory studies of biocorrosion control using traditional and environmentally friendly biocides: an overview. *Latin Am Appl Res* 2005;35(4):295–300.
- [6]. Antony P.J., Chongdar S., Kumar P., Ramana R., *Electrochim. Acta.* 52 (2007) 3985.
- [7]. Beech I.B., Gaylarde C.C., *Rev. Microbiol.* 30 (1999) 177.
- [8] Beech I.B., *Int. Biodeterior. Biodegrad.* 53 (2004) 177.
- [9] Castaneda H., Benetton X.D., *Corros. Sci.* 50 (2008) 1169.
- [10]Wagner P ; Little B. *Materials Performance*,1993,9:65-68.
- [11] Ehrlich H.I. In:*Geo-microbiology*, M.Dekker, New York, 1996, 338.
- [12] Reza Javaherdashtia, R.K. Singh Ramanb, C. Panterc, E.V. Perelomad, *Microbiologically assisted stress corrosion cracking of carbon steel in mixed and pure cultures of sulfate reducing bacteria*, *Int. Biodeter. Biodegr.* 58 (2006) 27–35.
- [13] Reza Javaherdashti, *Impact of sulphate-reducing bacteria on the performance of engineering materials*, *Appl Microbiol Biotechnol*, 91 (2011)1507–1517.
- [14] W. Sand, T. Gehrke, *Microbially Influenced Corrosion of Steel in Aqueous Environments*, *Reviews in Environmental Science and Biotechnology*, Volume 2, Issue 2-4, (2003) 169–176.
- [15] Michael J. Franklin, David C. White, Hugh S. Isaacs, *Pitting corrosion by bacteria on carbon steel, determined by the scanning vibrating electrode technique*, *Corrosion Science*, 32 (1991) 945–952.

# Study of Glassy Carbon Films Synthesized Using Natural Precursor

Dattatray E. Kshirsagar\*<sup>1</sup>, Harish K. Dubey<sup>1</sup>, K. D. Barhate<sup>2</sup>, Maheshwar Sharon<sup>3</sup>

<sup>1</sup>Nanotech Lab., Department of Physics, B. K. Birla College, Kalyan (W), Maharashtra, India

<sup>2</sup>Department of Chemistry, B. K. Birla College, Kalyan (W), Maharashtra, India

<sup>3</sup>Walchnad Centre for Nanotechnology and Bionanotechnology, Walchand College of Arts and Science, Solapur, Maharashtra, India

## ABSTRACT

Thick films of glassy carbon were synthesized at 800°C using natural oil vapour deposition of Pongamia glabra oil. Scanning electron microscopy, X-ray diffraction, and micro-Raman spectroscopic study of the sample showed the disordered graphitic nature of films. Study of magnetic behaviour with hysteresis loop has shown a ferromagnetic nature.

**Keywords:** Glassy Carbon, Natural Oil Vapour Deposition, Magnetic Behaviour

## I. INTRODUCTION

Films of glassy carbon (GC) are an interesting form of disordered carbon, having physical and chemical properties similar to those of diamond like carbon (DLC) [1]. It is a mixture of amorphous and nano crystalline carbon, commonly having sp<sup>3</sup> and sp<sup>2</sup> chemical bonds. These carbon materials have a variety of potential applications due to their characteristics similar to those of DLC films and additional properties of higher conductivity and thermal resistance than DLC. The physical properties of GC including low density, chemical inertness, closed porosity, thermal stability, electrical conductivity and glass-like isotropic properties allow its application in the aerospace, medical, mechanical, chemical, semiconductor industries [2-10]. As an interesting material, we have performed some magnetic measurement on GC films and reporting the experimental evidences of its ferromagnetic behaviour.

## II. METHODS AND MATERIAL

Natural oil of Pongamia glabra seeds was used for synthesis of thick films of glassy carbon with natural oil vapour deposition method. Here, the crude oil of pongamia glabra seed was pyrolysed and deposited on quartz substrate at reaction temperature of 800°C. Hydrogen was used as carrier gas to carry the oil vapours in the reaction zone of the furnace and deposited as a film. Samples were annealed for 45 minutes in hydrogen atmosphere.

## III. RESULTS AND DISCUSSION

Micro-Raman Spectrum of GC film shows three broad peaks at 1356 cm<sup>-1</sup>, 1600 cm<sup>-1</sup> and 1930 cm<sup>-1</sup>. Here, Raman shift Peak located at 1356 cm<sup>-1</sup> corresponds to sp<sup>3</sup> carbon bond of multi-crystalline graphite[11] and is designated as the D-peak that means disordered[12, 13] allowed zone edge, A<sub>1g</sub> mode of graphite. Such peak is due to the breathing modes of A<sub>1g</sub> symmetry involving phonons near the K-zone boundary [13-16]

and has contributions from both highly defective  $sp^3$  carbon and disordered  $sp^3$  carbon. This mode is forbidden in perfect graphite and only becomes active in the presence of disorder [17]. The second peak at  $1600\text{ cm}^{-1}$  is more intense and related to the  $sp^2$  carbon bond, designated as G-peak, zone centre  $E_{2g}$  phonon mode at around  $1580\text{ cm}^{-1}$  to  $1600\text{ cm}^{-1}$ . The peak located at  $1930\text{ cm}^{-1}$  of Raman spectra (figure 1), indicates that GC film can have a significant fraction of carbon-carbon  $sp$  chains and peak assigned to a stretching vibration of the  $sp$  carbon chain, normally located at about  $1900\text{--}2000\text{ cm}^{-1}$  [18]. The decrease in intensity of this peak may be a result of destruction of  $sp$  phase due to its exposure to air [19].

Ratio of intensity of D- peak ( $I_D$ ) and G-peak ( $I_G$ ) for film was calculated to be  $\sim 0.95$ . This ratio correlates with the in-plane graphite crystallite size  $L_a$ , according to the relationship,  $L_a = 4.4I_G/I_D$  (in nm) [13]. The calculated value of  $L_a$  is  $4.6\text{ nm}$ , implying the microcrystalline graphite planar crystal size is about  $4.6\text{ nm}$  in the formed GC film. By using the polynomial equation [20] developed on the basis of data presented in the references [17, 21],

$$sp^3\text{content} = 0.24 - 48.9(\omega_G - 0.1580) \quad (1)$$

Here, unit of  $\omega_G$  has taken as inverse of micrometre unit [22]. Using the shift in G-peak position in the above equation, the changes in  $sp^3$  content in the films can be calculated. In our GC film  $\sim 15\%$  of  $sp^3$  type of carbon was found for  $1600\text{ cm}^{-1}$ . SEM image of GC film (figure 2) shows that the film is made of a continuous amorphous carbon layer.

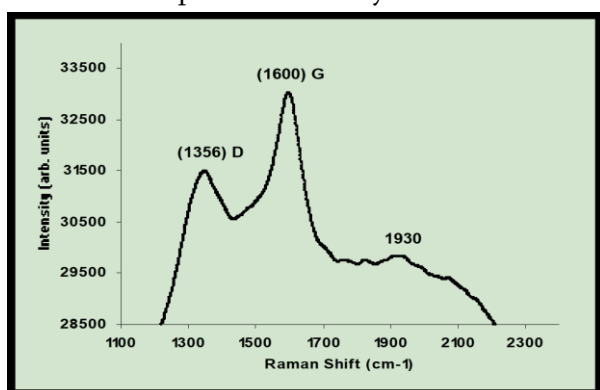


Figure 1 .Raman spectra of GC film

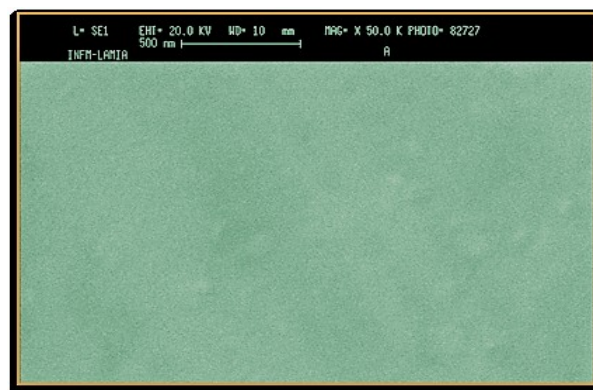
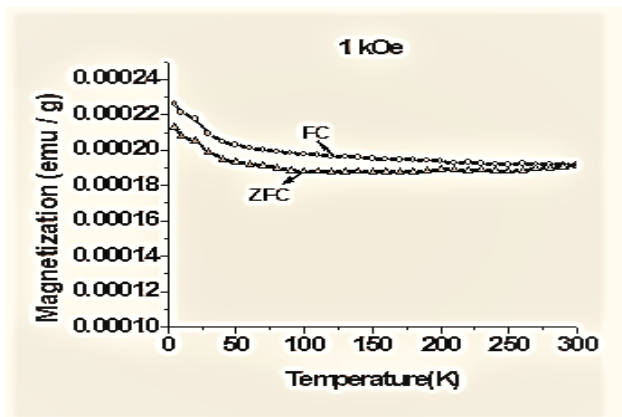


Figure 2. SEM image of GC film

In the XRD data spectrum, which is analogous to the spectrum [3] given by Z. Zeng *et al* for glassy carbon [23], two broad peaks at (002) and (101) was observed. These broad peaks were the indication of a disordered material, where the crystallinity of the sample was far from the crystal material [24].

A hysteresis for the GC film (figure 3) at comparatively low field  $H=1\text{ kOe}$ , clearly gives the evidence of ferromagnetic behaviour. Moreover, the curve asymptotically tends to a quite large positive value possibly due to the presence of ferromagnetic impurities [24]. To confirm such ferromagnetic behaviour magnetization hysteresis loops were measured in the field range between  $-50\text{ kOe}$  to  $+50\text{ kOe}$ . A typical ferromagnetic like hysteresis loop was observed for GC films (figure 4) which provides a relation between the magnetization ( $M$ ) and applied field ( $H$ ). The saturation magnetization ( $M_s$ ) was observed  $\sim 4.4\text{ kOe}$  at  $0.000618\text{ emu/g}$ . It is a main characteristic of the hysteresis loop, which is normally observed, when all the magnetic moments are aligned along a common direction that results in the largest value of the magnetization.



**Figure 3.** M–T curves for GC film under zero-field-cooling (ZFC) and field cooling (FC)

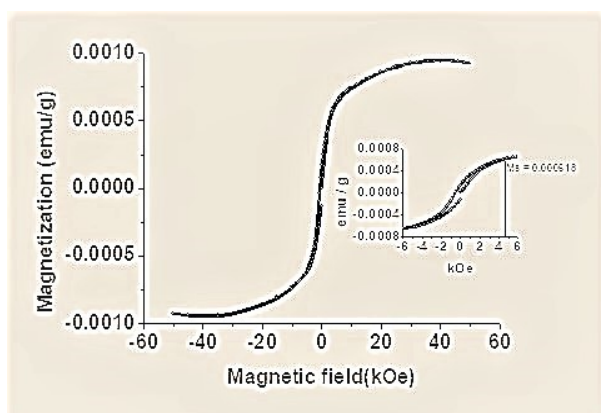


**Figure 4.** Hysteresis loop for GC films

Remnant magnetization, which is the leftover magnetization, has value 0.000121 emu/g. From the above data of SQUID measurement, it is clear that, the GC films synthesized from Pongamia glabra oil have ferromagnetic property. Here, the ferromagnetism may couple the paramagnetism of common amorphous carbon with some ferromagnetic clusters formed by defects during the formation of film. This possibility is supported by the micro-Raman spectrum of GC film (figure 1), as the film is made of disordered  $sp^2$  and  $sp^3$  network along with some carbon-carbon  $sp$  state. It means, such ferromagnetic behaviour of material can be ascribed to the structural instability that can coexist during the process of graphitization.

## IV. CONCLUSION

Carbon films with glassy surface can synthesized from pongamia glabra oil by vapour deposition method. Study of its morphology as well as reasonable magnetic response reveals occurrence of ferromagnetic response in accordance with applied field, if we take into account that the structural changes have a great impact on this magnetic behaviour evolution. However, further study is necessary to explain the magnetic behaviour of such films.

## V. REFERENCES

- [1] Yasumaru N., Miyazaki K. and Kiuchi J.2004. Appl. Phys. A ( 2004).
- [2] Lausevic Z. and Jenkins G.M. 1986 . Carbon(1986)
- [3] Yun-Soo Lim, Hee-Seok Kim, Myung-Soo Kim, Nam-Hee Cho and Sahn Nahm.2003 .Macromol. Res.(20030)
- [4] Fukuyama K. and Nishizawa T.,Nishikawa K.2001. Carbon( 2001)
- [5] Fukuyama K., Nishizawa T. and Nishikawa K.2001. Carbon, (2001)
- [6] Gary W. J., Morgan W.C., Cox J. H.and Woodruff E. M.1972. Carbon( 1972)
- [7] Yoshida A., Kaburagi Y.and Hishiyama Y.1991. Carbon ( 1991)
- [8] Botelho E.C., Scherbakoff N.and Rezende M.C.2001. Carbon, (2001)
- [9] Kaae J. L.1985. Carbon ( 1985)
- [10] Fischbach, D.B.1971. Carbon( 1971)
- [11] Paul K. Chu, Liuhe Li.2006. Mater. Chem. Phys.( 2006)
- [12] Robertson J.2002. Mater. Sci. Eng. Rep.( 2002)
- [13] Tuinstra F. and Koenig J. L.1970. J. Chem. Phys.(1970)
- [14] Lespade P., Marchard A., Couzi M. and Cruege F.1984. Carbon, (1984)
- [15] Nemanich R. J.and Solin S. A. 1979. Phys. Rev. B( 1979)

- [16] Lespade P., Al-Jishi R. and Dresselhaus M. S. 1982. Carbon( 1982)
- [17] Ferrari A.C. and Robertson J. 2000. Phys. Rev. B(2000)
- [18] Qiang Wang, Fangyu Cao and Qianwang Chen. 2005. Green Chem.( 2005)
- [19] Ferrari A.C. and Robertson J. 2004. Phil. Trans. R. Soc. Lond. A( 2004)
- [20] Singha A., Ghosh A., Ray N.R. and Roy A. 2006. Cond. Mat. mtrl. sci.( 2006)
- [21] Tamor M.A., Vassell W.C. and Carduner K.R. 1991. Appl. Phys. Lett. ( 1991).
- [22] Dattatraya E. Kshirsagar, Vijaya Puri, Madhuri Sharon, Sandesh Jaybhaye, Rakesh A. Afre, Prakash Somani, and Maheshwar Sharon. 2009. Advanced Science Letters (2009)
- [23] Zeng Z., Natesan K. and Maroni V. A. 2002. Oxid. Met.( 2002)
- [24] D. E. Kshirsagar, Harish K. Dubey, Vijay Jadhav and Maheshwar Sharon. 2015. Advanced Science, Engineering and Medicine (2015), doi:10.1166/asem.2015.1706



# Effect of Euphorbia Tirucalli L. Extracts on Brain and Muscle Proteins of Fish

Kranti Ozarkar\*<sup>1</sup>, Mayur Rao<sup>2</sup>, Geetha Unnikrishnan<sup>3</sup>

\*<sup>1</sup>Department of Zoology, Birla College, Kalyan, Maharashtra, India

<sup>2</sup>Department of Biotechnology, Birla College, Kalyan, Maharashtra, India

<sup>3</sup>Department of Zoology, Birla College, Kalyan, Maharashtra, India

## ABSTRACT

Euphorbia tirucalli has a number of medicinal uses along with toxic effects attributed to the plant. This plant is mainly used for its fish stupification and piscicidal activities by tribals of Gond tribe of Kawal Wild Life Sanctuary, Andhra Pradesh, southern Rajasthan, southern Maharashtra in India and Africa [2][3][4][5]. The present study aims to identify the effect of E. tirucalli extracts on skeletal muscles and brain protein composition, as the contraction and relaxation of skeletal muscles is responsible for normal swimming movements of the fish. The altered swimming movements are indicative of effect of plant extracts on these proteins. For the current study three different extracts of E. tirucalli were prepared and their effects were observed on the fish, Tilapia. Protein samples were prepared from skeletal muscles and brain tissues. These samples were separated with the help of SDS-PAGE and Agarose Gel Electrophoresis. The results indicated denaturation of certain protein bands in the plant extract treated muscle and brain proteins of the fishes.

**Keywords:** Euphorbia tirucalli, Piscicidal activity, Stupification of Fish, Protein, SDS-PAGE, AGE

## I. INTRODUCTION

Fish catching with the aid of plants is an ancient practice. Plants have been used in various parts of the world by people from times immemorial for poisoning or stupifying fish. This practice is one of the great biological and ethnological interest. All parts of the plants are used; but in most cases a certain part such as the bark or root in which the toxic principles are located are utilized. Such plants contain different phytochemicals like alkaloids, coumerins, resins, saponins, diosgenin etc. [1] [2][4][5]

Family Euphorbiaceae has a reputation of having incredibly toxic plants. Some of the Euphorbia plants are used in folk medicine to cure skin diseases, gonorrhoea, migraines, intestinal parasites, and warts. The genus Euphorbia has been the source of large number of biological active compounds. Tannins,

flavonoids, unsaturated sterols/triterpenes, carbohydrates, lactones and proteins/amino acids were reported as major active constituents of some Euphorbia species [6]. Euphorbia tirucalli L. (Family: Euphorbiaceae) is a succulent cactus-like plant growing to a height of about 10 M. It was introduced from Africa as a garden plant. E. tirucalli grows in arid zones as well as zones that are more mesophytic, the species makes a good living fence post. E. tirucalli is also called petroleum plant because it produces a hydrocarbon substance similar to gasoline [6]. Whole plant harvesting is worthwhile from energy point-of-view with rubber, petroleum, and alcohol as energy products and resins, which may find use in the linoleum, oilskin and leather industries. The charcoal derived from plant can be used in gunpowder[7][8]. The dried latex contains resin which is a principle constituent (75.8-82.1%). The stem contains

hentriacontene, hentriacontanol, the antitumor steroid 4-deoxy-phorbol ester, beta-sitosterol, caoutchouc, casuarinin, corilagin, cycloeuphordenol, cyclotrucanenol, ellagic acids, euphorbins, euphol, euphorone, euphorcinol, gallic acids and glucosides[9][10]. A variety of diterpenoids with antibacterial, anticancer, prostaglandin E2-inhibitory, antifeedant, anti-HIV, and analgesic activity have also been isolated from different *Euphorbia* species [22]. They include jatrophone, ingenol and myrsinane diterpenoids. These diterpenoids are reported to act in diverse ways; they are found to be skin- irritants, tumour-promoters [11]. In addition to anti-tumour activity, several species of this genus have been investigated for their immunomodulatory activity and some immunotoxic, immunosuppressive and immunostimulatory effects. These broad range and diversity of biological activities in the *Euphorbia* genus, is perhaps due to the presence of various components with different modes of action in the plants [13][14][15][16]. Adverse effect of aqueous extracts of *Euphorbia tirucalli* on respiratory pathway of fish is studied. The extract also cause energy crisis during stress by suppressing ATP level [17][18].

Many workers in India have documented their work on piscicidal effect of various plants and plant parts including *Euphorbia tirucalli*. Piscicidal effect of some common plants were studied against target animals of fresh waterbodies in India by Digvijay Singh and Ajay Singh in 2002 [19]. In 1995, Poisonous effects of *Euphorbia tirucalli* on fish was studied by Kamat and Muthe [20]. Effects of *Euphorbia tirucalli* latex on blood calcium and phosphate of the freshwater air-breathing catfish *Heteropneustes fossilis* was studied by Abhishek Kumar et al(2010) [18]. In 2003, Toxicity of *Euphorbia tirucalli* plant against fresh water target and non-target organisms were studied by Tiwari et al.[21] From literature survey it is evident that though piscicidal effect of *Euphorbia tirucalli* is studied, toxic effects of *Euphorbia tirucalli* on skeletal muscles and brain protein of fish are not investigated. The current

study gives an insight on the effects of various extracts of *Euphorbia tirucalli* on fish muscles and brain, which are required for swimming action and its co-ordination. During the current investigation proteins from muscles and brain are analyzed using electrophoretic technique so as to observe any degenerative changes.

## II. METHODS AND MATERIAL

### A. Extraction of Plant material and Treatment Given to *Tilapia* Fish:

A plant material of *Euphorbia tirucalli* was collected from college campus. The twigs and stem of plant *Euphorbia tirucalli* were dried in shade and were powdered. Extractions were prepared using dried plant powder as well as fresh plant materials. Three types of extracts were prepared as follows-

1. **Extract 1: Crude aqueous extract:** Fresh stem and twigs were macerated in 3 ml of distilled water using mortar and pestle and filtered using muslin cloth.
2. **Extract 2: 100% Ethanolic Soxhlet extract:** Fresh stem and twigs of the plant were macerated and then extracted using ethanol in Soxhlet apparatus for 8hrs. The ethanolic extract thus obtained was dried using flash evaporator. A dried extract was dissolved in 10 ml of ethanol. This extract was used as ethanolic plant extract for estimation of change in protein profile (Kamath & Muthe, 1995) [7].
3. **Extract 3: Alkaloid extract:** Plant alkaloids are major fraction playing important role in piscicidal activity; hence alkaloids were extracted from the stem and twigs of *E. tirucalli*.

These extracts were used for the study of stupification and piscicidal activity on commonly available fresh water fish *Tilapia*. The fishes were divided in four groups and each group containing six fishes. They were acclimatized for a period of 24 hrs to the laboratory conditions and the doses of above

mentioned extracts were prepared as mentioned in table 1

**Table 1**

EXTRACT	CONCENTRATION	QUANTITY	TIME PERIOD
1	2ppm	100 µl	6 hrs
2	2ppm	100 µl	6 hrs
3	2ppm	100 µl	6 hrs
1	10 ppm	100 µl	6 hrs
2	10 ppm	100 µl	6 hrs
3	10 ppm	100 µl	6 hrs
1	20 ppm	100 µl	6 hrs
2	20 ppm	100 µl	6 hrs
3	20 ppm	100 µl	6 hrs
Control-1	Ethanol	100 µl	6 hrs
Control-2	Distilled Water	100 µl	6hrs

During the treatment period of 6hrs, the fishes were observed for behavioural and physiological changes. After the treatment period, fishes from all four groups were sacrificed and skeletal muscles and brain tissue was procured. The tissues thus procured were then used for analysis of proteins.

### B. Extraction Of Protein From Fish and Quantitative Protein Estimation by Barfords' Method:

Fishes were dissected to obtain muscle and brain tissue at 4-6 °C.



Muscle and brain tissue were taken in separate petriplates containing 1X Phosphate buffer (pH 7.4)



Homogenize the tissues with chilled 1X phosphate buffer (pH 7.4)



The homogenized tissue sample was cold centrifuged at



4 °C at 3000 rpm for 10 minutes (Gupta & Mullins, 2010) [23]

Supernatant was collected in pre-chilled centrifuge tube and was used as protein sample.

Fishes from control group were used for quantitative protein estimation by Barfords' method.

The protein samples extracted from all four groups were separated by SDS-PAGE and Agarose gel electrophoresis.

### C. Electrophoresis of Fish Brain and Muscle protein:

1. SDS-Polyacrylamide Gel Electrophoresis was performed by using standard HIMEDIA SDS-PAGE Kit (HTP001) for all four groups with brain and muscle proteins extracts. The gels thus obtained were stained with Coomassie Brilliant Blue R (CBB-R) stain and Silver Stain. Silver staining is the most sensitive protein staining method available for gel electrophoresis. It can efficiently detect minute quantity such as 5 ng protein in a 2.5 mm wide band in 0.75 mm thick gel. Different proteins give different intensity of the staining. [22]
2. Agarose Gel Electrophoresis was performed for separation of muscle and brain protein samples from fish.

It was carried out using HIMEDIA Genomic DNA isolation AGE kit. A standard procedure of gel preparation was followed.

## III. RESULTS AND DISCUSSION

The fishes were exposed to 2ppm, 10ppm and 20ppm concentrations of crude aqueous extract, 100%

ethanolic Soxhlet extract and alkaloid extract for a period of 6hrs as mentioned in the Table II.1.

The results indicated that on exposure to low concentration of 2ppm of all three extracts, fishes survived the treatment period of 6 hrs without any signs of discomfort or irritation. When the fishes were treated with 10ppm concentration of all three extracts, they exhibited primary irritation for 15min. to 20 min. Redness near gills region was also observed. After exposure to 20ppm concentrated extracts, fishes showed increased levels of discomfort and irritation. There was a prominent redness near gills. Fishes were also observed to gasp for air. For crude extract and ethanolic extract, these symptoms lasted for 30mins. But the fishes eventually recovered. In case of 20 ppm alkaloid extract, these symptoms persisted for almost 40 mins and fishes also exhibited stupification. Surfacing of the fishes was seen with no swimming activity.

Muscle and brain proteins were extracted from treated and control fishes. Proteins from muscles and brain were quantified calorimetrically by Barford's Method. The amount of protein in muscle was found to be 0.3194 % and in brain it was 0.8429 %. The protein quantity was observed to be sufficient to carry out protein separation by SDS-PAGE and Agarose gel electrophoresis (AGE).

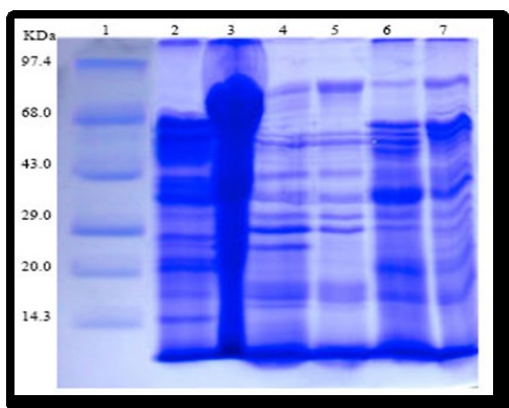


**Figure 1.** Brain Protein Separation By SDS- PAGE

Lane 1- Protein Marker.

Lane 2- Control Muscle Protein.

Lane 4- Muscle Protein Treated with Extract 1.

Lane 5- Muscle Protein Treated with Extract 2.

Lane 6- Muscle Protein Treated with Extract 3.

Lane 7- Muscle Protein Treated with Extract 3

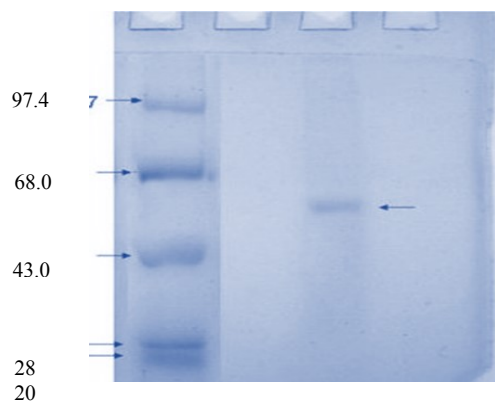


**Figure 2.** Brain Protein Separation By SDS- PAGE

Lane 1- Protein Marker

Lane 3- Control Fish Brain Protein

Lane 4- Treated Fish Brain Protein

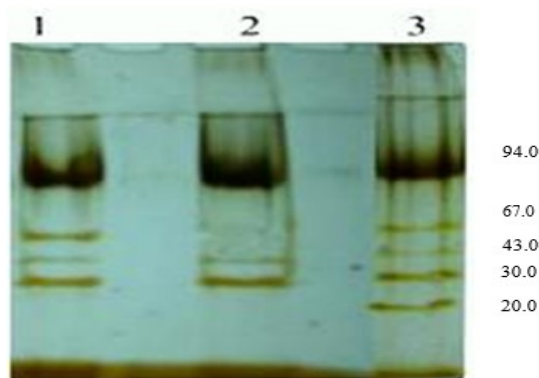


**Figure 3.** Silver Staining of SDS-PAGE of Muscle Protein

Lane 1- Control Fish Muscle Protein.

Lane 2- Extract 3 Treated Fish Muscle Protein.

Lane 3- Protein Marker.

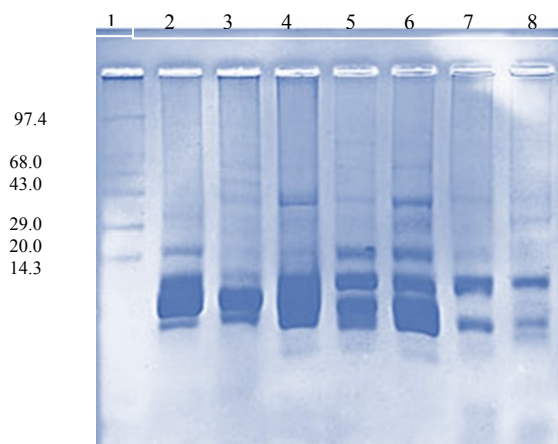


**Figure 4.** AGE Separation of Fish Muscle and Brain Protein By CBB Staining

Lane 1- Protein Marker.  
Lane 2- Control Brain Protein.  
Lane 3- Extract 2 Treated Brain Protein.  
Lane 4- Extract 3 Treated Brain Protein.  
Lane 5- Extract 1 Treated Muscle Protein.  
Lane 6- Control Muscle Protein.  
Lane 7- Extract 2 Treated Muscle Protein.  
Lane 8- Extract 3 Treated Muscle Protein.

Muscle and brain protein samples extracted from treated and control fish were separated by SDS- PAGE and Agarose Gel Electrophoresis

#### **Separation of Muscle Protein:**

Muscle protein separation carried out using SDS-PAGE, resulted in an altered protein behavior between 97.4 KDa and 68.0 KDa molecular weight region. Hence, it can be concluded that protein in this region is sensitive to the phytochemical constituents of Euphorbia tirucalli extract.

#### **Silver Staining Evaluation of Muscle Protein:**

Silver staining of muscle protein showed alteration pattern in protein, where in it was observed that a single band of molecular weight 68.0 KDa was absent. This also indicates alteration of protein structure of fish under the influence of phytochemical fractions of the Euphorbia tirucalli extract.

#### **Separation of Brain Protein:**

When brain protein samples were separated on SDS-PAGE, it showed a single band from control protein sample. Treated protein samples did not show any band separation on electrophoresis. These type of results may be observed due to denaturation of brain proteins under the influence of phytochemicals of the extracts or due to unfavourable laboratory conditions.

#### **Separation of Proteins By Agarose Gel Electrophoresis (AGE):**

When muscle and brain protein samples were separated by agarose gel electrophoresis, it showed following results-

When alcoholic and alkaloid extracts treated fish muscles and brain proteins were separated on AGE; it was observed that there was absence of bands situated at position 97.4 KDa, 68.0 KDa and one more band at 43.0 KDa molecular weight region. This indicated that fish muscle and brain contains proteins which are sensitive to phytochemicals of Euphorbia tirucalli. This result was more prominent in alkaloid extract of E. tirucalli.

### **IV. CONCLUSION**

The present study, thus reveals the protein denaturation from muscles and brain of fish Tilapia under the influence of extracts of Euphorbia tirucalli. The alkaloid fraction of plant extract was observed to show degenerative effect on muscle protein of molecular weight 97.4 KDa to 68.0 KDa as these bands were absent in the separated brain and muscle proteins by SDS-PAGE and AGE of treated fishes. It was also observed that one more band of protein situated at 43.0 KDa region was absent, when brain and muscle proteins were separated by Agarose gel electrophoresis. All these results thus indicate that the piscicidal and stupification activities exhibited by Euphorbia tirucalli are due to denaturation of certain proteins which are required for normal swimming behavior of the fish. The contraction and relaxation of skeletal muscles is responsible for normal swimming movement. The degeneration of brain proteins lead to loss of control and co-ordination. The altered swimming movement was indicative of effect of Euphorbia tirucalli extracts on these proteins. It was also observed that alkaloid extract (Extract 3) was most effective in denaturation of these proteins as compared to other two extracts. The alkaloid component was also observed to cause air grasping problem which leads to redness near gill region of Tilapia.

## V. REFERENCES

- [1] Indian Plants Reported as Fish Poison, Raizada M. B. & Verma S. B., Indian Fors. , 1937, 63, 198
- [2] Fish Stupifying Plants employed by tribals of southern Rajasthan- A Probe, Curr.Sci, 1986, 55, 647-650
- [3] Fish Stupifying plants used by Tribals of North Maharashtra, Pawar S, Patil M. V. and Patil D. A., Ethanobotany, 2004, 16, 136-138.
- [4] Plants used for poison fishing in tropical Africa, Neuwinger, H. D., Toxicon (2004), 44 (4), 417-430CODEN: TOXIA6; ISSN: 0041-0101. (Elsevier)
- [5] Piscicidal plants used by Gond tribe of Kawal wild life sanctuary, Andra Pradesh, India, E. N. Murthy, C. Pattanaik, C. S. Reddy, v. S. Raju., Indian Journal of natural Products and Resources, V1(1), March 2010, pp 97-101.
- [6] Euphorbia tirucalli L. (Euphorbiaceae)-the miracle tree: current status of available knowledge. Julius M, Damme PV. Sci Res Essay 2011; 6(23): 4905-14.
- [7] Biogas production potential of Euphorbia tirucalli L. along with cattle manure; Rajasekaran, P.; Swaminathan, K. R.; Jayapragasam, M.; Biological Wastes (1989), 30 (1), 75-7CODEN: BIWAED; ISSN:0269-7483.
- [8] Hydrocarbons from plants: analytical methods and observations; Calvin, Melvin; Naturwissenschaften (1980), 67 (11), 525-33CODEN: NATWAY; ISSN: 0028-1042.
- [9] Tirucallicine - a new macrocyclic diterpene from Euphorbia tirucalli; Khan, Abdul Qasim; Rasheed, Tahir; Malik, Abdul; Heterocycles (1988), 27 (12), 2851-6CODEN: HTCYAM; ISSN:0385-5414.A taraxerane type triterpene from Euphorbia tirucalli; Rasool, Nazli; Khan, Abdul Qasim; Malik, Abdul; Phytochemistry (1989), 28 (4), 1193-5CODEN: PYTCAS; ISSN:0031-9422.
- [10] A new macrocyclic diterpene ester from the latex of Euphorbia tirucalli; Khan, Abdul Qasim; Malik, Abdul; Journal of Natural Products (1990), 53 (3), 728-31CODEN: JNPRDF; ISSN:0163-3864.
- [11] Toxicological screening of Euphorbia tirucalli L.: developmental toxicity studies in rats.,Silva Aldo Cesar Passilongo; de Faria Dieime Elaine Pereira; Borges Nathalia Barbosa do Espirito Santo; de Souza Ivone Antonia; Peters Vera Maria; Guerra Martha de Oliveira, Journal of ethnopharmacology (2007), 110 (1), 154-9 ISSN:0378-8741.
- [12] Activation of the Epstein-Barr virus lytic cycle by the latex of the plant Euphorbia tirucalli; MacNeil, A.; Sumba, O. P.; Lutzke, M. L.; Moormann, A.; Rochford, R.; British Journal of Cancer (2003), 88 (10), 1566-1569CODEN: BJCAAI; ISSN:0007-0920. (Nature Publishing Group)
- [13] African Burkitt's lymphoma: a plant, Euphorbia tirucalli, reduces Epstein-Barr virus-specific cellular immunity; Imai S; Sugiura M; Mizuno F; Ohigashi H; Koshimizu K; Chiba S; Osato T; Anticancer research (1994), 14 (3A), 933-6 ISSN:0250-7005.
- [14] The skin irritant and tumor promoting diterpene esters of Euphorbia tirucalli L. originating from South Africa; Fuerstenberger, G.; Hecker, E.; Zeitschrift fuer Naturforschung, C: Journal of Biosciences (1985), 40C (9-10), 631-46CODEN: ZNCBDA; ISSN:0341-0382.
- [15] Tumor promotion by Euphorbia lattices; ROE F J; PEIRCE W E; Cancer research (1961), 21 (), 338-44 ISSN: 0008-5472.
- [16] Why do Euphorbiaceae tick as medicinal plants? A review of Euphorbiaceae family and its medicinal features. Mwine JT, Damme PV. J Med Plants Res 2011; 5(5): 652-62.
- [17] Effects of Euphorbia tirucalli latex on blood calcium and phosphate of the freshwater air-

- breathing catfish *Heteropneustes fossilis*, Abhishek Kumar, ManiRam Prasad, Diwakar Mishra, Sunil K. Srivastav & Ajai K. Srivastav, *Toxicological & Environmental Chemistry*, Volume 93, Issue 3, pages 585-592, 2011
- [18] Piscicidal effect of some common plants of India commonly used in freshwater bodies against target animals, Singh D, Singh A., *Chemosphere*. 2002 Oct; 49 (1):45-9. Ramesh, A. Malarvizhi, R. Petkam, *Journal of Tropical Forestry and Environment*, Vol 1, No 1 (2011)
- [19] Poisonous effects of *Euphorbia tirucalli* on fish, Kamat, DV & Muthe, PT, *Journal of Animal Morphology and Physiology*. Vol. 42, no. 1-2, pp. 65-68. Dec 1995.
- [20] Toxicity of *Euphorbia tirucalli* plant against fresh water target and non- target organisms, Sudhanshu Tiwari, Pratibha Singh, Ajay Singh, *Pakistan Journal of Biological Sciences*, 6(16):1423-1429(2003)
- [21] Antiviral Activities of Extracts of *Euphorbia hirta* against HIV-1, HIV-2 and In Vivo; Gyuris, A., szlavik, L., Minarovits, J., Vasas, A., Molnar, J. and Hohmann, J (2009); *International Journal of Experimental and Clinical Pathophysiology and Drug Research*. Vol. 23 (3), pp. 429-432.
- [22] A modified silver staining protocol for visualization of proteins compatible with matrix-assisted laser desorption/ionization and electrospray ionization- mass spectrometry; Jun X. Yan, Robin Wait, Tom Berkelman, Rachel A. Harry, Jules A. Westbrook, Colin H. Wheeler, Michael J. Dunn, 2000, *Electrophoresis*, Vol.21(17), pp.3666-3672, First published: 22 November 2002.
- [23] Dissection of organs from the adult Zebrafish; Gupta T, Mullins MC.; *J Vis Exp*. 2010 Mar 4; (37). pii: 1717. doi: 10.3791/1717.

# EPR Study of Nickel Doped Mn-Zn Ferrite Nanoparticles

L. N. Singh, F. A. Ahmed

Department of Physics, Dr. Babasaheb Ambedkar Technological University, Lonere, Raigad, Maharashtra, India

## ABSTRACT

In the present work we have synthesized  $Mn_{0.5-x}Ni_xZn_{0.5}Fe_2O_4$  ( $x=0.0, 0.1, 0.2, 0.3$ ) ferrite nanoparticles by sol-gel method. The XRD patterns confirm the synthesis of single crystalline nanoparticles. The effective g-factor,  $g_{eff}$ , linewidth  $\Delta H_{PP}$ , resonance field have been investigated at room temperature. Scanning electron microscopy (SEM) was used to characterize the surface morphology of the samples.

**Keywords:** Ferrite nanoparticles; sol-gel; XRD; SEM

## I. INTRODUCTION

Ferrites are ferromagnetic materials having a spinel structure. The general chemical formula of ferrites is  $MFe_2O_4$  where M represents divalent metallic ion like Fe, Mn, Ni, Zn, or a mixture of these. The spinel structure predicated on a face centred cubic lattice in which the sites fascinated by the cations are of two types, tetrahedral and octahedral sites [1]. This type of compounds having spinel structure exhibit a diversity of new properties which depend on the character of the cations and their site distribution through tetrahedral and octahedral sites. The electrical and magnetic properties of ferrite nanoparticles have attracted significant concentration in recent years. The properties of ferrite nanoparticles depend on method of preparation and particle size [2]. Various preparation methods have been used to synthesize ferrite nanoparticles such as sol-gel method [3], hydrothermal technique [4], ball milling [5], coprecipitation method [6]. Among these methods sol-gel method is attractive because it is simple, fast, needs cheap raw materials which consequence good homogeneity and morphology of the prepared material [7].

The properties of manganese ferrite and nickel ferrite can be changed by substitution of nonmagnetic  $Zn^{2+}$  ions which replacing  $Mn^{2+}$  ions in the A site and  $Ni^{2+}$  ions in the B site. In the substituted ferrites, Mn-Zn and Ni-Zn ferrites are commercially important class of magnetic material. Mn-Zn ferrites are the one of the most important soft ferrite which have high initial permeability, saturation magnetization and low core losses. Mn-Zn ferrites are widely used in various electronic applications such as transformers, chock coils, noise filters, recording heads, medical diagnosis etc. [8]. Ni-Zn ferrites are inexpensive magnetic materials which are useful for various technological application [9]. Ni-Zn ferrites have been used in radio frequency circuits, filters, microwave devices, antennas and transformer cores due to its high resistance and low eddy current losses [10]. Mn-Ni-Zn ferrites are technologically important materials for scientific and industrial applications. These ferrites are widely used in high frequency applications. To synthesize the ferrites with high resistivity and permeability Ni has been substituted in Mn-Zn ferrite. In this work, we investigate the influence of  $Ni^{2+}$  ions substitution on  $Mn_{0.5-x}Ni_xZn_{0.5}Fe_2O_4$  ( $x=0.0, 0.1, 0.2, 0.3$ ) ferrite nanoparticles.



## II. METHODS AND MATERIAL

Nickel substituted Mn-Zn ferrite nanoparticles were synthesized by sol-gel method. Analytical grade manganese chloride, nickel chloride, zinc chloride and iron chloride were used as a starting materials. In the first, calculated amount of metal chlorides were weighed accurately and dissolved in distilled water. The solution was then heated with constant stirring and appropriate amount of ammonia solution was added to preserve the pH between 6 and 7. We added citric acid to remove the insoluble residue and ethylene glycol for homogeneity. After getting gel, it was then heated in an oven at 250°C for instinctive ignition and the slack powders were then crushed adequately. The obtained powders were then annealed at 800°C for 3 hours and sintered at 1100°C for 1 hour. The prepared samples were characterized for phase identification, crystallite size, lattice parameter, crystallite density resolution by using x-ray diffractometer. EPR spectra were recorded by using X-band Varian's (E-112) spectrometer. For morphology analysis of the samples scanning electron microscope (Hitachi-48000) was used.

## III. RESULTS AND DISCUSSION

### A. Structural Characterization

The sol-gel prepared ferrite nanoparticles were characterized by XRD for structural studies. The X-Ray Diffraction patterns for the samples  $Mn_{0.5-x}Ni_xZn_{0.5}Fe_2O_4$  ( $x=0.0, 0.1, 0.2, 0.3$ ) is shown in figure 1. This XRD patterns exhibit the configuration of single phase cubic spinel structure and the diffraction peaks were indexed by using JCPDS. All the experimental peaks were in good agreement with the theoretically generated one. The peaks indexed to (220), (311), (222), (400), (422), (511), (440), (531) and (622) planes correspond to cubic spinel structure. Besides the ferrite peaks, extra peaks comparable to the haematite phase has been observed in XRD pattern of the samples, haematite phase forms with large particle size [11]. The SEM photograph of the samples is

shown in figure 2. The morphology of the samples is porous and agglomerated.

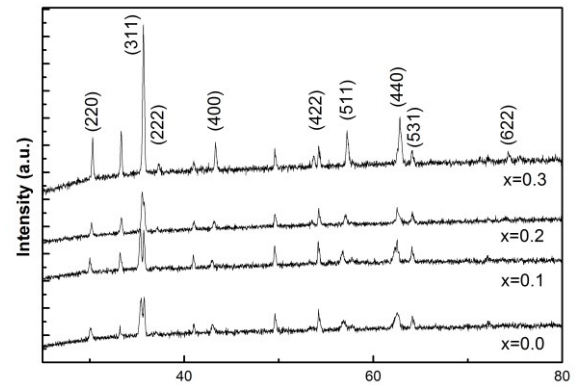


**Figure 1.** The X-ray diffractograms of  $Mn_{0.5-x}Ni_xZn_{0.5}Fe_2O_4$  ( $x=0.0, 0.1, 0.2, 0.3$ ).

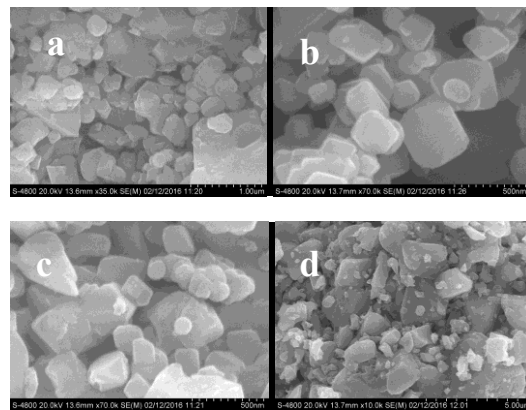


**Figure 2.** SEM photographs of  $Mn_{0.5-x}Ni_xZn_{0.5}Fe_2O_4$  ferrite nanoparticles, (a)  $x=0.0$ , (b)  $x=0.1$ , (c)  $x=0.2$ , (d)  $x=0.3$ .

### B. EPR Study

The EPR spectra of  $Mn_{0.5-x}Ni_xZn_{0.5}Fe_2O_4$  ( $x=0.0, 0.1, 0.2, 0.3$ ) were recorded at 9.1 GHz at room temperature. The EPR is important for exploring the magnetic properties of ferrite nanoparticles at high frequency since the resonance arises from the interaction among spin and electromagnetic waves. All the EPR spectra were analysed to acquire the values of different parameters such as linewidth ( $\Delta H_{PP}$ ), resonance field (B) and g-value using Lorentzian distribution function and the values are presented in table 1. The g-value is deliberated by the relation [12].

$$g = h\nu/\beta H$$

Where,  $h$  is a Planck's constant,  $\nu$  is the microwave frequency,  $\beta$  is Bohr magneton and  $H$  is the magnetic field at the resonance.

**Table 1.** EPR parameters of  $Mn_{0.5-x}Ni_xZn_{0.5}Fe_2O_4$  ( $x=0.0, 0.1, 0.2, 0.3$ )

Ni Content (x)	Linewidth ( $\Delta H_{PP}$ ) Gauss	Resonance Field (B) Gauss	g-value
0.0	1180	2930	2.22
0.1	1680	2340	2.78
0.2	1780	2190	2.97
0.3	1820	2230	2.92

G. S. Shane et al. [13] reported the decrease in spin-spin relaxation time constant with increase in nickel ion concentration. The decrease in spin-spin relaxation time is accredited to the decrease in electron motion and weakening of superexchange interaction and strengthening dipole interaction with increase in nickel ion substitution. The strong dipole interactions contribute a large linewidth ( $\Delta H_{PP}$ ) and g-value. It has been observed that the linewidth ( $\Delta H_{PP}$ ) increases with the increase in nickel substitution. This is probably due to increasing dipolar interaction through cations and oxygen ions [14].

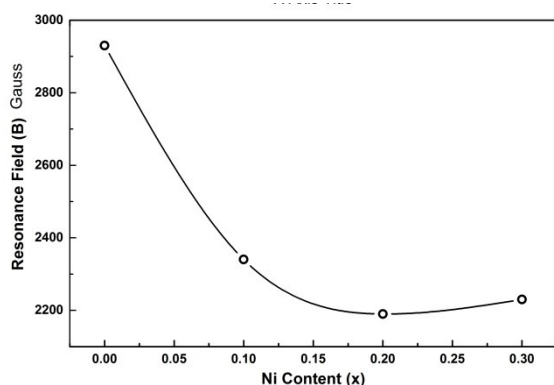


**Figure 3.** Variation of Resonance Field with Ni content.

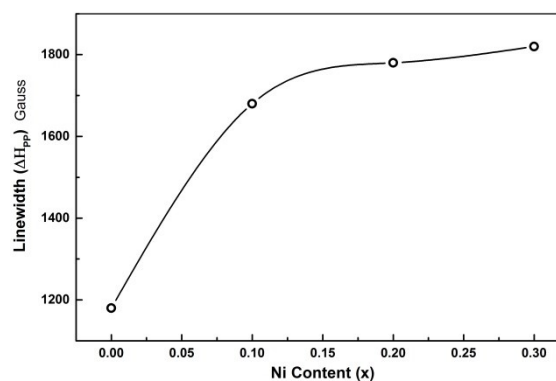


**Figure 4.** Variation of Linewidth ( $\Delta H_{PP}$ ) with Ni content.

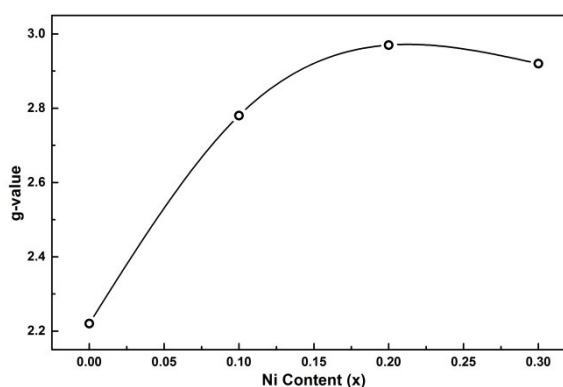


**Figure 5.** Variation g-value with Ni content.

#### IV. CONCLUSION

We have investigated structural and magnetic properties of sol-gel prepared  $Mn_{0.5-x}Ni_xZn_{0.5}Fe_2O_4$  ( $x=0.0, 0.1, 0.2, 0.3$ ) ferrite nanoparticles. The linewidth increases with increase of nickel ion concentration which is due to leading dipole-dipole interactions. It has been observed that g-value increases by Ni substitution from 2.22 to 2.97. This can be interpreted by spin-spin and spin lattice relaxation.

#### V. REFERENCES

- [1] Kurian M., Nair D. S., Journal of Saudi Chemical Society (2013), <http://dx.doi.org/10.1016/j.jscs.2013.03.003>
- [2] S. R. Kulkarni, Priyanka U. Londhe, N. B. Chaurse, J. Mater Sci: Mater Electron (2013) 24:4186-4191, DOI 10.1007/s 10854-013-1381-1

- [3] C. Venkataraju, R. Paulsingh, *Int. J. Nano Dimens.* 6(3): xxx-xxx, Summer 2015, ISSN: 2008-8868
- [4] Kandasamy Velmurugan, Vellaiyappan Sangli Karuppanan Venkatachalapathy, Sechassalom Sendhilmathan, *Materials Research*, 2010; 13(3): 299-303
- [5] Xuebo Cao and Li Gu, *Nanotechnology* 16(2005), 180-185, doi: 10.1088/0957-4484/16/2/002.
- [6] Kurikka V. P. M. Shafi and Aharon Gedanken, *Chem. Mater.* 1998, 10, 3445-3450.
- [7] Majid Niaz Akhtar, Nadeem Nasir, Muhammad Kashif Noorhana Yahya, Mukhtar Ahmad, Gulam Murtaza, Muhammad Azhar Khan, M. H. Asif, A. Sattar, R. Raza, M. Saleem, S. N. Khan, *Progress in Natural Science Materials International* (2014), <http://dx.doi.org/10.1016/j.pnsc.2014.06.005>.
- [8] I. C. Masthoff, A. Gutsche, H. Nirsche, H. Nirsche G. Garnweitner, *Royal Society of Chemistry* (2015), 17, 2464-2470.
- [9] Yang Yiqing, Zheng Liang, Zheng Hui, Yan Xui, Yan Xuefei, *Proceedings of the 2012, 2<sup>nd</sup> International Conference on Computer and Information Application (ICCIA 2012)*.
- [10] K. Rama Krishna, K. Vijaya Kumar, C. Ravindernathgupta, Dachepalli Ravinder, *Advances in Materials Physics and Chemistry*, 2012, 2, 149-154.
- [11] C. Rath, K. K. Sahu, S. Anand, S. K. Date, N. C. Mishra, R. P. Das, *Journal of Magnetism and Magnetic Materials* 202 (1999) 77-84.
- [12] Kisan Zipare, Jyoti Dhumal, Sushil Bandgar, Vikas Mathe, Guruling Shahane, *Journal of Nanoscience and Nanoengineering* Vol. 1, No. 3, 2015, pp. 178-182
- [13] G. S. Shahane, Ashok Kumar, Manju Arora, R. P. Pant, Krishan Lal, *Journal of Magnetism and Magnetic Materials*, 322 (2010) 1015-1019
- [14] Ashok Kumar, Promod Kumar, Geeta Rana, M. S. Yadav and R. P. Pant, *Appl. Sci. Lett.* 1(2) 2015, 33-36.

# Synthesis & Thermal, Optical & Dielectric characteristics of Gadolinium doped $\text{EuF}_3$ nanoparticles in presence of $\alpha$ - glycine

Manoj P Mahajan<sup>\*1</sup>, M. M. Khandpekar<sup>2</sup>

<sup>1</sup>Department of Physics, A. P. Shah Institute of Technology, Opp. Hypercity Mall, G. B. Road, Thane, Maharashtra, India

<sup>2</sup>Material Research Laboratory, Birla College of Arts, Science & Commerce, Kalyan, 421304, Maharashtra, India

## ABSTRACT

$\text{EuF}_3$ : Gd nanoparticles have been synthesized in the presence of  $\alpha$ - glycine via chloride route at room temperature. The synthesised nanoparticles shows hexagonal phase with lattice parameters  $a = b = 6.920 \text{ \AA}$  and  $c = 7.085 \text{ \AA}$  (JCPDS No. 32-0373). The average size of nanoparticles calculated with Debye- Scherer equation was found to be 51 nm. Thermal characteristics were studied from TGA/DTA spectrum and it shows decomposition in two stages. UV-VIS studies show three wavelengths which find applications in optoelectronic devices. Dielectric studies explained d.c conduction process.

**Keywords:** Glycine, Chloride Route, Hexagonal Phase, Decomposition, Optoelectronic.

## I. INTRODUCTION

Dielectric material plays vital role in the construction of microcircuits. Because of the high permittivity and stable thermal as well as chemical properties rare earth materials have attracted researcher and are widely used as dielectric materials [1,2]. Literature review tells us that there are fewer reports on dielectric properties of  $\text{EuF}_3$  nanoparticles. Because of sharp emission lines, rare earth material also finds application in the field of optoelectronic devices. Water solubility limits the use of rare earth material in biological fields. Surface modification makes it water soluble that can be done by adding organic ligands.

## II. EXPERIMENTAL

$\text{EuF}_3$  nanoparticles were synthesised via chloride route and to reduce agglomeration microwave drying was employed. The solution of  $\text{EuCl}_3 \cdot 6\text{H}_2\text{O}$  (0.064 mol, 1.65 gm),  $\text{GdCl}_3 \cdot 6\text{H}_2\text{O}$  (0.064 mol, 0.8435 gm), Glycine  $\text{C}_2\text{H}_5\text{NO}_2$  (0.064 mol, 0.0480

gm) and  $\text{NH}_4\text{F}$  (0.576 mol, 3.200 gm) was prepared in distilled water. Ammonium fluoride forms three parts and the other reagents forms one part (molar ratio of 1:3). A mixture of 7 ml of europium chloride ( $\text{EuCl}_3 \cdot 6\text{H}_2\text{O}$ ), 1.5 ml of gadolinium chloride ( $\text{GdCl}_3 \cdot 6\text{H}_2\text{O}$ ) and 1.5 ml of glycine ( $\text{C}_2\text{H}_5\text{NO}_2$ ) is taken in a clean beaker. 10 ml of Ammonium fluoride ( $\text{NH}_4\text{F}$ ) is then swiftly injected into the mixture using a syringe. The white precipitate appears instantly which is dried in microwave oven for 30 minutes. The nanocrystals thus obtained are washed with distilled water several times and kept for drying each time in the oven. The finished product is stored in sealed tubes for further characterisation.

## III. RESULTS AND DISCUSSION

### A. Thermal Studies

The TGA analysis of  $\alpha$ - glycine modified  $\text{EuF}_3$ :Gd nanoparticles can be divided in to two stages in temperature range from room temperature to

830°C. The first stage shows prominent decomposition occurring at 270°C with nearly 50% weight loss. This is seen as a sharp endothermic peak in the DTA curve. A small endothermic peak at around 530 °C marks the second stage where there is liberation of NH<sub>4</sub>, Cl<sub>2</sub> etc from the sample. Thus heating the sample removes the surface attachments making EuF<sub>3</sub>:Gd nanoparticles water insoluble. The TGA/DTA profile is shown in Figure 1.

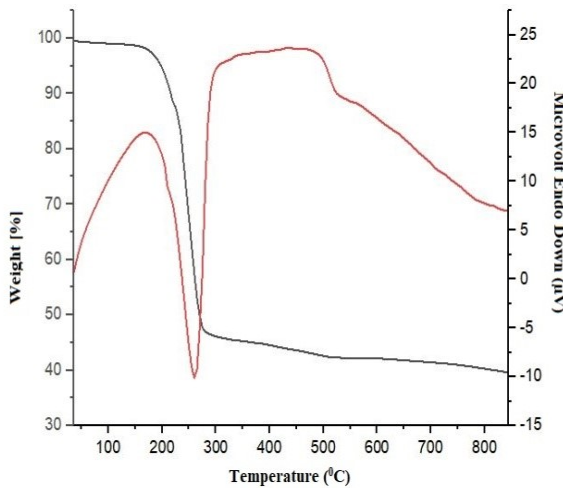


Figure 1. TGA/DTA plot of EuF<sub>3</sub>: Gd @ glycine

### B. Optical Studies

The UV-VIS spectra of EuF<sub>3</sub>: Gd @ glycine is shown in Fig. 2. The spectra shows absorption edges at 460 nm, 580 nm & 625 nm corresponding to band gap energies ( $E_g = hc/\lambda$ )  $E_1 = 2.70$  eV,  $E_2 = 2.14$  eV &  $E_3 = 1.98$  eV respectively. These multiple absorption edges indicate quantum dot like nature of the synthesized nanoparticles. Beyond 400nm a wide transparent window suggests that the synthesized nanoparticles can be used in optoelectronics devices.

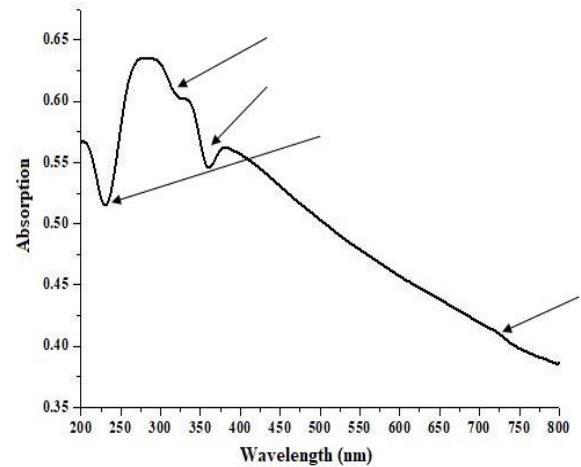


Figure 2. UV-VIS spectra of of EuF<sub>3</sub>: Gd @ glycine

### C. Dielectric Studies

The variation of dielectric constant and dielectric loss as function of frequency (log F) in range 1 KHz to 5 MHz is studied and shown in Fig. 3. The dielectric constant has highest value at low frequency which gradually decreases when the frequency changes to 10 KHz. This decrease in the value of dielectric constant is due to space charge polarization taking place in the dielectric material. For higher frequency values the dielectric constant and dielectric loss remains constant which means for higher frequencies dielectric constant is independent of frequency.

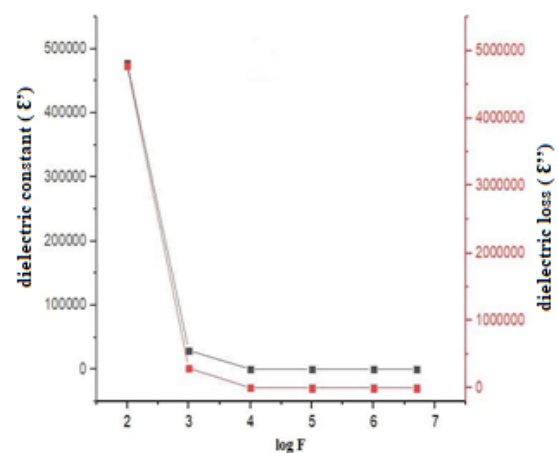
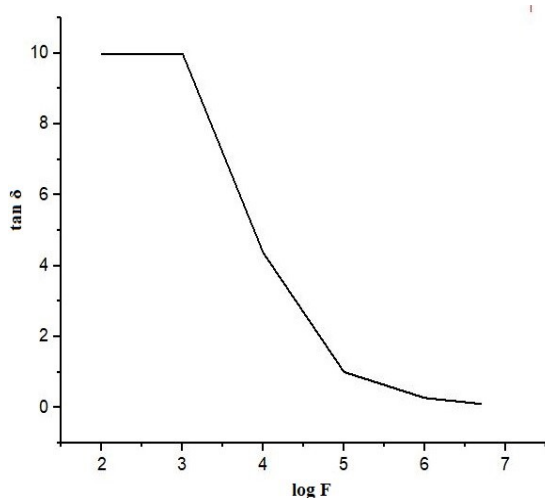


Figure 3. Variation of dielectric constant and dielectric loss as function of log F

The variation of dielectric loss as function of frequency also studied in the frequency range 1 KHz to 5 MHz for synthesised nanoparticles which is shown in Fig. 4. For low value of frequency the dielectric loss is constant. For higher frequency the dielectric loss gradually decreases. This is due to the fact that at higher frequencies dipole follows the variation in the field the dielectric loss decreases.



**Figure 4.** Variation of  $\tan \delta$  as function of Frequency (log F)

#### IV. CONCLUSION

Gadolinium doped  $\text{EuF}_3$  nanoparticles have been synthesised in the presence of glycine as modifier with subsequent drying in microwave to obtain the final finished product. The synthesised nanoparticles shows hexagonal phase with particle size of 51 nm. The TGA/DTA shows two stage decomposition at around 270 °C (sharp) and 530 °C (weak). The UV-VIS spectra shows presence of three absorption edges are obtained at 460 nm, 580 nm & 625 nm corresponding to band gap energies ( $E_g = hc/\lambda$ )  $E_1 = 2.70$  eV,  $E_2 = 2.14$  eV &  $E_3 = 1.98$  eV respectively. The dielectric study shows sharp decrease in value at lower frequency which is independent at higher frequencies. The dielectric loss gradually decreases as observed in graph. This is due to the fact that at higher frequencies dipole

follows the variation in the field and dielectric loss decreases.

#### V. ACKNOWLEDGMENTS

The authors wish to thank Material research laboratory, Birla College, Kalyan (W) for providing research facilities and A.P.Shah Institute of Technology for Institutional support. MPM wishes to thank IIT Mumbai (SAIF) and IIT Madras for providing the experimental facilities for advanced characterisation.

#### VI. REFERENCES

- [1] A. Goswami and R. Ramesh Varma, *Thin films*, 28 (1975) 157.
- [2] B.J.M.Reddy , G.P.Jyothi, M.V.R.Reddy, M.N.Chary and F.N.Reddy, *Phy. Stat.ol.(a)* 137 (1993) 241.
- [3] Amit T Singh, M.M.Khandpekar, *Material Research Express* 2 (2015) 055401.
- [4] M M Khandpekar and S G Gaurkhede, *Journal of Crystal Growth* 401 (2014) 453-457
- [5] Anatoly Safronikhin , Tatyana Shcherba, Heinrich Ehrlich, Georgy Lisichkin, *Applied Surface Science* 255(2009)7990- 7994

# Study of Antibacterial Properties of *Azadirachta indica* and *Trachyspermum ammi* A Commonly Used Plant Material That Aids Digestion

Nutan. B. Kamble, Roothmary. S. Nadar, Greeshma. R. Bale, Vinod. S. Narayane

Department of Zoology, Birla College Kalyan (West), M.S, India

## ABSTRACT

*Azadirachta indica* commonly called neem is a plant known for its medicinal value all over the world. In India it has been used as antibacterial, antifungal, anti-inflammatory agents in Ayurveda and unani medicine. Neem leaf extracts in specific are used to cure digestive problems and disturbances, intestinal parasites and also reduce discomfort. *Trachyspermum ammi* commonly known as ajwain is another plant material used to improve the digestion and the flavor of food. It is commonly added in those recipes which are difficult for digestion and lead to acidity and gas troubles. Aqueous extract of neem leaves and ajwain seeds were prepared to demonstrate their antimicrobial efficacy using pure culture of *E.coli*. *Escherichia coli* popularly abbreviated as *E.coli* is a common bacterial flora of human intestine, which helps in preventing the entry of pathogenic microorganisms. Thus it can serve as a better experimental model for bacteriological and anti-microbial studies. Growth curve was studied with the help of optical density with the help of Elico CL63 photometer. Growth curve and well diffusion were the methods used for the study. In comparative analysis of dry and fresh neem sterile aqueous extract it was found that fresh neem was more effective in inhibiting the growth of *E.coli*; whereas in further investigation with ajwain and fresh neem it was found that neem is more potent in inhibiting the *E.coli* growth.

**Keywords :** *Escherichia Coli*, *Trachyspermum Ammi*, *Azadirachta Indica*, Growth Inhibition.

## I. INTRODUCTION

India is well known for its deep-rooted traditional medicinal knowledge and values. Ayurveda, Siddha, and Unani are some of the greatly known fields [1, 3-6, 8]. Before the development of science and technology the age old traditional methods were the only ones for the rescue of human race. Countries like India has rich array of herbal diversity. Many of them are widely used for various medicinal purposes [2]. Medicinal properties of these plants were explored and put to use under our indigenous field of medicine called Ayurveda in Vedic Period between 2500 and 500 BC in India [1]. Ayurveda is also called the “science of longevity”

because it offers a complete system to live a long healthy life. It offers programs to revitalize the body through proper diet and nourishment [1]. It not only includes treatment methods to cure commonly found diseases like cough, cold, fever, headache, but also the cancer, cardio vascular diseases, asthma, kidney stones, etc., which are considered to be deadly [3-6]. In comparison with the modern allopathic medicines they are highly cost effective, easily available and also efficient to cure the diseases with minimum side effects [1].

List of the herbs having medicinal properties grown in Asia would be enormous but incomplete without adding the two plants of immense importance as far

as their known medicinal properties are concern. Azadirachta indica and Trachyspermum ammi commonly called neem and amla are the plants known for their medicinal values easily availability and sustainability in tropical conditions.

Azadirachta indica commonly known as neem, nim tree or Indian lilac or Margosa, is a tree in the mahogany family Meliaceae. It is one of two species in the genus Azadirachta, and is native to the Indian subcontinent, i.e. India, Nepal, Pakistan, Bangladesh, Sri Lanka, and Maldives. It is typically grown in tropical and semi-tropical regions [7]. Neem trees also grow in islands located in the southern part of Iran. Its fruits and seeds are the source of neem oil. Neem products are believed by siddha and Ayurveda practioners to be antibacterial [10], antifungal [11], anti-inflammatory, anti-viral, anthelmintic, antidiabetic, and sedative [7]. Neem leaves are also proved to be effective in treating skin diseases and disorders [9].

Trachyspermum ammi also known as ajowan, ajwain, or carom is an annual herb in the family Apiaceae. Ajwain is a plant primarily found in countries like India Pakistan, south east and near east of Iran, where these seeds are predominantly used as a spice [17]. In Asian countries these seeds hold an important place in cuisines. They are better to taste, with a flavor similar to anise and oregano. Even a small amount can add great flavor to the dish. Ajwain is efficiently used in traditional Ayurvedic medicine primarily for stomach disorders such as indigestion, flatulence, and diarrhea. In Siddha medicine, it is used as a cleanser, detox, and antacid. The indigenous Indian system of

medicine uses ajwain as an antimicrobial, anti-hypersensitive, antispasmodic, bronchodialating and antilithiasis [19]. Ethanol and acetone extract of ajwain seeds possessed an antibacterial activity against two Gram negative food spoilage bacteria Pseudomonas aeruginosa and Escherichia coli [3, 18].

Escherichia coli being the commonly present bacterium in the human intestine, helps in preventing the entry of pathogenic microorganisms. E. coli are non-pathogenic in normal conditions, but if present in excess, can turn out to be a causative agent of various diseases like urinary tract infection, diarrhoea, vomiting etc. With increasing resistance of microorganisms to antibiotics, people have spun their way towards herbal medicines.

## II. METHODS AND MATERIAL

**Collection of Sample:** Fresh Neem leaves were collected from Birla College campus and Ajwain seeds were procured from the local market.

### **Preparation of Extracts:**

Aqueous soxhlet extract of neem:

The neem leaves were washed and divided in two parts. One part was used directly as fresh leaves to prepare the aqueous extract and the other part was kept at 40°C for drying. The aqueous extracts of fresh as well as dried neem leaves were prepared using the soxhlet apparatus. 25 Gms of fresh as well as dried neem leaves powder was used for preparing 100 ml of extract separately using distilled water. The extracts were further concentrated to 25 ml, autoclaved and stored in sterile condition at 4°C till further use.



Aqueous soxhlet extract of ajwain seeds: Sterile aqueous extract of ajwain seeds was prepared as explained above.

Crude extract preparation of fresh neem leaves and ajwain seeds:

Crude extract was prepared by boiling 25 Gms of sample (fresh neem leaves, ajwain seeds) in 50ml of distilled water and condensed to 25 ml by evaporation, cooled and preserved at 4°C till further use.

#### **Preparation of bacterial culture:**

Pure isolated colonies of the E.coli were obtained from the Department of Microbiology, Birla College Kalyan. E.coli was sub-cultured by growing the colonies on nutrient agar slants and Preserved in refrigerator.

#### **Preparation of nutrient broth:**

25 ml of sterile nutrient broth was prepared using distilled water, and stored at 4°C.

#### **Preparation of nutrient agar plates:**

20 ml of sterile nutrient agar was poured on sterile plates.

### **ANTIMICROBIAL ASSAY BY GROWTH CURVE METHOD:**

#### **A. Growth curve analysis using sterile aqueous extract:**

24 ml of sterile nutrient broth was inoculated with 1ml of sterile fresh neem leaves extract and 1ml of

E.coli culture, and was incubated in Remi Orbital shaking incubator at 37°C for 24 hrs. The growth was analyzed at regular intervals of 1 hr. similarly growth analysis of E.coli was studied using ajwain extract. Parallel study was performed using 0.5ml of neem and ajwain extract separately. All the studies were performed in triplicates. Control was maintained similarly using sterile distilled water.

#### **B. Growth curve analysis using crude extract:**

24 ml of sterile autoclaved nutrient broth was inoculated 1ml of E.coli culture and 1ml of crude fresh neem leaves extract. Parallel study was also carried out using 0.5ml extract, and incubated in shaker incubator at 37°C for 3hrs. The growth was analysed at regular intervals of 10 min. Similar study was performed using 0.5ml and 1ml of ajwain extract individually. All the studies were performed in triplicates. Control was maintained similarly using sterile distilled water.

### **ANTIMICROBIAL ASSAY BY AGAR DITCH METHOD:**

Sterile nutrient agar plates were used as medium for screening antibacterial activity. 100µl of E.coli culture was uniformly spread on sterile plates using a sterile spreader. Wells of 1cm were dug using a sterile cork borer in solidified pre inoculated agar medium. The plates were divided into 3 quadrants I, II, and III, each having 100µl of 1%, 10% and 100% individual crude extract of fresh neem leaves and ajwain seeds. The plates were incubated at 37°C for 8hrs and observed for clear inhibition zone formed around the wells.

### III. RESULTS AND DISCUSSION

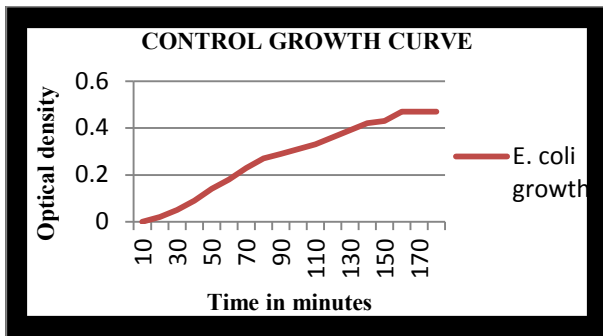


Fig.1

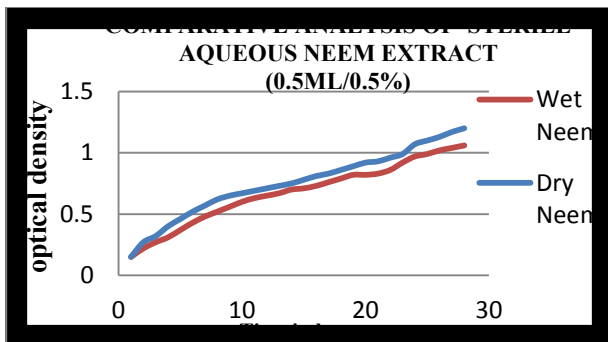


Fig.2

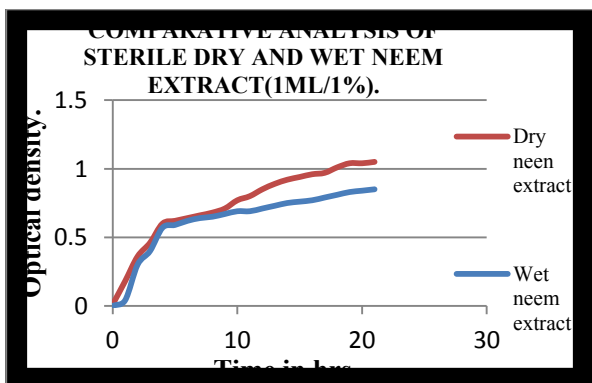


Fig.3

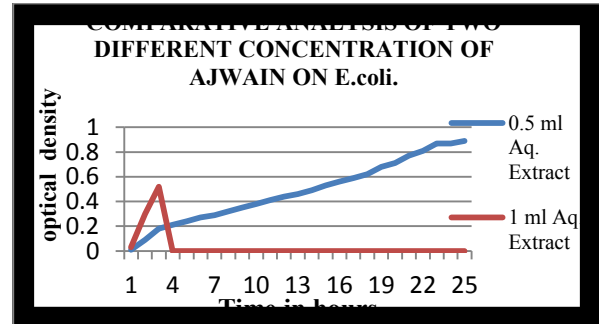


Fig.4

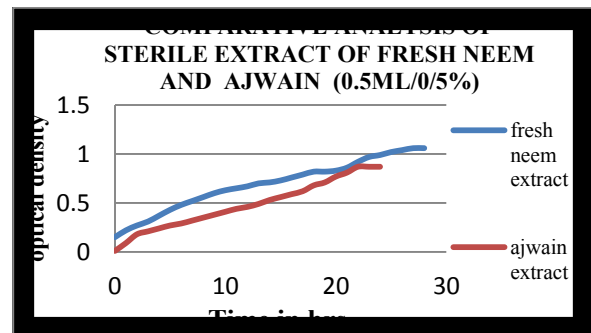


Fig.5

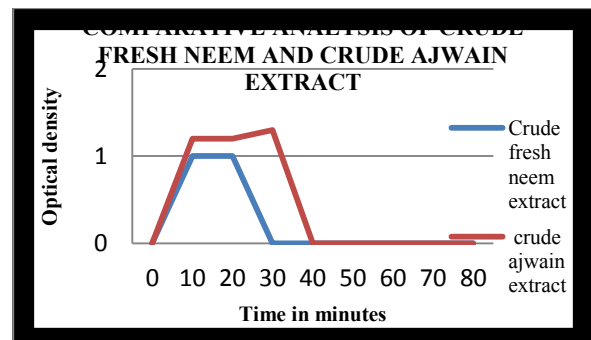


Fig.6.



Fig.7 Control inhibition zone on agar plate

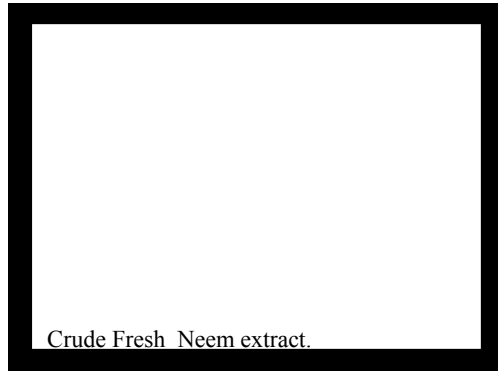


Fig.8. Inhibition zone of crude fresh neem extract at different concentrations.

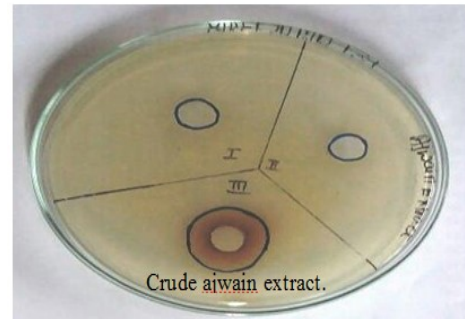


Fig.9 Inhibition zone of crude ajwain extract at different concentrations

Table 1: showing the inhibition zone of crude extract of fresh neem leaves and ajwain seeds at three different concentrations

	Crude extract of fresh neem leaves.			Crude extract of ajwain seeds.			Control
<b>Concentration.</b>	1%	10%	100%	1%	10%	100%	100µl E.coli.
<b>Inhibition zone.(cm)</b>	1.2cm	1.4cm	3.4cm	1.2cm	1.4cm	3cm	0 cm

Fig. 1 represents the growth curve of control sample which was not exposed to any herbal extract while the Fig. 2 represents the growth curve of E. coli where the sterile aqueous extract of fresh neem leaves was incorporated with the culture medium at the concentration of 0.5 ml/25 ml of nutrient broth and dry neem leaf sterile aqueous extract at the same concentration. It was found that sterile aqueous extract of fresh neem leaves was more effective in inhibiting the growth of E.coli. Studies carried out using 1ml of sterile aqueous extract of fresh neem and dry neem leaves / 25ml of nutrient broth also shows similar results indicating that fresh neem leaves extract is more effective than dry neem leaves, as seen in Fig 3. Fig 4 represents that

in comparative analysis of sterile aqueous extract of ajwain seeds, 1ml extract /25 ml of nutrient broth is more effective than 0.5ml of extract. From Fig 5 it is evident that sterile aqueous extract of ajwain seed is effective than neem leaves extract. On similar lines on comparing fig 3 and fig .4, it is observed that ajwain seed extract is much effective in inhibiting the bacterial growth in less time in comparison to fresh neem leaves extract at the concentration of 0.5ml as well as 1ml /25ml NB. Fig.6 indicates the potential growth inhibition obtained using crude extract of fresh neem leaves than in comparison to crude extract of ajwain seed. The agar ditch method primarily focus on the inhibition zones formed using three different

concentrations of crude extracts of fresh neem leaves and ajwain seeds respectively. As seen in fig .7 no inhibition zone is seen in control agar ditch filled with sterile distilled water. Whereas the inhibition zones formed around the neem leaves extract and ajwain seed extract increases with an increase in concentration used (fig 8, 9, table 1).

Margosa that is *Azadirachta Indica* is well known plant for the wide range of medicinal uses it has. It is possible that the medicinal properties of the plant are due to the different active components present in the plant. The most important active constituent is azadirachtin and the others are nimbolinin, nimbin, nimbidin, nimbidol, sodium nimbinate, gedunin, salannin, and quercetin. Leaves contain ingredients such as nimbin, nimbanene, 6-desacetylnimbinene, nimbandiol, nimbolide, ascorbic acid, n-hexacosanol and amino acid, 7-desacetyl-7-benzoylazadiradione, 7-desacetyl-7-benzoylgedunin, 17-hydroxyazadiradione, and nimbiol. Quercetin and  $\beta$ - sitosterol, polyphenolic flavonoids, were purified from neem fresh leaves and were known to have antibacterial and antifungal properties and seeds hold valuable constituents including gedunin and azadirachtin<sup>[21]</sup>. In past many workers have assessed the antimicrobial properties of this plant using various extraction solvents such as ethanol, methanol etc<sup>[20,21,23]</sup>. As stated above in this investigation water was used as solvent when compared with the earlier literature where methanolic samples were used<sup>[20]</sup>. It was found that results obtained using aqueous crude extract were less effective than methanolic extract<sup>[20]</sup>.

Ajwain also known as *Trachyspermum ammi* is a commonly used across India in various Indian cuisines. It is used to add flavor as well to help in digestion of food. Apart from these values it is also a

fundamental remedy on acidity problems, stomach ache, and other problems related to indigestion. Ajwain seeds contain several phytochemicals such as, tannins, glycosides, saponins, flavones and mineral matter like calcium, phosphorus, iron and nicotinic acid. Essential oil present in the ajwain contains the major constituent thymol. The remainder non-thymol fractions called thymene contains p-cymene,  $\beta$ -pinene, limonene with  $\gamma$ -pinenes and  $\beta$ -pinene. Alcoholic extract contains highly hygroscopic saponin. It has been reported that minute amount of camphene, myrcene and D3-carene is also present. A yellow crystalline flavone and steroid like substance have been isolated from the fruit of ajwain and it also contains a glucoside 6-O- $\beta$ - glucopyranosyloxythymol. The major constituents of *T. ammi* are carvone, limonene and dillapiole<sup>[24]</sup>. Ajwain was studied in the past and was reported that it has antimicrobial properties and a great pharmacological use<sup>[24]</sup>. In the current investigation it was found that ajwain seeds aqueous soxhlet extract shows better antimicrobial activity than neem in growth curve assay.

#### IV. CONCLUSION

The growth curve experimental set up for 24hrs proved that ajwain seeds are more effective in inhibiting the growth of gram negative bacteria *E.coli*. Whereas the agar ditch method indicated that the crude extract of neem leaves was more effective than the ajwain extract in inhibiting the *E.coli* growth.

## V. REFERENCES

- [1]. M. M. Pandey, Subha Rastogi, and A. K. S. Rawat.(2013) .Indian Traditional Ayurvedic System of Medicine and Nutritional Supplementation, Evidence-Based Complementary and Alternative Medicine Volume 2013, Article ID 376327.
- [2]. PreetamSarkar Iolith kumar DHa et,al.: Traditional and ayurvedic foods of Indian origin, Journal of Ethnic Foods (September 2015), Volume 2, Issue 3, , Pages 97-109
- [3]. R. A. Mashelkar, "Second world Ayurveda congress (theme: Ayurveda for the future) inaugural address: part III," (2008), Evidence-Based Complementary and Alternative Medicine, vol.5, no. 4, pp. 367–369.
- [4]. E. L. Cooper (2008), "Ayurveda is embraced by eCAM," Evidence-Based Complementary and Alternative Medicine, (2008) vol. 5, no. 1, pp. 1–2.
- [5]. E. L. Cooper, "Ayurveda and eCAM: a closer connection,"Evidence-Based Complementary and Alternative Medicine, (2008.) vol.5, no. 2, pp. 121–122.
- [6]. K. Joshi, Y. Ghodke, and B. Patwardhan, "Traditional medicineto modern pharmacogenomics: Ayurveda Prakriti type andCYP2C19 gene polymorphism associated with the metabolic variability," Evidence-Based Complementary and Alternative Medicine, (2011.) vol. 2011, Article ID 249528, 5 pages.
- [7]. Venugopalan Santhosh Kumar1,\* and Visweswaran Navaratnam1, 2: Neem (Azadirachta indica): Prehistory to contemporary medicinal uses to humankind; Asian Pac J Trop Biomed. 2013 Jul; 3(7): 505–514.
- [8]. San Francisco: Wikipedia; Siddha medicine. [Online] Available from: [http://en.wikipedia.org/wiki/Siddha\\_medicine](http://en.wikipedia.org/wiki/Siddha_medicine) .
- [9]. Mohammad A. Alzohairy \*(2016); Therapeutics Role of Azadirachta indica (Neem) and Their Active Constituents in Diseases Prevention and Treatment. Evid Based Complement Alternat Med. 2016; 2016: 7382506.
- [10]. Govindachari T. R., Suresh G.,et,al.. Identification of antifungal compounds from the seed oil of Azadirachta indica . Phytoparasitica. 1998; 26 (2):109–116. doi: 10.1007/bf02980677.
- [11]. Kher A., Chaurasia S. C. Antifungal activity of essential oils of three medical plants. Indian Drugs. 1997; 15: 41–42.
- [12]. Bandyopadhyay U., Biswas K., Sengupta A., et al. Clinical studies on the effect of Neem (Azadirachta indica) bark extract on gastric secretion and gastroduodenal ulcer. Life Sciences. 2004;75(24):2867–2878. doi: 10.1016/j.lfs.2004.04.050.
- [13]. Sultana B., Anwar F., Przybylski R. Antioxidant activity of phenolic components present in barks of Azadirachta indica, Terminalia arjuna, Acacia nilotica, and Eugenia jambolana Lam. trees. Food Chemistry. 2007; 104 (3):1106–1114. doi: 10.1016/j.foodchem.2007.01.019.
- [14]. Ebong P. E., Atangwho I. et, al. The antidiabetic efficacy of combined extracts from two continental plants: Azadirachta indica (A. Juss) (Neem) and Vernonia amygdalina (Del.) (African Bitter Leaf) The

- American Journal of Biochemistry and Biotechnology. 2008;4(3):239–244. doi: 10.3844/ajbbbsp.2008.239.244.
- [15]. Paul R., Prasad M., Sah N. K. Anticancer biology of *Azadirachta indica* L (neem): a mini review. *Cancer Biology and Therapy*. 2011;12 (6):467–476. doi: 10.4161/cbt.12.6.16850.
- [16]. Biswas K., Chattopadhyay I., Banerjee R. K., Bandyopadhyay U. Biological activities and medicinal properties of neem (*Azadirachta indica*) *Current Science*. 2002; 82 (11):1336–1345.
- [17]. Zahin MI, Ahmad Aqil F. Antioxidant and antimutagenic activity of *Carum copticum* fruit extracts. *Toxicology in Vitro*. 2010; 24:1243-1249.
- [18]. Venugopal Amrita, Dasani Sonal\*,et.al.; Antibacterial Effect of Herbs and Spices Extract on *Escherichia coli*; *Electronic Journal of Biology*, (2009), Vol. 5(2): 40-44
- [19]. M. K. Prashanth 1 , H. D. Revanasiddappa 1\*,et.al.; Antioxidant and antibacterial activity of ajwain seed extract against antibiotic resistant bacteria and activity enhancement by the addition of metal salts.; *Journal of Pharmacy Research* 2012,5(4),1952-1956.; ISSN: 0974-6943.
- [20]. Poonam Panchal et al., Oct-Dec 2013 *Guru Drone Journal of Pharmacy and Research*,;1(1):18-21.
- [21]. Mohammad A. Alzohairy, *Evidence-Based Complementary and Alternative Medicine* Volume 2016 (2016), Article ID 7382506, 11 pages
- [22]. <http://dx.doi.org/10.1155/2016/7382506>.
- [23]. Zarshenas MM, Moein M, Samani SM, Petramfar P. An overview on ajwain (*Trachyspermum ammi*) pharmacological effects (2013); *Modern and traditional. Journal of Natural Remedies.*, 14:98
- [24]. Josephin Sheeba.B et al (2012) *Asian J. Plant Sci. Res.*, 2 (2):83-88.
- [25]. Hafiz MuhammadAsif et .al (2014), A panoramic view on phytochemical, nutritional, ethanobotanical uses and pharmacological values of *Trachyspermum ammi* Linn. <https://doi.org/10.12980/APJTB.4.APJTB-2014-0242>

# Protease Production Using Solid State Fermentation

Dhaliwal MK\*, Patil RN, Sambare S

Department of Microbiology, Birla College, Kalyan, Maharashtra, India

## ABSTRACT

Proteases are enzymes that break down protein molecules through peptide bond hydrolysis. Microbial proteases are the most important industrial enzymes with considerable applications in food, medicines and pharmacy. They are extracellular enzymes that can be produced by both submerged and solid state fermentation (SSF). *Aspergillus* sp. are known to produce various types of proteases. Solid state fermentation processes generally use natural raw materials as carbon and energy source. Different agro-industrial waste products will be evaluated to check possibility of potential utilization of substrates in SSF. The production of enzymes by bioprocesses is a good value added to agro industry residues. A comparative study was carried out on the production of protease using Wheat bran and Rice bran as substrates in solid state fermentation by *Aspergillus niger* ATCC 16404. Among them Wheat bran produced higher activity protease as 1.785 U/ml than Rice bran 1.487 U/ml activity under solid state fermentation conditions. The optimized conditions for producing maximum yield of protease were incubation at room temperature ( $28\pm 2$ )°C, 120hours, pH 6, concentration of nitrogen source 0.5% and additional carbon source is 1% sucrose. The protease production from agricultural waste products can be commercially used in detergents and leather industry and it adds great value to agro-industrial wastes.

**Keywords:** Bioprocess, Protease, Solid State Fermentation, Bran, Optimization.

## I. INTRODUCTION

Enzymes are biocatalysts that determine the patterns of chemical and energy transformations. The most striking characteristics of enzymes are their catalytic power and specificity. Proteolytic enzymes are included in a sub-class of the enzymes hydrolases. These enzymes hydrolyse proteins into smaller peptides and amino acids by cleavage of peptide bonds (Munawar et. al., 2014). Their involvement in the life cycle of disease-causing organisms has led them to become a potential target for developing therapeutic agents against fatal diseases such as cancer and AIDS (Sawant et. al., 2014).

### A. Classification of proteases

On the basis of the site of action on protein substrates, proteases are broadly classified as endopeptidases or exopeptidases enzymes (Sawant et. al., 2014). The endopeptidases are divided into four subgroups based on their catalytic mechanism, serine protease, aspartic protease, cysteine protease, and metalloproteases (Rawlings and Barrett, 1993). Several species of strains including fungi (*Aspergillus flavus*, *Aspergillus melleus*, *Aspergillus niger*, *Chrysosporium keratinophilum*, *Fusarium graminearum*, *Penicillium griseofulvum*, *Scedosporium apiosermum*) and bacteria (*Bacillus licheniformis*, *Bacillus firmus*, *Bacillus alcalophilus*, *Bacillus amyloliquefaciens*, *Bacillus proteolyticus*, *Bacillus subtilis*, *Bacillus thuringiensis*) are reported to

produce proteases. Fungi elaborate a wide variety of proteolytic enzymes than bacteria and also offer an advantage as the mycelium can be grown on cheaper substrate, broad range of pH and the mycelium can also be easily removed from the final product (Sri lakshmi et. al., 2014).

Protease production under solid-state fermentation has been investigated using *Bacillus* sp. (Prakasham et. al., 2005; Akcan et. al., 2011, Imtiaz et. al., 2013, Mukhtar et. al., 2013; Sathyavrathan et. al., 2014; Pant et. al., 2015; Ortiz et. al., 2016). **Solid state**

### **fermentation**

Solid-state fermentation has been defined as the process with solid materials as substrate with near-absence of water content, generally using natural raw materials as carbon and energy source. Solid-state fermentation has many advantages including superior volumetric productivity, use of inexpensive substrate, simpler downstream processing, lower energy requirement and low wastewater output (Özkan et. al., 2011; Sri lakshmi et. al., 2014). Solid-state fermentation is especially suited for the growth of fungi because of their lower moisture (30 to 80%) requirements compared with the bacteria (Sankeerthana et. al., 2013; Mukhtar et. al., 2009). Rice bran was used as the substrate for screening nine strains of *Rhizopus* sp. for neutral protease production by Solid state fermentation (Alagarsamy et. al., 2006; Chutmanop et. al., 2008).

The growth and production of protease by *Aspergillus* has been studied by using rice bran, rice mill waste, vegetable waste, oil cakes, wheat bran, fruit waste (Mukhtar et. al., 2009; Paranthaman et. al., 2009; Madhumithah et. al., 2011; Kranthi et. al., 2012; Sankeerthana et. al., 2013; Dutta et. al., 2014; Munawar et. al., 2014; Santhi, 2014).

Protease production by *Fusarium oxysporum* on rice bran under solid-state fermentation was studied (Ali et. al., 2013).

Protease production by a thermophilic fungus *Humicola grisea* was evaluated in solid state fermentation (SSF) with different substrates and also under the influence of different activators and inhibitors. The environmental conditions of the fermentation play a vital role in the growth and metabolic production of microbial population (Sri lakshmi et. al., 2014). Optimization of different media components can greatly affect the enzyme production cost (Joo et. al., 2003; Wang et. al., 2008; Schrickx et. al., 1995).

### **Applications of proteases**

Viral proteases have gained importance due to their functional involvement in the processing of the proteins of viruses that cause diseases such as AIDS and cancer (Rawlings and Barrett, 1993). All of the virus-encoded peptidases are endopeptidases. Retroviral aspartyl proteases that are required for viral assembly and replication are homo-dimers and are expressed as a part of the poly protein precursor. The mature protease is released by autolysis of the precursor (Kuo et. al., 1994).

Besides extended application for nutritional and pharmaceutical purposes, proteases from natural sources are also widely used tools in biotechnological practices. Their degradative properties make them useful for general protein digestion in tissue dissociation, cell isolation, and cell culturing. The specificity and the predictability of cleavages by proteases enables their use for more specific tasks such as antibody fragment production, the removal of affinity tags from recombinant proteins and specific protein digestion in the proteomics field mainly for protein sequencing (Mótyán et al., 2013). Due to their key role in the life-cycle of many hosts and pathogens they have great medical, pharmaceutical, and academic importance (Li et al., 2013; Gupta and Khare, 2007). In view of the recent trend of developing environmentally friendly technologies, proteases are envisaged to have extensive applications in leather tanning industries and in several bioremediation processes (Gupta et



al., 2002). Proteases that are used in the food and detergent industries are prepared in bulk quantities and used as crude preparations; whereas those that are used in medicine are produced in small amounts but require extensive purification before they can be used (Bholay and Niranjana, 2012).

In the present work we have studied the production of protease by solid-state fermentation using different agro-industrial waste products like rice bran and wheat bran as cheap substrates and the effect of physico-chemical parameters like pH, temperature, concentration of nitrogen and different carbon sources on protease production.

## II. MATERIALS AND METHOD

The organism used in the present study was *Aspergillus niger* ATCC 16404 obtained from Microbial Type Culture Collection & Gene Bank and maintained on potato dextrose agar slants.

### 1. Collection of substrates:

Different agro-industrial waste residues- rice bran and wheat bran were used. Rice bran was collected from rice-mill from the area nearby Kalyan, India in polythene bag. The sample was grounded in dry blender until the size of the particles reached the desired size and stored at ambient condition for further use. Wheat bran was purchased from online store amazon.in and used as it is as substrate.



**Figure 1:** Substrates used for solid state fermentation

### 2. Inoculum Preparation:

The inoculum was prepared by dispersing the spores from a week-old fungal slant culture in 0.1 % Tween-80 solution with a sterile inoculation loop (Paranthaman et. al., 2009).

### 3. Solid-State Fermentation:

Ten grams of each substrate (rice bran and wheat bran) was taken in a 250 ml Erlenmeyer flask separately, moistened with 15 ml of the salt solution (Ammonium chloride-0.5g; Sodium nitrate-0.5; Potassium dihydrogen orthophosphate-0.2g; Magnesium sulphate-0.2mg; Sodium chloride-0.1g per 100ml distilled water). The flasks were plugged tightly with cotton wool, sterilized at 121.5°C for 15 min, cooled, inoculated with 1 ml of fungal spore suspension (100 spores/ml) and incubated at 37°C for 120 hr (Paranthaman et. al., 2009).

### 4. Extraction of Crude Enzyme:

A solution of Tween-80 (0.1 %) was added in to the 100 ml of distilled water. 50 ml, of this water was added to the fermented substrate and homogenized the substrate on a rotary shaker at 120 rpm for 12 h. The content of flask was filtered with help of 4-fold muslin cloth. The suspended solids were removed by centrifuging the homogenate at 8000 x g at 4°C for 15 min and the resultant supernatant was used for analytical studies (Paranthaman et. al., 2009).

### 5. Protein Estimation in Crude Enzyme

Amount of protein in crude enzyme was determined by Lowry's method of protein estimation, in which 0.5ml of crude enzyme, 0.5ml of distilled water was reacted with 5ml of Lowry's reagent C (Folin-

Ciocaltaeu reagent) and 0.5ml of Reagent D (0.5N NaOH) and the absorbance was read at 660nm. Absorbance was compared with the standard graph prepared by reacting known concentration of protein ranging from 50 µg/ml to 250 µg/ml with the Lowry's reagents and plotting a graph between concentration of protein Bovine Serum Albumin and OD at 660 nm (Lowry et.al., 1951).

#### **6. Measurement of enzymatic activity**

Protease activity in the culture supernatant was determined according to the method of Tsuchida et. al., (1986) using casein as a substrate. A mixture of 500 µl of 1% (w/v) of casein in 50 mM phosphate buffer, pH 7 and 200 µl crude enzyme extract were incubated in a water bath at 40°C for 20 minutes. After 20 minutes, the enzyme reaction was terminated by the addition of 1 ml of 10% (w/v) trichloroacetic acid (TCA) and was kept at room temperature for 15 minutes. Then, the reaction mixture was centrifuged to separate the unreacted casein at 10,000 rpm for 5 minutes. The supernatant mixed with 2.5 ml of 0.4M Na<sub>2</sub>CO<sub>3</sub> and 1 ml of 3-fold diluted Folin Ciocalteu reagent. The resulting solution was incubated at room temperature in the dark for 30 minutes and absorbance of the blue color developed was measured at 660 nm against a reagent blank using a tyrosine standard. One international unit (IU) of protease activity is the amount of enzyme, which liberates 1 µmol of tyrosine per min. (Mohapatra et. al., 2003).

#### **7. Optimization of fermentation conditions**

Production of protease from *Aspergillus niger* was optimized by controlling different physico chemical parameters like pH, temperature, carbon source and concentration of nitrogen source.

#### **8. Initial pH of medium**

The effect of initial pH on protease production was studied by changing the initial growth medium pH from 2, 3 and 6 with 1N Lactic acid/ NaOH before sterilization at 121°C for 15 min. and optimum pH for protease production was determined.

#### **9. Incubation temperature:**

The effect of temperature was studied by incubating the inoculated flasks at different temperatures viz. room temperature (28±2)°C, 37°C and 55°C.

#### **10. Effect of concentration of supplementary nitrogen sources**

Whether the addition of supplementary nitrogen sources could enhance the production of protease was tested by supplying an inorganic nitrogen source (NaNO<sub>3</sub> and NH<sub>4</sub>Cl) at a level of 0.5% w/w in the medium. The flasks were then incubated for 5 days at room temperature. At the end of the incubation period, protease production in cell free supernatant was determined. Further, nitrogen source was optimized with different concentrations [0.3, 0.5, 0.7% (w/v)].

#### **11. Effect of carbon sources**

The effect of carbon sources on enzyme production was investigated by supplementing the basal salt solution, pH 7, with 1% (w/v) of different carbon sources, viz., maltose, lactose, and sucrose. The flasks were then incubated for 5 days at room temperature. At the end of the incubation period, protease production in cell free supernatant was determined.

#### **12. Partial purification of Protease:**

About 20 ml of the crude enzyme extract prepared was brought to 80% saturation by adding solid ammonium sulphate salt with continuous stirring. The mixture was left overnight at 4°C. The mixture was centrifuged at 10,000 rpm for 20 minutes and the pallette was dissolved in 30ml of 50mM phosphate buffer (pH 7) which was then subjected to dialysis (Shanmugapriya et. al., 2012).

The precipitate dissolved in phosphate buffer at pH 7 is dialyzed against the same buffer overnight at 4°C (Immanuel et. al., 2006). The partially purified sample was assayed for enzyme activity and protein content.

### III. RESULT AND DISCUSSION

#### 1. Protease production by solid state fermentation

The production of protease by the standard culture *Aspergillus niger* ATCC 16404 in solid state fermentation using solid substrates that have been moistened with a salt solution is done. The enzyme activity of protease produced was calculated using tyrosine standard by Folin-Lowry method.

The selection of an ideal agro-biotech waste for enzyme production in solid state fermentation process depends upon several factors, mainly related with cost and availability of substrate material (Paranthaman et. al., 2009).

#### 2. Effect of different substrates on protease production

Two different agro-waste substrates were used for solid state fermentation viz., wheat bran and rice bran. Five grams of each substrate were weighed and hydrated with 10 ml of basal salt solution containing (g): NaCl; 0.1g, MgSO<sub>4</sub>.7H<sub>2</sub>O; 0.2g, KH<sub>2</sub>PO<sub>4</sub>; 0.2g, NH<sub>4</sub>Cl<sub>2</sub>; 0.5g and NaNO<sub>3</sub>; 0.5g dissolved in 100ml of distilled water (Coral et al. 2003). Flasks containing fermentation medium were autoclaved, cooled and inoculated with 1.0ml of *Aspergillus niger* ATCC 16404 spore suspension prepared in 0.1% Tween 80 solution, incubated for 120 hrs at 30°C. Rice bran and Wheat bran were used as substrate. Wheat bran was the suitable substrate for production of protease at pH 6 and (28±2)°C, enzyme activity 0.850 U/ml. When grown on rice bran, the fungus produced protease showing 0.799 U/ml enzyme activity [Table 1]. The protein content of wheat bran (14-16%) is higher compared to rice bran (7-8%). This could be the factor for lower production of protease when rice bran was used as a substrate.

**Table 1:** Enzyme activity of protease produced by the culture on rice bran (RB) and wheat bran (WB) by SSF

Substrate	Extinction at 670nm	Tyrosine formed (µmole)	Enzyme activity (units/ml)
RB 1	0.34	0.95	0.20
RB 2	0.30	0.85	0.18
RB 3	0.35	1.00	0.21
WB 1	0.59	1.65	0.35
WB 2	0.62	1.75	0.37
WB 3	0.68	1.90	0.40

#### 3. Optimization of fermentation conditions for protease production by SSF

Different fermentation conditions that may affect production of protease from *A. niger* were optimized as follows:

Production of the enzymes by mold culture mostly depends on the pH of medium. Therefore, the effect of different pH values on the production of protease by *A. niger* was studied. Production of the protease has increased with pH. Maximum enzyme activity [0.439units/ml] was observed at pH 6 for wheat bran and [0.255U/ml] (Table 2). Generally, protease production by microorganism depends on the extracellular pH because culture pH strongly influences many enzymatic processes and transport of various components across the cell membranes, which in turn support the cell growth and product production (Paranthaman et al., 2009). Changes in the pH may also cause denaturation of enzyme resulting in loss of catalytic activity. It may also cause change in the ionic state of substrate which may result in the formation of charged particles which may not correspond with the ionic active sites of enzyme (Karuna and Ayyanna, 1993).

**Table 2:** Enzyme activity of protease using different substrates at different pH values

Substrate	pH 2	pH 4	pH 6
Enzyme activity WB	0.323	0.429	0.439
Enzyme activity RB	0.17	0.201	0.255

Maximum protease production was obtained at room temperature (28±2)°C and protease activity was found to be 0.850 Units/ml for wheat bran and 0.799 Units/ml for rice bran (Table 3). In contrast, by reports of Paranthaman *et. al.*, (2009), fermentation carried out at 35°C was best suited for protease production. Protease activity was decreased with increase in temperature. Higher temperature (55°C) is found to have some adverse effect on metabolic activities of microorganisms and cause inhibition of growth of the fungus. The enzyme is denatured by losing its catalytic properties at high temperature due to stretching and breaking of weak hydrogen bonds within enzyme structure.

**Table 3:** Enzyme activity of protease using different substrates at different temperatures

Substrate	(28±2)°C	37°C	55°C
Enzyme activity WB	0.850	0.828	0.00
Enzyme activity RB	0.799	0.733	0.00

The effect of the concentration ammonium chloride and sodium nitrate on the protease production was studied using the range of 0.3-7.0% of nitrogen sources. A gradual increase in protease activity was observed with the increment of nitrogen source concentration and it declines after 0.5% (Table 4).

**Table 4,** Enzyme activity of protease using different concentrations of nitrogen sources during SSF

Substrate	Concentration of nitrogen source
-----------	----------------------------------

	0.3%	0.5%	0.7%
Enzyme activity WB	1.615	1.402	1.36
Enzyme activity RB	1.402	1.44	0.977

The highest protease activity (1.8Units/ml) was obtained when sucrose was used as a carbon source while the least protease activity (1.59Units/ml) was produced when maltose was used (Table 5). Madzak *et al.* (2000) also recorded that sucrose was a good substrate for production of extracellular proteases.

**Table 5:** Enzyme activity of protease using different carbon sources during SSF

Substrate	Carbon source		
	Sucrose	Maltose	Lactose
Enzyme activity WB	1.785	1.46	1.657
Enzyme activity RB	1.487	1.402	1.326

#### IV. CONCLUSION

Proteases are specialized proteolytic enzymes that are widely distributed nearly in all plants, animals and microorganisms. Proteases from microbial sources are preferred to those from other sources since they possess almost all the characteristics desired for their biotechnological applications. Fungal proteases are more preferred by researchers due to high diversity, broad substrate specificity, and stability under extreme fermentation conditions. In this study, the conditions for protease production by *A.niger* in solid state fermentation medium were optimized.

Wheat bran is a promising substrate for the production of protease by *A.niger* under solid state fermentation conditions. Optimum conditions for protease production by *A.niger* under solid state fermentation were: pH 6.0, 0.5% of a nitrogen source, (28±2)°C temperature during 120hrs incubation period.

## V. REFERENCES

- [1] Akcan, N., Uyar, F. (2011). Production of extracellular alkaline protease from *Bacillus subtilis* RSKK96 with solid state fermentation. *Eurasian Journal of Biosciences* 5:64-72.
- [2] Alagarsamy, S., Paul, D., Chandran, S., Szakacs, G., Soccol, C. R. and Pandey, A., (2006). Rice bran as a substrate for proteolytic enzyme production. *Brazilian Archives of Biology and Technology-an International Journal* 49 (5): 843-851.
- [3] Ali, S. S., Vidhale, N. N. (2013). Protease production by *Fusarium oxysporum* in solid-state fermentation using rice bran. *American Journal of Microbiological Research* 1(3):45-47.
- [4] Bholay, A. D. and Niranjana, P., (2012). Bacterial extracellular alkaline proteases and its industrial applications. *International Research Journal Biological Science*, 1(7):1-5.
- [5] Chutmanop, J., Chuichulcherm, S., Chisty, Y. and Srinophakun, P., (2008). Protease production by *Aspergillus oryzae* in solid-state fermentation using agroindustrial substrates. *Journal of Chemical Technology and Biotechnology*, 83:1012-1018.
- [6] Coral, G., Arikana, B., unaldi, M. N. and Guvenmez, H., (2003). Thermostable alkaline protease produced by an *Aspergillus niger* strain. *Annals of Microbiology* 53(4): 491 – 498.
- [7] Dutta, M., Chamendra, N., Pai, S. G., Pramod, T. and Siddalingeshwara, K.G., (2014). Isolation and screening of agro-waste substrates for protease production through solid state fermentation. *International Journal of Current Microbiology and Applied Sciences* 3(3): 774-781.
- [8] Gupta, A. and Khare, S. K., (2007). Enhanced production and characterization of a solvent stable protease from solvent tolerant *Pseudomonas aeruginosa*. *Enzyme Microbiological Technology*, 42: 11-16.
- [9] Gupta, R., Beg, Q. K., Khan, S. and Chauhan, B., (2002). An overview on fermentation, downstream processing and properties of microbial alkaline proteases. *Applied Microbiology Biotechnology*, 60: 381-395.
- [10] Immanuel, G., Bhagavath, C., Raj, P. I., Esakkiraj, P., and Palavesam, A., (2006). Production and partial purification of cellulase by *Aspergillus niger* and *A. fumigatus* fermented in Coir waste and sawdust. *The Internet Journal of Microbiology*, 3(1):11
- [11] Imtiaz, S., Mukhtar, H. and Ikram, H. (2013). Production of alkaline protease by *Bacillus subtilis* using solid state fermentation. *African Journal of Microbiology Research*, 7(16): 1558-1568.
- [12] Joo, H. S., Kumar, C. G., Park, G. C., Paik, S. R. and Chang, C. S., (2003). Oxidant and SDS-stable alkaline protease from *Bacillus clausii* I-52, production and some properties, *Journal of Applied Microbiology*, 95: 267-272.
- [13] Karuna, J. and Ayyanna, C., (1993). Production of semi-alkaline protease enzyme from *Aspergillus* spp. Proceedings of the Ninth National Convention of Chemical Engineers and International Symposium on Importance of Biotechnology in Coming Decades, Viskhapatnam India.
- [14] Kranthi, V.S., Rao, D. M. and Jaganmohan, P. (2012). Production of protease by *Aspergillus flavus* through solid state fermentation using different oil seed cakes. *International Journal of Microbiological Research* 3(1):12-15.
- [15] Kuo, L. C. and Shafer, J. A., (1994). Retroviral proteases. *Methods Enzymology*, 3: 178-241.
- [16] Li, Q., Yi, L., Marek, P. and Iverson, B. L., (2013). Commercial proteases: Present and future. *FEBS Letters*, 587: 1155-1163.
- [17] Lowry O.H., Rosebrough N.J. Farr A.L. and Randall R.J., (1951). Protein measurement with Folin phenol reagent. *Journal of Biological Chemistry*, 193: 265-275.
- [18] Madhumithah, C. G., Krithiga, R., Sundaram, S., Changam, S. S., Guhathakurta, S. and Cherian, K. M. (2011). Utilization of vegetable wastes for production of protease by solid state

- fermentation using *Aspergillus niger*. World Journal of Agricultural Sciences 7(5): 550-555.
- [19] Madzak, C., Treton, B. and Blanchin-Roland, S., (2000). Strong hybrid promoters and integrative expression/secretion vectors for quasi-constitutive expression of heterologous proteins in the yeast *Yarrowia lipolytica*, Journal Molecular Microbiology Biotechnology, 2(2): 207-216.
- [20] Mohapatra, B. R., Bapuji, M. and Sree, A., (2003). Production of industrial enzymes (amylase, carboxymethylcellulase and protease) by bacteria isolated from marine sedentary organisms. Acta Biotechnology, 23: 75-84.
- [21] IMótyán, J. A., Tóth, F. and Tozsér, J., (2013). Research applications of proteolytic enzymes in molecular biology. Biomolecules, 3: 923-942.
- [22] Mukhtar, H. and Haq, I., (2013). Comparative evaluation of agroindustrial byproducts for the production of alkaline protease by wild and mutant strains of *Bacillus subtilis* in submerged and solid state fermentation. The Scientific World Journal 538067.
- [23] Mukhtar, H. and Ikram, H. (2009). Production of acid protease by *Aspergillus niger* using solid state fermentation. Pakistan Journal of Zoology 41(4):253-260.
- [24] Munawar, T. M., Aruna, K., Swamy, A.V.N., (2014). Production, purification and characterization of alkaline protease from agro industrial wastes by using *Aspergillus terreus* (AB661667) under solid state fermentation. International Journal of Advanced Research in Engineering and Applied Sciences 3(10): 12-23.
- [25] Ortiz, G. E., Nosedá, D. G., PonceMora, M. C., Recupero, M. N., Blasco, M. and Albertó, E., (2016). A comparative study of new *Aspergillus* strains for proteolytic enzymes production by solid state fermentation. Enzyme Research 3016149.
- [26] Ozkan, E. and Ertan, F. (2011). Production and determination of some biochemical properties of protease enzyme by *Trichothecium roseum* under solid state fermentation. Romanian Biotechnological Letters 17(1):6903-6912.
- [27] Pant, G., Prakash, A., Pavani, J. V. P., Bera, S., Deviram, G. V. N. S., Kumar, A., Panchpuri, M., Prasuna, R. G. (2015). Production, optimization and partial purification of protease from *Bacillus subtilis*. Journal of Taibah University for Science 9:50-55.
- [28] Paranthaman, R., Alagusundaram, K. and Indhumathi, J. (2009). Production of protease from rice mill wastes by *Aspergillus niger* in solid state fermentation. World Journal of Agricultural Sciences 5(3):308-312.
- [29] Prabhavathy, G., Pandian, M. R. and Senthilkumar, B., (2012). Optimization and production of extracellular alkaline protease by solid state fermentation using *Bacillus subtilis*. Journal of Academic and Industrial Research, 1(7): 427-430.
- [30] Prakasham, R.S., Rao, C. S. and Sharma, P.N., (2006). Green gram husk-an inexpensive substrate for alkaline protease production by *Bacillus* sp. in solid-state fermentation. Bioresource Technology, 97: 1449-1454.
- [31] Rawling, N.D. and Barrett, A.J., (1994). Families of aspartic peptidases, and those of unknown mechanism. Methods Enzymology, 248: 105-120.
- [32] Rawlings, N.D. and Barrett, A.J., (1993). Evolutionary families of peptidases. Biochemistry Journal, 290: 205-218.
- [33] Sankeerthana, C., Pinjar, S., Jambagi, R. T., Bhavimani, S., Anupama, S., Sarovar, B., and Inamdar, S.R., (2013). Production and partial characterization of protease from *Aspergillus flavus* using rice mill waste as a substrate and its comparison with *Aspergillus niger* protease. International Journal of Current Engineering and Technology, (1):143-147.
- [34] Santhi, R. (2014). Extracellular protease production by solid state fermentation using *Punica granatum* peels waste. Indo American Journal of Pharmaceutical Research, 4(6):2706-2712.

- [35] Sathyavrathan, P. and Krithika, S., (2014). Production and optimization of protease from *Bacillus licheniformis* NRRL-NRS-1264 using cheap source substrates by submerged (SMF) and solid-state fermentation (SSF). *International Journal of Chemical Technology and Research*, 6(1): 286-292.
- [36] Sawant, R. and Nagendran, S. (2014). Protease: An enzyme with multiple industrial Applications. *World Journal of Pharmacy and Pharmaceutical Sciences*, 3(6):568-579.
- [37] Schrickx, J. M., Stouthamer, A. H. and Verseveld, H. W., (1995). Growth behaviour and glucoamylase production by *Aspergillus niger* N402 and a glucoamylase overproducing transformant in recycling culture without a nitrogen source. *Applied Microbiology and Biotechnology*, 43: 109–116.
- [38] Shanmugapriya, K., Saravana, P. S., Krishnapriya, Monoharan M., Mythili, A., and Joseph S., (2012). Isolation, screening and partial purification of cellulase from cellulose producing bacteria. *International Journal of Advanced Biotechnology and Research*, 3(1): 509-514.
- [39] Sri lakshmi, J., Madhavi, J. and Ammani, K. (2014). Protease production by *Humicola grisea* through solid state fermentation. *Global Journal of Bio-science and Biotechnology*, 3(3): 230-235.
- [40] Tsuchida, O., Yamagota, Y., Ishizuka, J., Arai, J., Yamada, J., Takeuchi, M. and Chishima, E., (1986). An alkaline protease of an alkalophilic *Bacillus* sp. *Current Microbiology*, 14: 7-12.
- [41] Wang, Q., Hou, Y., Xu, Z., Miao, J. and Li, G., (2008). Optimization of cold-active protease production by the psychrophilic bacterium *Colwellia* sp NJ341 with response surface methodology. *Bioresource Technology*, 99: 1926-1931.

# LC-MS analysis of dye extracted from *Butea monosperma* (Lamk.) Taub. flowers

Pooja Gupta\*, Naresh Chandra

Department of Botany, Birla College of Arts, Science & Commerce, Kalyan, Maharashtra, India

## ABSTRACT

In the present study dye was extracted from *Butea monosperma* (Lamk.) Taub. flowers using solvents like methanol and water. LC-MS analysis was carried out to identify major phytochemicals responsible for colour in *Butea monosperma* (Lamk.) Taub. flowers. The preparative HPTLC plate of methanolic dye was analysed. The three visible bands were further scraped and reconstituted in methanol for LC-MS analysis to obtain mass to charge ratio. Dye extracted from *Butea monosperma* (Lamk.) Taub. flowers exhibited several noticeable peaks and numerous small peaks. This showed butrin, isobutrin, butein and lanceoletin are some phytoconstituents which may be responsible for the yellow colour in *Butea monosperma* (Lamk.) Taub. flowers.

**Keywords :** *Butea monosperma*, LCMS, HPTLC, Flavonoids

## I. INTRODUCTION

The plant kingdom is a treasure house of potential drugs and in the recent years there has been an increasing awareness about the importance of medicinal plants. Colour is one of the element of nature that made the human living more aesthetic and fascinating in the world. They are supposed to be associated with emotions, human qualities, seasons, festivals and passion in our life. In the past, at dawn of the civilization, people tried to ornament their surroundings similar to that of natural colours observed in the plant, soil, sky and other sources. This gave birth to the new science of colours from natural origin (Vankar, 2007). Colours in flowers are adaptations that attract insects and other animals that in turn pollinate and help the plants to reproduce. Flavonoids are one of the most important phytochemical in some plants and they can be easily recognised as flower pigment (Mishra *et al.*, 2012).

*Butea monosperma* (Lamk.) Taub. commonly known as Flame of forest, belongs to the family Fabaceae. It is said that this tree is a form of Agnidev, God of Fire. *Butea monosperma* (Lamk.) Taub. showed anti-inflammatory, anti-stress, anti-diarrhoeal and anti-cancer property. In the present study dye was extracted from *Butea monosperma* (Lamk.) Taub. flowers using various solvents. HPTLC and LC-MS analysis was carried out to identify major phytochemical responsible for colour in *Butea monosperma* (Lamk.) Taub. flowers.

## II. METHODS AND MATERIAL

### Material

Dried powder of *Butea monosperma* (Lamk.) Taub flowers.

### Methods

#### 1) Preparation of dye

The extract was prepared for dye using 2g of dried powder of *Butea monosperma* (Lamk.) Taub.



flowers in 20ml methanol and water(aqueous). The dye was extracted in various solvents under optimized condition of extraction, by heating it in water bath for 30 minutes (Samanta and Konar, 2011).

The extracts were filtered to obtain 40% clear extracts of coloured solution using Whatmann paper 42 and observations were noted. Methanolic and aqueous dye showed intense colour so further analysis of only these dye was carried out by studying absorption spectra by using UV-spectrophotometer at different wavelengths (400nm to 620nm) (Plummer, 2003).

## 2) HPTLC analysis and LC-MS analysis

Methanolic and aqueous dye extracted from *Butea monosperma* (Lamk.) Taub. flowers was further analysed by HPTLC. The samples were loaded on TLC plate and simultaneously mobile phase was saturated in the saturation chamber for 20 minutes. TLC plate was kept in the chamber and the mobile phase was allowed to run upto 3/4 length of TLC plate. Then the plate was removed and dried to observe and scan.

10µl of the extract of *Butea monosperma* (Lamk.) Taub. flowers was loaded on TLC plates 60F254 using Camag Linomat V and were developed using ethyl acetate-formic acid-glacial acetic acid-water (100:11:11:26) as a solvent system for flavonoids separation. After drying the plates were observed under UV light at 254nm and 366nm and 520nm, using the UV cabinet and the separated spots were visualized. The plates were scanned by Camag TLC scanner at 520nm. The images were captured with Camag photo documentation at 254nm, 366nm and white light (without derivitisation).

The preparative HPTLC plate of methanolic dye was prepared for further analysis. The three

visible bands were further scraped and reconstituted in methanol for LC-MS analysis to obtain mass to charge ratio. The equipment used in the LC-MS study was of AB SCIEX make with model API 2000 with Q1 tuning mode.

## III. RESULTS AND DISCUSSION

The methanolic and aqueous dye extracted from *Butea monosperma* (Lamk.) Taub. flowers showed yellow dye as compared to other solvents. Methanolic and aqueous dye were further analysed to study maximum absorption using UV spectrophotometer. Maximum absorption of methanolic dye was observed at 520nm and aqueous dye was observed at 490nm as showed in (Figure 1).

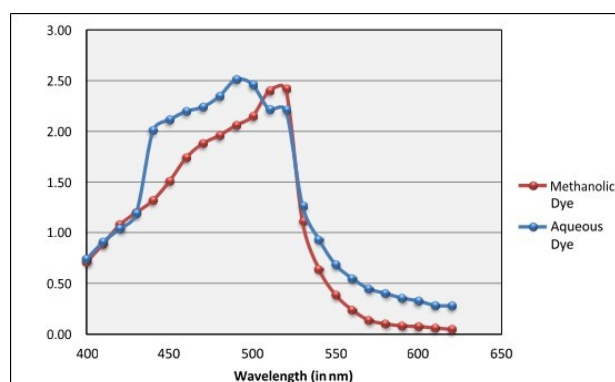


**Figure 1.** Absorption spectra of methanolic and aqueous dye extracted from *Butea monosperma* (Lamk.) Taub. flowers at different wavelengths

HPTLC analysis of 10µl methanolic dye extracted from *Butea monosperma* (Lamk.) Taub. flowers at 520nm showed 10 spots with Rf value 0.02, 0.14, 0.32, 0.42, 0.50, 0.75, 0.82, 0.84, 0.90, 0.91 (Table I). In 10µl aqueous dye of *Butea monosperma* (Lamk.) Taub. flowers at 520nm showed 10 spots 0.02, 0.06, 0.10, 0.31, 0.41, 0.75, 0.84, 0.86, 0.89, 0.91 (Table I). As observed in Plate 1 in white light.

The methanolic dye extracted from *Butea monosperma* (Lamk.) Taub. flowers with Rf value 0.32 and aqueous dye extracted from *Butea monosperma* (Lamk.) Taub. flowers with Rf value 0.31 at 520nm showed dark yellow visible band, which may corresponds to butrin. While Rf value

0.42 at 520nm in methanolic dye extracted from *Butea monosperma* (Lamk.) Taub. flowers and 0.41 at 520nm in aqueous dye showed light yellow visible band, which may correspond to isobutrin and Rf value 0.91 at 520nm in methanolic and aqueous dye extracted from of *Butea monosperma* (Lamk.) Taub. flowers showed yellow visible band, which may corresponds to butein. This showed that flavonoids were the major phytochemical responsible for the colour in *Butea monosperma* (Lamk.) Taub. flowers. These bands of methanolic dye extracted from *Butea monosperma* (Lamk.) Taub. were visible when separated from preparative HPTLC fingerprint, so these bands were scraped using scalpel and reconstituted in methanol for further analysis by LC-MS (Plate 2). Dye extracted from *Butea monosperma* (Lamk.) Taub. flowers exhibited several noticeable peaks and numerous small peaks.

In the present study the molecular mass 597.8 may correspond to butrin (596) in spot 1 with Rf 0.32, 597.5 may correspond to isobutrin (596.17) in spot 2 with Rf 0.42 and 273.5 may correspond to butein (272) in spot 3 with Rf 0.91 (high intensity peak). It was observed that the molecular mass 302.50 may correspond to lanceoletin (302) in spot 3 with Rf 0.91. This showed that butrin, isobutrin, butein and lanceoletin are some phytoconstituents which may be responsible for the yellow colour in *Butea monosperma* (Lamk.) Taub. flowers. Many other flavonoids may be in combination or pure forms are present in *Butea monosperma* (Lamk.) Taub. flowers.

**Table 1.** Hptlc Fingerprint Of Methanolic And Aqueous Dye Extracted From *Butea Monosperma* (Lamk.) Taub. Flowers

Peak No.	Methanolic dye	Aqueous dye
	Max Rf at 520nm	
1	0.02	0.02
2	0.14	0.06
3	<b>0.32</b>	0.10
4	<b>0.42</b>	<b>0.31</b>
5	0.50	<b>0.41</b>
6	0.75	0.75
7	0.82	0.84
8	0.84	0.86
9	0.90	0.89
10	<b>0.91</b>	<b>0.91</b>

Further investigation is necessary for standardising the other flavonoids and extraction of other compounds from *Butea monosperma* (Lamk.) Taub. flowers. In the earlier study it was observed that *Butea monosperma* (Lamk.) Taub. flowers contains phytoconstituents butrin, isobutrin and butein as suppressor of tumour cells (Rasheed et al., 2010). A flavone was isolated from the flowers of *Butea monosperma* (Lamk.) Taub. identified for the first time as lanceoletin (Oberoi and Ledwani, 2010).

Similar work was observed in flavonoids extracted from marigold flowers which were investigated for their dyeing potential. Patulitrin and patuletin were isolated and their structures established using HPLC-MS (Guinot et al., 2008). Standard extraction procedure for examining chromophoric substances of turmeric was investigated. Acetone and methanol were used as extracting solvents with different extraction procedures and pH levels. GC-MS analysis identified curcumin (6.7 min), feruloylmethane (8.3min), coumaran (6.09min), vanillin (6.2min), and zingiberene (10.5min) as the major products. Curcumin which has been known

as the major chromophoric substance of turmeric was not detected in any samples (Cheunsoon and Obendorf, 2006).

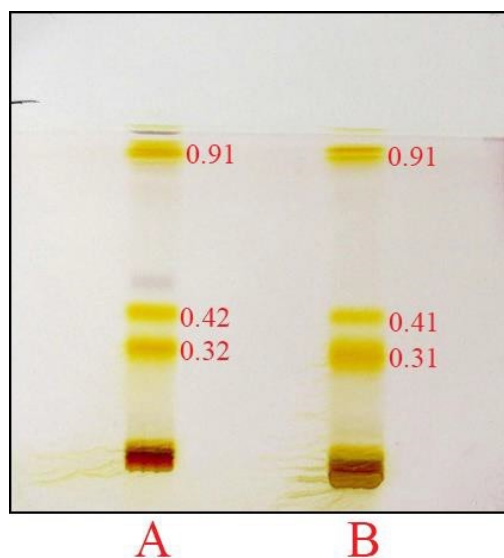


**Plate 1.** HPTLC fingerprint of methanolic and aqueous dye extracted from *Butea monosperma* (Lamk.) Taub. flowers at white light

**Keywords:** A – Methanolic dye, B – Aqueous dye

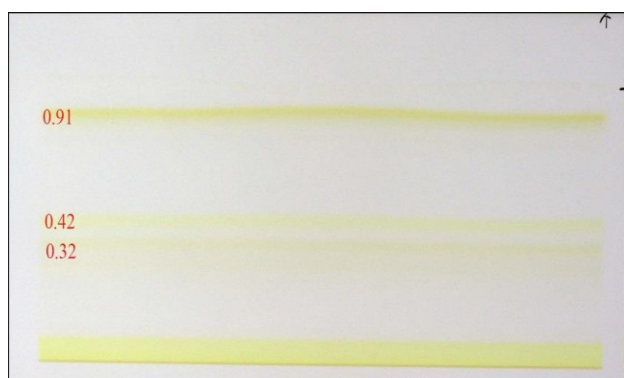


**Plate 2.** Preparative HPTLC fingerprint of methanolic dye extracted from *Butea monosperma* (Lamk.) Taub. flowers

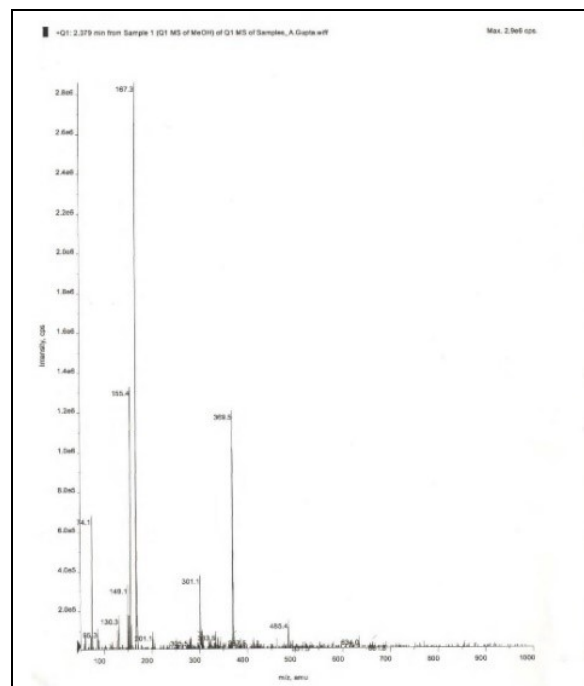


**Figure 2.** Q1-MS observation for methanol

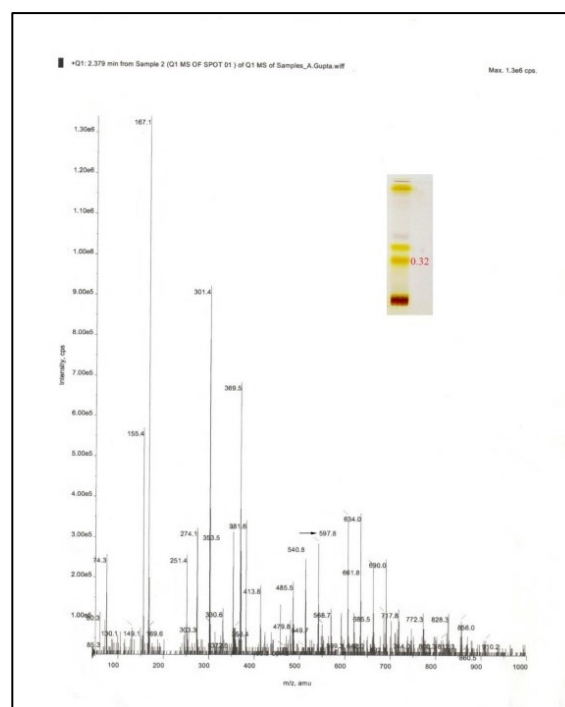


**Figure 3.** Q1-MS observation for methanolic dye extracted from *Butea monosperma* (Lamk.) Taub. flowers for spot 1

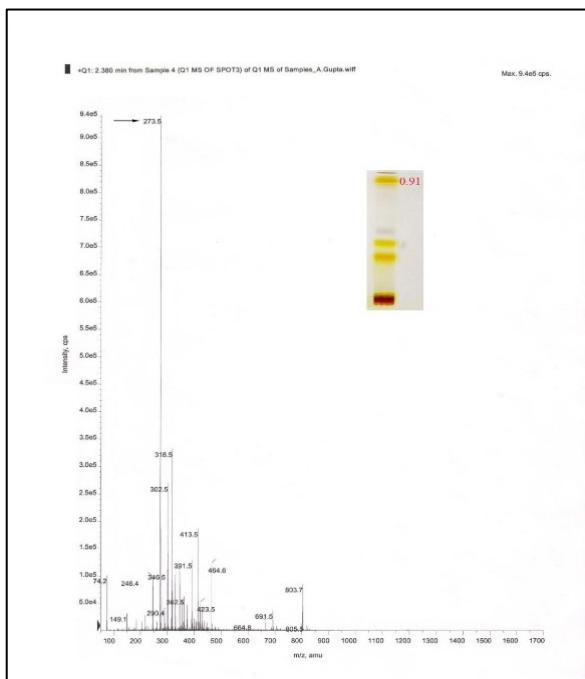


**Figure 4.** Q1-MS observation for methanolic dye extracted from *Butea monosperma* (Lamk.) Taub. flowers for spot 3

#### IV. CONCLUSION

It was observed from the present study that the methanolic and aqueous dye extracted from *Butea monosperma* (Lamk.) Taub. flowers showed intense yellow colour. The HPTLC and LC-MS analysis confirmed the presence of flavonoids responsible for the yellow colour in *Butea monosperma* (Lamk.) Taub. flowers. The flowers are good source of flavonoids which can be used as natural colour. Flavonoids also have many medicinal properties and can be used in therapeutic treatment.

**Table 2.** Q1-MS observation for methanolic dye extracted from *Butea monosperma* (Lamk.) Taub. Flowers

Q1 MS of MeOH	Q1 MS of Spot 1	Q1 MS of Spot 2	Q1 MS of Spot 3
74.10	74.30	74.10	74.20
85.30	85.30	-	-
130.30	130.10	130.30	-
149.10	149.10	-	-
155.40	155.40	155.40	-
167.30	167.10	-	-
201.10	-	-	-
-	251.40	-	-
-	274.10	-	<b>273.50</b>
301.10	301.40	301.50	-
-	-	-	<b>302.50</b>
305.50	-	-	-
-	-	-	318.50
-	353.50	353.50	-
367.50	-	-	-
369.50	369.50	369.50	-
-	381.60	381.50	-
383.50	-	-	-
-	413.80	-	413.50
-	-	437.40	-
-	-	-	464.60
485.40	485.50	-	-
531.50	-	-	-
-	540.80	-	-
-	568.70	-	-
-	<b>597.80</b>	<b>597.50</b>	-
-	-	619.80	-
634.00	634.00	-	-
661.80	661.80	-	-
-	685.50	-	-
-	690.00	-	-
-	717.80	-	-
-	-	739.80	-
-	-	-	803.70

## V. REFERENCES

- [1] Vankar, P. S. (2007). Natural Dyes for Industrial Applications. Publisher: National Institute of Industrial Research, 1.
- [2] Mishra, G. J.; Reddy M. N. and Rana J. S. (2012). Isolation of flavonoid constituent from *Launaea procumbens* Roxb. by preparative HPTLC method. *IOSR Journal of Pharmacy*. 2(4):05-11.
- [3] Samanta, A. K. and Konar, A. (2011). Dyeing of textiles with natural dyes. Dr. Emriye Akcakoca Kumbasar edition. 978-953-307-783-3.
- [4] Plummer, D. T. (2003). An introduction to Practical biochemistry. Tata McGraw- Hill Publishing Company Limited. Twentieth reprint. 122-130
- [5] Oberoi, S and Ledwani, L. (2010) Isolation and characterization of new plant pigment along with three known compounds from *Butea monosperma* petals. *Archives of applied science research*. 2(4): 68-71.
- [6] Rasheed, Z.; Akhtar, N.; Khan, A.; Khan, K. A. and Haqqi, T. M. (2010). Butrin, isobutrin and butein from medicinal plant *Butea monosperma* selectively inhibit nuclear factor-kappa B in activated human mast cells: suppression of tumour necrosis factor-alpha, interleukin (IL)-6 and IL-8. *J. Pharmacol Exp Ther*. 333(2):354-63.
- [7] Guinot, P.; Annick, G.; Gilles, V.; Alain, F. and Claude, A. (2008). Primary flavonoids in marigold dye: extraction, structure and involvement in the dyeing process. *Phytochem. Anal*. 19: 46-51.
- [8] Cheunsoon, A. and Obendorf, S. K. (2006). GC-MS analysis of dye extracted from turmeric. *Fibres and Polymers*. 7(2): 158-163.

# Study of 1,2,4-Triazole As Effective Corrosion Inhibitor For Mild Steel Used In Oil And Gas Industries In 1M HCl

Pratap Kamble , R. S. Dubey

Department of Chemistry, R. Jhunjhunwala College, Ghatkopar (W), Mumbai, Maharashtra, India

## ABSTRACT

The corrosion inhibition effect of 1,2,4-triazole on mild steel in 1 M HCl solution has been investigated by weight loss, open circuit potential (OCP) and potentiodynamic polarization methods. The experimental results revealed that the compound having significant inhibiting effect on the corrosion of mild steel in 1M HCl solution. The inhibition efficiency was found to increase with increasing concentration of inhibitor and attain maximum value of 93% at 500 ppm concentration. Potentiodynamic polarization studies have shown that the compound acted as mixed-type inhibitor retarding the corrosion of mild steel by blocking the active sites of metal surface. The values of inhibition efficiency obtained from weight loss and polarization measurements are in good agreement. The adsorption of the inhibitor on mild steel surface followed Langmuir adsorption isotherm with negative value of the free energy of adsorption  $\Delta G^0_{ads}$ . The surface morphology of the mild steel specimen was evaluated by using scanning electron microscopy (SEM) and energy dispersive x-ray analysis (EDAX) techniques.

**Keywords:** Triazole, Mild Steel, Inhibitor, Surface Morphology.

## I. INTRODUCTION

Mild steel is an important category of material due to wide range of industrial applications [1-4]. Hydrochloric acid solutions are widely used for pickling, descaling, acid cleaning and oil well acidizing industry which leads to electrochemical corrosion. Among the various methods available, use of corrosion inhibitor is one of the most practical and economical method for corrosion protection of steel especially in acid media [4-8]. An organic corrosion inhibitor is a chemical material applied to a liquid or gas within industrial processes to decrease the corrosion rate of metal or its alloy [9]. Organic inhibitors containing heteroatom such as O, N, S and P are frequently used in order to minimize the corrosion attack on metal in acid media [10-15]. Organic inhibitors are generally adsorbed on metal

surface and forms protective film which acts as barrier between the metal and aggressive solutions. The efficiency of organic compounds as an inhibitor depends on its ability to get adsorbed on the metal surface by replacing water molecule from metal surface. Nitrogen containing heterocyclic compounds are found very effective and efficient corrosion inhibitor of mild steel in acidic media. Pursual of literature reveals that many N-heterocyclic compounds such as pyrazole, bipyrazole, benzimidazole, triazole, tetrazole, quinoline, isoquinoline, indole and quinoxaline have been used for corrosion inhibition of mild steel in acidic media [16-20]. Triazole and its derivatives are important constituents of pharmacologically active compounds. They possess wide spectrum of activities ranging from antibacterial, anti-inflammatory, anticonvulsant and

anti-neoplastic[21].A few triazole have been reported as corrosion inhibitor in different corrosive environment.

The present study was undertaken to investigate the inhibition of corrosion of mild steel in 1M hydrochloric acid by 1,2,4-triazole.The study was conducted by using weight loss, electrochemical technique, Scanning electron microscopy (SEM) and energy dispersive X-ray spectroscopy (EDX) techniques.

## II. METHODS AND MATERIAL

### 2.1. Material and sample preparation

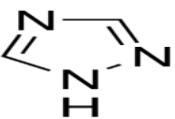
The weight loss and electrochemical experiments were performed on mild steel specimen having chemical composition, C-0.16%, Si-0.10%, Mn-0.40%, P-0.013%, S-0.02% and remaining iron. The exposed dimensions were 1cm x 3cm x 0.025cm and 1cm<sup>2</sup> for the weight loss and electrochemical experiment respectively. Before exposure to test solution exposed areas were polished successively with different grades of metallographic emery paper,1/0,2/0,3/0 and 4/0, washed with doubled distilled water, degreased with acetone and finally dried and stored in desiccators.

### 2.2. Test solution

1 M HCl was prepared by dilution of 36% HCl (analytical grades) in bi-distilled water.

The characterization data, IUPAC name, structure and abbreviation used for the studied compound are given below in Table 1.

**Table 1.** IUPAC name, molecular structure, melting point and analytical data of studied inhibitor.

Inhibitor	Molecular Structure	Analytical data
1,2,4-Triazole		MP- 120-122 °C

### 2.3. Weight loss measurement:

The weight loss experiment was performed by immersing mild steel specimen in 50 ml of test solution with and without different concentration of inhibitors. After 24 h immersion time, the mild steel specimens were taken out, cleaned with distilled water, dried and accurately weighed. Each experiment was performed in triplicate to obtain good result and the mean value is reported. The inhibition efficiency was calculated by using the following relation:

$$\eta\% = \frac{W_0 - W_{\text{corr}}}{W_0}$$

Where  $W_0$  and  $W_{\text{corr}}$  are the weight loss in absence and presence of inhibitors .The surface coverage is given by following relation

$$\theta = \eta\%/100.$$

### 2.4 Electrochemical measurement:

Polarization studies were carried out using electrochemical measurement system, DC 105, containing software of DC corrosion technique from M/S Gamry instrument, 734, Louis Drive, Warminster, PA, USA. For polarization studies, mild steel specimens having surface area of 1cm<sup>2</sup> were exposed to acid solution .Mild steel as working electrode, saturated calomel (SCE) as reference electrode and graphite as auxiliary electrode were used for all electrochemical measurement. Before each measurement the specimen were allowed to corrode freely, and their OCPs were measured as a function of time to obtain a steady-state potential. The anodic and cathodic Tafel curves were obtained by changing the electrode potential automatically from - 0.5 to 0.5 V at the scan rate of 5mv/s. Polarization study was done with and without inhibitors in 1M HCl.

### 2.5 Surface measurement:

The surface film formed on the metal specimen was evaluated by SEM-EDX analysis. This was carried out by using SEM/EDX model PHENOM PROX from the

Netherlands. The spectra were recorded for a sample exposed for 24 hours in 1M HCl in the absence and presence of 500 ppm inhibitor. The energy of acceleration beam employed was 20 kV.

### III. RESULTS AND DISCUSSION

#### 3.1 Weight loss measurement:

Weight loss data of mild steel in 1 M HCl in the absence and presence of various concentrations of inhibitor were obtained and given in table 2. Inhibition efficiencies were calculated according to following equation:

$$\%IE = \frac{W_0 - W_{corr}}{W_{corr}} \quad (1)$$

$W_{corr}$  and  $W_0$  are weight loss of mild steel in presence and absence of inhibitors respectively. The results showed that the inhibition efficiency increases with increasing the concentration of inhibitors. The results obtained from the weight loss measurement were in good agreement with those obtained from electrochemical measurements.

**Table 2.** The weight loss parameter obtained for mild steel in 1 M HCl containing different concentrations of 1, 2, 4-triazole.

Inhibitor	Concentration (ppm)	Weight loss (mg)	Surface coverage	Inhibition efficiency (%E)
Blank	-	235	-	-
1,2,4-triazole	100	42	0.8212	82.12
	200	30	0.8723	87.23
	300	28	0.8808	88.08
	400	21	0.9106	91.06
	500	16	0.9319	93.19

#### 3.2 Adsorption isotherm

The surface coverage values  $\theta$ , (defined as  $\theta = \%IE/100$ ), increased with increasing inhibitor concentration as a result of adsorption of more inhibitor molecules on the steel surface (Table-2). If molecular adsorption at the metal/solution interface is the mechanism through which the corrosion inhibition occurs, several adsorption isotherms can be tested. The simplest, being the Langmuir isotherm, is based on the assumption that all adsorption sites are equivalent and that molecular binding occurs independently from nearby sites being occupied or not. Under these circumstances, the proportionality between surface coverage  $\theta$  and bulk concentration  $C$  of the adsorbing compound is as follows [22]:

$$KC = \theta / (1-\theta) \quad (2)$$

Here  $K$  is the equilibrium constant. It is convenient to rearrange the equation, yielding:

$$C / \theta = C + 1/K \quad (3)$$

The graph of  $C/\theta$  vs  $C$  obtained straight line with  $R^2$  value obtained varied close to unity confirming the validity of this approach. The slope of the straight line was almost close to unity, suggesting that adsorbed molecule formed monolayer on mild steel surface.

Free energy of the adsorption ( $\Delta G_{ads}^0$ ) can be calculated by using the following equation:

$$\Delta G_{ads}^0 = -RT \ln (55.5 k_{ads}) \quad (4)$$

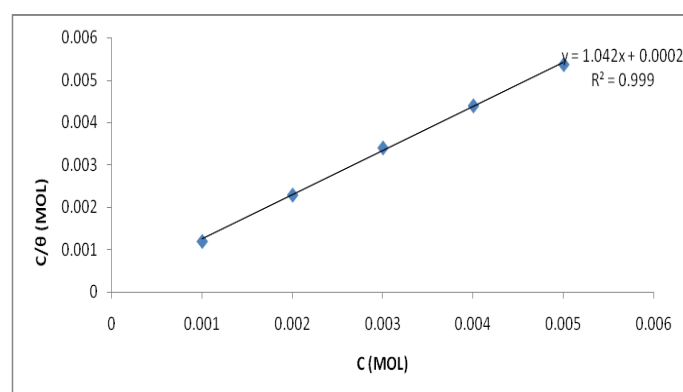


**Figure 1.** Langmuir isotherm plot for adsorption of 1,2,4-triazole on mild steel surface in 1 M HCl.



Generally, value of  $\Delta G_{ads}^0$  up to  $-20 \text{ kJmol}^{-1}$  are associated with physisorption while those around  $-40 \text{ kJmol}^{-1}$  or higher are associated with chemisorptions. In present case the value was  $-31.05$ . This was lower than  $-40 \text{ kJ mol}^{-1}$  but higher than  $-20 \text{ KJmol}^{-1}$  indicating that the adsorption was neither typical physisorption nor chemisorption but it is mixed type. Thus in the present case adsorption of inhibitor molecule on the mild steel involved both physisorption and chemisorptions but physisorption was the predominant mode of adsorption. The negative value of  $\Delta G_{ads}^0$  indicated the spontaneous adsorption of inhibitors on the surface of the metal [23,24]

### 3.3 Open circuit potential (OCP) measurement

The electrochemical behaviour of mild steel in 1M HCl was studied by monitoring change in corrosion potential ( $E_{corr}$ ) with time. The change in open circuit potential of mild steel in absence and presence of various concentrations of inhibitors is shown in Figure 2.

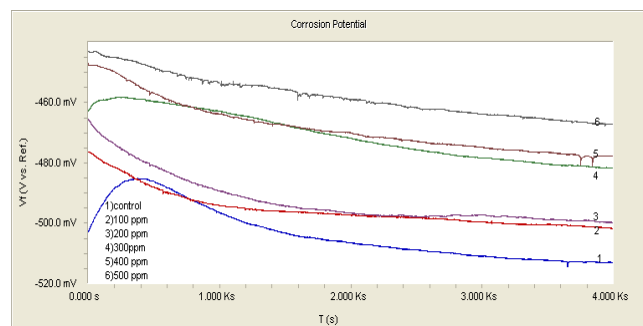


**Figure 2.** Open circuit potential diagram for mild steel in 1 M HCl without and with different concentrations of 1,2,4-Triazole.

The change in OCP of mild steel in absence and presence of inhibitors were measured for period of one hour with sample period of one data per second. The potential attains steady state after exposure of approximately 30 minutes. The steady state potential is an equilibrium state at which  $i_{ox}$  equal to  $i_{red}$ . It has been observed that OCP of mild steel from moment of immersion in 1M HCl tends towards more

negative value in absence of inhibitor. This shows corrosiveness of medium which is due to breakdown of pre-immersion, air formed oxide film on the metal surface. In the presence of various concentrations of inhibitors the steady state potential of mild steel shifts more towards positive value. This is due to adsorption of inhibitors on metal surface resulting in passivation of metal.

### 3.4 Potentiodynamic polarisation studies

The polarization behaviour of mild steel in 1 M HCl in the absence and presence of different concentration of inhibitors are shown in Figure 3.

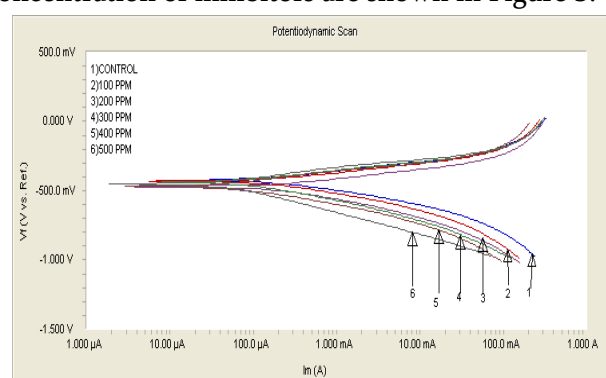


**Figure 3.** Polarization curve of mild steel in the absence and presence of 1,2,4-Triazole.

Electrochemical parameters such as corrosion current ( $I_{corr}$ ), corrosion potential ( $E_{corr}$ ), and Tafel slopes constant  $\beta_a$  and  $\beta_c$  calculated from Tafel plots are given in table 3. From the evaluated  $I_{corr}$  value,  $\eta\%$  can be calculated using the relation  $\eta\% = \frac{i_0 - i_{corr}}{i_0}$ . where  $i_0$  and  $i_{corr}$  are the corrosion current densities in the absence and presence of inhibitors. From the data of table 3 and figure 2, it is clear that in the presence of tetrazole there was remarkable decrease in  $i_{corr}$  value by shifting both anodic and cathodic Tafel slopes towards low current densities [25]. It was further confirmed that the shape of polarization curves were similar in absence and presence of inhibitors, suggesting that 1,2,4-triazole inhibited mild steel corrosion by simply adsorbing on the mild steel surface without changing the mechanism

of mild steel dissolution[26]. An inhibitor can be classified as anodic, cathodic or mix type depending upon the displacement in  $E_{corr}$  value. If the displacement in  $E_{corr}$  for the inhibited and uninhibited solution is more than 85mV it can be classified as cathodic or anodic type. But the displacement in  $E_{corr}$  is less than 85 mV then it can be classified as mixed-type. Since the maximum displacement for studied compound was 23 mV indicating that tetrazole is mixed type of inhibitor [27].

**Table 3.** Tafel polarization parameters for mild steel in 1 M HCl in absence and presence of 1,2,4-triazole.

Acid Medium	Concentration (ppm)	$-E_{corr}$ (mv)	$I_{corr}$ ( $\mu A/cm^2$ )	$\beta_a$ (v/dec)	$\beta_c$ (v/dec)	IE %
1 M HCl	-	-470.0	704.0	103.3 $e^{-3}$	196.4 $e^{-3}$	-
	100	-475.0	128.0	71.50 $e^{-3}$	144.3 $e^{-3}$	81.81
	200	-473.0	90.90	68.30 $e^{-3}$	133.6 $e^{-3}$	87.08
	300	-475.0	84.00	69.70 $e^{-3}$	164.5 $e^{-3}$	88.06
	400	-483.0	63.40	83.00 $e^{-3}$	169.3 $e^{-3}$	90.99
	500	-	36.90	93.1 $e^{-3}$	154.6	93.

#### IV. SURFACE STUDIES

##### 4.1 SEM studies

To support our conclusion that the 1, 2, 4-triazole form protective surface film, SEM micrograph of the mild steel surface were recorded in the absence and presence of 500 ppm concentration of triazole. The result shows that the surface of polished mild steel

coupon (Figure 4a) was considerably smoother with minimum undulation or pitting. (Fig-4b) shows the surface of coupon immersed in 1 M HCl solution which is strongly damaged due to acid corrosion. However the coupon immersed in the solution containing 500 ppm of 1,2,4-triazole was relatively smooth compared to free acid solution(Figure 4c).

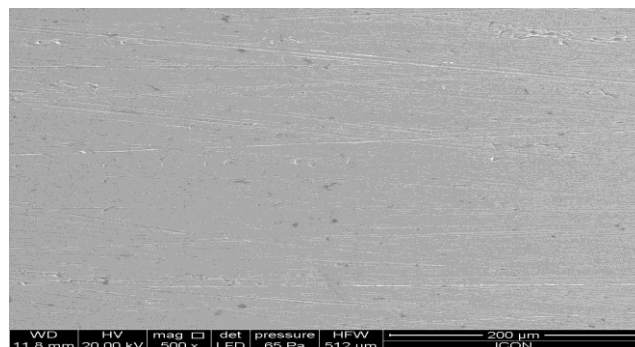


**Figure 4(a).** SEM micro graphs of mild steel surface before immersion in 1 M HCl

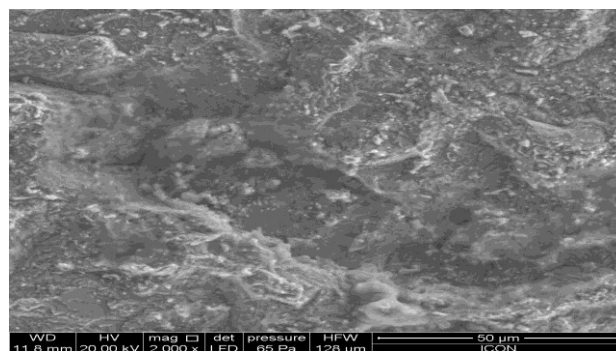


**Figure 4(b).** SEM micro graphs of mild steel surface after one day immersion in 1 M HCl

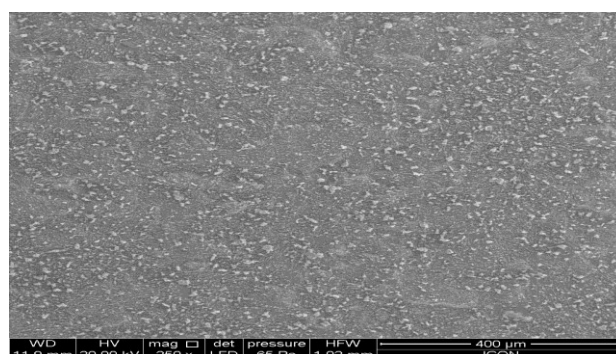


**Figure 4(c).** SEM micro graphs of mild steel surface after one day of immersion in 1 M HCl+500 ppm of 1,2,4-Triazole.

## 4.2 EDX studies

To further support our weight loss and electrochemical finding that 1, 2, 4-triazole inhibit mild steel corrosion by forming a protective film on surface, we recorded the EDX spectra in absence and presence of 500 ppm of 1, 2,4-triazole.

The spectral profile of the polished mild steel sample before immersion in 1M HCl shows the signal for Fe, C and O. On immersion in 1M HCl, the signal for O disappeared due to breaking of preimmersion air formed oxide film. Signal for Fe and carbon also slightly decreased. The profile in presence of 1, 2, 4-triazole shows additional signal for nitrogen atoms. This is due to adsorption of inhibitor on the mild steel surface.

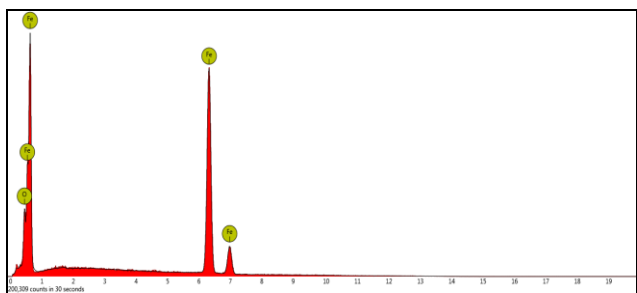


Figure 5. EDX of (a) polished mild steel surface

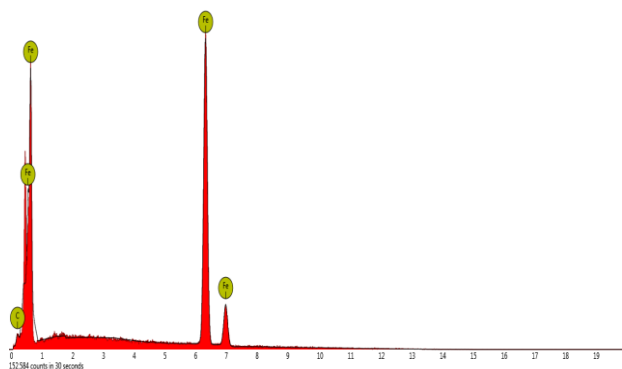


Figure 5. EDX of (b) after one day immersion in 1 M HCl

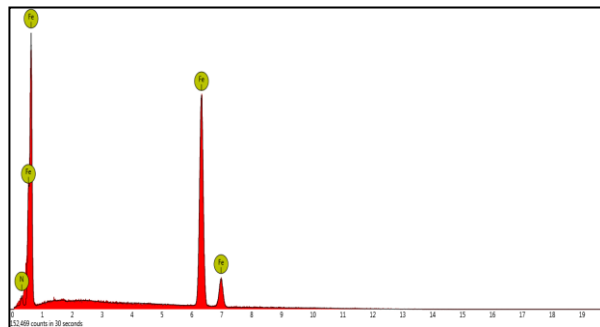


Figure 5. EDX of (c) after one day of immersion in 1 M HCl +500 ppm of 1,2,4-Triazole.

## V. MECHANISM OF INHIBITION

Corrosion inhibitors are believed to act by adsorption on metal surface by either physical or chemical means. The physical adsorption occurs via electrostatic interaction between the oppositely charged inhibitor molecule and metal surface, whereas chemical adsorption takes place via donor-acceptor interaction between lone pair electrons of heteroatom (N,S,O),  $\pi$  electrons of aromatic rings and polar functional groups with vacant d orbital of metal. The compound inhibits corrosion by controlling both anodic as well as cathodic reactions. In acid solution, inhibitor can exist as protonated species. The nitrogen atom present in the molecule can be easily protonated in acidic solution which can get adsorbed onto the cathodic sites of the mild steel and decrease the evolution of hydrogen. The adsorption on the anodic sites occurs through  $\pi$  electrons of triazole ring and lone pairs of electrons of nitrogen atoms which decrease the anodic dissolution of mild steel.

## VI. CONCLUSION

The corrosion behaviour of mild steel in 1 M HCl in absence and presence of tetrazole compound was investigated using the weight loss, open circuit potential and potentiodynamic polarization technique and surface analytical techniques. From the result obtained the following conclusion can be drawn:

1. 1, 2, 4-Triazole acted as a good and efficient corrosion inhibitor for the corrosion of mild steel in 1M HCl solution.
2. The inhibition efficiency increased with an increase in the concentration of inhibitor.
3. The adsorption of the inhibitor on mild steel surface obeyed Langmuir adsorption isotherm. The negative Gibbs free energy value indicated that the adsorption of inhibitor on surface is spontaneous process.
4. Polarization studies showed that 1,2,4-triazole acts as mixed inhibitor
5. The surface morphology techniques revealed the formation of smooth uniform surface on mild steel in presence of inhibitor.

## VII. REFERENCES

1. R. Winston revie, Herbert H. Uhlig, Corrosion and corrosion control; An introduction to corrosion science and Engineering, Fourth edition, Wiley Interscience 2008.
2. M. A. Amin, K. F. Khaled, Sahar A. Fadi. allah, Corros. Sci. 52 (2010) 140.
3. A. Ostovari, S. M. hoseinieh, M. Peikari, S. R. Shadizadeh, S. J. Hashemi, Corros. Sci. 51 (2009) 1935-1949.
4. Z. Tao. , S. Zang. , Li W. B. Hou. Corrosion Sci. , 2009, 51, 2588.
5. Raheem jafar aziz. , Study of some drugs as corrosion inhibitors of mild steel in 1M H<sub>2</sub>SO<sub>4</sub>. Int. j. curr. Res. Chem. Pharma. Sci. (2016). 3(12):1-7.
6. E. E. Oguzie, Y. Li, F. H. Wang, Corrosion inhibition and adsorption behavior of methionine on mild steel in sulfuric acid and synergistic effect of iodide ion, J. Colloid and Interface cience 310, Issue 1 (2007) 90-98.
7. S. M. A. Hosseini, A. Azimi, Corros. Sci. 51 (2009) 728-732.
8. O. K. Abiola, Adsorption of 3-(4-amino-2-methyl-5-pyrimidyl methyl)-4- methyl thiazolium chloride on mild steel, Corros. Sci 48, issue 10 ( 2006) 3078- 3090.
9. Raheem jafar aziz. , Study of some drugs as corrosion inhibitors of mild steel in 1M H<sub>2</sub>SO<sub>4</sub>. Int. j. curr. Res. Chem. Pharma. Sci. (2016). 3(12):1-7.
10. Qing Qu, Zhengzheng Hao, Lei Li, Wei Bai, Yongjun Liu, Zhongtao Ding, Synthesis and evaluation of Tris-hydroxymethyl-(2-hydroxybenzylidenamino)-methane as a corrosion inhibitor for cold rolled steel in hydrochloric acid, Corros. Sci 51, issue 3 (2009) 569-574.
11. V. S. Sastry, Corrosion inhibitors: Principals and application, John wiley and sons ltd. , 2001, p. 637-751.
12. F. Bentiss, M. Traisnel, L. Lagrenee, M. Lagrenee, Appl. Surf. Sci. 161 (2000) 194-202.
13. H. Ashassi-Sokhabi, D. Seifzadeh, M. G. Hosseini, Corros. Sci. 50 (2008) 3363- 3370.
14. M. A. Qurashi, I. Ahmed, A. K. Singh, S. K. Shukla, B. Lal, V. Singh, Mater. chem. Phys. 112 (2008) 1035-1039.
15. G. K. Gomma, Mater. chem. phy55 (1998) 241.
16. A. Chetouani, A. Aounti, B. Hammouti, T. Benhadda, M. Daoudi, Appl. surf. Sci. 249 (2005) 375.
17. H. H. Hassan, E. Abdelghani, M. A. Amima. Electrochem. Acta 52(2007)6359.
18. S. Kertit, B Hammouti. Appl. surf. Sci. 161 (1996)59.
19. Eno E. Ebenso, Ime B. Obot, L. C. Murulana. Quinoline and its derivatives as effective corrosion inibitors for mild steel in acidicmedium. Int. J. Electrochem. Sci. , 5(2010)1574-1586.
20. I. B. Obot, N. O. Obi-Egbedi, Corros. Sci. 52 (2110)282.
21. M. A. Qurashi, Suddir, K. R. Ansari, Eno Ebenso. 3-Aryl substituted triazole derivative as a new and effective corrosion inhibitor for mild steel in hydrochloric acid solution. medium. Int. J. Electrochem. Sci. , 7(2012)7476-7492.

22. M. G. Hosseini, S. F. L. Mertens, M. R. Arshadi, Synergism and antagonism in mild steel corrosion inhibition by sodium dodecylbenzenesulphonate and hexamethylene tetramine, *Corros. Sci.* 45 (2003) 1473–1489
23. Chandrabhan varma, M. A. Quraishi, A. singh “5-substituted 1H-tetrazole as effective corrosion inhibitors for mild steel in 1M hydrochloric acid”. *Journal of Taibah university for science*. Vol. 10, issue 5, 2016. pp. 718-733.
24. j. , Shukla, K. S. Pitre, “Electrochemical behavior of brass in acid solution and the inhibitor effect of imidazole” , *corrosion Rev.* , 2002 , 20(3), pp. 217-230.
25. I. Ahamad and M. A. Qurashi, “Bis(benzimidazole-2-yl)disulfide , an efficient water soluble inhibitors for corrosion of mild steel in acid media” . *Corrosion science* vol. 51, no. 9 pp2006-2013, 2009.
26. A. K. Singh, M. A. Quraishi, Inhibitive effect of diethylcarbazine on the corrosion of mild steel in hydrochloric acid, *Corros. Sci.* 52, issue 4 (2010) 1529-1535.
27. M. Abdallah, Rhodanine azosulpha drugs as corrosion inhibitors for corrosion of 304 stainless steel in hydrochloric acid solution, *Corros. Sci.* 44, issue 4 (2002)717-728.

# Inhibitive effect of 8-hydroxy Quinoline on the corrosion of mild steel in 1M HCl

R. S. Dubey, Pratap Kamble

Department of Chemistry, R. Jhunjhunwala College, Ghatkopar (W), Mumbai, Maharashtra, India

## ABSTRACT

The inhibitive action 8-Hydroxy quinoline on corrosion of mild steel in 1 M HCl was investigated by weight loss, open circuit potential (OCP) and potentiodynamic polarization technique. The results showed that the 8-hydroxy Quinoline inhibited mild steel corrosion and inhibition efficiency increased with increase in concentration of inhibitor. The adsorption is spontaneous and followed Langmuir's adsorption isotherm. Polarization study indicated that the inhibitor acted as mixed-type. The protective film formed on surface is confirmed by scanning electron microscopy (SEM) and energy dispersive analysis by X-ray (EDX). Result obtained from weight loss technique are in good agreement with electrochemical and surface analytical results.

**Key words:** Mild Steel, Corrosion, HCl, SEM, EDX.

## I. INTRODUCTION

Corrosion is the deterioration of a metal as a result of chemical reaction between it and the surrounding. Corrosion causes heavy economic losses. In India with GDP of amount 2 trillion, loses as much as 100 billion dollar every year on account of corrosion. Mild steel is widely used as construction material in most of major industries due to its excellent mechanical properties and low cost. The major problem of mild steel is its dissolution in acidic medium [1-6]. Acids is widely used for acid pickling, descaling, oil well acidizing and other applications. Due to their high corrosive nature acid may cause damage to the system components. Thus it is necessary to develop some effective corrosion inhibitors. The use of organic inhibitor is the most effective and most economic method for protection of metal from corrosion. Generally, organic inhibitors inhibit metallic corrosion by adsorbing on the surface and thereby forming a protective barrier [7-14]. The adsorption of an inhibitor is influenced

by various factors such as electron density of donor site, presence of functional groups, electronic structure of inhibiting molecule, molecular area and molecular weight of inhibitor. Organic compounds containing heteroatoms including nitrogen, sulphur, and/or oxygen with polar functional groups and conjugated double bonds have been reported as effective corrosion inhibitor [14-20].

The aim of present work is to study the inhibition effect of 8-hydroxy Quinoline on mild steel in presence of 1 M HCl by using various techniques such as weight loss measurement, open circuit potential (OCP), and potentiodynamic polarization. Surface analytical techniques such as SEM AND EDX were also used to characterize corrosion product formed.

## II. EXPERIMENTAL PROCEDURE

### 2.1. Material and sample preparation

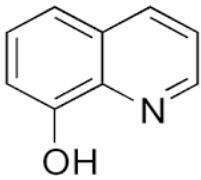
Mild steel of commercial grade in sheet form having composition as follows: C-0.16%, Si-0.10%, Mn –

0.40%, P - 0.012%, S - 0.02%, and Iron- balance, were used in the present investigation. For electrochemical polarization, samples of 1cm x 3cm were sheared from the commercial grade sheets. The surface of these samples was successively polished by using the Emery papers of grades 1 / 0, 2 / 0, 3 / 0, and 4 / 0 obtained from Signor, Switzerland to obtain a scratch free mirror finish surface. The polished samples were washed with detergent solution, rinsed with distilled water and finally degreased with acetone. The specimens were dried and stored in a desiccators containing silica gel as a dehydrating agent. The test solution of 1M HCl was prepared by diluting analytical grade HCl (MERCK, 37%) in double distilled water.

## 2.2. Synthesis of inhibitor

The 8-hydroxy quinoline used in present study was synthesized according to a previously described procedure [21].The completion of the reaction was verified by the disappearance of starting material on TLC plate. The IUPAC name, chemical structure and analytical data for synthesized compound given below.

**Table 1.** IUPAC name, molecular structure, melting point and analytical data of studied inhibitor.

Inhibitor	Molecular Structure	Analytical data
8-Hydroxy quinoline		MP – 74°C - 76°C. FT-IR- $\nu_{max}/cm^3$ . 3500,1680,1400,1550, 1360,1150 1080.

## 2.3weight loss measurements

Weight loss measurements were carried out in a glass vessel with 100 ml of 1M HCl solution with and without concentration of inhibitor ranges from 100-500 ppm. The immersion time for weight loss

was 24 h at 27 °C.After dilution the mild steel specimens were withdrawn, rinsed with double distilled water, washed with acetone, dried and weight. The experiments were carried out in duplicate and the average value of weight loss was noted.

## 2.4 electrochemical measurements

The variation of corrosion potential of mild steel in 1 M HCl was measured against saturated calomel electrode in absence and presence of various concentrations of inhibitors. The time dependence of OCP for different experiments was recorded for 1 hours exposure period .Then the sample was used for potentiodynamic polarization experiments .The potential was swept between -0.5V to 0.5 V at the scan rate 5mV/second. Electrochemical Measurement System, DC 105,containing software of DC corrosion techniques from M/S Gamry Instruments Inc., 734, Louis Drive, Warminster, PA-18974, USA has been used for performing corrosion potential and polarization experiments. For electrochemical polarization studies (corrosion potential, and potentiodynamic polarization) flag shaped specimens with sufficiently long tail were cut from the stainless steel sheet. These samples were polished as described earlier leaving a working area of 1cm<sup>2</sup> on both sides of the flag and a small portion at the tip for providing electrical contact. Rest of the surface was isolated from the corroding solution by coating with enamel lacquer including side edges. The test specimen was connected to the working electrode holder with the help of a screw. About 50ml of the corrosive medium was taken in a mini corrosion testing electrochemical cell. This volume was appropriate to permit desired immersion of electrodes. The electrochemical investigation was carried out using microprocessor based corrosion measurement system (CMS-105, Gamry Instruments Inc., USA.). The three-electrode system cell i.e.

working electrode, reference electrode (Saturated Calomel Electrode), and counter electrode (Graphite rod), was used throughout the electrochemical measurements. Open circuit potential measurements and potentiodynamic polarization experiments were carried out at the concentration of 100, 200,300,400 and 500 ppm of the inhibitor.

### 2.5 SEM AND EDX STUDIES

The composition and surface morphology of corrosion product on mild steel sample after immersion for 24 hours in 1 M HCl in the absence and presence of 500 ppm of 8-hydroxy Quinoline was studied using a scanning electron microscope and EDX examination using energy dispersive spectrometer. The accelerating voltage for SEM picture was 20.0 kv.

## III. RESULTS AND DISCUSSION

### 3.1. Weight loss measurement

Weight loss data of mild steel in 1M HCl in the absence and presence of various concentrations of inhibitor were obtained and are given in Table 1. Inhibition efficiencies (%IE) were calculated according to [46]:

$$(\% \text{ IE}) = \frac{(W_0 - W_{\text{corr}})}{W_0} \times 100 \quad (1)$$

Where,  $W_{\text{corr}}$  and  $W_0$  are the weight loss of mild steel in the presence and absence inhibitors, respectively.

The results show that the inhibition efficiencies increase with increasing inhibitor concentration. The results obtained from the weight loss measurements are in good agreement with those obtained from the electrochemical methods.

**Table 2.** The weight loss parameter obtained for mild steel in 1 M HCl containing different concentrations of 8-hydroxy quinoline.

Inhibitor	Concentration (ppm)	Weight loss (mg)	Surface coverage	Inhibition efficiency (%E)
Blank	-	431	-	-
8-Hydroxy quinoline	100	280	0.350	35.03
	200	185	0.570	57.07
	300	146	0.661	66.12
	400	99	0.770	77.03
	500	77	0.821	82.13

### 3.2 Adsorption isotherm

Fundamental information on the adsorption of inhibitor on metal surface can be provided by adsorption isotherm. The weight loss temperature results were used to calculate the adsorption isotherm parameters. The most frequently used isotherms are Langmuir, Frumkin, Temkin, Florry-Huggins and thermodynamic /kinetic model of El-Awady isotherm. It is found that the adsorption of studied inhibitor on mild surface obeys Langmuir adsorption isotherm. Langmuir adsorption isotherm is given by following equation:

$$C/\theta = 1/K_{\text{ads}} + C \quad (2)$$

Where  $\theta$  is the degree of surface coverage,  $C$  is the molar inhibitor concentration in the bulk solution and  $K_{\text{ads}}$  is the equilibrium constant of the process of adsorption. Plot of  $C/\theta$  versus  $C$  of 8- hydroxyl quinoline presented in fig.(4).The obtained plots are almost linear with correlation coefficient ( $R^2=0.999$ ) for Langmuir adsorption isotherm . $K_{\text{ads}}$  can be



calculated from intercepts of the straight lines in figure 1

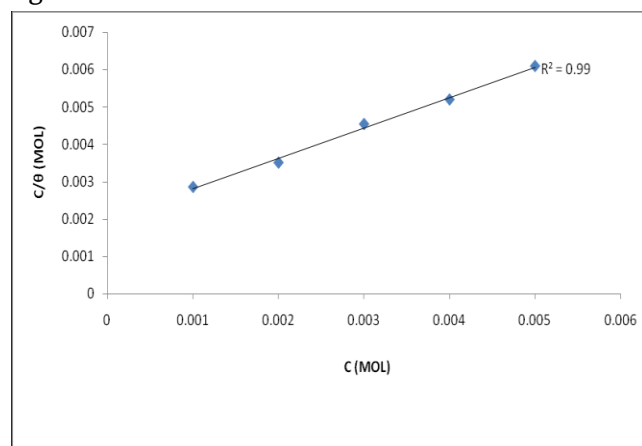


**Figure 1.** Langmuir adsorption isotherm for mild steel in 1 M HCl at various temperatures.

The standard free energy of adsorption ( $\Delta G_{ads}$ ) is calculated from equation [22].

$$K_{ads} = (1/55.5) \exp(-\Delta G_{ads}/RT) \quad \text{----- (3)}$$

Where the constant 55.5 is the molar concentration of water in solution in mol L<sup>-1</sup>. R is universal gas constant and T is absolute temperature. The negative values of  $\Delta G_{ads}$  ensured the spontaneity of the adsorption process and stability of the adsorbed layer on the steel surface [23]. Generally, values of  $\Delta G_{ads}$ , around -20 KJ mol<sup>-1</sup> or lower are consistent with the electrostatic interaction between the charged molecules and charge metal, such as physisorption. When it is around -40 KJ mol<sup>-1</sup> or higher values it involves charge sharing or charge transfer from organic molecules to the metal surface to form coordinate type of bond that is chemisorptions [24]. In the present work the calculated value of  $\Delta G_{ads}$  is 25.53 kJ/mol, which indicate adsorption of inhibitor on mild steel surface involves both physical and chemical adsorption.

### 3.3. Open Circuit Potential Measurement (OCP)

Inherent reactivity of the metallic materials in a particular environment is determined from its open

circuit potential (corrosion potential). The influence of the corrosive and inhibitive species present in the electrolyte may be predicted by analysing the nature of the OCP curve. The variation of open circuit potential of Mild Steel exposed to 1M HCl solution containing inhibitor i.e. 8-hydroxy quinoline in the concentration range 100-500ppm is shown in Figure 2. The steady state potential is obtained after 3600 seconds of the exposure period. In the presence of different concentration of inhibitors, OCP is shifted towards the positive potential direction in comparison to without inhibitor and get stabilized thus indicating the adsorption of the inhibitors on the metal surface. The magnitude of shift of polarization curve towards positive direction was found proportional to the concentration of the inhibitor.

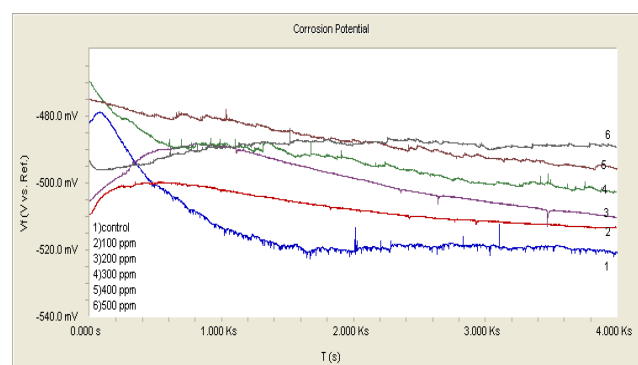


**Figure 2.** Open circuit potential diagram for mild steel in 1 M HCl without and with different concentrations of 8-hydroxy quinoline.

### 3.4. Potentiodynamic polarization curves

Potentiodynamic polarization curves of mild steel in 1 M HCl in the absence and presence of 8-hydroxy Quinoline are illustrated in fig.3. The presence of 8-hydroxy quinoline caused a clear decrease in both anodic and cathodic current densities with increase in inhibitor concentration, probably due to the adsorption of at the active sites of the electrode surface, retarding both metallic dissolution and hydrogen evolution reaction [25]. The

electrochemical kinetic parameters, i.e., corrosion current densities ( $i_{corr}$ ), corrosion potential ( $E_{corr}$ ), cathodic Tafel slope ( $\beta_c$ ) anodic Tafel slope ( $\beta_a$ ) are presented in table (6).

Here, the IE% is defined by following equation:

$$IE\% = \frac{i_0 - i_{corr}}{i_0} \quad \text{----- (4)}$$

Where  $i_0$  and  $i_{corr}$  are the corrosion current density values without and with inhibitor respectively. The corrosion current density decreased with increasing the concentration of the inhibitor, which indicates that the presence of 8-hydroxy quinoline retard the dissolution of mild steel in 1 M HCl solution and degree of inhibition depends on the concentration of inhibitor. It can also be observed that the corrosion

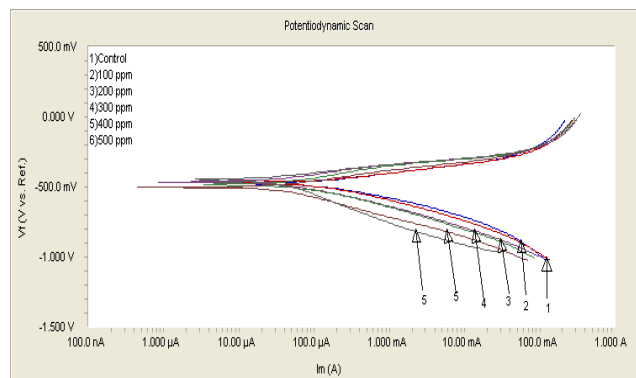


**Figure 3.** Potentiodynamic Polarization curves of mild steel in 1 m HCl in the absence and presence of different concentration of 8-hydroxy quinoline

Potential values remained almost constant in presence of inhibitor, suggesting that 8-hydroxy quinoline acted as mixed-type inhibitor. Furthermore, it is observable that the shape of polarization curves are similar in the absence and presence of 8-hydroxy quinoline, suggesting that the inhibitor inhibits mild steel corrosion by simply adsorbing on mild steel surface without changing the mechanism of mild steel dissolution [26].

**Table 3.** Polarization data of mild steel in 1M HCl solution in absence and presence of different concentration of 8-hydroxy quinoline.

Acid Medium	Concentration (ppm)	$-E_{corr}$ (mv)	$I_{corr}$ ( $\mu A/cm^2$ )	$\beta_a$ (v/dec)	$\beta_c$ (v/dec)	IE %
1 M HCl	-	475.0	133.0	$76.90 e^{-3}$	$134.4 e^{-3}$	
	100	472.0	85.10	$65.70 e^{-3}$	$127.0 e^{-3}$	53.84
	200	481.0	54.10	$90.40 e^{-3}$	$126.0 e^{-3}$	68.15
	300	503.0	40.20	$85.30 e^{-3}$	$140.1 e^{-3}$	72.77
	400	508.0	35.20	$86.90 e^{-3}$	$146.2 e^{-3}$	79.65
	500	463.0	26.64	$85.30 e^{-3}$	$125.20 e^{-3}$	85.42

## IV. SURFACE STUDIES

### 4.1. SEM studies

In order to evaluate the condition of metal surface in contact with acid solution in absence and presence of inhibitor, a surface analysis is carried out using scanning electron microscope and Energy dispersive X- ray spectrometer.

The surface morphology of the mild steel specimens immersed in 1M HCl for 24 h without and with optimum concentration of the 8-hydroxy Quinoline is shown in following figure. A micrograph of the polished mild steel surface before immersion in 1M HCl is shown in figure 4(a). The micrograph shows the surface was smooth and without pits. Fig.4(b) represents SEM micrograph of mild steel surface immersed in 1M HCl without 8-hydroxy Quinoline which appears to be highly corroded and damaged due to free acid attack. Fig.4(c) represents SEM micrograph of mild steel in the presence of optimum concentration of the 8-hydroxy Quinoline in acid solution causes significant improvement in the surface morphology. Thus it can be concluded that 8-hydroxyl Quinoline forms protective surface film on the metal surface through adsorption which protect the metal from acid solution.

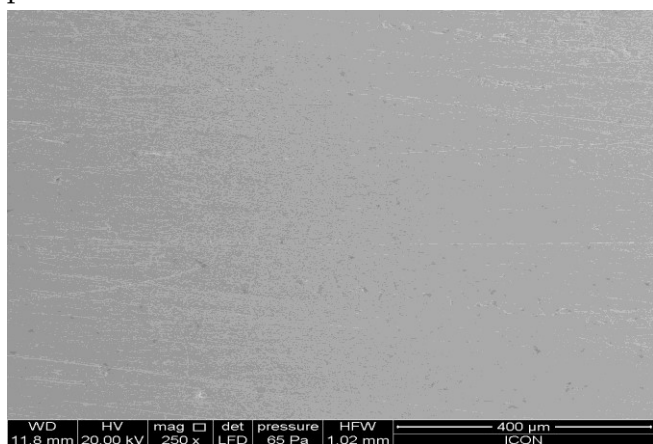


**Figure 4.(a).** SEM micro graphs of mild surface before immersion in 1 M HCl

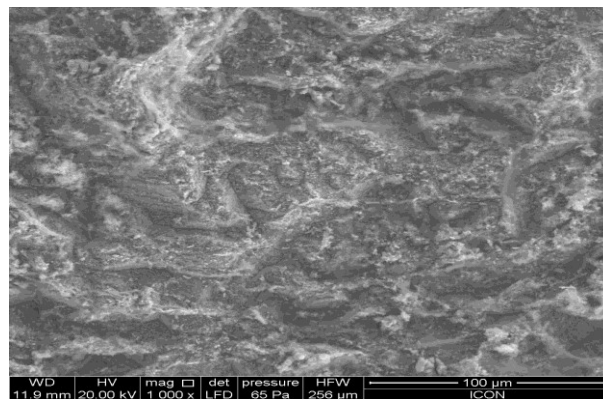


**Figure 4.(b).** SEM micro graphs of mild surface after one day immersion in 1 M HCl and

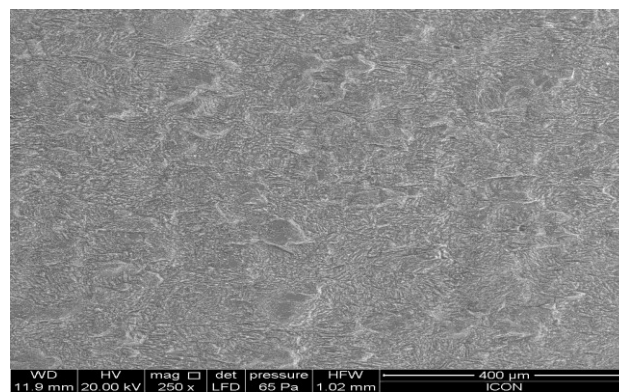


**Figure 4(c).** SEM micro graphs of mild surface after one day of immersion in 1 M HCl+500 ppm of 8-nitro quinoline.

### 4.2 EDX studies

Figure 5 (a) shows spectra of mild steel specimen before immersion in 1 M HCl which shows a signal for Fe and oxygen. Figure 5(b) shows EDX spectra of mild steel specimen immersed in 1 M HCl in the absence of 8-hydroxy Quinoline which is characterized by signal corresponding only for Fe. However, Figure 5(c) shows EDX spectrum in the presence of 8-hydroxy Quinoline with additional signal for nitrogen (N) which attributed due to adsorption of 8-hydroxy Quinoline on mild steel surface.

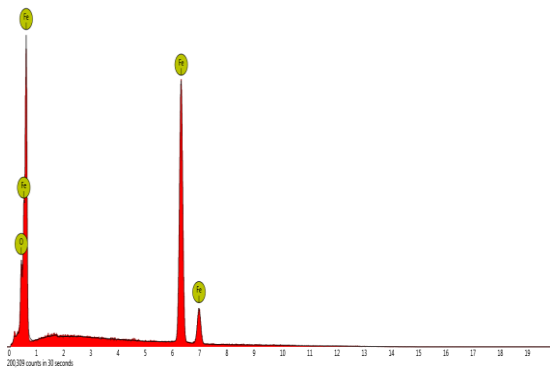


**Figure 5(a).** EDX spectra of polished mild steel surface

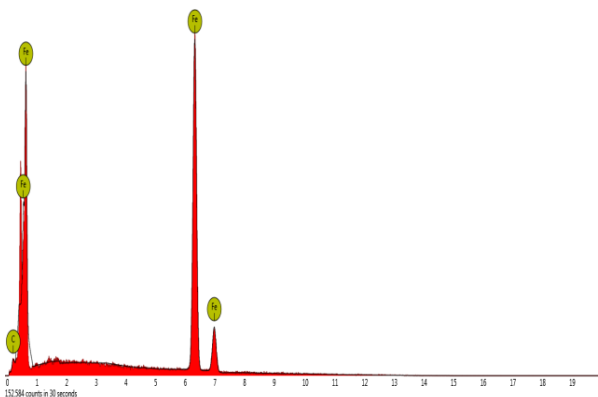


**Figure 5 (b).** EDX spectra of mild steel after one day immersion in 1 M HCl

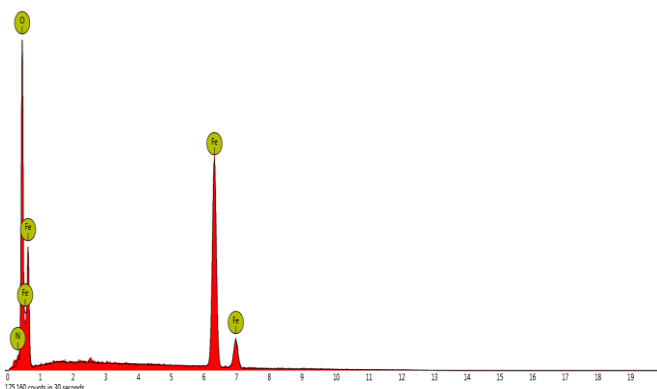


**Figure 5(c).** EDX spectra of mild steel after one day of immersion in 1 M HCl +500 ppm of 8-hydroxy Quinoline.

## V. MECHANISM OF INHIBITION

Corrosion inhibition of mild steel in acid solution can be described on the basis of adsorption phenomenon. 8-hydroxy Quinoline contains various functional groups such as  $-OH$ ,  $C=C$  and  $C=N$

through which it can adsorb on metal surface. The adsorption can be chemisorption or physisorption and some time both processes can take place. 8-hydroxy Quinoline can adsorb onto metal surface by three different ways.

1. Sharing of electrons of nitrogen and oxygen with iron surface.
2. Interaction between pi electrons of benzene ring of 8-hydroxy Quinoline with the metal surface.
3. It is also possible that the N atom of 8-hydroxy Quinoline can be easily protonated in acid medium. This protonated N atom can show electrostatic interaction with negatively charged metal surface.

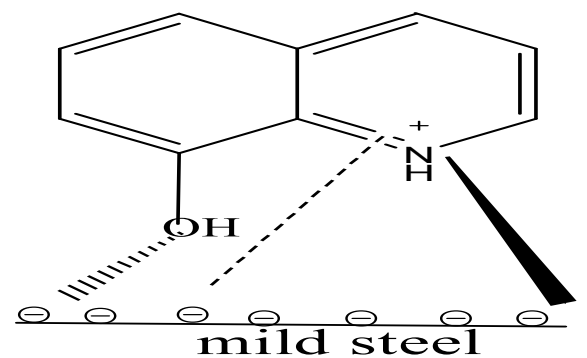


**Figure 6.** Pictorial representation of adsorption behaviour of the 8-hydroxy quinolone on mild steel in 1M HCl

## VI. CONCLUSION

On the basis of the above results the following conclusion can be drawn.

1. 8-hydroxy Quinoline acted as an effective corrosion inhibitor for mild steel in 1M HCl solution.
2. The corrosion process was inhibited by adsorption of inhibitor molecule on the mild steel surface.
3. The inhibition efficiency increased with increase in the concentration of the inhibitor.

4. Adsorption study showed that the inhibition mechanism obeyed Langmuir adsorption isotherm.
5. The negative value of free energy of adsorption indicated strong and spontaneous adsorption of inhibitor on mild steel surface.
6. Potentiodynamic polarization studies shown that inhibitor retards both the anodic and cathodic partial reactions. Thus 8-hydroxy Quinoline acted as mixed type inhibitor.
7. SEM/EDX studies revealed that corrosion inhibition is due to the adsorption of 8-hydroxy Quinoline at mild steel/acid solution interface.

## VII. REFERENCES

- [1] W. Machu, in: Proceedings of the Third European Symposium on Corrosion Inhibitors, Ferrara, Italy, University of Ferrara, 1970, p. 107.
- [2] F. Bentiss, M. Traisnel, M. Lagrene 'e, Corros. Sci. 42 (2000) 127.
- [3] A. Chetouani, A. Aouniti, B. Hammouti, N. Benchat, T. Benhadda, S.Kertit, Corros. Sci. 45 (2003) 1675.
- [4] M. Lagrene 'e, B. Mernari, N. Chaibi, M. Traisnel, H. Vezin, F. Bentiss, Corros. Sci. 43 (2001) 951.
- [5] S.S. Abd El-rehim, S.A.M. Refaey, F. Taha, M.B. Saleh, R.A. Ahmed, J. Appl. Electrochem. 31 (2001) 429.
- [6] A.B. Tadros, B.A. Abd El-nabey, J. Electroanal. Chem. 246 (1988) 433.
- [7] H. Luo, Y.C. Guan, K.N. Han, Corrosion 54 (1998) 721.
- [8] S.T. Arab, E.A. Noor, Corrosion 49 (1993) 122.
- [9] F. Bentiss, M. Traisnel, N. Chaibi, B. Mernari, H. Vezin, M. Lagrene 'e, Corros. Sci. 44 (2002) 2271.
- [10] K. Tebbji, H. Oudda, B. Hammouti, M. Benkaddour, M. El Kodadi, F. Malek, A. Ramdani, Appl. Surf. Sci. 241 (2005) 326.
- [11] M. Bouklah, A. Attayibat, S. Kertit, A. Ramdani, B. Hammouti, Appl. Surf. Sci. 242 (2005) 399.
- [12] S. Muralidharan, K.L.N. Phani, S. Pitchumani, S. Ravichandran, S.V.K. Iyer, J. Electrochem. Soc. 142 (1995) 1478.
- [13] E.E. Oguzie, V.O. Njoku, C.K. Enenebeaku, C.O. Akalezi, C. Obi, Effect of hexamethyl pararosaniline chloride (crystal violet) on mild steel corrosion in acidic media, Corros. Sci. 50 (2008) 3480–3486.
- [14] V. R. Saliyan, A. V. Adhikari, Quinolin-5-ylmethylene-3-[[8-(trifluoromethyl)quinolin-4-yl] thio} propanohydrazide as an effective inhibitor of mild steel corrosion in HCl solution, Corros. Sci. 50 (2008) 55–61.
- [15] K. C. Emregal, O. Atakol, Corrosion inhibition of mild steel with Schiff base compounds in 1 M HCl, Material Chem. Phys. 82, issue 1 (2003) 188–193.
- [16] F. Kandemirli, S. Sagdin, Theoretical study of corrosion inhibition of amides and thio semicarbazones, Corros. Sci. 49 (2007) 2118–2130.
- [17] N. Hackerman, R.M. Hurd, in: Proc. Int. Congress of Metallic Corrosion, Butterworths, London, 1962, p. 166.
- [18] F.B. Growcock, W.W. Frenier, V.R. Lopp, in: Proc. 6th European Symposium on Corrosion Inhibitors, Ann. Univ. Ferrara, N.S., Sez. V. Suppl. No. 7, 1980, p. 1185.
- [19] D. Jayaperumal, S. Muralidharan, P. Subramaniam, G. Venkatachari, S. Senthilrel, Anti-Corros. Methods Mater. 44 (1997) 265.
- [20] Yiwei Ren, Yi Luo, Kaisong Zhang, Gefu Zhu, Xiaolin Tan, Lignin terpolymer for corrosion

- inhibition of mild steel in 10% hydrochloric acid medium, *Corros. Sci.* 50 (2008) 3147–3153.
- [21] B.S.Furniss, A.J.Hannaford, P.W.G.Smith, A. R. Tatchell, *Vogel's textbook of practical organic chemistry*, fifth edition 1989.
- [22] Fouda A. S, Shalabi K, E- Hossiany A,(2016), Moxifloxacin antibiotic as green corrosion inhibitor for carbon steel in 1 M HCl. *J.Bio. Tribo .corros.*2:18.DOI 10.1007//s40735-016-0048-x.
- [23] Ahamad I, Prasad R, Qurashi MA,(2010), Thermodynamic, electrochemical and quantum chemical investigation of some Schiff bases as corrosion inhibitors for mild steel in hydrochloric acid solutions. *Corros. Sci.*52,933-942.
- [24] Elyn Amira WAW, Rahim AA, Osman H, Awang k, Bothi Raja P.(2011), Corrosion inhibition of mild steel in 1M HCl solution by *Xylopiya Ferruginea* Leaves from different extract and partitions. *Int .J.Electrochem .Sci.*6, 2998-3016.
- [25] Wang X, Wan Y, Zeng Y, GuY(2012), Investigation of benzimidazole compound as a novel corrosion inhibitor for mild steel in hydrochloric acid solution . *Int.J.Electrochem.Sci.*7 ,2403-2415.
- [26] ChandrabhanVarma. A.Qurashi, A.Singh(2016), 5-substituted 1H-tetrazoles as effective corrosion inhibitors for mild steel in 1M hydrochloric acid. *Journal of Taibah University for science* 10,718-733.

# Study of Ground Water Pollution in Roha, District Raigad, Maharashtra, India

Ranjana A. Kularni , G. R. Bhagure\*

Department of Chemistry, Satish Pradhan Dnyansadhana College, Thane, Maharashtra, India

## ABSTRACT

Roha is a small city & taluka in the Raigad District of the Maharashtra State of India and is situated on the banks of river Kundalika. Ground water is major source of drinking water & In Roha taluka availability of ground water is much more. Samples at Raigad District were collected during Pre-Monsoon Season i.e. from March 2016 to May 2016. The 10 sampling Sites were selected for sampling that are located in Roha, Killa, Tambdi Khurd, Muthavde, Furgarewadi, Ghosale, Muthawali, khari, Pingalsai, and Tareghar. 27 water quality parameters were determined as per the standard procedure as prescribed by APHA AWWA and BIS. It was found that the physical parameters like pH, Colour, odour, Turbidity, were Acceptable. The presence of chloride may be due to discharge of sewage, industrial water in water body, Chloride values are in well within the limits. Also Higher concentration of TDS was found which may cause heart & kidney diseases, TDS concentration In Ground water of Roha & nearby villages are within the standard limits.

**Key words:** Roha, Water quality, TDS, Industrial water

## I. INTRODUCTION

Groundwater is the water found underground in the cracks and spaces in soil, sand and rock. It is stored in and moves slowly through geologic formations of soil, sand and rocks called aquifers. Ground water is the Most Major source of fresh water for drinking, Agriculture & Industrial desires, Groundwater is often cheaper, more convenient and less vulnerable to pollution than surface water. Therefore, it is commonly used for public water supplies. For example, groundwater provides the largest source of usable water. Many municipal water supplies are derived solely from groundwater. Polluted groundwater is less visible, but more difficult to clean up, than pollution in rivers and

lakes. Groundwater pollution most often results from improper disposal of wastes on land. Major sources

include industrial and household chemicals and garbage landfills, excessive fertilizers and pesticides used in agriculture, industrial waste lagoons, tailings and process wastewater from mines, industrial fracking, oil field brine pits, leaking underground oil storage tanks and pipelines, sewage sludge and septic systems.

## II. STUDY AREA & PERIOD

The samples were collected around the Roha town. Roha is a small city & taluka in the Raigad District of the Maharashtra State of India and is situated on the banks of river Kundalika. Ground water is major source of drinking water & In Roha taluka availability of ground water is much more. Samples at Raigad District were collected during Pre Monsoon Season i.e. from March 2016 to May 2016. The ten sampling Sites are located in 1.Roha 2.Killa 3.Tambdi Khurd

4.Muthavde 5.Furgarewadi 6.Ghosale 7.Muthawali  
8.khari 9.Pingalsai 10.Tareghar.

**The Map of RAIGARH District Roads, Rivers Railway Tracks, Taluka.**



**Figure 1**

**III. METHODOLOGY**

The samples were collected in Pre- Monsoon. the samples were collected in Plastic (polypropylene) container (capacity: 2 litre ). The collection, transportation and preservation were done as per the Standards & as per CPCB guidelines. The various water quality parameters such as, Colour, Odour, pH, TDS, Iron, Sulphate, Fluoride, Nitrate, Salinity, Hardness, EC, Boron, Free Residual Chlorine, Turbidity, Phenolic compounds, cyanide ) & heavy metals Cu, Zn, Cr<sup>+6</sup>, Nickel, Lead, Cadmium.

**Instruments :**

3.1 Atomic Absorption Spectrophotometer (Make Chemito now takeover by Thermofisher) Model No. AA203: For Heavy metals

3.2 UV-Visible Spectrophotometer (make Chemline): For Sulphate, Nitrate, Fluoride, Boron, Phenolic compounds.

3.3 Methods used: APHA 22nd Edition & IS 3025.

**Depth to Water Level :Premonsoon (Average Level)**

The Average depth to water levels in the district during premonsoon ranges between 0.55 m bgl (Nagothan) and 8.60 m bgl (Chinchwad). Depth to water levels during Pre monsoon is Shallow water levels i.e., less than 2 m bgl are seen in the central part of the district. The water levels 5 to 10 m bgl are seen in the southern part of the district i.e. around Poladpur and Mahad and also as scattered patches across the district. In the major part of the district water level ranges from 2 to 5 m bgl.

**Ground Water Development**

Physiographic, geology and rainfall of the district plays a major role in the Ground water resource availability and sustainability. The high, steep hill ranges, isolated hillocks, undulation etc give rise to high run off. The predominance of hard rock formation in the form of basaltic lava flows facilities the run off rather than natural recharge due to the poor ground water storage and transmission capabilities. The formation due to poor storage and transmission characteristics gets fully saturated during monsoon and a situation of rejected recharge is resulted. These aquifers then are drained naturally due to slopping and undulation topography.

The district despite of high rainfall of (1500 – 3500 mm) faces water scarcity situation following January or February month. Development of ground water has taken place on a limited scale in Deccan Trap Basalt area. However, ground water development for



irrigation purpose has taken place on a good scale in the alluvial area of coastal tract.

#### IV. METHODS

Methods used for analysis of samples are as per APHA 22<sup>nd</sup> Edition & IS 3025

Table 1

Sr. No	Name of the Water Quality Parameter	Bureau of Indian Standard (IS-10500:1994)	Pre Monsoon march 2016 to may 2016 (Parameters Range)
1	pH	6.5 - 8.5	6.63 - 7.28
2	Total Hardness mg/l	200	72 - 179
3	TDS mg/l	500	111- 433
4	Chlorides (as Cl) mg/l	250	32 - 54
5	Sulphates (as SO <sub>4</sub> ) mg/l	200	19 - 51
6	Nitrates as (NO <sub>3</sub> ) mg/l	45	0.22 - 0.46
7	Fluorides (as F) mg/l	1.0	<0.2 - 0.75
8	Cu mg/l	0.05	0.030 -0.037
9	Fe mg/l	0.3	0.23 - 0.28
10	Zn mg/l	5	0.31 - 0.58

#### V. RESULTS AND DISCUSSION

The suitability of ground water for drinking purpose is determined keeping in view the effects of various chemical constituents in water on the biological System of human being. The classification of water was carried out as per the Bureau of Indian Standards (BIS) for drinking water to assess the suitability of Ground water.

##### a. pH value :

The pH value of water is indication of its quality. pH values usually changes due to contamination from industrial waste, carbonate and bicarbonate. The pH values for the samples Collected at Ten Locations the Minimum pH was Recorded 6.63 at **GW 10** and the maximum value recorded was 7.28 at **GW1**.

##### b. Electrical Conductivity:

It indicates mineral, geological effect and organic pollution. It increases as dissolved salt concentration increases. The minimum conductivity in the Study region was 0.125 mS/cm recorded at **GW8** and the Maximum Value 0.493 mS/cm was recorded at **GW9**.

##### c. Total Hardness:

The total Hardness value of water is due to the calcium and magnesium salts. The total Hardness values for samples are within the range of permissible limit. Minimum Value Observed was 72mg/l at **GW8** and the Maximum Value was 179mg/l at **GW6**

##### d. Total Dissolved Solids:

Total dissolved solids values does not cause harm to human but higher concentration may cause heart and kidney diseases. Total dissolved solids values for all sampling sites are within the range of permissible limit. The lowest value observed was 111mg/l at **GW8** and the maximum value 433mg/l at **GW4**.

##### e. Turbidity:

The turbidity is due to existence of many types of pathogenic organisms. It is an indicator of pollution. All samples were within the Standards.

##### f. Chloride:

The presence of chloride is an indicator of organic pollution. The presence of chloride in water body is mainly due to discharge of sewage, industrial effluents and agricultural fertilizers .The values for all samples are well below the standard limit. The minimum value recorded was 32mg/l at **GW1** and the Maximum Value was 54mg/l at **GW10**

**g. Sulfate:**

The sulfate in water is due to leaching of gypsum and other minerals. The values of the present study lie below the standard limit. The minimum value recorded was 19mg/l at **GW8** and the maximum Value recorded was 51mg/l. at **GW4**.

**h. Heavy Metals:**

Heavy Metals are also the important factor, at all the ten locations the parameters analyzed were. Heavy metals Cu, Zn, Cr<sup>+6</sup>, Nickel, Lead, Cadmium. Fe, Cyanide, Boron, Aluminum, Arsenic & Mercury. So all the Heavy Metals in the Study region were below the detectable limits.

Micro Biological Parameters like MPN (Most Probable Number) & E.coli were analysed but were not detected.

## VI. CONCLUSION

The presence of chloride may be due to discharge of sewage, industrial water in water body, Chloride values are in well within the limits. Also Higher concentration of TDS may cause heart & kidney diseases, TDS concentration In Ground water of Roha & nearby villages are within the standard limits.

Ground water quality for 10 locations for Roha & villages coming under Roha Block were analyzed for physical & chemical parameters. It was observed that ground water quality is satisfactory in Roha.

**Ground water Collection at Industrial Area.**

The ground water sample was collected at MIDC Industrial area, at Dhatav Village, Roha, Raigad District. The physical parameters like pH, Colour, odour, Turbidity, were Acceptable. Being Chlorides with in limit but at the higher side of 104.7mg/l when compared to the ground water collection at 11 locations during the pre-monsoon period. Also the Total dissolved solids was Beyond the limits 1586 mg/l which was on a higher side. The calcium was also crossing the limits with a value of 87.13 mg/l. Magnesium with a value of 56.1 mg/l was crossing the limits. Heavy metals were not detected at this location.

# Applications of Hyphenated Analytical Techniques to Pharmaceutical Drug Analysis : A Review

Ratnakar Hole<sup>1</sup>, Vinod Lohakane<sup>2</sup>, Sandesh Jaybhaye<sup>2</sup>, Rajesh Dwivedi<sup>1</sup>, Achyut Munde<sup>3</sup>

<sup>1</sup>Glenmark Research Center, Mahape, New Mumbai, Maharashtra, India

<sup>2</sup>Birla College of Arts, Commerce & Science, Kalyan-West, Maharashtra, India

<sup>3</sup>Milind College of Science, Aurangabad, Maharashtra, India

## ABSTRACT

As far analytical evaluations are concerned, today's advanced pharmaceutical organizations are facing increased number of challenges starting from raw materials right upto the finished product. The challenges are related to the accuracy, sensitivity, ease of laboratory demands, the purity, composition and performance of various drugs. Nowadays there is a vast array of scientific techniques available to the analytical scientists that enable this characterization. But the available analytical techniques are lacking to fulfill the increased demand of pharmaceutical analysis. In such contradictory environment, hyphenated technique had opened window of opportunities to the analytical scientists. Hyphenated techniques refer to combination of two or more analytical techniques to characterize the pharmaceutical drugs. These hyphenated techniques offer shorter analysis time, higher degree of automation, higher sample throughput, better reproducibility, reduction of contamination because it is a closed system, Enhanced combined selectivity and therefore higher degree of information. This review discusses the current trends in analytical evaluations of various types of materials which will provide unique path to the researchers to move a step forward.

**Keywords :** Analytical tools, Hyphenated techniques, Drugs analysis, Pharma Drugs

## I. INTRODUCTION

In the past two decades, demands on analytical support for pharmaceutical drugs have intensified. As a result, new technology is continually evolving to meet these challenges. In addition, the use of more established methodologies is being enhanced by incremental improvements in technology and protocol. Hyphenation (combination) of analytical techniques [1, 2] is one such approach adopted by modern pharmaceutical analysts in meeting the needs of today's industry.

A hyphenated technique is combination (or) coupling of two different analytical techniques with the help of

proper interface. The term hyphenated techniques range from the combination of separation-separation, separation-identification & identification-identification techniques [3].

The term "hyphenation" was first adapted by Hirschfeld in 1980 to describe a possible combination of two or more instrumental analytical methods in a single run (Hirschfeld, 1980). The aim of the coupling is to obtain an information-rich detection for both identification and quantification compared to that with a single analytical technique [3].

The new dimension in the area of hyphenated techniques that offers some very significant benefits in pharmaceutical analysis is that of multi-dimensional

chromatography. Various set-ups involving coupling GC, HPLC and CE systems together in different configurations have been studied for analyzing many different sample types [4]. Examples include Size exclusion chromatography coupled with RP-HPLC, CE and GC coupled with LC. Since, RP-HPLC and CE techniques are capable of high resolution separation with orthogonal separation mechanism, combining both techniques in a two-dimensional mode can produce very high peak capacities and extremely high resolving power, particularly useful for complex mixtures [5]. This hyphenated technique not only provides appropriate sensitivity but also unique capabilities for identification and confirmation of the species of interest.

In Pharmaceutical analysis mass spectrometric detection is always preceded by some kind of separation that enables the qualitative and quantitative analysis of the different species by separating them from each other and also from matrix interferences [6]. They consist of two main parts: a separation technique (GC, HPLC or Electrophoresis) and a detector (UV, AAS, ICP-MS or ESI-MS) that are connected by an interface. The most frequently applied coupled analytical techniques are HPLC-ICP-MS, HPLC-ESI-Q-TOF-MS and HPLC-Orbitrap-MS [7].

Among the spectroscopic techniques available to date, NMR is probably the least sensitive, and yet it provides the most useful information toward the structure elucidation of pharmaceutical products. Technological developments have allowed the direct parallel coupling of HPLC systems to NMR, giving rise to the new practical technique HPLC-NMR or LC-NMR, which has been widely known for more than last 15 years [8]. Combined CE-NMR can offer the separation capability of CE and the superior detection of NMR [12]. GC-NMR provides the structural information of molecule from the separated components [13, 14].

The FTIR is a useful spectroscopic technique for the identification of organic compounds, because in the mid-IR region the structures of organic compounds have many absorption bands that are characteristic of particular functionalities, e.g., -OH, -COOH but the hyphenation of HPLC with FTIR spectrometry is again brain-storming [9]. Gas chromatography coupled with transform Fourier infrared spectrometry is capable of obtaining Infrared spectra from the peaks as they elute from the capillary columns thus combining the separation power of gas chromatography with the identification power of infrared spectrometry [10].

TLC combined with mass spectrometry is most efficient analytical tools for structural elucidation. TLC-MS technique is used for indirect and direct characterization of analytes on the surfaces of TLC plates [11].

The combination of a Thermogravimetric Analyzer (TGA) with an Infrared Spectrometer (TG-IR) is the most common type of Evolved Gas Analysis (EGA) in use today. The combination of TGA with a Mass Spectrometer (TG/MS) is becoming increasingly popular due to its ability to detect very low levels of impurities [15].

Combining Differential Scanning Calorimetry (DSC) with Raman spectroscopic technique (DSC-Raman) allows us to apply the precise temperature control of the DSC with the ability of Raman to detect the different polymorphic structures, and obtain precise characterization of the material [16].

## II. APPLICATIONS OF HYPHENATED TECHNIQUES

1. Identification of drug degradation products
2. Isolation and identification Low-level impurities into drugs
3. Differentiation of isomers and identification without reference compounds

4. Drug metabolism to analyze biofluids such as plasma or urine
5. Separation and characterization of peptide libraries
6. Identification and separation of chiral compound
7. Detection & characterization of bulk drug impurities obtained during drug stability study
8. Analysis of unstable compounds or compounds formed in situ
9. Composition profiling to analyze the content and structure of components in a mixture, thus providing valuable insights of molecular back-bone
10. Identification and quantification of polymorphic forms of drug substance and drug products

### III. TYPES OF HYPHENATED TECHNIQUES

1. Double hyphenated techniques
2. Triple hyphenated techniques

#### 1. Double Hyphenated Techniques

- LC-MS
- GC-MS
- TLC-MS
- LC-NMR
- GC-NMR
- CE-NMR
- LC-FTIR
- GC-FTIR
- CE-MS
- TG-MS
- DSC-Raman

#### 2. Triple Hyphenated Techniques

- LC-MS-MS
- GC-MS-MS
- LC-ICP-MS
- GC-ICP-MS
- GC-FTIR-MS

### IV. REVIEW OF HYPHENATED TECHNIQUES

#### 1. LC/MS:

Liquid Chromatography/Mass Spectrometry (LC/MS) is a powerful analytical technique that combines the resolving power of liquid chromatography with the detection specificity of mass spectrometry. Liquid chromatography (LC) separates the sample components and then introduces them to the mass spectrometer (MS). The MS creates and detects charged ions. The LC/MS data may be used to provide information about the molecular weight, structure, identity and quantity of specific sample components [17]. A typical automated LC-MS system (Figure 1) consists of double three-way diverter in-line with an auto sampler, LC system, the Mass spectrometer. The diverter generally operates as an automatic switching valve to divert undesired portions of eluting from the LC system to waste before the sample enters the MS [18]. LC-MS is highly selective and sensitive technique. The flow rate of HPLC is around 1ml/min which is difficult to accommodate in mass spectrometry vacuum system also the diluent which is used has to be vaporized which leads to damage of the thermally labile compounds by excessive heating [19]. By hyphenation of these two techniques capabilities of both the techniques are improved.

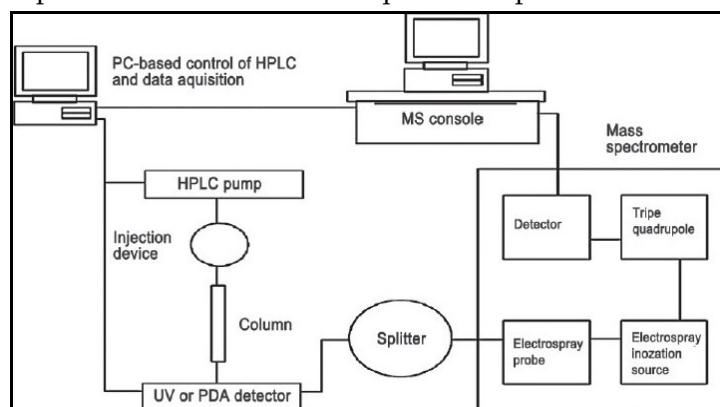


Figure 1. Schematic presentation of LC/MS

The ionization techniques used in LC-MS are generally soft ionization techniques that mainly display the molecular ion species with only a few fragment ions. Nowadays, various types of LC-MS systems incorporating different types of interfaces are available commercially. The interfaces are designed in such a way that they offer adequate nebulization and

vaporization of the liquid, ionization of the sample, removal of the excess solvent vapour, and extraction of the ions into the mass analyser. The two most widely used interfaces are electrospray ionization (ESI) and atmospheric pressure chemical ionization (APCI). The latter is considered as “the chromatographer's LC-MS interface” because of its high solvent flow rate capability, sensitivity, response linearity, and fields of applicability [20].

## 2. GC/MS:

Gas Chromatography/Mass Spectrometry (GC/MS) is the first of its kind hyphenated technique which became inevitable for pharmaceutical analysis [21]. Mass spectra obtained by this technique offer more structural information based on the interpretation of fragmentations. Compounds that are adequately volatile, small, and stable in high temperature in GC conditions can be easily analyzed by GC-MS. Sometimes, polar compounds, especially those with a number of hydroxyl groups, need to be derivatized for GC-MS analysis. In GC-MS, a sample is injected into the injection port of GC device, vaporized, separated in the GC column, analyzed by MS detector, and recorded. The equipment used for GC-MS (Figure 2) generally consists of an injection port at one end of a metal column (often packed with a sand-like material to promote maximum separation) and a detector (MS) at the other end of the column. A carrier gas (argon, helium, nitrogen, hydrogen etc.) propels the sample down the column. The GC separates the components of a mixture in time and the MS detector provides information that aids in the structural identification of each component.

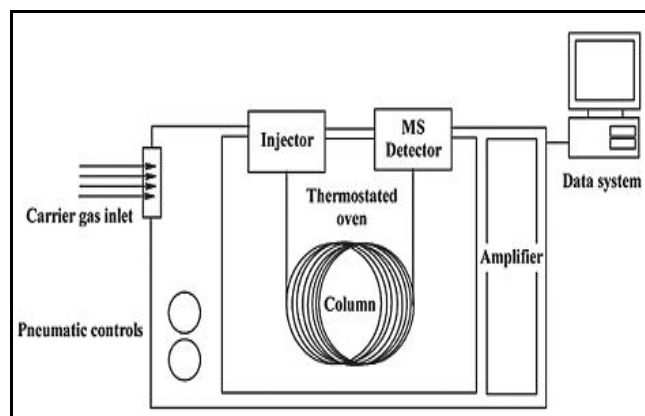


Figure 2. Schematic presentation of GC/MS

The GC-MS columns can be of two types: capillary columns, macrobore columns and packed columns. The process of ionization not only ionizes the molecule but also breaks the molecule into the fragments and detect these fragments with the help of electron impact ionization and chemical ionization. The molecular ion of analyte forms a finger print spectrum which is different from other analytes. The advantage of this technique is sometimes two different analyte will have same mass spectrum but the retention time of both the analytes is different so such type of analytes can be separated or analyses with the help of GC-MS.

Two widely used Ionization techniques in GCMS are the electron impact ionization (EI) and the alternative chemical ionization (CI) in either positive or negative modes [22].

## 3. TLC/MS:

Many different Thin Layer Chromatography/Mass Spectrometry (TLC/MS) techniques have been reported in the literature. According to differences in their operational processes, the existing TLC/MS systems can be classified into two categories: Indirect mass spectrometric analyses, performed by scraping, extracting, purifying, and concentrating the analyte from the TLC plate and then directing it into the mass spectrometer's ion source for further analysis; Direct mass spectrometric analyses, where the analyte on the TLC plate is characterized directly through mass

spectrometry without the need for scraping, extraction, or concentration processes. Direct TLC/MS analysis is performed under vacuum, but the development of ambient mass spectrometry has allowed analytes on TLC plates to be characterized under atmospheric pressure.

#### 4. LC/NMR:

The first on-line LC/NMR experiment using superconducting magnets was reported in the early 1980s. However, the use of this hyphenated technique in the analytical laboratories started in the latter part of the 1990s. LC/NMR promises to be of great value in the analysis of complex pharmaceutical mixtures. LC/NMR experiments can be performed in both continuous-flow and stop-flow modes. A wide range of bio analytical problems can be addressed using 500, 600, and 800 MHz systems with  $^1\text{H}$ ,  $^{13}\text{C}$ ,  $^2\text{H}$ ,  $^{19}\text{F}$ , and  $^{31}\text{P}$  probes. The main prerequisites for on-line LC/NMR, in addition to the NMR and HPLC instrumentation, are the continuous-flow probe and a valve installed before the probe for recording either continuous-flow or stopped-flow NMR spectra [8]. The analytical flow cell was initially constructed for continuous-flow NMR acquisition. However, the need for full structural assignment of unknown compounds, especially during research & development of novel pharmaceutical products, has led to the application in the stopped-flow mode.

Generally, in LC/NMR system, the LC unit comprises (Figure 3) auto-sampler, LC pump, column, and a non-NMR detector (e.g., UV, DAD, EC, refractive index, or radioactivity). From this detector, the flow is guided into the LC-NMR interface, which can be equipped with additional loops for the intermediate storage of selected LC peaks. The flow from the LC/NMR interface is then guided either to the flow-cell NMR probe-head or to the waste receptacle. Following passage through the probe-head, the flow is routed to a fraction collector for recovery and further investigation of the various fractions analyzed by NMR. In most of the LC/NMR operations, reversed-

phase columns are used, employing a binary or tertiary solvent mixture with isocratic or gradient elution. To enhance the potential of LC/NMR, it is recommended to use eluents that have as few  $^1\text{H}$  NMR resonances as possible (e.g.,  $\text{H}_2\text{O}$ , Acetonitrile or Methanol), at least one deuterated solvent (e.g.,  $\text{D}_2\text{O}$ ), buffers that have as few  $^1\text{H}$  NMR resonances as possible (e.g., TFA or ammonium acetate), ion pair reagents that have as few  $^1\text{H}$  NMR resonances as possible (e.g., ion pairs with *t*-butyl groups create an additional resonance).

The major applications of LC/NMR tools are the identification of drug degradation products and isolation and identification of low level impurities.

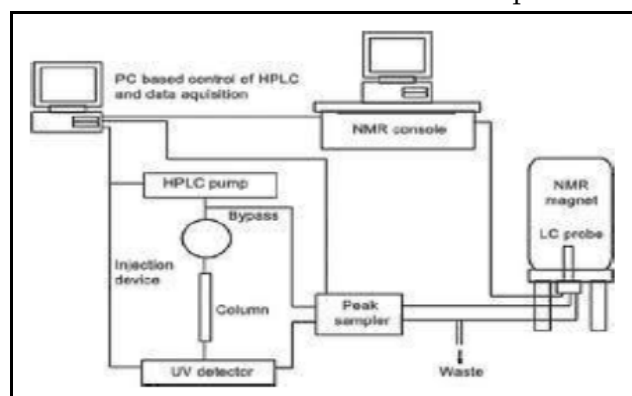


Figure 3. Schematic presentation of LC/NMR

#### 5. GC/NMR:

In GC/NMR technique, NMR perform the identification of the components and GC is used for the separation of the components. A special processing technique was developed to handle the recorded NMR spectrum in the gas phase with very low sample amounts. The chromatographic and spectroscopic conditions were optimized with respect to the  $^1\text{H}$  NMR detection. The identification of volatile cis/trans-stereoisomers can be accomplished by employing a hyphenated GC-NMR system [23]. The separation of constitutional and configurational isomers is also the major application of GC/NMR technique in pharmaceutical analysis. Also during GC/NMR evaluation of chiral compounds, the

enantiomers show the same spectra at different retention time.

## 6. CE/NMR:

The low-mass sample requirements with high separation efficiencies and fast separations are keys to the success of CE/NMR technique. Analyte peaks in CE/NMR typically contain low nano-litre volumes. High resolution CE electro-pherograms and NMR spectrum can be obtained using nano-litre volumes. The CE/NMR experiments histidine in phosphate buffer. The NMR microcoil probe can be coupled to the capillary CE system with no major modification to the existing CE instrumentation.

Figure 4 illustrates novel CE–NMR instrumentation with a dual microcoil probe to record continuous flow NMR data under stopped-flow conditions [24].

Using CE–NMR technique the major metabolites of paracetamol in human urine has been demonstrated [25, 26]. In this study CE–NMR successfully analyzed two major metabolites, paracetamol glucuronide and paracetamol sulfate conjugates, as well as endogenous material (hippurate). CE/NMR has been designed and shown to be a promising tool to analyze complex mixtures [27]. Capillary techniques are especially useful for analyzing mass limited samples as required in pharmaceutical analysis.

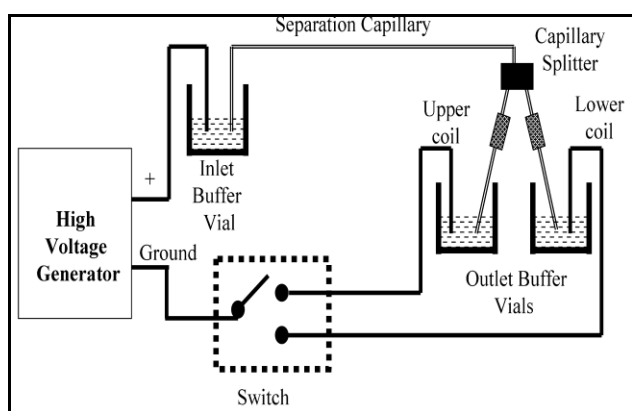


Figure 4. Schematic presentation of CE/NMR

## 7. LC/FTIR:

The recent developments in LC/FTIR technology have incorporated two basic approaches based on interfaces applied in LC/FTIR. One is a flow-cell approach and the other is a solvent-elimination approach. The approach used with the flow cell in LC/FTIR is similar to that used in UV/Visible and other typical HPLC detectors. In this case, absorption of the mobile phase induces the interference of the detection of sample component absorption bands, but some transparent region of the mid-IR range produces detection possibility. Generally, KBr or KCl salts are used for the collection of sample components in the eluent, and heating up the medium before IR detection eliminates the volatile mobile phase solvents.

Since FT-IR is an absorbance process, the geometry of sample during the measurement process matters. For a fixed mass or volume of the analyte, reducing the diameter by a factor of two creates a deposit with four times the thickness and four times the optical density. Further as the IR detector is total light limited, this deposit diameter reduction of two improves the signal-to-noise ratio by four times. Therefore, to achieve a useful instrument that produces full mid-infrared spectrum, the LC/FTIR hyphenation process must [28].

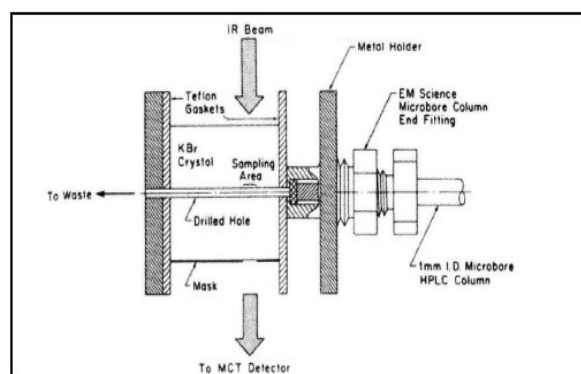


Figure 5. Schematic presentation of LC/FTIR

## 8. GC/FTIR:

This technique is very sensitive and sample recovery is also possible because IR is non-destructive technique. In this technique the GC does the separation part where as IR perform the function of



identification. The analyte components separated by Gas chromatography travel through the column. These two techniques are linked through glass column or vacuum tubes. Interface used in this technique is internally gold coated small glass pipe connected to column by narrow tubing [29]. Light pipe is heated in order to rid condensation and maximize path length for enhanced sensitivity. Effluent from GC is directly forwarded into the heated pipe of IR at atmospheric pressure. Infrared red spectroscopy identifies the compound by identifying the functional groups.

GC/FTIR technique is particularly useful for distinguishing between structural isomers, such as *ortho*-, *meta*- and *para*-xylene, whose electron-impact and chemical-ionization mass spectra are identical.

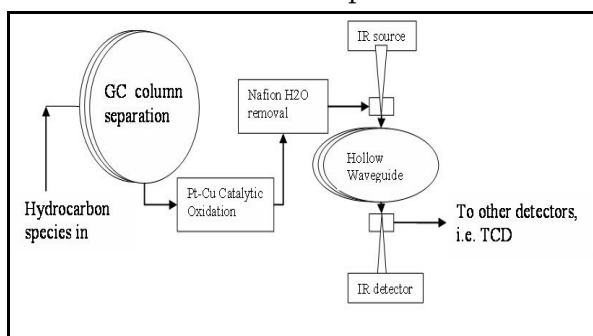


**Figure 6.** Schematic presentation of GC/FTIR

### 9. CE/MS:

Capillary Electrophoresis coupled with Mass Spectrometry is an online separation technique in which molecules are distinguished according to their differences in electrophoretic mobilities and structural information [30]. This technique is speedy, efficient and low solvent and sample is required for the analysis. The CE is connected to the MS with the help of the long capillaries which increases the analysis time for better sensitivity. The detectors used for the CE analysis are UV and DAD. The electrolytes used in this technique are inorganic and non-volatile. Ionisation interfaces used are electrospray; fast atom bombardment interface and ion spray ioniser. Detectors used in mass spectroscopy are TOF, ion trap and Quadrupole. Main advantage of quadrupole detector is sensitivity [31].

The major pharmaceutical applications of this technique include the identification of basic and acidic compounds using non-aqueous CE/MS, the analysis of complex arabino oligosaccharides and drug bioanalysis & biomarker discovery.

### 10. TG/MS:

Heating a sample on the TGA causes a sample to release volatile materials or generate combustion components as it burns. These gases are then transferred to MS for identification. Hyphenating TG/MS is a powerful approach for analysis of an unknown mixture to determine its primary components and identify additives or contaminants. This information may be needed, for example, to evaluate a competitor's product or to determine compliance with regulations [15].

TG/MS technique basically consists of a take-off tube placed very close to the specimen crucible in the TGA, a narrow and heated passage tube for gas transfer without condensation. This tube terminates with a micro metering valve connected to a rotary pump. This acts as the first stage of pressure reduction and gives the desired viscous flow required for faster transfer. The second stage of pressure reduction is achieved through a molecular leak valve. This ensures both a clean sample entry and the low operating pressure at the mass spectrometer [32].

This system is used to study temperature programmed decomposition of many oxyanion based inorganic salts. In conjunction with off-line analytical techniques, the chemical, structural evaluation of the intermediates/products with complete kinetic/reaction pathways is determined.

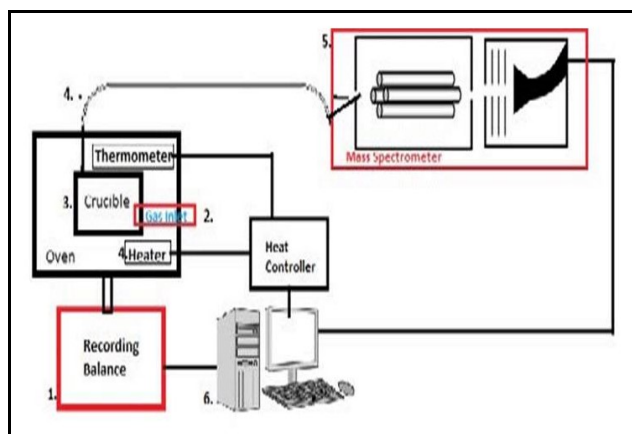


**Figure 7,** Schematic presentation of TG/MS

### 11. DSC/Raman:

DSC allows scientists to see the transitions between crystalline forms in a drug but but the forms must be determined by another method. Simultaneous DSC/Raman technique solves this problem. One of the great strengths of DSC/Raman is that a spectroscopist is able to determine structural information from the spectrum. For example, in semicrystalline sample, where the drug exists in mixtures of crystalline and amorphous forms, the ability to understand crystallinity is an obvious advantage.

The Raman spectrometer can collect data during the rapid heating of the material to the melt, although the fast heating will limit the number of spectra collected, and then on both the cooling and isothermal hold stages. After this experiment, the data are more conclusive in the Raman and in the DSC. In other words, DSC/Raman complements each other because Raman spectra can provide qualitative information to supplement the quantitative information from DSC.

In this technique, Raman Station allows the use of a remote probe for collecting spectrum. This makes an optical fibre connection between the spectrometer and the DSC. The lid of the DSC is modified to hold the focusing and collecting optics, with adjustment to align the laser beam with the sample. These modifications serve to protect the remote probe from high temperatures in the DSC, as well as to protect and maintain the controlled thermal environment required for proper DSC operation. The laser illuminates a spot approximately 200  $\mu\text{m}$  across. The

sample will normally be in an open pan, although a quartz window can be used for volatile materials [33].

### 12. LC/MS/MS:

LC-MS/MS can detect the sample components of different class by low injection volume. Minimal sample pre-treatment is required and it also reduces the time of analysis. LC-MS is the first step of LC/MS/MS. This technique is more sensitive and specific than that of the LC/MS. It is around 20-100 times sensitive than LC-/MS. More specific because in this technique second filtering process is also involved.

### 13. GC/MS/MS:

This technique is sensitive as well as specific and can be used for ultra-trace analysis. For qualitative identification with MS/MS, product ion scan, precursor ion scan and neutral loss with a triple quadrupole or product scan with an ion trap can be used. In recent years the sensitivity of the quadrupole is increased instead of loss. Also the scanning speed is high [22].

## V. CONCLUSION

The hyphenated techniques, in which separation techniques are coupled with diverse selective and sensitive detection methods, are widely used in pharmaceutical drug analysis. These techniques create new and ever greater possibilities. Their main advantages include extremely low limits of detection and quantification, insignificant influence of interferences on the determination process, as well as very high precision and repeatability of determinations. Nevertheless, the hyphenated techniques have been constantly developing and gaining more and more importance in pharmaceutical research & development, which is corroborated by the rising number of works pertaining to the subject. Further, the regulatory agencies are also encouraging the pharmaceutical organizations to best utilize the hyphenated techniques.

## VI. REFERENCES

- [1] Sweedler, J.V., The continued evolution of hyphenated instruments. *Analytical & Bio-analytical Chemistry*, 2002, 373, 321–322.
- [2] Albert, K. Hyphenated techniques. . *Analytical & Bioanalytical Chemistry*, 2002, 372, 25–26.
- [3] Ruchira chin hole et.al. Recent applications of hyphenated liquid chromatography techniques. *International journal of pharmaceutical sciences review and research*: 2012, 14(1); 57-63.
- [4] Bruins, A. P.; Covey, T. R.; Henion, J. D., Ion spray interface for combined liquid chromatography-atmospheric pressure ionization mass spectrometry. *Analytical Chemistry*. 1987, 59,2642-2646.
- [5] Nishino, I., Fujitomo, H. & Umeda, T. (2000) *J. Chromatogr. B: Biomedical Sciences and Applications*, 749(1), 101.
- [6] Hirschfeld, T. 1980. The hy-phen-ated methods. *Anal. Chem.* 52(2): 226–232.
- [7] Dressler, V.L., Antes, F.G., Moreira, C.M., Pozebon, D., and Duarte, F.A. 2011. As, Hg, I, Sb, Se and Sn speciation in body fluids and biological tissues using hyphenated-ICP-MS techniques: A review. *Int. J. Mass Spectrom.* 307(1-3): 149–162.
- [8] Albert K. *On-line LC-NMR and Related Techniques*. London: Wiley; 2002.
- [9] Jinno K, Fujimoto C, Hirata Y. An interface for the combination of micro high performance liquid-chromatography and infrared spectrometry. *Appl. Spectrosc.* 1982;36:67–9.
- [10] Bourne S, Haefner AM, Norton KL, Griffiths PR. Performance characteristics of a real-time direct deposition gas-chromatography fourier-transform infrared spectrometry system. *Anal Chem.* 1990;62:2448–52.
- [11] Cheng SC1, Huang MZ, Shiea J. Thin layer chromatography/mass spectrometry, *Journal of Chromatography A*. 2011 May 13; 1218(19):2700-11.
- [12] Dimuthu A. Jayawickrama, Jonathan V. Sweedler, Hyphenation of capillary separations with nuclear magnetic resonance spectroscopy *Journal of Chromatography A*, 1000 (2003) 819–840.
- [13] Buddrus J, Herzog H. Coupling of Chromatography and NMR Study of Flowing Gas Chromatographic Fractions by Proton Magnetic Resonance. *Organic Magnetic Resonance*, February 1981; 15(2):211-213.
- [14] Herzog H, Buddrus J. Coupling of Chromatography and NMR. Part 5: Analysis of High-Boiling Gas-Chromatographic Fractions by On-line Nuclear Magnetic Resonance. *Chromatographia* 18(1):31-33.
- [15] PerkinElmer *Material Characterization Instrument Guide*
- [16] Kevin P. Menard, Richard Spragg, Greg Johnson, and Craig Sellman, *Hyphenation: The Next Step in Thermal Analysis*, American Laboratory January 2010.
- [17] Arpino, P.J. 1982. On-line liquid chromatography/mass spectrometry? An odd couple! *TrAC Trends Anal. Chem.* 1(7): 154–158.
- [18] *Pharmaceutical analysis modern methods*, W.MUNSON part –a 2001 edition.
- [19] Munson JW, *pharmaceutical analysis:modern methods part A*, Mumbai International medical Book Distributors, 2011.
- [20] Wilson ID, Brinkman UA. Hyphenation and hypernation: the practice and prospects of multiple hyphenation. *J Chromatogr A*. 2003;1000:325–56.
- [21] Jinno K. In: *Infrared Detect*, in *Encyclopedia of Chromatography*. Cazes J, editor. New York, USA: Marcel Dekker; 2001.
- [22] Guo X, Lankmayr E, *Hyphenated Techniques in Gas Chromatography*, Institute of Analytical Chemistry and Food Chemistry, Graz University of Technology, Austria, 14-19.
- [23] Klaus Albert, *Online Coupling of Gas Chromatography to Nuclear Magnetic*

Resonance Spectroscopy: Method for the Analysis of Volatile Stereoisomers, Institute of Organic Chemistry, Chemisches Zentralinstitut, University of Tuebingen, Auf der Morgenstelle 18, D-72076 Tuebingen, Germany.

- [24] A .M. Wolters, D.A. Jayawickrama, A.G. Webb, J.V. Sweedler *Anal. Chem.* 21 (2002) 5550.
- [25] K . Pusecker, J. Schewitz, P. Gfrorer, L.H. Tseng, K. Albert, E. Bayer, I.D. Wilson, N.J. Bailey, G.B. Scarfe, J.K. Nicholson, J.C. Lindon, *Anal. Commun.* 35 (1998) 213.
- [26] J. Schewitz, P. Gfrorer, K. Pusecker, L.H. Tseng, K. Albert, E. Bayer, I.D. Wilson, N.J. Bailey, G.B. Scarfe, J.K. Nicholson, J.C. Lindon, *Analyst* 123 (1998) 2835.
- [27] K. Pusecker, J. Schewitz, P. Gfrorer, L.H. Tseng, K. Albert, E. Bayer, *Anal. Chem.* 70 (1998) 3280.
- [28] Londhe SV, Mulgund SV, Chitre TS, Mallade PS, Barival JB, Jain KS. Hyphenated techniques in the analytical world, *Indian J Pharm educ Res* dec2008; 42(4).
- [29] Griffiths PR, Pentoney SL, Giorgetti A, ShaferKH: The hyphenation of chromatography and FTIR spectrometry, *Anal. Chem* 1986; 58:1349A-1364A.
- [30] Cai J, Henion J, Review Capillary electrophoresis-mass spectrometry, *Journal of Chromatography A* 1995; 703:667-692.
- [31] Schmitt-Kopplin P, Frommberger M. Capillary electrophoresis- mass spectrometry: 15 years of developments and applications. *Electrophoresis* 2003; 24:3831-3867.
- [32] Baldev Raj: Thermogravimetry-evolved gas analysis-mass spectrometry system for materials research, *Bull. Mater. Sci.*, Vol. 26, No. 4, June 2003, pp. 449-460
- [33] Perkin Elmer: Applications of Simultaneous DSC-Raman Technique.

# Growth, Structural and Optical Studies of Semi Organic Mixed Amino-Nitrate (GSA) Crystal

S S Dongare\*<sup>1</sup>, S B Patil<sup>2</sup>, M M Khandpekar<sup>3</sup>

<sup>1</sup>Department of Physics, JSM's SGAS & GPC College, Shivle, Murbad, Maharashtra, India

<sup>2</sup>Department of Physics K G Karjat College of ASC, Karjat, Raigad, Maharashtra, India

<sup>3</sup>Material Research Laboratory, Birla College, Kalyan, Maharashtra, India

## ABSTRACT

The mixed amino-nitrate (GSA) crystals were grown from saturated solutions by slow evaporation technique with molar ratio (3:0.5:0.5), Transparent, elongated crystals of appreciable sizes (16 x 11 x 5 mm) were obtained in about 3-4 weeks time. The solubility of GSA has been determined in water. The grown crystal belongs to orthorhombic system with cell  $a= 18.478$  a.u,  $b= 12.739$  a.u and  $c= 5.015$  a.u. with unit cell volume  $1180.69$  A.U<sup>3</sup>. The presences of chemical components/ groups have been identified by CHN and EDAX analysis. Comparative IR and Raman studies indicate a molecule with a lack of centre of symmetry. A wide transparency window useful for optoelectronic applications is indicated by the UV Studies. Using Nd- YAG laser (1064nm), the optical second harmonic generation (SHG) conversion efficiency of GSA have been carried out. Also photoconductivity, I-V characteristics, dielectrics studies, and Vickers micro hardness measurement have been carried out.

**Keywords:** Crystal Growth, Structure, Optical Properties, SHG efficiency, Hardness

## I. INTRODUCTION

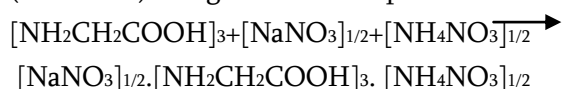
The field of non-linear optics is based on the development of new materials which have strong interaction with the light beam. Semi-organic compounds have been recently recognized as potential candidates for such second harmonic generation (SHG). Amino acid complexes with variety of ionic salts are found to be suitable as non linear optical materials [1, 2]. The basic amino acid alpha glycine has been employed to synthesize many organic and semi organic materials exhibiting dielectric, ferroelectric, non linear optical and light sensing behavior [3, 4]. The molecular arrangement with large inter-atomic distances however leads to poor thermal and mechanical properties. The presence of inorganic element in the organic matrix is seen to enhance mechanical strength of the material making it suitable for applications.

These materials are promising element for feature photonic technologies, which involves application for information, image processing, frequency conversion and optical switching etc. The large NLO coefficients of organic molecules have been combined with mechanical strength imparted by the inorganic component. Varieties of amino acids like glycine, L-arginine, L-histidine etc. have been used [5, 6]. Glycine is found to exist in three polymeric crystalline forms namely  $\alpha$ ,  $\beta$ ,  $\gamma$ , the simplest being the alpha form.  $\alpha$ -glycine has been combined with  $\text{NaNO}_3$  [7],  $\text{AgNO}_3$  [8] and  $\text{CaNO}_3$  [9] to produce interesting non linear optical compounds. In glycine sodium nitrate molecule the zwitterion of glycine is retained. The Na atom is seen to exhibit eight fold coordination and the polyhedron assumes the shape of a distorted hexagonal bipyramid. Moreover the glycine molecules are found to link through head-to-tail hydrogen bonds which are 'sandwiched' between the layers [10].

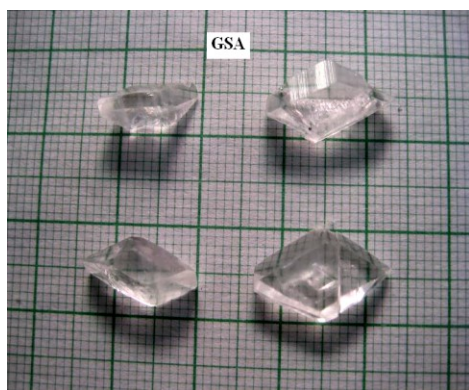
The organic matrix of glycine is found to be flexible to a variety of organic and inorganic components. In the present investigation single crystals of glycine barium- calcium nitrate (GSA) were grown and have been characterized by X-ray diffraction, FTIR, UV, SHG studies, I-V characteristics.

## II. GROWTH AND SOLUBILITY

GSA crystals were grown by slow evaporation technique from saturated solution in doubled distilled water at 30°C with a pH of 4.6. The A.R grade  $\alpha$ -glycine, sodium nitrate ( $\text{NaNO}_3$ ), ammonium-nitrate ( $\text{NH}_4\text{NO}_3$ ) supplied by Merck (India) with molar ratios 3:0.5:0.5. Transparent crystals of about  $16 \times 11 \times 5 \text{ mm}^3$  were obtained in four weeks time (Figure 1). The size of a crystal is found to depend on the amount of the material available in the solution. The solubility was determined by dissolving the known amount of substance in distilled water at various temperatures (300-350K) using constant temperature bath.



The size of a crystal was found to be depending on the amount of the material available in the solution which in turn is decided by the solubility of the material in solvent. The solubility of the synthesized material (GSA) was determined in distilled water at four different temperatures using constant temperature bath (Figure 2). The solubility is found to increased with temperature from 300-350K.



Maharashtra As grown GSA crystal

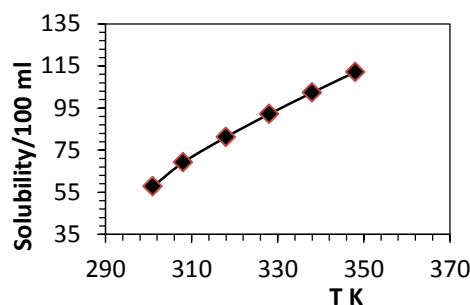


Figure 2. Solubility curve for GSA crystal

## III. CHARACTERIZATION

The grown crystal were subjected to X-ray powder diffraction using JEOL JDX-8030 Series, a highly sophisticated X-Ray diffractometer system with characteristic Cu-K $\alpha$  radiation ( $\lambda = 1.541 \text{ \AA}$ ). The sample was scanned in range from  $10^\circ$ - $70^\circ$  at rate of  $5^\circ$  per min [11, 12]. Density of GSA crystals was determined using the flotation method and a value of  $1.251 \text{ g/cc}$  was recorded. The melting point was found to lie at  $145^\circ\text{C}$  and the sample was found to finally decompose at  $265^\circ\text{C}$ . Heated sample showed effervescence near to decomposition temperature their by leading to bumping as also recorded in thermal (TGA/DTA) measurements. The FTIR spectra of sample were recorded in KBr phase in the frequency range from  $400$ - $4500 \text{ cm}^{-1}$  using Perkin Elmer 1600 series infrared spectrometer with resolution of  $4 \text{ cm}^{-1}$  and scanning speed of  $2 \text{ mm/s}$  [13, 14]. Laser Raman Spectra was recorded in solid form using Ramanor HG-2S, Jobin Yvon spectrometer with Argon ion laser source ( $\lambda = 5145 \text{ \AA}$ ) in range  $200 \text{ cm}^{-1}$ - $3500 \text{ cm}^{-1}$ . The absorption spectrum UV-Vis was recorded using U-2900, Hitachi system in range  $100$ - $1200 \text{ nm}$  covering the entire ultraviolet and near visible region [15]. The nonlinear optical conversion efficiency was tested using a modified Kurtz and Perry setup [16-17]. A Q-switched Nd:YAG laser beam of wavelength  $1064 \text{ nm}$  was used for SHG measurements with an input power  $2.69 \text{ mJ/pulse}$ . The pulse width was maintained at  $8 \text{ ns}$  at a repetition rate of  $100 \text{ Hz/pulse}$ . The crystal of GSA were ground to a uniform particle size of about  $125$ -

150  $\mu\text{m}$  and then packed in a capillary of uniform bore and exposed to laser radiations. The second harmonic signal generated in crystalline sample was confirmed from the emission of green radiation (532nm) from the crystal. The intensity of green light was measured using photo multiplier tube and CRO. The I-V characteristic and photoconductivity was recorded using digital pico ammeter Model DPM 111. Polished crystals of thickness 4mm were silver plated on the opposite faces Silver coating was applied on the opposite sides of polished crystal and was placed between two copper electrodes forming a parallel plate capacitor. The dc input was increased from 0 to 30V in steps and the corresponding readings were recorded. A 100 Watt Tungsten filament lamp with iodine vapors' was used to expose the samples for photoconductivity measurements. The dark characteristics were recorded by covering the sample with a black cloth.

#### A. X-ray diffraction

The new GSA crystal was characterized by powered X-ray diffraction to confirm the phase. The analysis of the observed spectra was carried out using POWD- Interactive powder diffraction data interpretation and indexing software program, Version 2.2 (Australia). The XRD peaks were indexed and the grown crystal was found to have orthorhombic symmetry with lattice parameters  $a=18.478$  a.u,  $b=12.739$  a.u and  $c=5.015$  a.u. and the unit cell volume  $1180.69$  A.U<sup>3</sup>. The intense peaks were recorded at  $2\theta = 20^\circ$  to  $40^\circ$  with maximum intensity of around 7128 on plane (4 2 1) as shown in spectrum (Figure 3)

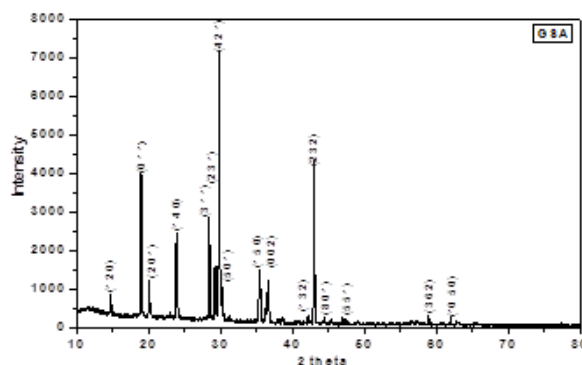


Figure 3. XRD Profile of GSA Crystal

#### B. FTIR and Raman Studies

Figure 4 shows FTIR spectrum of the grown GSA crystal. The characteristic absorption peaks have been observed in the range  $400\text{ cm}^{-1}$  to  $3200\text{ cm}^{-1}$  and active IR peaks were found to lie in region from  $400\text{ cm}^{-1}$  to  $1800\text{ cm}^{-1}$ .

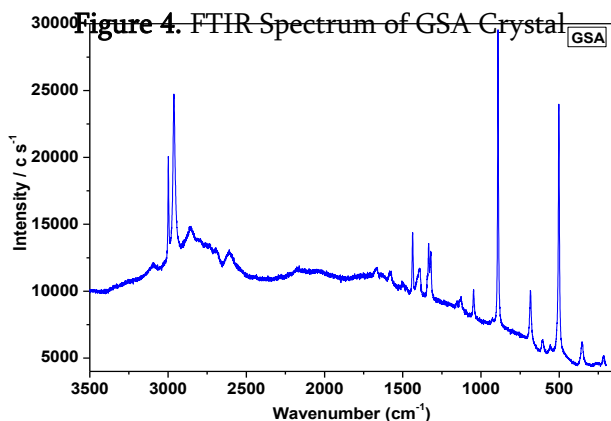
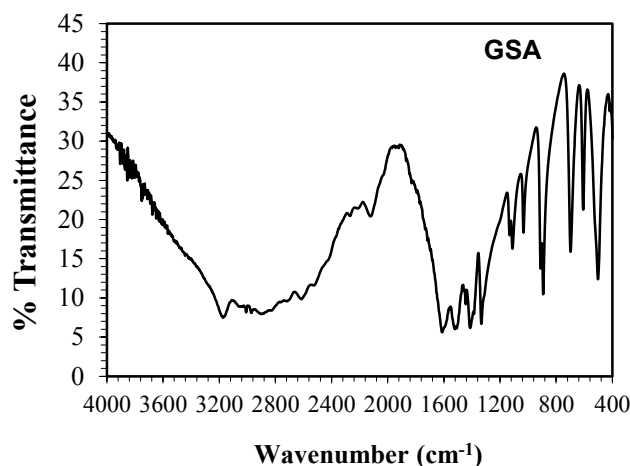


Figure 5. Raman Spectrum of GSA Crystal

A broad characterization peak appears between  $1700\text{ cm}^{-1}$ -  $2800\text{ cm}^{-1}$ . Free glycine exists as a

zwitterion in which the carboxyl group is present as carboxylate ions and amino group exist as ammonium ion. The absorptions due to carboxylate group of free glycine are observed between 501 and 690  $\text{cm}^{-1}$ . In the IR spectrum  $\text{CH}_2$  stretching occurs at 2962.4  $\text{cm}^{-1}$ . Amino acid combination band is found at 2166.9  $\text{cm}^{-1}$ . The strong  $\text{NH}_3^+$  deformation occurs between 1499  $\text{cm}^{-1}$ - 1637.3  $\text{cm}^{-1}$  and  $\text{NH}_3^+$  stretching occurs between 2609  $\text{cm}^{-1}$  & 2798.3  $\text{cm}^{-1}$ . The  $\text{CH}_2$  stretching is found to be weak in FTIR at 2966.3  $\text{cm}^{-1}$ . The  $\text{NO}_3^-$  symmetric stretch appears at 1048.2  $\text{cm}^{-1}$  and  $\text{NO}_3^-$  asymmetric stretching frequency lying at 1338  $\text{cm}^{-1}$ . The Raman profile for the GSA crystals is shown in Figure 5. The both spectrum shows prominently  $\text{COO}^-$  rocking/wagging/bending, CCN symmetric stretching,  $\text{CH}_2$  wagging/twisting,  $\text{CH}_2$ -Scissor,  $\text{NH}_3^+$  deformation, Amino acid combination bond,  $\text{NH}_3^+$  deformation,  $\text{CH}_2$  stretching and the presence of  $\text{NO}_3^-$  symmetric/asymmetric stretching etc.

### C. UV Studies

The UV absorption spectrum for GSA crystal was recorded in the UV-vis region (Figure 6). The peak at 200-221 nm is due to  $n-\pi^*$  transition [18-19]. The cut off wavelength  $\lambda_{\text{max}}$  lies at 221.5 nm with corresponding energy gap of 5.61 eV. A wide transparent window is present between 265 nm-1200 nm suggesting its use in optoelectronics devices.

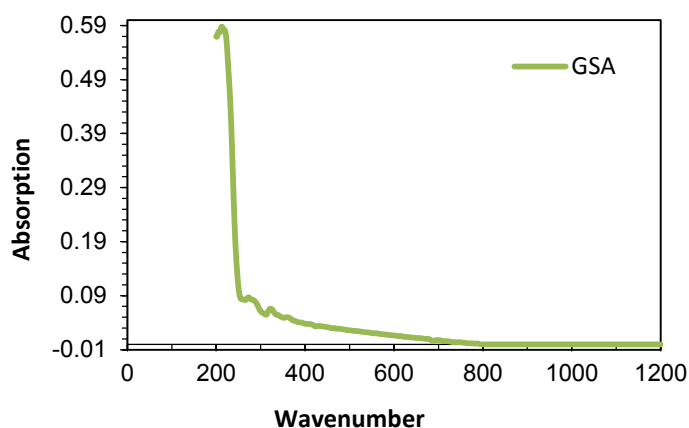


Figure 6. UV-Vis-NIR Spectrum of GSA Crystal

### D. Powder SHG measurement

The grown GSA crystals were subjected to second harmonic generation test for NLO property. Using Nd:YAG Q-switched laser source, the crystal was ground into powder with particle size is about 125-150  $\mu\text{m}$  and densely packed into two transparent slide was illuminated by pulse-laser beam with a wavelength of 1064nm. The SHG signal generated in the crystalline sample was collected and displayed as green light radiation ( $\lambda = 532\text{nm}$ ) on a cathode ray oscilloscope. A SHG signal of 5 mV was obtained compared to 185 mV of that of standard KDP crystal for the same input energy of 2.69 mJ/pulse. The SHG efficiency is found to depend upon the method and conditions during growth, composition and size of crystallites exposed during measurements.

### E. I-V and Photoconductivity Studies

The I-V and photoconductivity characteristic (dark and bright current) of the GSA crystals with applied field is as shown in Figure 7. The voltage (V) was found to increase with current (I) linearly up to voltage of 100 V/cm. On exposure to light radiation bright current is found to be greater than dark current (positive photoconductivity). This enhancement of field dependent conductivity of the sample is due to the generations of mobile charge carrier caused due the absorption of photons [20].

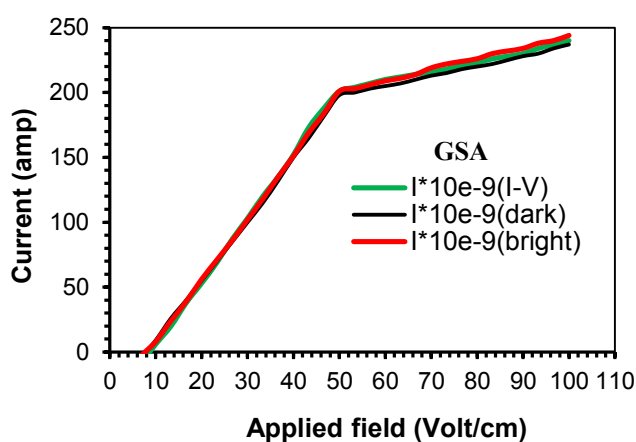


Figure 7. I-V and Photoconductivity plot



#### IV. CONCLUSION

Transparent crystals of acid mixed glycine -sodium-ammonium nitrate (GSA) crystal was successfully grown using slow evaporation method at room temperature from the aqueous solution and characterized by various techniques. The solubility was found to vary linearly in temperature range 300K-350K. The presence of fundamental groups has been verified by the comparative FTIR and Raman spectroscopic studies. The close match between the IR and Raman peaks indicate a molecule with lack of center of symmetry. The optical studies showed that the crystal have wide transparent window in the region 265 nm- 1200 nm useful for optoelectronic applications. The optical SHG efficiency of GSA crystal was carried out with respect to standard KDP. The I-V characteristics found to be linear upto 100 V/cm and on exposures to light sample show positive photoconductivity which may be attributed to due to the enhancement of charge carrier through absorption of photons.

#### V. ACKNOWLEDGMENTS

Thanks are due to the staff of Department of Material Science at TIFR, IIT, UICT, Material Research Lab, Kalyan and Indian Institute of Science, Bangalore for providing experimental facilities.

#### VI. REFERENCES

- [1] J. H. Paredes, D. G. Mintik, O. H. Negrete, H. E. Ponce, M. E. Alvarez R, R. R. Mijangos, A. D. Moller, *J. Phys. Chem. of Solids*. 69 (2008) 1974.
- [2] J. H. Paredes, D. G. Mintik, O. H. Negrete, H. E. Ponce, M. E. A. Ramos, A. D. Moller, *J. Mol. Struc.* 875 (2008) 295.
- [3] R. Pepinsky, Y. Okaya, D.P. Eastman, *T.Mitsui, Phys. Rev.* 107 (1957) 1538.
- [4] M.M. Khandpekar, S.P. Pati, *J. Opt. Commun.* 283 (2010) 2700.
- [5] D. Eimert, S. Velsko, L. Davis, F. Wang, G. Loiacono, G. Kennedy, *IEEE, J.Quantum. Electron.* 25 (1989)179.
- [6] M. D. Agarwal, J .Choi, W. S.Wang, K.Bhat, R. B. Lal, A.D.Shied, B. G. Penn, D.O. Frazier, *J.Crystal Growth* 204 (1999)179.
- [7] M. N. Bhat, S. M. Dharmaprakash, *J. Cryst. Growth*, 235 (2002) 511.
- [8] J. K. Mohan Rao, M. A. Vishwamitra, *Acta. Crystallogr. B*28 (1972) 1484.
- [9] S. Natarajan, *Z. Kristallgr.* 163 ( 1983) 305.
- [10] R. V. Krishnakumar, M. S. Naandhini, S. Natarajan, K. Sivakumar, B. Varghese, *Acta. Cryst. C*57 (2001) 1149.
- [11] S. A Martin Britto, S. Natarajan, *Opt. Commun.* 281 (2008) 457.
- [12] S .Dhanuskodi, K .Vasanta., *Spectrochimica. Acta. Part A* 61(2005)1777.
- [13] T. Mallik, T .Kar, *J.Cryst.Growth*, 274 (2005) 251.
- [14] S. Dhanuskodi, A. P Jeyakumari, S. Manivannan, *J. Cryst.Growth.* 282 (2005)72.
- [15] S. Manikandan, S. Dhanuskodi, *Spectrochimica.Acta Part A* 67(2007)160.
- [16] S.K. Kurtz, T.T.Perry, *J.Appl. Phys.*39 (1968) 3798.
- [17] A. Joseph Arul Pragasam, J. Mhadavan, M.G. Mohamed, S. Selvakumar, K.Ambujan, P.Sagayaraj, *Opt. Mater.* 29 (2009)173.
- [18] R. M. Silverstein, G. C. Bassler, C. Morrck, *Spectroscopic Identification of Organic compounds*, fourth ed. Wiley USA, 1991.
- [19] T. Balakrisnan, K. Ramamurthi, *Cryst.Res.Technol.*12 (2006)1184.
- [20] S.Brahadeeswaran, H.L Bhat, N.S.Kini, A.M. Umarji,P. Balaya, P. S. Goyal, *J. Appl. Phys.*88 (2000) 5935.

# Growth, Structural and Optical Studies of Semi Organic Mixed Amino-Nitrate (GSA) Crystal

S S Dongare\*<sup>1</sup>, S B Patil<sup>2</sup>, M M Khandpekar<sup>3</sup>

\*<sup>1</sup>Department of Physics, JSM's SGAS & GPC College, Shivle, Murbad, Maharashtra, India

<sup>2</sup>Department of Physics K G Karjat College of ASC, Karjat, Raigad, Maharashtra, India

<sup>3</sup>Material Research Laboratory, Birla College, Kalyan, Maharashtra, India

## ABSTRACT

The mixed amino-nitrate (GSA) crystals were grown from saturated solutions by slow evaporation technique with molar ratio (3:0.5:0.5), Transparent, elongated crystals of appreciable sizes (16 x 11 x 5 mm) were obtained in about 3-4 weeks time. The solubility of GSA has been determined in water. The grown crystal belongs to orthorhombic system with cell  $a= 18.478$  a.u,  $b= 12.739$  a.u and  $c= 5.015$  a.u. with unit cell volume  $1180.69$  A.U<sup>3</sup>. The presences of chemical components/ groups have been identified by CHN and EDAX analysis. Comparative IR and Raman studies indicate a molecule with a lack of centre of symmetry. A wide transparency window useful for optoelectronic applications is indicated by the UV Studies. Using Nd- YAG laser (1064nm), the optical second harmonic generation (SHG) conversion efficiency of GSA have been carried out. Also photoconductivity, I-V characteristics, dielectrics studies, and Vickers micro hardness measurement have been carried out.

**Keywords:** Crystal Growth, Structure, Optical Properties, SHG efficiency, Hardness

## I. INTRODUCTION

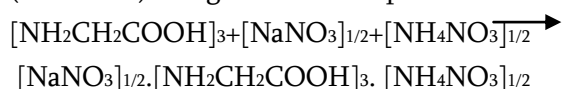
The field of non-linear optics is based on the development of new materials which have strong interaction with the light beam. Semi-organic compounds have been recently recognized as potential candidates for such second harmonic generation (SHG). Amino acid complexes with variety of ionic salts are found to be suitable as non linear optical materials [1, 2]. The basic amino acid alpha glycine has been employed to synthesize many organic and semi organic materials exhibiting dielectric, ferroelectric, non linear optical and light sensing behavior [3, 4]. The molecular arrangement with large inter-atomic distances however leads to poor thermal and mechanical properties. The presence of inorganic element in the organic matrix is seen to enhance mechanical strength of the material making it suitable for applications.

These materials are promising element for feature photonic technologies, which involves application for information, image processing, frequency conversion and optical switching etc. The large NLO coefficients of organic molecules have been combined with mechanical strength imparted by the inorganic component. Varieties of amino acids like glycine, L-arginine, L-histidine etc. have been used [5, 6]. Glycine is found to exist in three polymeric crystalline forms namely  $\alpha$ ,  $\beta$ ,  $\gamma$ , the simplest being the alpha form.  $\alpha$ -glycine has been combined with  $\text{NaNO}_3$  [7],  $\text{AgNO}_3$  [8] and  $\text{CaNO}_3$  [9] to produce interesting non linear optical compounds. In glycine sodium nitrate molecule the zwitterion of glycine is retained. The Na atom is seen to exhibit eight fold coordination and the polyhedron assumes the shape of a distorted hexagonal bipyramid. Moreover the glycine molecules are found to link through head-to-tail hydrogen bonds which are 'sandwiched' between the layers [10].

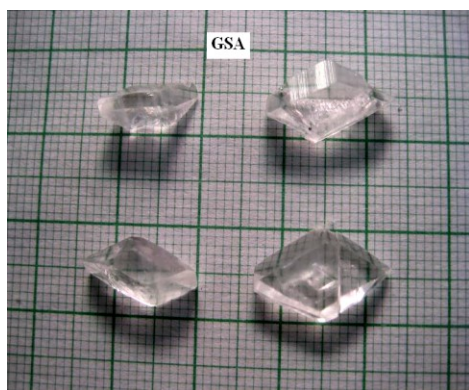
The organic matrix of glycine is found to be flexible to a variety of organic and inorganic components. In the present investigation single crystals of glycine barium- calcium nitrate (GSA) were grown and have been characterized by X-ray diffraction, FTIR, UV, SHG studies, I-V characteristics.

## II. GROWTH AND SOLUBILITY

GSA crystals were grown by slow evaporation technique from saturated solution in doubled distilled water at 30°C with a pH of 4.6. The A.R grade  $\alpha$ -glycine, sodium nitrate ( $\text{NaNO}_3$ ), ammonium-nitrate ( $\text{NH}_4\text{NO}_3$ ) supplied by Merck (India) with molar ratios 3:0.5:0.5. Transparent crystals of about  $16 \times 11 \times 5 \text{ mm}^3$  were obtained in four weeks time (Figure 1). The size of a crystal is found to depend on the amount of the material available in the solution. The solubility was determined by dissolving the known amount of substance in distilled water at various temperatures (300-350K) using constant temperature bath.



The size of a crystal was found to be depending on the amount of the material available in the solution which in turn is decided by the solubility of the material in solvent. The solubility of the synthesized material (GSA) was determined in distilled water at four different temperatures using constant temperature bath (Figure 2). The solubility is found to increased with temperature from 300-350K.



Maharashtra As grown GSA crystal

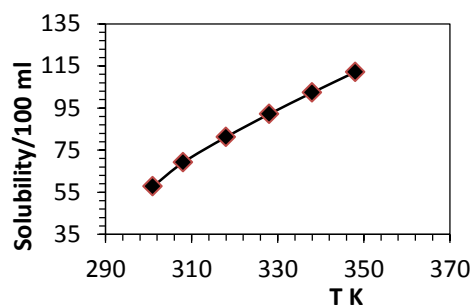


Figure 2. Solubility curve for GSA crystal

## III. CHARACTERIZATION

The grown crystal were subjected to X-ray powder diffraction using JEOL JDX-8030 Series, a highly sophisticated X-Ray diffractometer system with characteristic Cu-K $\alpha$  radiation ( $\lambda = 1.541 \text{ \AA}$ ). The sample was scanned in range from  $10^\circ$ - $70^\circ$  at rate of  $5^\circ$  per min [11, 12]. Density of GSA crystals was determined using the flotation method and a value of  $1.251 \text{ g/cc}$  was recorded. The melting point was found to lie at  $145^\circ\text{C}$  and the sample was found to finally decompose at  $265^\circ\text{C}$ . Heated sample showed effervescence near to decomposition temperature their by leading to bumping as also recorded in thermal (TGA/DTA) measurements. The FTIR spectra of sample were recorded in KBr phase in the frequency range from  $400$ - $4500 \text{ cm}^{-1}$  using Perkin Elmer 1600 series infrared spectrometer with resolution of  $4 \text{ cm}^{-1}$  and scanning speed of  $2 \text{ mm/s}$  [13, 14]. Laser Raman Spectra was recorded in solid form using Ramanor HG-2S, Jobin Yvon spectrometer with Argon ion laser source ( $\lambda = 5145 \text{ \AA}$ ) in range  $200 \text{ cm}^{-1}$ - $3500 \text{ cm}^{-1}$ . The absorption spectrum UV-Vis was recorded using U-2900, Hitachi system in range  $100$ - $1200 \text{ nm}$  covering the entire ultraviolet and near visible region [15]. The nonlinear optical conversion efficiency was tested using a modified Kurtz and Perry setup [16-17]. A Q-switched Nd:YAG laser beam of wavelength  $1064 \text{ nm}$  was used for SHG measurements with an input power  $2.69 \text{ mJ/pulse}$ . The pulse width was maintained at  $8 \text{ ns}$  at a repetition rate of  $100 \text{ Hz/pulse}$ . The crystal of GSA were ground to a uniform particle size of about  $125$ -

150  $\mu\text{m}$  and then packed in a capillary of uniform bore and exposed to laser radiations. The second harmonic signal generated in crystalline sample was confirmed from the emission of green radiation (532nm) from the crystal. The intensity of green light was measured using photo multiplier tube and CRO. The I-V characteristic and photoconductivity was recorded using digital pico ammeter Model DPM 111. Polished crystals of thickness 4mm were silver plated on the opposite faces Silver coating was applied on the opposite sides of polished crystal and was placed between two copper electrodes forming a parallel plate capacitor. The dc input was increased from 0 to 30V in steps and the corresponding readings were recorded. A 100 Watt Tungsten filament lamp with iodine vapors' was used to expose the samples for photoconductivity measurements. The dark characteristics were recorded by covering the sample with a black cloth.

#### A. X-ray diffraction

The new GSA crystal was characterized by powered X-ray diffraction to confirm the phase. The analysis of the observed spectra was carried out using POWD- Interactive powder diffraction data interpretation and indexing software program, Version 2.2 (Australia). The XRD peaks were indexed and the grown crystal was found to have orthorhombic symmetry with lattice parameters  $a=18.478$  a.u,  $b=12.739$  a.u and  $c=5.015$  a.u. and the unit cell volume  $1180.69$  A.U<sup>3</sup>. The intense peaks were recorded at  $2\theta = 20^\circ$  to  $40^\circ$  with maximum intensity of around 7128 on plane (4 2 1) as shown in spectrum (Figure 3)

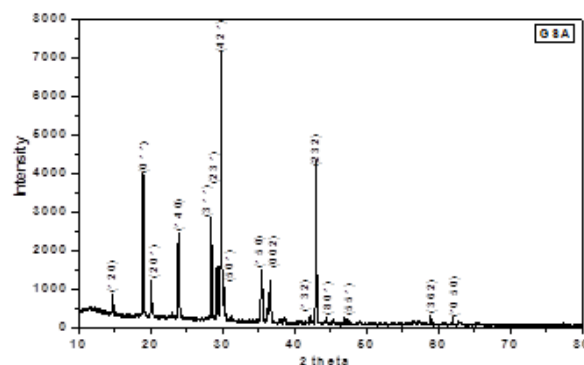


Figure 3. XRD Profile of GSA Crystal

#### B. FTIR and Raman Studies

Figure 4 shows FTIR spectrum of the grown GSA crystal. The characteristic absorption peaks have been observed in the range  $400\text{ cm}^{-1}$  to  $3200\text{ cm}^{-1}$  and active IR peaks were found to lie in region from  $400\text{ cm}^{-1}$  to  $1800\text{ cm}^{-1}$ .

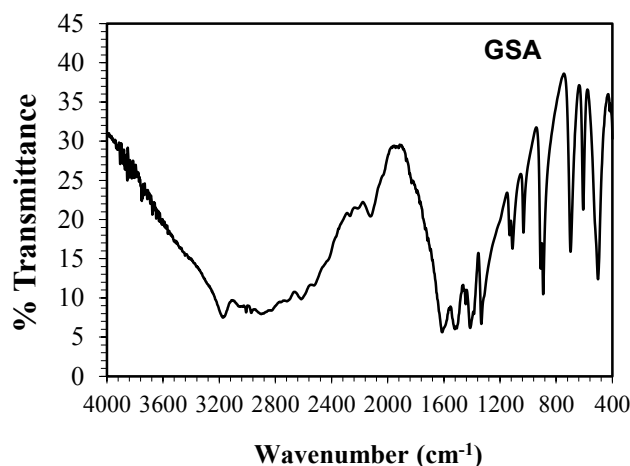


Figure 4. FTIR Spectrum of GSA Crystal

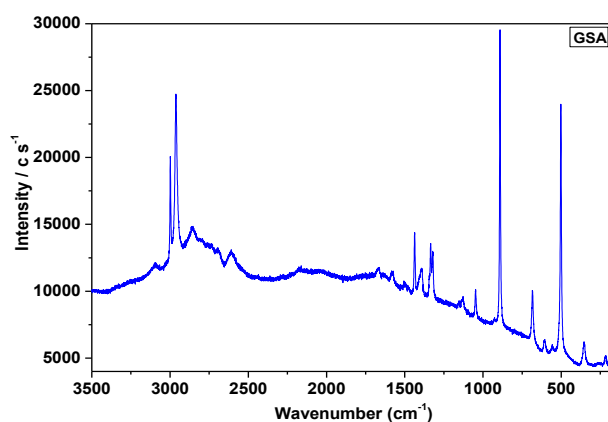


Figure 5. Raman Spectrum of GSA Crystal

A broad characterization peak appears between  $1700\text{ cm}^{-1}$ -  $2800\text{ cm}^{-1}$ . Free glycine exists as a

zwitterion in which the carboxyl group is present as carboxylate ions and amino group exist as ammonium ion. The absorptions due to carboxylate group of free glycine are observed between 501 and 690  $\text{cm}^{-1}$ . In the IR spectrum  $\text{CH}_2$  stretching occurs at 2962.4  $\text{cm}^{-1}$ . Amino acid combination band is found at 2166.9  $\text{cm}^{-1}$ . The strong  $\text{NH}_3^+$  deformation occurs between 1499  $\text{cm}^{-1}$ - 1637.3  $\text{cm}^{-1}$  and  $\text{NH}_3^+$  stretching occurs between 2609  $\text{cm}^{-1}$  & 2798.3  $\text{cm}^{-1}$ . The  $\text{CH}_2$  stretching is found to be weak in FTIR at 2966.3  $\text{cm}^{-1}$ . The  $\text{NO}_3^-$  symmetric stretch appears at 1048.2  $\text{cm}^{-1}$  and  $\text{NO}_3^-$  asymmetric stretching frequency lying at 1338  $\text{cm}^{-1}$ . The Raman profile for the GSA crystals is shown in Figure 5. The both spectrum shows prominently  $\text{COO}^-$  rocking/wagging/bending, CCN symmetric stretching,  $\text{CH}_2$  wagging/twisting,  $\text{CH}_2$ -Scissor,  $\text{NH}_3^+$  deformation, Amino acid combination bond,  $\text{NH}_3^+$  deformation,  $\text{CH}_2$  stretching and the presence of  $\text{NO}_3^-$  symmetric/asymmetric stretching etc.

### C. UV Studies

The UV absorption spectrum for GSA crystal was recorded in the UV-vis region (Figure 6). The peak at 200-221 nm is due to  $n-\pi^*$  transition [18-19]. The cut off wavelength  $\lambda_{\text{max}}$  lies at 221.5 nm with corresponding energy gap of 5.61 eV. A wide transparent window is present between 265 nm-1200 nm suggesting its use in optoelectronics devices.

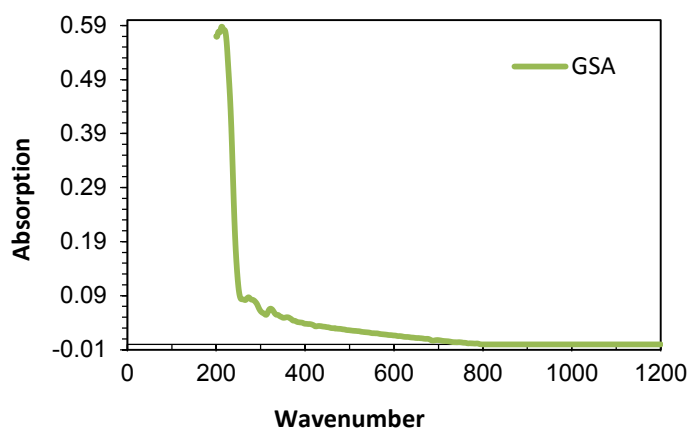


Figure 6. UV-Vis-NIR Spectrum of GSA Crystal

### D. Powder SHG measurement

The grown GSA crystals were subjected to second harmonic generation test for NLO property. Using Nd:YAG Q-switched laser source, the crystal was ground into powder with particle size is about 125-150  $\mu\text{m}$  and densely packed into two transparent slide was illuminated by pulse-laser beam with a wavelength of 1064nm. The SHG signal generated in the crystalline sample was collected and displayed as green light radiation ( $\lambda = 532\text{nm}$ ) on a cathode ray oscilloscope. A SHG signal of 5 mV was obtained compared to 185 mV of that of standard KDP crystal for the same input energy of 2.69 mJ/pulse. The SHG efficiency is found to depend upon the method and conditions during growth, composition and size of crystallites exposed during measurements.

### E. I-V and Photoconductivity Studies

The I-V and photoconductivity characteristic (dark and bright current) of the GSA crystals with applied field is as shown in Figure 7. The voltage (V) was found to increase with current (I) linearly up to voltage of 100 V/cm. On exposure to light radiation bright current is found to be greater than dark current (positive photoconductivity). This enhancement of field dependent conductivity of the sample is due to the generations of mobile charge carrier caused due the absorption of photons [20].

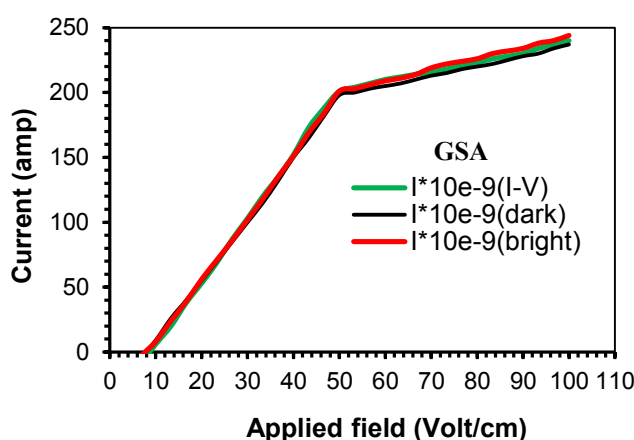


Figure 7. I-V and Photoconductivity plot

#### IV. CONCLUSION

Transparent crystals of acid mixed glycine -sodium-ammonium nitrate (GSA) crystal was successfully grown using slow evaporation method at room temperature from the aqueous solution and characterized by various techniques. The solubility was found to vary linearly in temperature range 300K-350K. The presence of fundamental groups has been verified by the comparative FTIR and Raman spectroscopic studies. The close match between the IR and Raman peaks indicate a molecule with lack of center of symmetry. The optical studies showed that the crystal have wide transparent window in the region 265 nm- 1200 nm useful for optoelectronic applications. The optical SHG efficiency of GSA crystal was carried out with respect to standard KDP. The I-V characteristics found to be linear upto 100 V/cm and on exposures to light sample show positive photoconductivity which may be attributed to due to the enhancement of charge carrier through absorption of photons.

#### V. ACKNOWLEDGMENTS

Thanks are due to the staff of Department of Material Science at TIFR, IIT, UICT, Material Research Lab, Kalyan and Indian Institute of Science, Bangalore for providing experimental facilities.

#### VI. REFERENCES

- [1] J. H. Paredes, D. G. Mintik, O. H. Negrete, H. E. Ponce, M. E. Alvarez R, R. R. Mijangos, A. D. Moller, *J. Phys. Chem. of Solids*. 69 (2008) 1974.
- [2] J. H. Paredes, D. G. Mintik, O. H. Negrete, H. E. Ponce, M. E. A. Ramos, A. D. Moller, *J. Mol. Struc.* 875 (2008) 295.
- [3] R. Pepinsky, Y. Okaya, D.P. Eastman, *T.Mitsui, Phys. Rev.* 107 (1957) 1538.
- [4] M.M. Khandpekar, S.P. Pati, *J. Opt. Commun.* 283 (2010) 2700.
- [5] D. Eimert, S. Velsko, L. Davis, F. Wang, G. Loiacono, G. Kennedy, *IEEE, J.Quantum. Electron.* 25 (1989)179.
- [6] M. D. Agarwal, J .Choi, W. S.Wang, K.Bhat, R. B. Lal, A.D.Shied, B. G. Penn, D.O. Frazier, *J.Crystal Growth* 204 (1999)179.
- [7] M. N. Bhat, S. M. Dharmaprakash, *J. Cryst. Growth*, 235 (2002) 511.
- [8] J. K. Mohan Rao, M. A. Vishwamitra, *Acta. Crystallogr. B*28 (1972) 1484.
- [9] S. Natarajan, *Z. Kristallgr.* 163 ( 1983) 305.
- [10] R. V. Krishnakumar, M. S. Naandhini, S. Natarajan, K. Sivakumar, B. Varghese, *Acta. Cryst. C*57 (2001) 1149.
- [11] S. A Martin Britto, S. Natarajan, *Opt. Commun.* 281 (2008) 457.
- [12] S .Dhanuskodi, K .Vasanta., *Spectrochimica. Acta. Part A* 61(2005)1777.
- [13] T. Mallik, T .Kar, *J.Cryst.Growth*, 274 (2005) 251.
- [14] S. Dhanuskodi, A. P Jeyakumari, S. Manivannan, *J. Cryst.Growth.* 282 (2005)72.
- [15] S. Manikandan, S. Dhanuskodi, *Spectrochimica.Acta Part A* 67(2007)160.
- [16] S.K. Kurtz, T.T.Perry, *J.Appl. Phys.*39 (1968) 3798.
- [17] A. Joseph Arul Pragasam, J. Mhadavan, M.G. Mohamed, S. Selvakumar, K.Ambujan, P.Sagayaraj, *Opt. Mater.* 29 (2009)173.
- [18] R. M. Silverstein, G. C. Bassler, C. Morrck, *Spectroscopic Identification of Organic compounds*, fourth ed. Wiley USA, 1991.
- [19] T. Balakrisnan, K. Ramamurthi, *Cryst.Res.Technol.*12 (2006)1184.
- [20] S.Brahadeeswaran, H.L Bhat, N.S.Kini, A.M. Umarji,P. Balaya, P. S. Goyal, *J. Appl. Phys.*88 (2000) 5935.

# Green synthesis of silver nanoparticles from plant sources and evaluation of their antimicrobial activity

Sapna G. Yadav<sup>1</sup>, Sudeep H Patil<sup>2</sup>, Pratima Patel<sup>3</sup>, Vineetha Nair<sup>4</sup>, Shahida Khan<sup>5</sup>, Shivani Kakkar<sup>6</sup>, Annika Durve Gupta<sup>\*7</sup>

<sup>1-7</sup>Department of biotechnology, university of Mumbai, Kalyan, Maharashtra, India.

## ABSTRACT

Nanoparticles are used widely due to its small size, orientation, physical properties, which are reportedly shown to change the performance of any other material which is in contact with these particles. Silver nanoparticles have received substantial attention in the field of antimicrobial research due to the antimicrobial activity of silver. These particles can be synthesized easily by different chemical, physical, and biological approaches. The biological approach is the most emerging approach of preparation, as this method is easier than the other methods, ecofriendly, non toxic and less time consuming. In the present study green synthesis of silver nanoparticles was carried out using the plant extracts of Neem (*Azadirachta indica*), Tea (*Camellia sinensis*), Peels from kitchen waste and the mixture of all the three extracts. Silver was of a particular interest for this process due to its evocative physical and chemical properties. The reduction process of  $Ag^+$  to  $Ag^0$  was observed by formation of brown colour within 24 hours of incubation period and synthesized SNPs showed an absorption peak at around 450 nm in the UV-visible spectrum. The reaction was followed by the characterization of the silver nanoparticles using UV-Vis and FTIR. The antimicrobial activity was tested using agar well method with Gram positive and Gram negative microorganism. It was observed that the antimicrobial activity was higher against Gram negative bacteria. Local plants such as tea leaves and waste is an alternative to a safer, more eco-friendly alternatives of synthesizing silver nanoparticles. This environment friendly, method provides simple, easy and cost effective faster synthesis of nanoparticles than chemical method and can be used in several areas such as catalysis, medical application etc.

**Keywords:** Silver nanoparticles, UV-Visible Spectroscopy, FTIR, Antimicrobial activity

## I. INTRODUCTION

Nanotechnology is the branch of technology that deals with dimensions and tolerances of less than 100 nanometers, especially the manipulation of individual atoms and molecules. They exhibit novel and significantly improved physical, chemical and biological properties, phenomena and processes because of their size [1]. Nanoparticle may or maynot exhibit size-related properties that differ significantly from those observed in fine particles or bulk materials

[2]. Some of the applications of nanoparticles to biology or medicine are in tissue engineering, cancer therapy, multicolour optical coding for biological assays, manipulation of cells and biomolecules, protein detection, drug and gene delivery, bio detection of pathogens, probing of DNA structure, tumour destruction via heating (hyperthermia), MRI contrast enhancement and phagokinetic studies.

Among the various metal nanoparticles, silver (Ag) nanoparticle has received substantial attention in the

field of antimicrobial research. Silver has long been recognized as having an inhibitory effect towards many bacterial strains and microorganisms [3]. Synthesising silver nanoparticles by plants is a major advantage that they are easily available, safe and nontoxic in most cases, have a broad variety of metabolites that can aid in reduction of silver ions and are quicker than microbes in the synthesis. Biosynthesis of nanoparticles is a kind of bottom up approach, where the main mechanism of action is redox reaction. The need for biosynthesis of nanoparticles arises from the fact that the physical and chemical processes became costly and the use of hazardous chemicals in various steps [4]. Phytochemical mediated metal nanoparticle syntheses are effective, economical and environmental friendly. Plants are considered as biosynthetic laboratories of wide spectrum of phytochemicals such as phenolics, alkaloids and flavonoids. These phytochemicals are expected to self assemble and cap the metal nanoparticles formed in their presence and thereby induces some shape control during metal ion reduction [5]. Metallic nanoparticles obtained by biosynthesis employing plant extracts have been reviewed and reported by different authors [6,7].

In this work we have synthesized and characterized the silver nanoparticles from plant sources like leaves of Tea, Neem, Peels from kitchen waste and also from the combination of all three extracts and have checked the antibacterial activity of the synthesized silver nanoparticles

## II. MATERIALS AND METHODS

### Test chemicals

$\text{AgNO}_3$  were purchased from SD Fine Company, India and used without further purification. The purity was

at least 99.5%. The solutions for the metal salts were prepared in deionised water. The media for bacterial growth was obtained from Himedia, India.

### Sample Collection:

The sample sources for synthesis of nanoparticles were dried Tea leaves (*Camellia sinensis*) from local market, fresh Neem leaves (*Azadirachta indica*) from Ambivili area and Peels of mango, sweet potato, drumstick, tomato, carrot, pumpkin, snake gourd collected from normal kitchen waste.

### Preparation of extract:

Samples used were fresh leaves of Neem (*Azadirachta indica*), dried leaves of Tea (*Camellia sinensis*) and Peels of mango, sweet potato, drumstick, tomato, carrot, pumpkin, snake gourd. The solvent used was deionized water.

The samples were weighed 1g each and added to 50ml of deionized water in a flask. These flasks were kept in boiling water bath for 15min with inverted funnel. After cooling, the solution was filtered using Whatman filter paper no. 1. 2ml each of the filtrates were mixed in a conical flask and used as the fourth sample. The samples were named Tea, Peel, Neem and Mix [8].

### Synthesis of Silver nanoparticles:

1 ml of freshly prepared 5mM Silver nitrate solution was added to 5ml of the sample solutions respectively. This mixture was kept in boiling water bath for 10min until visible colour change (brown colour) was observed. The mixtures were kept in incubator at 37°C for 24hrs [8].

### UV-Vis spectral analysis

The reduction of pure  $\text{Ag}^+$  ions was monitored by using UV-Vis spectrum of reaction medium after 24



hrs. Sample was prepared by diluting the solution in deionized water in the ratio 1:10. Deionized water was used as blank. The analysis was carried out on a UV – Vis spectrophotometer (Jasco v-630 Spectrophotometer) from range 350-600nm.

### FTIR analysis of silver nanoparticles

The chemical composition of synthesized silver nanoparticles was studied by using FTIR spectrometer (JASCO FT/IR 4100 type A). The liquid samples were mixed with KBr and pellets were made. The solution were characterized in the range 4000-650  $\text{cm}^{-1}$

### Study of antimicrobial activity

The antibacterial activity of the synthesized silver nanoparticles was checked using Agar Well Diffusion method. 1 ml of the 24 hrs old grown bacterial culture was seed inoculated in molten sterile Nutrient agar butt and poured into petriplates. All the four samples (Neem, Tea, Veg peels, Mix) were tested against the five cultures - Staphylococcus aureus, Escherichia coli, Klebsiella pneumoniae, Corynebacterium diphtheriae and Pseudomonas aeruginos.

After the incubation period, the plates were examined for zone of inhibition. The diameter of the zones of clearance was measured and the mean value was calculated.

### III. RESULT AND DISCUSSION

The mixture showed colour change to brown colour at 37°C, after addition of plant extract to aqueous solution of  $\text{AgNO}_3$ . The colour is characteristic of the Surface Plasmon Resonance (SPR) of silver nanoparticles. The reduction of silver ion to silver nanoparticle was reflected in spectral data obtained by using a UV-Vis spectrophotometer. Absorbance

was found to be in range of 350-450nm which is specific for silver nanoparticles (Table 1, Figure 1) [9].

**Table 1: Absorbance of the AgNPs**

Silver nanoparticles	Maximum wavelength	Absorbance
Neem	443.8nm	0.477
Green tea	369.6nm	0.997
Vegetable Peels	431.6nm	0.556
Mixture of all three	447nm	0.791

Neem is found to exclude addition of external stabilizing agent during synthesis of silver nanoparticles and to offer synergistic effects to enhance the antimicrobial properties of the synthesized silver nanoparticles [10].

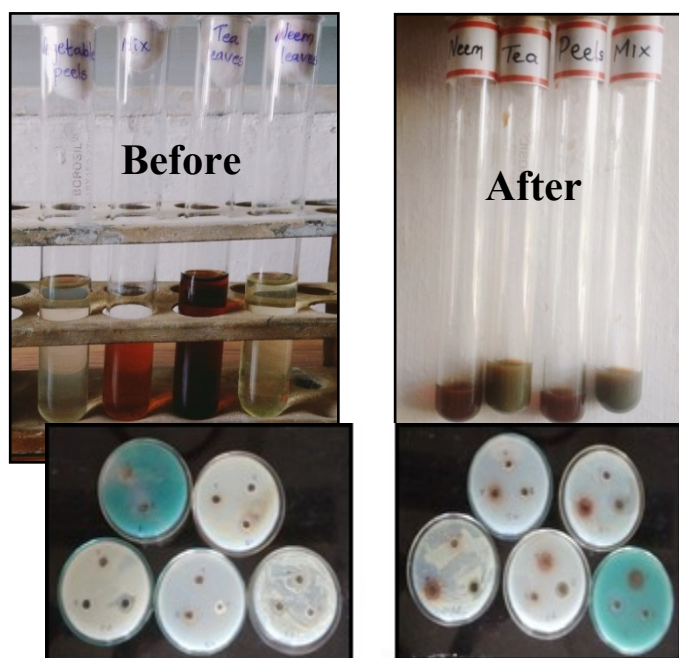


**Figure 1.** Colour change during synthesis of AgNPs before and after

The UV-Vis spectra confirmed the formation of Ag nanoparticles as the colour change occurred to reddish brown and maximum absorbance was found at 443.8nm for Neem AgNPs which lies in the range of earlier reported biosynthesized silver nanoparticles, 350-550nm [10] and 350-450nm [9] Other studies stated its range to be mostly around and at [11,12].

The Green tea leaves which were used for synthesis of silver nanoparticles showed peak at 369nm [13,14] The peels from kitchen waste also proved to be a good source for synthesis of nanoparticles. The UV-Vis spectral analysis showed its maximum absorbance at 431.6nm which was found to lie near the previously observed peak of 430nm with similar peels [15]

#### FTIR Analysis

FT-IR was carried to determine the functional groups responsible for reduction present in the plant sample and the synthesized nanoparticles. The FT-IR spectrum obtained for extracts displays a number of absorption peaks, reflecting its complex nature. Strong absorption peaks at 3263 to 3331  $\text{cm}^{-1}$  result from stretching of the -NH band of amino groups or is indicative of bonded -OH hydroxyl group. The absorption peaks at about 2929.87  $\text{cm}^{-1}$  could be assigned to stretching vibrations of -CH<sub>2</sub> and -CH<sub>3</sub> functional groups. The intense band at 1585  $\text{cm}^{-1}$

The characterization of Neem silver nanoparticles by FTIR showed the presence of alcohols and phenols, alkenes, aromatic group and ether which matched with the previously reported groups alkenes, alcohols and phenols with an additional primary amine group at 1634.90 $\text{cm}^{-1}$  [11]. In Peel AgNPs presence of aromatic groups, ketone groups and alcohols and

could be assigned to the aromatic C=C bending. FT-IR study indicates that the hydroxyl (-OH), and amine (N-H) groups in the extracts are mainly involved in reduction of Ag<sup>+</sup> ions to Ag<sup>0</sup> nanoparticles. For the plant extract, the FTIR results confirmed the presence the presence of -NH, -OH, C=C, and -CH group, which indicates that the plant extract containing the hydroxyl and amine group substituted flavonoids. It is observed that flavonoids act as a reducing agent, which reduces Ag<sup>+</sup> to Ag<sup>0</sup> and the amino group as stabilizing agents in the green synthesis of silver Nanoparticles. The FT-IR spectroscopic studies have also showed that the leaf extracts not only acts as reducing agent but as a stabilizer also, which prevents the agglomeration of AgNPs. The carbonyl group of amino acid residues has a strong binding ability with metal, suggesting the formation of a layer covering silver nanoparticles which act as a stabilizing agent to prevent agglomeration in the aqueous medium [16]. The observed intense band were compared with standard values of identify the functional groups.

The groups assisting reduction were found to be in the range of 1400-1600, 1640-1690, 2850-3000 and 1000-1300 $\text{cm}^{-1}$ . Thus the reduction of plant extracts by AgNO<sub>3</sub> was confirmed by FTIR analysis and the flavonoids present were found to be responsible for reduction.

phenols were observed indicating presence of flavonoids and other phytochemicals which were previously reported with an additional amine group at 3403.99 $\text{cm}^{-1}$  [15] The antimicrobial activity of the silver nanoparticles was studies against five different organisms viz. Gram positive organisms (Staphylococcus aureus and Corynebacterium

diphtheria) and Gram negative organisms (*Escherichia coli*, *Klebsiella pneumoniae* and *Pseudomonas aeruginosa*) (Figure 2, Table 2).

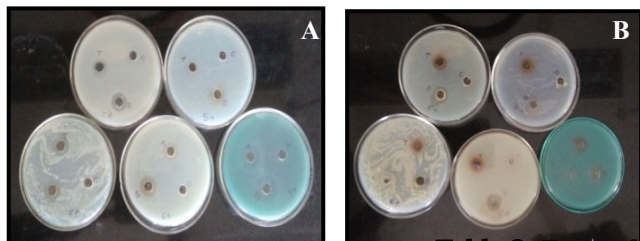


**Figure 2.** Antimicrobial activity of AgNPs prepared from [A] neem leaves, [B] tea leaves, [C] vegetable peels and [D] mixture of all.

**Table 2.** Zone of inhibition for the AgNPs

Organisms	Zone of inhibition(mm)					
	Neem AgNP	Tea AgNP	Peels AgNP	Mixture	Control A (1mM AgNO <sub>3</sub> )	Control B (Plant extract)
<i>Escherichia coli</i>	13	14	12	13	-	-
<i>Klebsiella pneumoniae</i>	12	14	15	16	-	-
<i>Pseudomonas aeruginosa</i>	11	11	13	12	-	-
<i>Staphylococcus aureus</i>	11	11	13	14	-	-
<i>Corynebacterium diphtheriae</i>	13	18	19	19	-	-

The figures show clear zone of inhibition in the well treated with silver nanoparticles whereas the well treated with only plant extract and silver nitrate did not show any inhibition. It was observed that the antibacterial activity of Mix AgNPs was more compared to Neem, Tea and Peels AgNPs against *Staphylococcus aureus*, *Escherichia coli*, *Klebsiella pneumoniae* and *Corynebacterium diphtheriae*. All the four nanoparticles showed maximum activity against *Corynebacterium diphtheriae* and minimum against *Pseudomonas aeruginosa*.

The Neem nanoparticles showed inhibitory action against *Staphylococcus aureus*, *Escherichia coli* and *Pseudomonas aeruginosa* which was previously reported [10]. In addition, antibacterial action against *Klebsiella pneumoniae* and *Corynebacterium diphtheriae* was also observed. Considerably good

antibacterial activity of Peel nanoparticles was observed against *Escherichia coli* and *Klebsiella pneumoniae* as earlier stated [15].

#### IV. CONCLUSION

The research work suggests that plants extract made from Neem, Tea and Peels from Kitchen waste and mixture of all capable of producing silver nanoparticles extracellular. The use of plant in synthesis of nanoparticles is advantageous in many ways in terms of production, economic viability and safety. The samples were environmental friendly, simple and efficient route for synthesis of benign nanoparticles. The characterization of silver nanoparticles was carried out using UV-Vis spectrometer and FTIR. The characterization by FTIR

showed the presence of aromatic groups, ketone groups and alcohols and phenols indicating presence of various phytochemicals including flavonoids which aid in reduction of silver. Plant extract can be used efficiently in synthesis of silver nanoparticles as greener route. Control over physical dimensions seems to be very easy with the use of plants. Nanoparticles produced from plants have various applications. The above silver nanoparticles revealed to have an effective antimicrobial property against *Staphylococcus aureus*, *Corynebacterium diptheria*, *Escherichia coli*, *Klebsiella pneumonia* and *Pseudomonas aeruginosa*. The present study emphasizes the use local plants and waste part for synthesis of silver nanoparticles with potent antibacterial effect. This green synthesis method has many advantages such as eco-friendly, cost effective and easily scaled up to large scale synthesis. The further characterization of the silver nanoparticles can be done by SEM analysis preferably to find its size and shape. Various parameters including pH, temperature and concentration of  $\text{AgNO}_3$  can be altered to obtain better results. Further, the checking of its antioxidant property may give new applications for the use of silver nanoparticles.

## V. REFERENCES

1. Kannan N., Shekhawat M.S., Ravindran C.P. and Manokari M. (2014). Preparation of silver nanoparticles using leaf and fruit extracts of *Morindacoreia Buck.*, Ham. –A green approach. *Journal of Scientific and Innovative Research*. 3(3): 315-318.
2. Banerjee P., Satapathy M., Mukhopahayay A. and Das P. (2014). Leaf extract mediated green synthesis of silver nanoparticles from widely available Indian plants: synthesis, characterization, antimicrobial property and toxicity analysis. *Bioresources and Bioprocessing*. 1:3.
3. Sriram T. and Pandidurai V. (2014). Synthesis of silver nanoparticles from leaf extract of *Psidium guajava* and its antibacterial activity against pathogens. *International Journal of Current Microbiology and Applied Sciences*. 3(3):146-152.
4. Ramya M, Sylvia Subapriya (2012) Green synthesis of silver nanoparticles. *Int J Pharm Med Bio Sc* 1: 54-61.
5. Ahmad N., Sharma S., Alam M.K., Singh V.N., Shamsi S.F. (2010) Rapid synthesis of silver nanoparticles using dried medicinal plant of basil. *Colloids Surf B* 81: 81-6.
6. Bali R., Razak N., Lumb A., Harris AT. (2006) The synthesis of metallic nanoparticles inside live plants. *Proce Int Conference Nanosci Nanotechnol (ICONN '06)* 224-7.
7. Victor S.M., Alfredo R.V.N. (2012) Green Synthesis of Noble Metal (Au, Ag, Pt) Nanoparticles, Assisted by Plant-Extracts. *Noble Metals: InTech* 392-408
8. Sankar R, Karthik A, Prabu A, Karthik S, Shivashangari KS, Ravikumar V. *Origanum vulgare* mediated biosynthesis of silver nanoparticles for its antibacterial and anticancer activity. *Colloids Surf B Biointerfaces*. 2013;108:80-4.
9. Bose D. and Chatterjee S. (2016). Biogenic synthesis of silver nanoparticles using guava (*Psidium guajava*) leaf extract and its antibacterial activity against *Pseudomonas aeruginosa*. *Applied Nanoscience*. 6:895–901.
10. Namratha N. and Monica P.V. (2013). Synthesis of silver Nanoparticles using *Azadirachta indica* (Neem) extract and usage in water purification. *Asian J. Pharm. Tech*. 3(4):170-174.
11. Agrawal P., Mehta K., Vashisth P., Sudarshan, Bhat P., Vishnu B. V. G. (2014). Green Synthesis of Silver Nanoparticles and Their Application in



- Dental Filling Material. International Journal of Innovative Research in Science, Engineering and Technology. 3(6):13038-13052.
12. Gavhane A. J., Padmanabhan P., Kamble S. P. and Jangle S. N. (2012). Synthesis of silver nanoparticles using extract of Neem leaf and Triphala and evaluation of their antimicrobial activities. International Journal of Pharma and Bio Sciences. 3(3):88-100.
  13. Loo Y. Y., Chieng B. W., Nishibuchi M. and Radu S. (2012). Synthesis of silver nanoparticles by using tea leaf extract from Camellia Sinensis. International Journal of Nanomedicine. 7:4263-4267.
  14. Shet A. R., Tantri S. and Bennal A. (2016). Economical biosynthesis of silver nanoparticles using fruit waste. Journal of Chemical and Pharmaceutical Sciences. 9(3):2306-2311.
  15. Sharma K., Kaushik S., Jyoti A. (2016). Green Synthesis of Silver Nanoparticles by Using Waste Vegetable Peel and its Antibacterial Activities. Journal of Pharmaceutical Science & Research. 8(5):313-316.
  16. Awwad A.M., Salem N.M., Abdeen A.O. (2013) Green synthesis of silver nanoparticles using carob leaf extract and its antibacterial activity. Int J Ind Chem 4: 2

# Loading of Anti Cancer Drug on Carbon Nanotubes

Seema Manchanda\*, Madhuri Sharon, Maheshwar Sharon

Department of Chemistry Birla College of Arts, Science and Commerce, Kalyan, University of Mumbai  
Maharashtra, India

## ABSTRACT

Carbon Nanotubes exhibit many unique intrinsic physical and chemical properties and have been intensively explored for biological and biomedical applications in the past few years. The presented work is a prelude in the direction of using Carbon Nano tubes as a vehicle for drug delivery to the desired sites. Anti cancer drug, Doxorubicin is loaded on functionalized Multiwalled Carbon Nano tubes at different pH conditions. Analysis done was FTIR, ATR, TEM, and UV Visible spectroscopy.

## I. INTRODUCTION

**Carbon Nano-tubes (CNT)** are concentric shells of graphite formed by one sheet of conventional graphite rolled up into a cylindrical form. The lattice of carbon atoms of graphite sheets remains continuous around the circumference of the Nano tubes. Hence, Carbon nanotubes are fullerene-related structures closed at either end with caps containing pentagonal rings.

CNTs are of two types Single Walled Carbon Nano Tubes (SWCNT) and Multi Walled Carbon Nano Tubes (MWCNT) (Figure 1)

In **SWCNT** there are only tubules and no graphitic layers around them. Diameter of SWCNT is up to 2 nanometer where as length varies as per production procedure from 3 to 10  $\mu\text{m}$ . The arrangement of carbon in a SWCNT can be of the arm-chair, zigzag, or chiral pattern. SWCNT are mostly produced in a bundle and then are separated by chemical or physical methods.

**MWCNTs** are stacks of graphene sheets rolled up into concentric cylindrical structures. Their diameter is in the range of 10 – 50 nm and length can be up to or

more than 10  $\mu\text{m}$ . The individual graphene sheets are separated by about 0.34 nm.

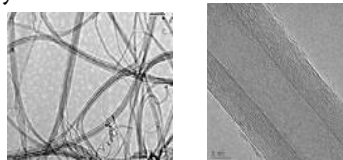


**Figure 1.** Single Walled (Left) and Multi Walled (right) Carbon Nanotube.

Whenever one thinks about loading any material to Carbon Nano tubes (CNTs), the thought that comes into the mind that (i) is it filling the lumen with the desired material or (ii) chemically attaching them onto the surface of the CNT.

Filling CNTs with metal like materials are easy as it can be done during the synthesis of CNT. However unloading them still remains a bigger task, as it is difficult to push out something from the 2-3 nm diameter lumen. Moreover, drugs are often temperature sensitive, hence their loading at higher temperature, at which CNT synthesis takes place is not possible.

So far as the attachment to the CNT surface is concerned, there are many possibilities (a) adsorbing

them on to the surface (b) attaching them to dangling bonds or (c) attaching through a linker or functionalized molecule.

Scientists have tried all such methods. Some of them are mentioned below.

Small drug molecules can be **covalently conjugated** to CNTs for *In vitro* delivery. Fluorescent dyes and drug cargoes were simultaneously linked to 1,3-dipolar cycloaddition functionalized CNTs via amide bonds for the delivery of an anti-cancer drug (Pastorin *et al* 2006) or an antifungal drug (Wiecowski *et al* 2005) into cells. Feazell and Lippard used non-covalently PEGylated SWNTs as a longboat delivery system to internalize a platinum (IV) complex, a pro-drug of the cytotoxic platinum (II), into cancer cells. The inert platinum (IV) pro-drug compounds developed by the Lippard's group are activated only after being reduced to the active platinum (II) form. SWNTs tethered with the platinum (IV) complexes through peptide linkages are taken into cancer cells by endocytosis and reside in cell endosomes, where reduced pH induces reductive release of the platinum (II) core complex, thus killing the cancer cells. The cytotoxicity of the platinum (IV) complex increases over 100-fold after attachment to SWNTs. They have also conjugated paclitaxel, a commonly used anti-cancer drug, to branched PEG-coated SWNTs via a cleavable ester bond (Liu *et al* 2008). The SWNT-PTX conjugate was tested both *In vitro* and *in vivo*.

**Noncovalent conjugation;** beside covalent conjugation, novel noncovalent supramolecular chemistry for loading aromatic drug molecules onto functionalized SWNTs by  $\pi - \pi$  stacking has been uncovered by (Liu *et al* 2007). Doxorubicin, a commonly used cancer chemotherapy drug, can be loaded on the surface of PEGylated SWNTs with remarkably high loading, up to 4 g of drug per 1 g of nanotube, owing to the ultrahigh surface area of SWNTs. The loading/binding is pH dependent and favorable for drug release in endosomes and lysosomes, as well as in tumor micro-

environments with acidic pH. Similar drug loading behaviors have been reported for MWNTs (Ali Boucetta *et al* 2008), single-walled carbon nanohorns (Murakami *et al* 2006) and nano-graphene oxide (Sun *et al* 2008 and Liu *et al* 2008). The supramolecular approach of drug loading on CNTs opens new opportunities for drug delivery.

**$\pi - \pi$  stacking,** for the delivery of aromatic drugs such as doxorubicin, which are directly loaded on the nanotube surface via  $\pi - \pi$  stacking, the functional groups on the SWNT coating molecules (e.g., PL PEG amine) can be conjugated with targeting molecules such as Arg – Gly – Asp (RGD) peptide for targeted delivery (Liu *et al* 2007).

**Encapsulation of drug molecules inside nanotubes;** apart from drug conjugation and loading on the external surfaces of nanotubes, the lumen of CNTs may allow the encapsulation of drug molecules inside nanotubes for drug delivery. Fullerene balls (Kataura *et al* 2001), metal ions (Jeong *et al* 2003), small compounds such as metallocenes (Li *et al* 2005), and even DNA molecules (Kaneko *et al* 2007) have been encapsulated inside CNTs. Although a number of theoretical modeling studies predicted the insertion of biomolecules including chemotherapy drugs (Hilder *et al* 2007 and Hilder *et al* 2008) into CNTs, drug delivery by encapsulation of drugs inside CNTs has been rarely reported. Further experimental studies are still needed to examine the possibility of utilizing the encapsulation strategy in CNT-based drug delivery.

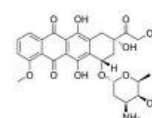
## II. METHODS AND MATERIAL

### Loading Doxorubicin on functionalized CNT

#### Drug Used:

#### **Doxorubicin**

- Structure:
- Molecular formula:  $C_{27}H_{29}NO_{11}$ .
- Mol. Wt. : 579.99
- M.P.: 204°C



- Appearance: Orange red crystalline Powder, hygroscopic
- Solubility: Soluble in water, slightly soluble in methanol.
- Storage: In air tight container

10 mg of f-MWCNT was suspended in 25ml of 0.2 mg/ml concentration of Doxorubicin in three different pH buffer solutions and kept overnight.

Calibration graph was plotted using the absorbance of 6 different dilutions of Doxorubicin (10, 20, 30, 40, 50 & 60 ppm) solutions.  $\lambda$  max was determined by scanning 0.05mg/ml solution of Doxorubicin from 400 to 580 nm using Spectrophotometer 169 of Systronics make.

To know whether Doxorubicin is loaded on f-MWCNT, FTIR, ATR and TEM was done.

Surface adsorption study was done by plotting a Calibration graph using 5 different concentrations of Doxorubicin (100,200,300,400,500 ppm) solutions.

5mg of f-MWCNT was added to 10ml of each concentration and absorbance of supernatant was taken after 24 hrs.

Graph of amount adsorbed Vs concentration of Doxorubicin was plotted and type of adsorption of drug on to the Carbon nano tubes was studied.

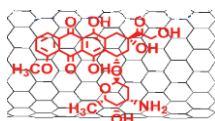


**Figure 2.** Schematic diagram of Doxorubicin loaded on to the CNT surface

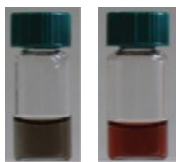


**Figure 3.** (Left) CNT in water and (Right) CNT + Doxorubicin in water

The loading capacity of Doxorubicin on CNT was determined by UV visible spectroscopy at 490 nm,

which was calculated by the difference of Doxorubicin concentrations between the original Doxorubicin solution and the supernatant solution after loading.

CNT shows distinctly different loading capacity toward Doxorubicin at different pH values.

**Table 1.** Effect of pH on loading of Doxorubicin on F-MWCNT as recorded at 490 nm by measuring remaining amount of Doxorubicin in water (the amount of Doxorubicin was calculated using standard calibration graph)

pH	Absorbance At 490 nm	mg/ml Doxorubicin remaining in water	Concn loaded (0.2-Concn) (mg/ml)	Amount loaded (mg)	% loading
4	0.152	0.045	0.155	3.87	77.5
7	0.121	0.036	0.164	4.10	82
9	0.140	0.0415	0.1585	3.96	79.25

To know Doxorubicin is loaded on f-MWCNT, FTIR, ATR and TEM was done

**FTIRs**

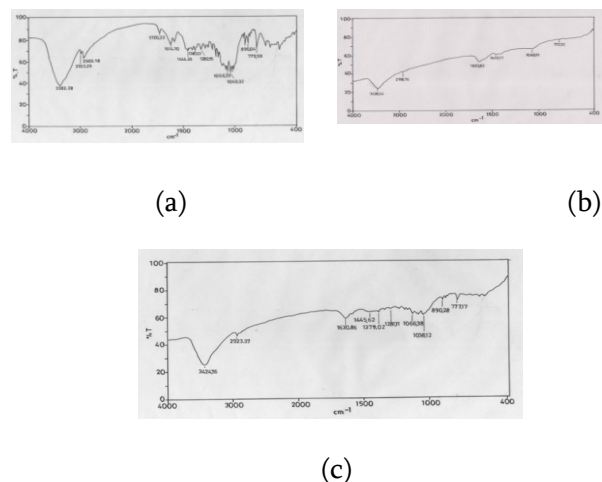


**Figure 4.** FTIR of (a) Doxorubicin and (b) f-CNT (c) f-CNT loaded with Doxorubicin



### ATRs

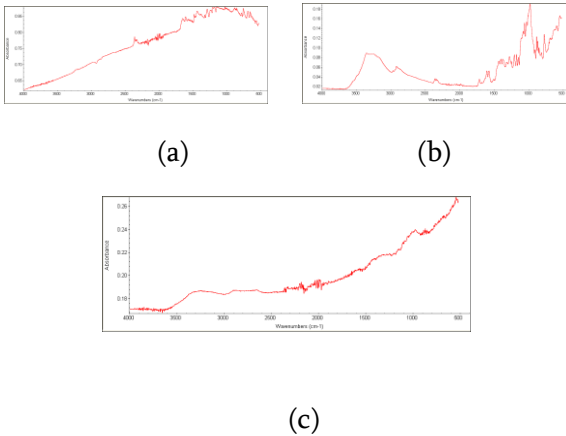


**Figure 5.** ATRs of (a) f-CNT (b) Doxorubicin (c) Doxorubicin loaded on F-MWNT

### TEM

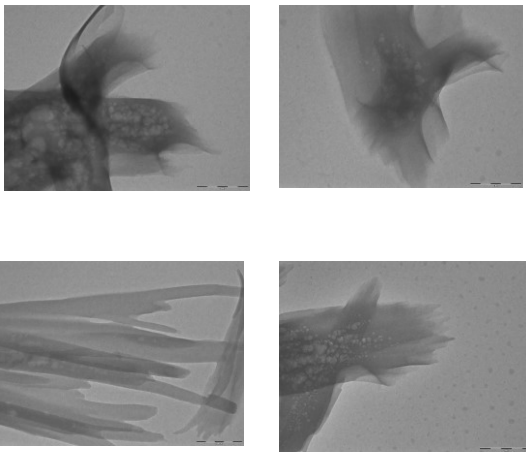


**Figure 6.** TEM of Doxorubicin

TEM of Doxorubicin shows that it cannot withstand high electron volt of transmission electron microscopy, as the images reveals that the drug degrades on the exposure of high electron volt. Therefore it was difficult to locate the drug on CNT by TEM.



**Figure 7.** TEM of Doxorubicin on CNT

## III. RESULTS AND DISCUSSION

FTIR of drug loaded on F-MWNT reveals the following facts:

- Peak at  $1630.86\text{ cm}^{-1}$  in FTIR of MWNT loaded with Doxorubicin is shifted from  $1633.82\text{ cm}^{-1}$  in FTIR of MWNT is due to the change in the environment of C=O group.
- Peak at  $1066.39\text{ cm}^{-1}$  in FTIR of Doxorubicin is due to C-O stretching of ether group which is also seen in the in FTIR of MWNT loaded with drug (peak at  $1066.38\text{ cm}^{-1}$ ).
- Peak at  $2923\text{ cm}^{-1}$  is due to C-H stretching.

ATR (Attenuated total reflection) of F-MWNT loaded with drug shows a broad peak at  $3000\text{-}3500\text{ cm}^{-1}$  which is also seen in the ATR of Doxorubicin. This further proves the loading of drug onto the MWNT. TEM of MWNT also shows the loading of drug, Doxorubicin onto the nanotube.

The FTIR spectra of CNT, Doxorubicin (Doxo), and CNT-Doxo nano hybrid show the following evidences. The peak at  $1633.82\text{ cm}^{-1}$  corresponding to  $\nu(\text{C}=\text{O})$  in the spectrum of CNT and the C=O peak ( $1720.23\text{ cm}^{-1}$ ) for Doxo shift to a lower position at  $1630.36\text{ cm}^{-1}$  after forming CNT- Doxo nano hybrid. This also indicates that Doxo be loaded onto CNT and the shift of characteristic peaks may be due to the hydrogen bonding between these two components. The -OH and -COOH groups on the CNT can form a strong hydrogen-bond with -OH and -NH<sub>2</sub> groups in Doxo. Therefore, Doxo was non-covalently loaded on CNT simply by mixing them in aqueous solution with the aid of slight sonication.

The highest loading capacity is observed at the neutral condition, rather than acidic or basic conditions. The pH-dependent loading may be due to the different degree of hydrogen-bonding interaction between these two species under different pH conditions. -COOH of CNT and the

-OH of Doxo, -COOH of CNT and the -NH<sub>2</sub> of Doxo, -OH of CNT and the -OH of Doxo, and -OH of CNT and the -NH<sub>2</sub> of Doxo (Table 2). Under acidic conditions, -NH<sub>2</sub> of Doxo forms -NH<sub>3</sub><sup>+</sup> with H<sup>+</sup> and therefore cannot participate in hydrogen bonding. In this case, two kinds of hydrogen bonding can occur between -COOH of CNT and the -OH of Doxo, and -OH of CNT and the -OH of Doxo. Furthermore, the H<sup>+</sup> in solution would compete with the hydrogen-bond-forming groups and then weaken the above hydrogen-bonding interaction. Under basic conditions, -COOH of CNT exists as -COO<sup>-</sup> and cannot form a hydrogen bond with -OH or -NH<sub>2</sub> groups of Doxo. Two kinds of hydrogen bonding interaction can occur between -OH of CNT and the -OH of Doxo, and -OH of CNT and the -NH<sub>2</sub> of Doxo. Therefore, the strongest hydrogen-bonding interaction between CNT and Doxo is expected under neutral conditions, and the highest loading of Doxo on CNT is obtained.

**Table 2.** Groups That Can Form Hydrogen Bonds with CNT and Doxo at Different pH Conditions

pH conditions	CNT	Doxo
Acidic	-OH, -COOH	-OH,
Neutral	-OH, -COOH	-OH, -NH <sub>2</sub>
Basic	-OH	-OH, -NH <sub>2</sub>

#### ADSORPTION STUDY:

To know how many layers of Doxorubicin has been loaded on to CNT, graph of different concentrations of Doxorubicin against amount of doxorubicin adsorbed was plotted.

**Table 3.** Amount of Doxorubicin loaded on CNT at different concentrations.

Concn + 5 mg CNT	Absorbance	Corr. Concn (mg/ml)	Concn Adsorbed	Amount adsorbed (mg)
100	0.098	0.025	0.075	0.75
200	0.233	0.070	0.130	1.30
300	0.418	0.125	0.175	1.75
400	0.577	0.170	0.230	2.30
500	0.590	0.175	0.325	3.25

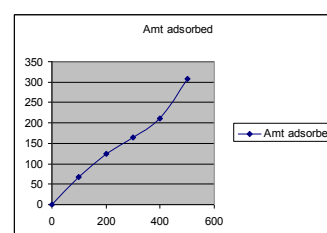


**Figure 8.** Graph of amount of Doxorubicin adsorbed Vs Different Concentration

The nature of graph shows adsorption of drug is multilayered adsorption which may be possible due to interactions within doxorubicin molecules also.

#### IV. CONCLUSION

With the advent of nanomaterials; interdisciplinary research has taken a big leap. The present work was a small effort to enter in this magnificent field of science having immense possibilities.

It was envisaged that the attachment of drug to the CNT surface could be by

- (a) getting adsorbed to the surface
- (b) or attached to the dangling bonds of CNT or
- (c) may be by attaching through a linker or functionalized molecule.

FTIR of functionalized CNT showed the introduction of -COOH and -OH group on the surface of CNT; which was thought to be suitable for Doxorubicin attachment by non-covalent bonding.

pH was considered as important parameters for **Loading of Doxorubicin** and UV-VIS Spectroscopy, ATR, FTIR and TEM assessment was chosen as the method for assessing the loading.

When Doxorubicin was added to f-MWCNT suspended in water a change in color from black (of CNT) to orange red was noticed, this was due to the Doxorubicin. After attachment procedure, the Doxorubicin remaining in the solution was assessed by UV-VIS spectrum taken at 490 nm was taken, which revealed that loading occurred at all the 3 tested pH viz. 4, 7 and 9 maximum being at neutral pH of 7 (i.e. 82%) and minimum at pH 4 (i.e. 77.5%). The pH-dependent loading may be due to the different degree of hydrogen-bonding interaction between these two species under different pH conditions.

Both ATR and FTIR spectra indicated the loading of Doxorubicin onto CNT. Moreover, the shift of characteristic peaks that appeared in FTIR spectrum suggested it to be due to the hydrogen bonding between these two components. The -OH and -COOH groups on the CNT can form a strong hydrogen-bond with -OH and -NH<sub>2</sub> groups in Doxorubicin. Therefore, it can be concluded that Doxorubicin was non-covalently loaded on CNT simply by mixing them in aqueous solution with the aid of sonication.

TEM Analysis of Doxorubicin Loaded on CNT was not a suitable technique because during TE Micrography of Doxorubicin showed deterioration of drug molecule due to electron beams of TEM were bombarded on to them. While taking the TEM micrograph, the structure started to bubble and eventually bursted.

To find out whether adsorption of Doxorubicin on to MWCNT was single layered or multi-layered due to possible interactions within Doxorubicin molecules, Langmuir adsorption isotherm graph was plotted, which showed that adsorption of drug is Multi-layered.

## V. REFERENCES

1. Pastorin G.; Wu.; Wieckowski, S.; Briand, J. P.; Kostarelos, K.; Prato, M.; Bianco, A. *Chem. Commun.* 2006, 1182-1184.
2. Wieckowski, S.; Pastiorin G.; Benincasa, M.; Klumpp, C.; Briand, J. P.; Gennaro, R.; Prato, M.; Bianco A.; *Angew. Chem. Int. Ed.* 2005, 44, 6358-6362.
3. Liu, Z.; Robinson, J. T. Sun, X.M.; Dai, H. J. *J. Am. Chem. Soc.* 2008, 130, 10876-10877.
4. Liu, Z.; Sun, X.; Nakayama, N.; Dai, H. *Supramolecular chemistry on water- soluble carbon nanotubes for drug loading and delivery.* *ACS Nano* 2007, 1, 50- 56.
5. Ali- Boucetta, H.; Al Jamal. K. T.; McCarthy, D.; Prato, M.; Bianco, A.; Kostarelos, K.; *Chem. Commun.* 2008, 459-461.
6. Murakani, T.; Fan, J.; Yudasaka, M.; Iijima, S.; Shiba, K.; *Mol. Pharmaceutics* 2006, 3, 407-414.
7. Sun, X.; Liu, Z.; Welsher, K.; Robinson, J. T.; Goodwin, A.; Zaric, S.; Dai, H. *Nano Res.* 2008, 1, 203-212.
8. Kataura, H.; Maniwa, Y.; Kodama, T.; Kikuchi, K.; Hirahara, K.; Suenga, K.; Iijima, S.; Suzui, S.; Achiba, Y.; Kratschmer, W. *Synth. Met.* 2001, 121, 1195-1196.
9. Jeong, G. H.; Farajian, A. A.; Hatakeyama, R.; Hirata, T.; Yaguchi, T.; Tohji, K.; Mizuseki, H.; Kawazoe, Y. *Phys. Rev. B* 2003, 68, 075410.
10. Li, L. J.; Khlobystov, A. N.; Wiltshire, J. G.; Briggs, G. A. D.; Nicholas, R. J. *Nat. Mater.* 2005, 4, 481-485.
11. Kaneko, T.; Okada, T.; Hatakeyama, R. *Contrib. Plasma Phys.* 2007, 47, 57-63.
12. Hilder, T. A.; Hill, J. M. *Micro Nano Lett.* 2008, 3, 41-49.
13. Hilder, T. A.; Hill, J. M. *Nanotechnology* 2007, 18, 275704

# GC-MS Analysis of *Luffa cylindrica* (L.) M.Roem. Vegetable Peel

Shivani Kakkar\*<sup>1</sup>, Annika Durve Gupta<sup>2</sup> and Meeta Bhot<sup>3</sup>

\*<sup>1</sup>Shivani Kakkar, Department of Biotechnology, Birla College, Kalyan, Maharashtra, India

<sup>2</sup>Annika Durve Gupta, Department of Biotechnology, Birla College, Kalyan, Maharashtra, India

<sup>3</sup>Meeta Bhot, Associate Professor, Department of Botany, Birla College, Kalyan, Maharashtra, India

## ABSTRACT

India is second major producer of fruits and vegetables in the world. Fruits and vegetables form the rich source of bioactive molecules. Due to the high consumption of vegetables and fruits, peel waste are generated in large quantities. Peel waste is a serious problem to processing industries and pollution monitoring agencies. Waste utilization is the one of the important and challengeable job around the world. The effect of resources depletion and environmental concerns have triggered new regulations and growing awareness throughout the world, thus promoting use of more and more fruit and vegetable waste to obtain by-products with health benefits. Thus, in present study an attempt was made to bring utilization of peel of *Luffa cylindrica* (L.) M.Roem. The aim of the study was to investigate the presence of different compounds from the methanolic extract of *Luffa cylindrica* (L.) M.Roem. peel by GC-MS method. 14 bioactive compounds were identified in the methanolic peel extract of *Luffa cylindrica* (L.) M.Roem. The identification of phytochemical compounds is based on the peak area, retention time molecular weight and molecular formula. Various bioactive compounds identified were found to possess biological and pharmacological activity such as antimicrobial, antifungal, anticancer, antioxidant properties. Recycling of fruit and vegetable waste is one of the most important means of utilizing it in a number of innovative ways yielding new products.

**Keywords:** *Luffa cylindrica* (L.) M.Roem. peel and GC-MS analysis

## I. INTRODUCTION

“Let food be thy medicine and medicine be thy food” was the famous dictum proclaimed by Hippocrates about 2500 years ago. Recently many scientific studies supported the above fact. It appears that diet containing some phytochemicals also termed as bioactive molecules, can provide protection against various chronic diseases like cancer, atherosclerosis, thrombosis, etc and also impart other health benefits (Wildman, 2001). Food of plant origin is capable of contributing appreciable quantities of nutrients, including proteins needed by both children and adults (Okaka *et al.*, 2002). Fruits and vegetables form the rich source of bioactive molecules. Over 10,000 bioactive phytochemicals have been identified in

different fruits and vegetables which are integral part of the human diet (Wise, 2001).

India is the second major producer of fruits and vegetables in the world. It contributes 10% of world fruit production. According to India Agricultural Research Data Book 2004, the total waste generated from fruits and vegetables comes to 50 million tons per annum (Uchakalwar *et al.*, 2014).

Due to the high consumption of vegetables and fruits, peel waste are generated in large quantities in big cities. Peel waste which are highly perishable and seasonal, is a problem to the processing industries and pollution monitoring agencies (Chacko *et al.*, 2014). These wastes if not disposed correctly are seen to

cause serious environmental problems such as water pollution, unpleasant odors, explosions and combustion and greenhouse gas emissions (Roy *et al.*, 2014). Thus, in the present study an attempt has been made to bring about the utilization of the vegetable peel waste for mankind.

## II. MATERIAL AND METHODS

### Collection of sample

The vegetable of *Luffa cylindrica* (L.) M.Roem. used in the present study was collected from the local market of Kalyan. It was identified from the Department of Botany, Agharkar Institute, Pune. The peels were washed properly under running tap water to remove dust particles. The peels were then shade dried for 5 days and once the moisture was reduced the peels were then completely dried in an oven at 50°C. The dried peels were then powdered using grinder and stored in air tight bottles.

### Preparation of sample for GC-MS study

About 5 grams of the peel powder of *Luffa cylindrica* (L.) M.Roem. was soaked in 50 ml methanol. Extraction was done in orbital shaker at 100 rpm (25°C) for 24 hours, followed by filtering of the extract using Whatman filter paper No.1. The residue was removed and supernatant was used for further analysis.

### GC-MS analysis

The dried peel powder of *Luffa cylindrica* (L.) M.Roem. was analyzed using GC-MS (Shimadzu capillary GC-quadrupole MS system QP 5000). The sample was injected into the GC-MS on a 30 m glass capillary column with a film thickness of 0.25 µm (30 m × 0.25 mm) with helium as carrier gas at 1 ml/min

constant flow mode. GC temperature programme was 50°C - 300°C at 10°C/min. The mass spectra were recorded in electron ionization mode at 50 eV.

## III. RESULT AND DISCUSSION

### GC-MS analysis of methanolic extract of *Luffa cylindrica* (L.) M.Roem. peel

Gas Chromatography and Mass spectroscopy analysis results of methanolic peel extract of *Luffa cylindrica* (L.) M.Roem. are shown in Table-1. GC-MS analysis of methanolic peel extract of *Luffa cylindrica* (L.) M.Roem. revealed the presence of 14 bioactive compounds. The identification of phytochemical compounds is based on the peak area, retention time molecular weight and molecular formula.

In the present investigation a variety of compounds have been detected including D-Limonene (8.81), 1-Hexadecanol (3.38), Stearic acid (0.48), 1-Monolinoleoylglycerol trimethylsilyl ether (1.12), Spirost-8-en-11-one (1.97), Glucopyranoside (1.24), 7-methyl-z-teradecen-1-ol acetate (0.59), 9,10-Secocholestra-5,7,10 (19)-triene-1,3-diol (1.75), Ethyl iso-allocholate (0.28), Cis-11-Eicosenoic acid (1.04), Estra-1,3,5 (10)- trien-17-ol (0.38), Pentadecanoic acid (8.43), Oleic acid (0.64) and Heptadecanoic acid (2.69) with retention time 6.47, 7.22, 7.48, 9.19, 9.87, 10.25, 10.99, 11.25, 11.98, 12.57, 12.70, 14.32, 15.39 and 15.64 respectively. Irrespective of the amount or concentration (high or low) in which these compounds were found to be present, almost all these compounds have been reported to possess some pharmacological or the other biological activity.

**Table 1.** GC MS analysis of methanolic extract of *Luffa cylindrica* (L.) M.Roem. vegetable peel

Sr. No.	Name of Compound	RT (min)	Area (%)	Formula	Molecular weight
1.	D-Limonene	6.47	8.81	C <sub>10</sub> H <sub>16</sub>	136
2.	1-Hexadecanol	7.22	3.38	C <sub>17</sub> H <sub>36</sub> O	256
3.	Stearic acid, 2-hydroxy-1-methylpropyl ester, 2-Hydroxy-1-methylpropyl stearate	7.48	0.48	C <sub>22</sub> H <sub>44</sub> O <sub>3</sub>	356

4.	1-Monolinoleoylglycerol trimethylsilyl ether	9.19	1.12	$C_{27}H_{54}O_4Si_2$	498
5.	Spirost-8-en-11-one	9.87	1.97	$C_{27}H_{40}O_4$	428
6.	Glucopyranoside	10.25	1.24	$C_{18}H_{32}O_{16}$	504
7.	7-methyl-z-teradecen-1-ol acetate	10.99	0.59	$C_{17}H_{32}O_2$	268
8.	9,10-Secocholestra-5,7,10 (19)-triene-1,3-diol	11.25	1.75	$C_{30}H_{52}O_3Si$	488
9.	Ethyl iso-allocholate	11.98	0.28	$C_{26}H_{44}O_5$	436
10.	Cis-11-Eicosenoic acid	12.57	1.04	$C_{20}H_{38}O_2$	310
11.	Estra-1,3,5 (10)- trien-17-ol	12.70	0.38	$C_{18}H_{24}O$	256
12.	Pentadecanoic acid	14.32	8.43	$C_{17}H_{34}O_2$	270
13.	Oleic acid	15.39	0.64	$C_{19}H_{36}O_2$	298
14.	Heptadecanoic acid	15.64	2.69	$C_{19}H_{38}O_2$	298

**Figure 1.** Mass spectrum of different compounds identified in methanolic extract of *Luffa cylindrica* (L.) M.Roem. vegetable peel by GC-MS analysis

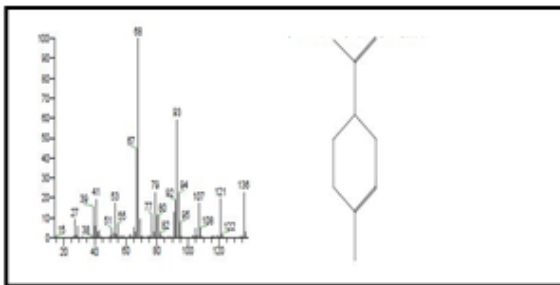


**Figure 1.1.** GC MS Spectrum of D-Limonene

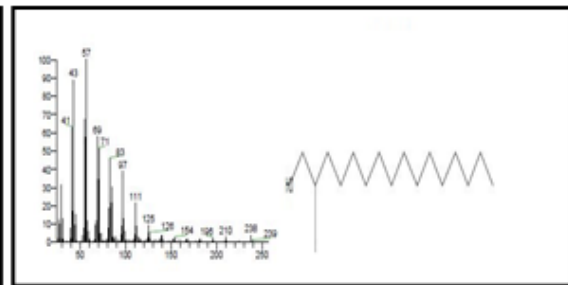


**Figure 1.2.** GC MS Spectrum of 1-Hexadecanol

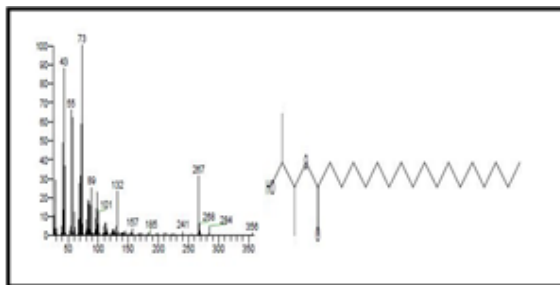


**Figure 1.3.** GC MS Spectrum of Stearic acid

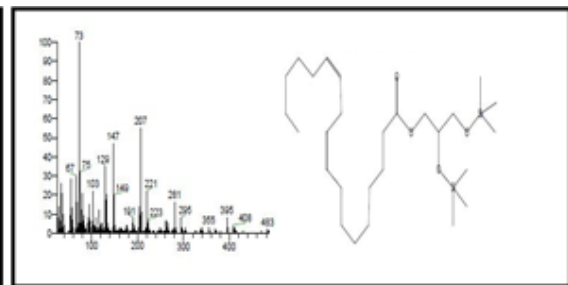


**Figure 1.4.** GC MS Spectrum of 1-Monolinoleoylglycerol trimethylsilyl ether

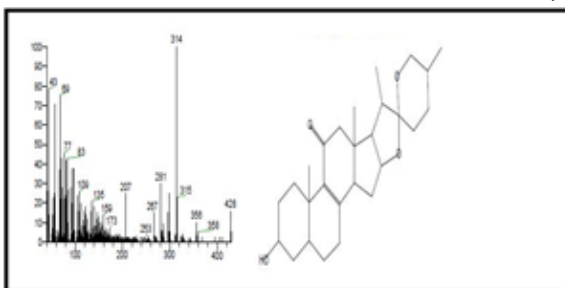


**Figure 1.5.** GC MS Spectrum of Spirost-8-en-11-one

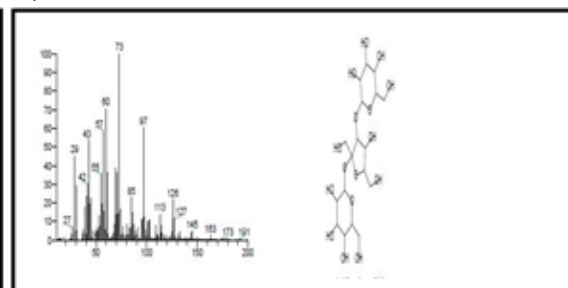


**Figure 1.6.** GC MS Spectrum of Glucopyranoside

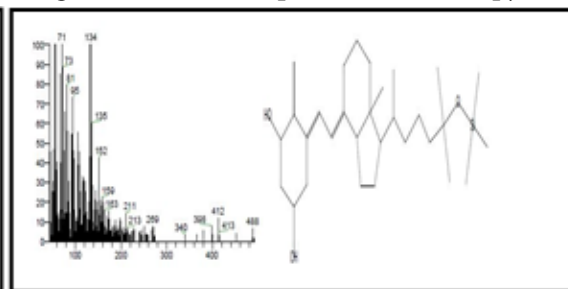
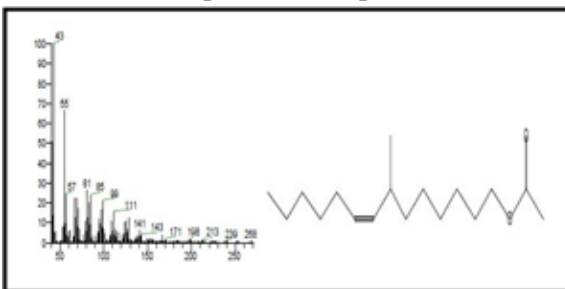


**Figure 1.7.** GC MS Spectrum of 7-methyl-z-teradecen-1-ol acetate **Figure 1.8.** GC MS Spectrum of 9,10-Secocholestra-5,7,10 (19)-triene-1,3-diol

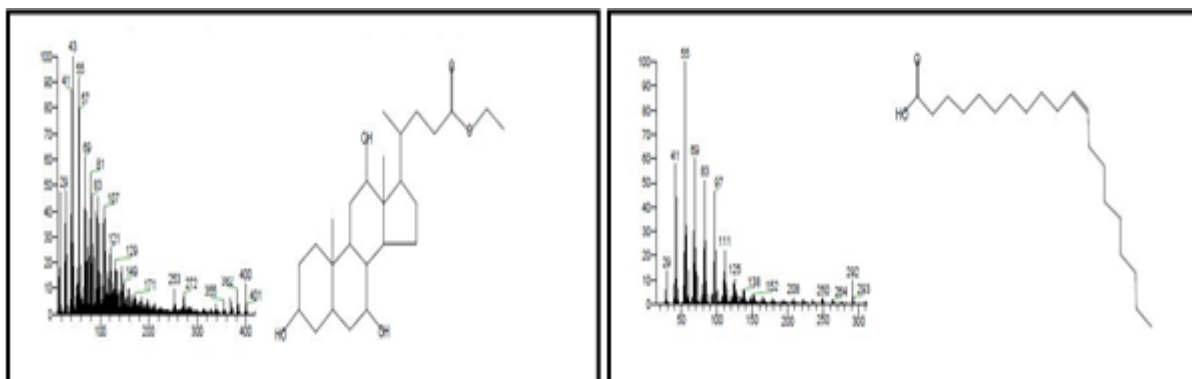


**Figure 1.9.** GC MS Spectrum of Ethyl iso-allochoolate **Figure 1.10.** GC MS Spectrum of Cis-11-Eicosenoic acid

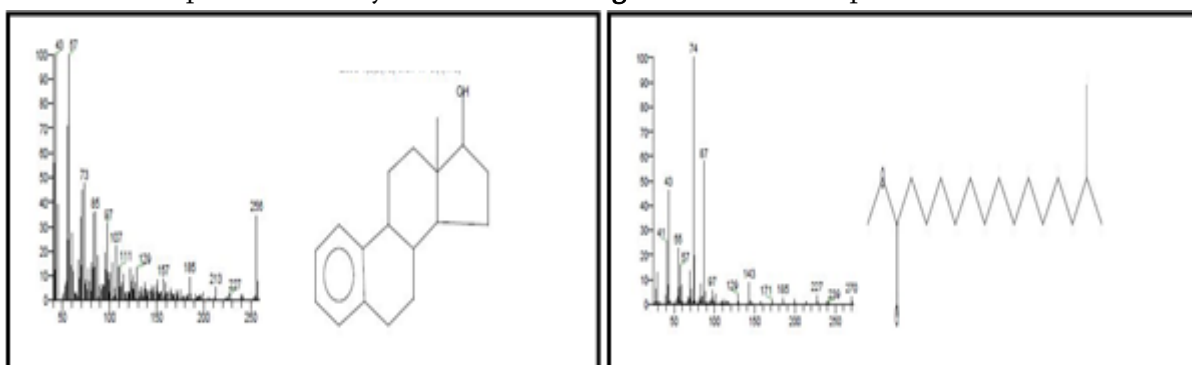


**Figure 1.11.** GC MS Spectrum of Estra-1,3,5 (10)- trien-17-ol **Figure 1.12.**GC MS Spectrum of Pentadecanoic acid

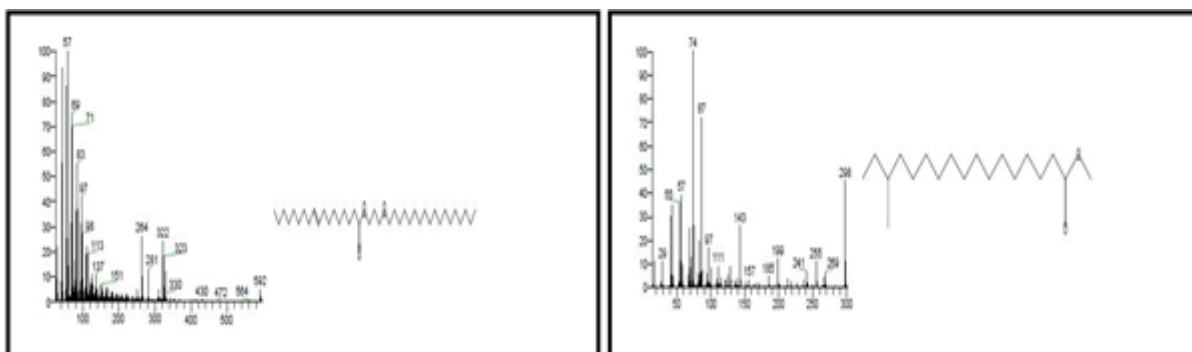


**Figure 1.13.** GC MS Spectrum of Oleic acid **Figure 1.14.** GC MS Spectrum of Heptadecanoic acid

#### IV. CONCLUSION

Recycling of fruit and vegetable waste is one of the most important means of utilizing it in a number of innovative ways yielding new products. The secondary metabolites (phytochemicals) and other chemical constituents of medicinal plants account for their medicinal value. Thus, the GC-MS analysis of methanolic extract of *Luffacylindrica*(L.) M.Roem. peel showed a highly complex profile, containing 14

bioactive constituents. This study further may be useful to explore the pharmacological and biosynthetic activity of the peel.

#### V. ACKNOWLEDGMENT

Authors are thankful to Department of Biotechnology, Birla College, Kalyan for providing the laboratory facilities.

## VI. REFERENCES

- [1] **Chacko C. and Estherlydia D.** (2014). Antimicrobial evaluation of jams made from indigenous fruit peels. *International Journal of Advanced Research*, **2(1)**: 202-207.
- [2] **Okaka JC, Akobundu ENT and Okaka ANC,** (2002). Human nutrition: An Integrated Approach. 2<sup>ed</sup>. OCJANCO Academic Publishers, Enugu, 312-320.
- [3] **Roy S. and Lingampeta P.** (2014). Solid wastes of fruits peels as source of low cost broad spectrum natural antimicrobial compounds furanone, furfural and benzenetriol. *International Journal of Research in Engineering and Technology*, **3(7)**: 273-279.
- [4] **Uchakalwar P. and Chandak A.** (2014). Production of Single Cell Protein from fruits waste by using *Saccharomyces cerevisiae*. *International Journal of Advanced Biotechnology and Research*, **5(4)**:770-776.
- [5] **Wildman, R.E.C.** (2001). Classifying nutraceuticals. In Handbook of nutraceuticals and functional foods (Edn. Wolinsky, Hickson and J.F. Jr., I). CRC press LLC.
- [6] **Wise, J.A.,** (2001). Health benefits of fruits and vegetables: the protective role of phytonutrients, in Vegetables, Fruits, and Herbs in health promotion Watson, R.R., Ed. CRC press, London, pp 147-176.



# Structural, Vibrational and Thermal Analysis of L-arginine Potassium Sulphate (LAKS) Crystal Having NLO Response

Smita S. Patil\*, Mahendra M. Khandpekar

\*<sup>1</sup>Department of Physics, Smt. Chandibai Himathmal Mansukhani College, Ulhasnagar-3, Dist-Thane, Maharashtra, India

<sup>2</sup>Material Research Laboratory, Department of Physics, Birla College, Kalyan, Maharashtra, India

## ABSTRACT

A new non-linear optical potassium sulphate crystal (LAKS) has been grown from aqueous solution by the slow evaporation technique at room temperature. Orthorhombic structure has been estimated as per XRD studies. CHNS, SEM and EDAX analysis were carried out for determining the chemical composition and surface morphology. Vibrational characterization, thermal studies and linear and non-linear optical studies were also done.

**Keywords:** Crystal Growth, Xrd, Vibrational, Thermal And Non-Linear

## I. INTRODUCTION

Among the 20 essential fundamental amino acids, L-arginine ( $C_6H_{14}N_4O_2$ ) is widely distributed in biological substances. The  $\alpha$ -carbon atom is attached with four groups, viz.; amino group, carboxyl group, guanidino group and hydrogen atom. Since all the carbon atoms in the L-arginine molecule are optically active, its related compounds are mostly non-centrosymmetric and exhibit second harmonic generation property. The long, linear carbon chain incorporates the character of flexibility in the l-arginine molecule. It has a catenarian structure at two ends of which carboxyl and guanidyl group form a dipole moment of about  $2.4 \times 10^{-8}$  esu. Thus l-arginine is a polar amino acid with positive guanidine group. Due to the highly basic nature of guanidine group l-arginine forms a number of salts with organic and inorganic acids viz L-arginine phosphate monohydrate, L-arginine diphosphate, L-arginine perchlorate, L-arginine nitrate, L-arginine maleate dihydrate, L-arginine formate, L-arginine acetate, L-arginine

oxalate, L-arginine fluoride [1] which are interesting NLO materials.

Present work reports the growth and characterization studies of L-arginine Potassium Sulphate (LAKS) crystals synthesized for first time in our laboratory.

## II. METHODS AND MATERIAL

AR grade L-arginine ( $C_6H_{14}N_4O_2$ ) and Potassium sulphate ( $K_2SO_4$ ) was used for the synthesis of L-arginine potassium sulphate (LAKS) crystals in the ratio 3:1. The crystals were obtained from aqueous solution (volume=200ml and pH=8.5) by slow evaporation method at room temperature ( $28^\circ C$ ). Optically good quality crystals of dimension 0.8 cm x 0.6 cm x 0.1cm were collected from the gel-like solution in about eight weeks of time (figure 1).



**Figure 1.** LAKS crystal

Since L-arginine is rich in nutrients, microbes formation is frequent during the growth of L-arginine crystals [2]. In our case the fungus formation may have been avoided as the solution was preheated to about 35°C and also the presence of sulphur in the compound may have further helped in this direction. For structure determination the crystal was subjected to powder x-ray diffraction using Panalytical Xpert MPO PRO which is highly sophisticated X-ray diffractometer system with characteristic CuK- $\alpha$  radiation ( $\lambda=1.5410\text{\AA}$ ). All the major reflection lines in the XRD spectra were indexed and the unit cell parameters were calculated using the computer program POWD-interactive powder diffraction data interpretation and indexing software program. Version 2.2 (Australia). The chemical composition of the LAKS crystal was determined by CHNS analyzer (THERMO FINNIGAN, FLASH EA 1112 series). SEM and EDAX analysis was done with a scanning electron microscope (ZEISS Ultra FESEM). For identifying the various functional groups present in the grown crystals FTIR and FT-Raman spectroscopic studies were carried out. FTIR spectra were recorded in the range 4000 - 400 $\text{cm}^{-1}$  using a Nicolet MAGMA<sub>550</sub> FTIR spectrometer with reference to a potassium bromide pellet. FT-Raman spectra were recorded in the spectral range 4000 - 100 $\text{cm}^{-1}$  using BRUKER RFS<sub>27</sub> stand alone FT-Raman spectrometer. The laser source used was ND: YAG 1054nm. Thermogravimetric analysis(TGA) and Differential thermal analysis(DTA) was carried out simultaneously for determining the thermal stability of the material in the temperature range 50 - 500°C in air atmosphere at a heating rate 10° C per min. The instrument used was PERKIN ELMER, DIAMOND TG/DTA thermal analyzer.

Linear optical properties of the grown crystals were studied using a Perkin Elmer model No.Lamda35 UV-Vis Spectrophotometer in the range 200nm - 1100nm. To confirm the non-linear optical property Kurtz powder SHG test was performed on the grown crystal.

### III. RESULTS AND DISCUSSION

#### X-ray diffraction studies

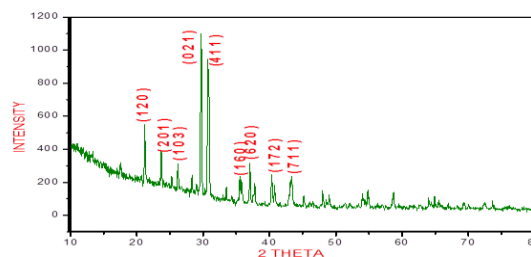


**Figure 2.** XRD of LAKS crystal

Powder XRD studies of grown LAKS crystal confirms the single phase formation with orthorhombic symmetry. The estimated crystal parameter are  $a=17.614\text{\AA}$ ,  $b=8.661\text{\AA}$ ,  $c=4.183\text{\AA}$  with unit cell volume= $632.87\text{\AA}^3$ . The intense xrd peak were recorded at 29.70° C with maximum intensity of 1107 on (0 2 1) plane (figure 2).

#### CHNS, SEM and EDAX Analysis

The chemical composition of the synthesized crystal was determined by CHNS analysis. The approximate empirical formula is thus established as  $\text{C}_3\text{H}_{10}\text{N}_4\cdot\text{K}_2\text{SO}_4$  for the crystal. SEM images of figure 3 shows layers with formation of crystallites sprinkled over the surface layers. Voids are clearly visible making the surface uneven. Crystalline formations of aggregates have been noted. EDAX spectrum shows peaks for potassium, oxygen and sulphur, suggesting thereby that the potassium sulphate has formed salt with l-arginine.

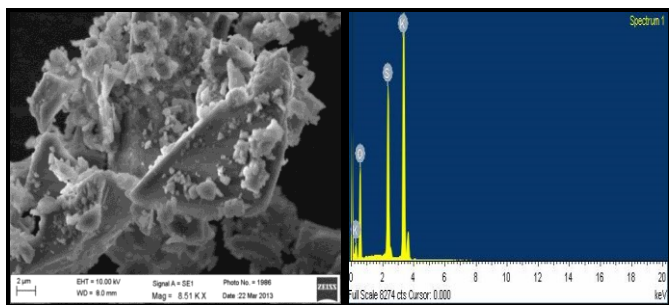


**Figure 3.** SEM and EDAX analysis of LAKS crystal

### FT-IR and FT-Raman Analysis

An attempt has been made to correlate the IR and Raman peaks and discuss the vibrational spectra of LAKS system (figure 4). It reveals that in the crystalline state, the l-arginine molecule is deprotonated at the carboxyl group ( $1605.22\text{cm}^{-1}$ ) [1, 3 4] and protonated at the guanidyl and amino groups ( $1682.56\text{cm}^{-1}$ ) [5,6]. An extensive system of hydrogen bonding extends throughout the molecule leads to deformation of stretching frequencies of  $\text{NH}_3^+$  and  $\text{COO}^-$  groups. Hence, LAKS crystal consists of an arginine molecule in the ionized form and a sulphate ion ( $982.06\text{cm}^{-1}$ ,  $983.42\text{cm}^{-1}$ ). Lack of any strong IR band at  $1700\text{cm}^{-1}$  clearly indicates the existence of the  $\text{COO}^-$  ion in zwitterionic form. In the high frequency region there is broad band between  $3700\text{--}2700\text{cm}^{-1}$ . In this broad band there are peaks at  $3347.76\text{cm}^{-1}$  due to N-H stretching vibrations of amino group and  $2955.42\text{cm}^{-1}$ ,  $2934.56\text{cm}^{-1}$ ,  $2870.90\text{cm}^{-1}$  due to C-H stretching vibrations of amino group. The protonation of amino group attached to  $\alpha$ - carbon atom can be proved because of the bands at  $1558.87\text{cm}^{-1}$  ( $\text{NH}_3^+$  symmetric deformation) at  $1682.56\text{cm}^{-1}$  ( $\text{NH}_3^+$  asymmetric deformation). The bands at  $2085.10\text{cm}^{-1}$  is due to the combination of  $\text{NH}_3^+$  deformation and  $\text{NH}_3^+$  torsion and is a very good indicator band for the identification of the charged  $\text{NH}_3^+$  group. And a band at  $454.31\text{cm}^{-1}$  is due to  $\text{NH}_3^+$  torsion mode. The numbers of IR bands arise due to the presence of the charged  $\text{NH}_3^+$  group confirm the protonation of the amino group in the LAKS crystal. Symmetry stretching of  $\text{SO}_4$  group appears at  $1114.47\text{cm}^{-1}$ ,  $1106.80\text{cm}^{-1}$ . The frequency bands observed at

$617.27\text{cm}^{-1}$ ,  $619.28\text{cm}^{-1}$  are assigned as asymmetric bending of the  $\text{SO}_4$  groups. No bands above  $3500\text{cm}^{-1}$  indicates the absence of water molecule in the crystal which also remains confirmed from the thermal study. Raman spectra are seen to be active in region up to about  $1100\text{cm}^{-1}$ . Most of the IR and Raman peaks in region between  $600\text{cm}^{-1}$  to  $1100\text{cm}^{-1}$  show one to one match indicating non-centrosymmetric nature.

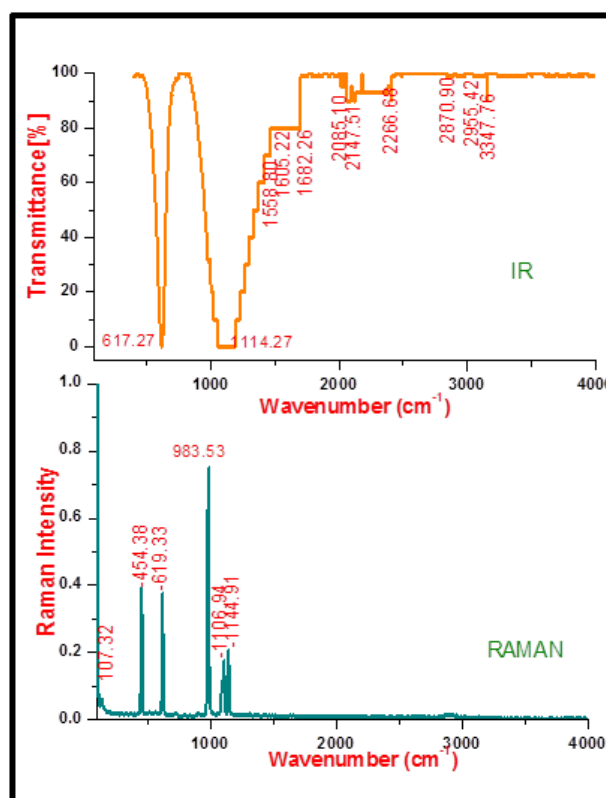


**Figure 4.** IR and RAMAN spectra of LAKS crystal

### Thermal Analysis

From the TGA curve of LAKS crystal (figure 5), it is observed that the material starts decomposing above  $210^\circ\text{C}$ . No weight loss up till  $200^\circ\text{C}$  indicates the absence of any physically absorbed or lattice water in the grown crystal [7]. Absence of water molecule is infact responsible for the long range stability of the grown crystals and is also evident from FTIR and FT-Raman studies. The DTA curve shows endothermic broad curve. Thus the grown crystal are highly stable as compared to LAP( $111^\circ\text{C}$ ), L-ADP( $173.9^\circ\text{C}$ ),

LAHClBr(92°C), LA-HCl(70°C), LAHBr(110°C), LAF(200°C) and LAAC(200°C).

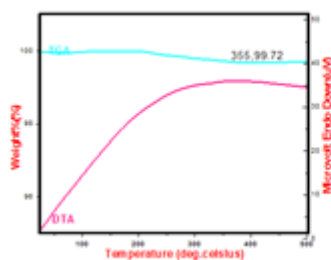


**Figure 5.** TGA and DTA curve of LAKS crystal

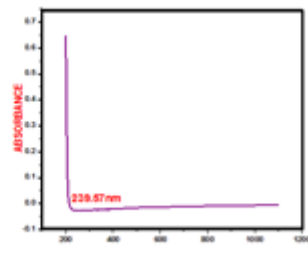


**Figure 6.** UV-VIS spectrum of LAKS crystal

### Linear and Non-linear optical Studies

The optical absorption spectrum of LAKS crystals of figure 6 shows a sharp UV cut-off at 239.57nm and the absorption is nearly zero in the entire visible region. The observed cut-off wavelength is may be due to weak n- $\pi$  transitions in carboxylate (-COO<sup>-</sup>) or guanidyl (NHC(NH<sub>2</sub>)-) ions. Wide transparency window makes the material useful for NLO studies. To check the nonlinear optical property of the grown crystal, Kurtz and Perry technique was used [8]. A high intensity Nd:YAG laser ( $\lambda = 1064\text{nm}$ ) with a pulse duration of 10ns and beam energy 24mJ per pulse was passed through the powdered sample. The generation of second harmonic was confirmed by the emission of green radiation. SHG efficiency of LAKS is found to be 0.39 times that of KDP crystal.

### IV. CONCLUSION

Optically good quality crystals of l-arginine potassium sulphate (LAKS) have been grown from aqueous solution by slow evaporation technique in about eight weeks. XRD studies confirm the crystalline nature with orthorhombic structure. SEM and EDAX analysis confirms the presence of potassium and sulphur in the crystal lattice of l-arginine. The study of FTIR and FT-Raman spectrum confirms the presence of amino, carboxyl and sulphate group in grown crystal. Thermal analysis revealed that the compounds are thermally stable upto 210°C. Linear optical property study revealed a good transparency of 100%. Kurtz

powder SHG test confirmed the non-linear optical behaviour of the LAKS crystals

### V. REFERENCES

- [1] M. D. Aggarwal, J. Stephens, A. K. Batra and R. B. Lal. 2003. *J. Optoelectronic & Advanced Materials* 5(3), 555-562.
- [2] G. Dhanaraj, T. Shripathi and H. L. Bhatt.1991. *J. Cryst. Growth* 113(3-4), 456-464.
- [3] L. J. Bellamy. 1975. *The Infrared Spectra of Complex Molecules*, 3rd Edition, Chapman and Hall, London.
- [4] D. Sankar, V. R. Menon, P. Sagayaraj and J. Madhavan. 2010. *PhysicaB* 405(1), 192-197.
- [5] M. Victor, A. Raj and J. Madhavan. 2011. *Scholars Research Library, Archives of Physics Research* 2(1), 183-189.
- [6] Z. Sun, G. Zhang, X. Wang, Z. Gao, X. Cheng, S. Zhang and D. Xu. 2009. *Cryst. Growth & Design* 9(7), 3251-3259.
- [7] S. Aruna, A. Anuradha, P. C. Thomas, M. Gulam Mohammed, S. A. Rajasekar, M. Vimalan, G. Mani and P. Sagayaraj.2007. *Indian J. Pure & Appl. Phys* 45, 524-528.
- [8] S. K. Kurtz and T. T. Perry. 1968. *J.Appl.Phys.* 39(8), 3798-3813.

# A Comparative study of Heavy Metals in Leachate and Groundwater near Solid Waste Dumpsite in Kalyan (MS)

Sonal Tawde

Birla College of Arts, Science and Commerce, Kalyan, Maharashtra, India

## ABSTRACT

Solid wastes are useless, unwanted or discarded materials that arise from man's activities and cannot be discarded through sewer pipe. A designated place for dumping of refuse is known as dumpsite. The municipal solid waste into our environment has contributed greatly to the increase in levels of heavy metals in soil and vegetations grown in dumpsites. Health risks of heavy metals include reduced growth and development, cancer, organ damage, nervous system damage, and in extreme cases, death. Dump sites have been identified as one of the major threats to groundwater resources. This leachate accumulates at the bottom of the dump site and percolates through the soil. Areas near dump sites have a greater possibility of groundwater contamination because of the potential pollution source of leachate originating from the nearby site. In the present study, the impact of leachate percolation on groundwater quality is estimated from an unlined dump site at Kalyan, Maharashtra. Heavy metals are analyzed in well water samples in different seasons to understand the possible link of groundwater contamination. The concentrations of heavy metals were determined by ICP OES.

**Keywords:** Solid Waste, Dumpsite, Leachate, Percolation, Ground water, Heavy Metals, ICP OES.

## I. INTRODUCTION

Water plays an important role for existence of mankind. The demand of water is rapidly increasing for drinking, irrigation and industrial uses. Large geographical area of Maharashtra State is occupied by hard rock. Kalyan city is nowadays suffering from availability of drinking water due to increase in population. If water from selected sources, is potable then the load on municipal water supply can be reduced. According to [11], solid wastes are useless, unwanted or discarded materials that arise from man's activities and cannot be discarded through sewer pipe. The non-flowing or sticky nature of solid waste gives rise to the accumulation of solid waste on some habitable parts of the earth surface. The soil and plants on these dumpsites will constitute a serious

threat to the health of people living around such areas [2].

The placement and compaction of municipal in landfills facilitates the development of facultative anaerobic conditions that promotes biological decomposition of land filled wastes. Hence, leachates of diverse composition are produced, depending on site construction and operational practices, age of the land filled [5]. Solid waste management has become a major environmental issue in India. The growth in Municipal Solid Waste (MSW) in urban centers has outpaced the population growth in recent years. The unsanitary methods adopted for disposal of solid wastes is, therefore, a serious health concern. Dump sites have been identified as one of the major threats to groundwater resources [10, 18]. The dumped solid

wastes gradually release its initial interstitial water and some of its decomposition by-products get into water moving through the waste deposit. Such liquid containing innumerable organic and inorganic compounds is called 'leachate'. The impact of dump site leachate on the surface and groundwater has given rise to a number of studies in recent years [1, 6, 8, 12, 14, 17]. The disposal of heavy metals is a consequence of several activities like chemical manufacturing, painting and coating, mining, extractive metallurgy, nuclear and other industries. Those metals exert a deleterious effect on fauna and flora of lakes and streams [9]. The extent of soil pollution by heavy metals and base metal ions some of which were soil micronutrients is very alarming. It has been observed that the larger the urban area, the lower the quality of the environment [9]. Heavy metals may enter the human body via food, water, air, or absorption through the skin in agriculture, industrial or residential settings [7, 13].

Kalyan city now a days suffering from availability of drinking water. Municipal Corporation of Kalyan is not able to supply drinking water for 24 hrs. for the city. Kalyan area is rich in ground water level. From olden times there are large number of wells which were in use. Water from wells near the dumpsite was used for various purposes including drinking. There are some sources, wells and bore wells which are still used by local people.

The present study is aimed at analyzing ground water samples at different dumpsites for their heavy metals concentration. In the present study, the impact of leachate percolation on groundwater quality is estimated from an unlined dump site at Kalyan, Maharashtra. Heavy metals are analyzed in leachate and in well water samples to understand the possible link of groundwater contamination. The objective of this study is to evaluate the groundwater pollution due to the dump site leachate. Such study could aid in quantifying information on the environmental impact of these metals. The data generated will serve as

baseline data for future studies which will help in suggesting various techniques that could be used to clean-up these metals from such harsh environment.

## II. METHODS AND MATERIAL

The quality of the ground waters from wells of five areas near Adharwadi Dumpsite of Kalyan where ground water is used at a considerable quantity were assessed for heavy metals using 'Standard methods for water and waste water treatment' [3]. The water samples were collected in summer and monsoon seasons. Leachate samples were collected from dumpsite at Adharwadi, Kalyan, Maharashtra State. Five groundwater wells within proximity of 1(one) Kms. from dumpsite which are used for drinking were selected as representative wells. Three samples were obtained from each well at different times. The samples were transported to the laboratory for analysis. In the determination of the availability and composition of heavy metals in the leachates and ground water from each sampling station, the digestive method, as recommended by [15] was used. The procedure was repeated for all the samples. The concentrations of heavy metals were determined by ICP OES (Agilent Technologies 700 series ICP OES). The samples were then analyzed for the metals Lead, Iron, Nickel, Cadmium, Chromium and Copper. Each sample was analyzed three times and the results are expressed as mean  $\pm$  SD (SD: standard deviation).

## III. RESULTS AND DISCUSSION

For the observations Refer Table 1. The graphs obtained from the analysis of metal concentrations are depicted in the figures 1, 2, 3, 4, 5, 6, 7 and 8 respectively.

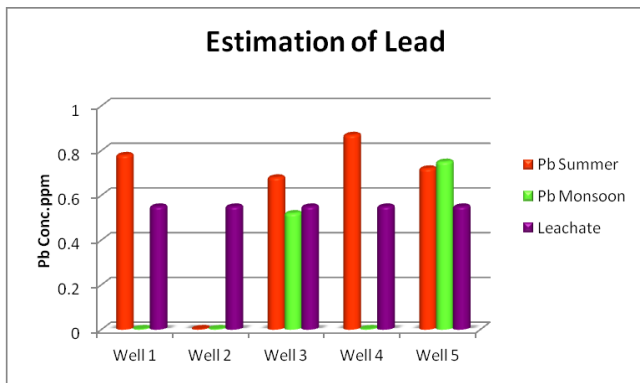


**Figure 1.** Estimation of Lead (Permissible Limit: 0.01ppm)

The drinking water standard (0.01 ppm) for Lead indicates that the water in the wells is highly contaminated in terms of Lead Pollution. The Lead levels are higher in the summer season than the monsoon season indicating dilution of well water in monsoon. When compared to lead present in leachate, the lead is more in summer as well as monsoon than the leachate. Out of the five wells only Well No. 3 and Well No.5 show high lead concentrations in monsoon. In Well No. 2 the lead levels are below detectable limits.

The risk of Lead poisoning through the food chain increases as the soil lead levels. [16]

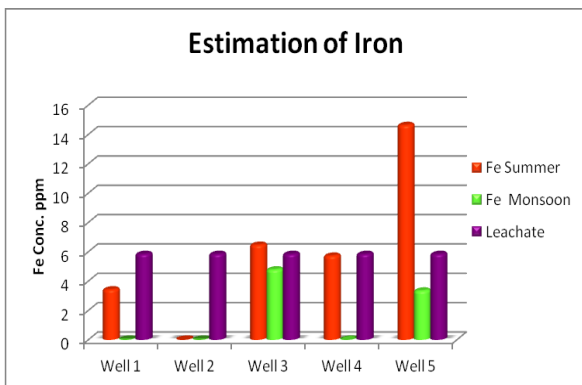


**Figure 2.** Estimation of Iron (Permissible Limit: 0.3 ppm)

The drinking water standard (0.3 ppm) for Iron indicates that the water in the wells is contaminated in terms of Iron Pollution. The Iron levels are higher in the summer season than the monsoon season indicating dilution of well water in monsoon. When

compared to iron present in leachate, the iron present in well water is more or less of similar concentration as the leachate, except in Well No. 5 where the iron concentration is extremely high. Out of the five wells only Well No. 3 and Well No.5 show lesser iron concentrations in monsoon. In Well No. 2 the iron levels are below detectable limits.

Iron may be hazardous to the environment; special attention should be given to plants, air and water. It is strongly advised not to let the chemical enter into the environment because it persists in the environment.

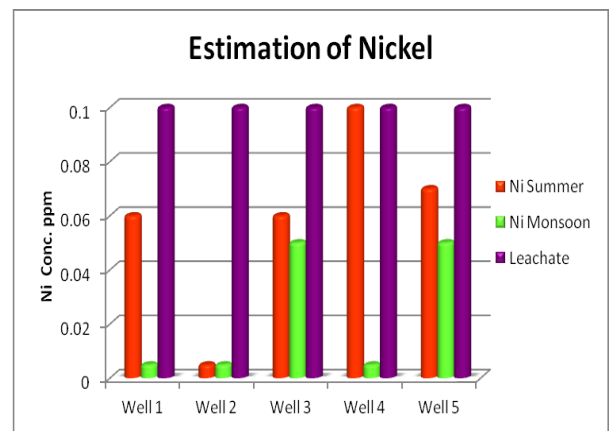


**Figure 3.** Estimation of Nickel (Permissible Limit: 0.02 ppm)

The drinking water standard (0.02 ppm) for Nickel indicates that the water in the wells is highly contaminated in terms of Nickel Pollution. The Nickel levels are higher in the summer season than the monsoon season indicating dilution of well water in monsoon. When compared to nickel present in leachate, the Nickel concentration is more in leachates as compared to well water except in Well No. 4, where the concentrations are similar in both. Out of the five wells, only Well No. 3 and Well No.5 show higher nickel concentrations in monsoon. In Well No. 2 the nickel levels are below detectable limits both in summer and monsoon. The highest concentration of nickel is more in Well No. 4. Acid rain increases the mobility of nickel in the soil and thus might increase nickel concentrations in groundwater [13].

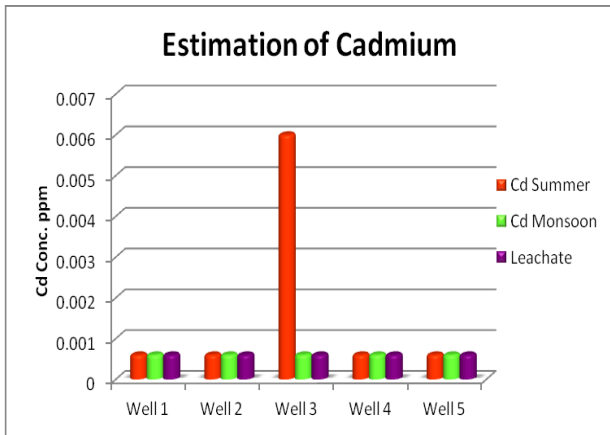


**Figure 4.** Estimation of Cadmium (Permissible Limit: 0.003 ppm)

The concentration of cadmium in all wells is below detectable limits and permissible limits in all seasons with an exception. Only in Well No. 3 the cadmium limits are higher and reach 0.006 ppm in the summer season. The cadmium limits in leachates is also below detectable levels.

Cadmium (Cd) leaching to water from contaminated soil is very low although it varies from soil to soil depending upon the textural and chemical properties which is evident in the above result showing concentrations below detectable levels.

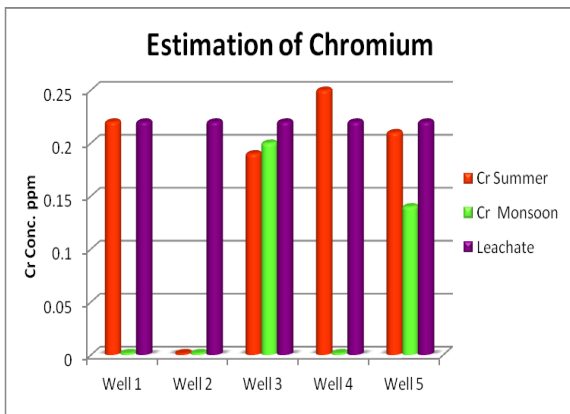


**Figure 5.** Estimation of Chromium (Permissible Limit: 0.05 ppm)

The drinking water standard (0.05 ppm) for Chromium indicates that the water in the wells is highly contaminated in terms of Chromium Pollution. The Chromium levels are highest in the summer season in Well No. 4. Out of the five wells, the

chromium concentrations above permissible limits in monsoon are found only in Well no. 3 and Well no. 5. Comparing the concentrations in summer and monsoon, in Well No. 3 the concentrations in monsoon are slightly higher than in summer. When compared to chromium present in leachate, the chromium is more in leachates in summer and monsoon, except in well no. 4. In Well No. 2 the chromium levels are well below detectable limits both in summer and monsoon.

Soluble and un-adsorbed chromium complexes can leach from soil into groundwater. This can be indicated in increased levels of chromium in the ground water which may be possible due to leaching from the dumpsite leachates.

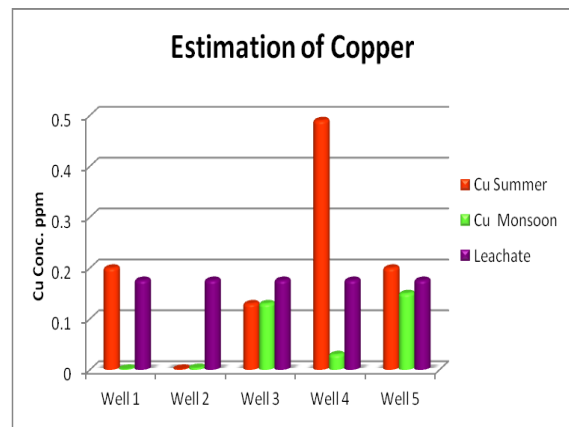


**Figure 6.** Estimation of Copper (Permissible Limit: 0.05 ppm)

The drinking water standard (0.05 ppm) for Copper indicates that the water in the wells is highly contaminated in terms of Copper Pollution. The Copper levels are higher in the all wells except Well No. 2, the highest concentration being in Well No. 4. Out of the five wells, the Copper concentrations above permissible limits in monsoon are found only in Well No. 3 and Well No. 5. When compared to Copper present in leachate, the Copper is more or less similar to the summer concentration levels except in Well No. 4 where it is highest. In Well No. 2 the chromium levels are well below detectable limits both in summer and monsoon.



In the soil, Cu strongly complexes to the organic fraction implying that only a small fraction of copper will be found in solution as ionic copper, Cu(II).

dumpsite to the wells is a possible reason for increase in metal concentrations.

#### IV. CONCLUSION

All the wells are being used for water usage by the local people. Presence of these heavy metals in ground water is showing the serious toxic risks of contamination due to percolation of leachate.

From the groundwater monitoring it is clearly evident that the leachate generated from the dumping site is affecting the groundwater quality in the adjacent areas through percolation in the subsoil. Therefore, some remedial measures are required to prevent further contamination. This can be achieved by the management of the leachate generated within the dumping site. Leachate management can be achieved through effective control of leachate generation, its treatment and subsequent recycling throughout the waste.

Adharwadi dumping site will soon be closed for MSW disposal since it has already received waste beyond its capacity. Remedial measures should be considered by taking this into account. Adharwadi dumping site is non-engineered landfill. It is neither having any bottom liner nor any leachate collection and treatment system. Therefore, all the leachate generated finds its paths into the surrounding environment. In such conditions only feasible options that could be followed are to limit the infiltration of the water through the landfill cover by providing impermeable clay cover. Due to this less water will enter and subsequently less leachate will be generated, thereby reducing the amount of leachate reaching the landfill base.

#### V. REFERENCES

- [1] Abu- Rukah, Y. and O. Al- Kofahi, (2001). The assessment of the effect of landfill leachate on ground-water quality—a case study. El-Akader

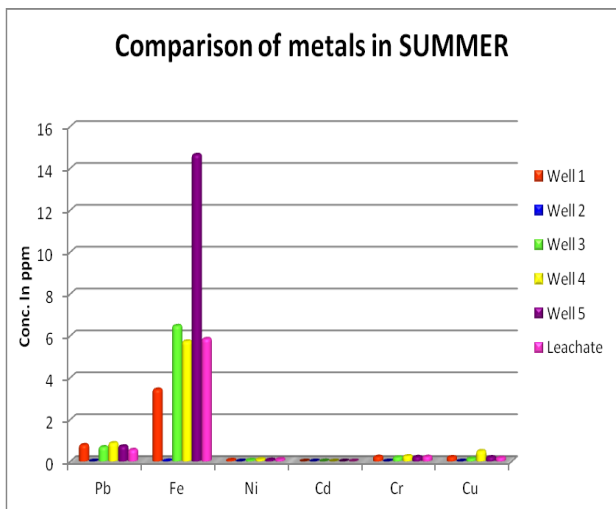


Figure 7. Comparison of all metals in Summer

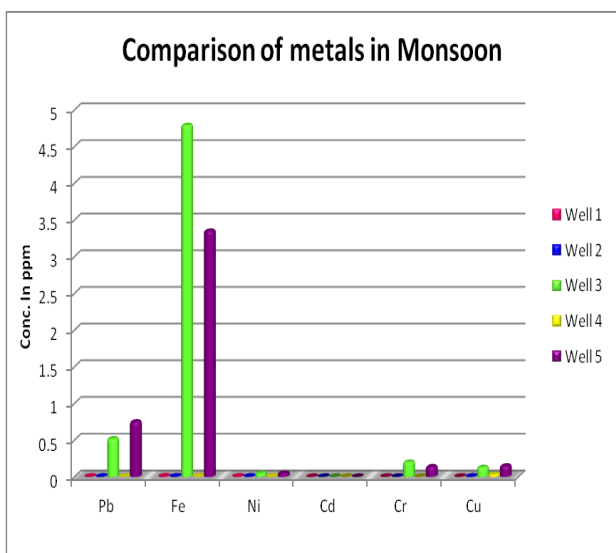


Figure 8. Comparison of all metals in Monsoon

The overall analysis of metals indicates that Iron is present in higher concentrations compared to other metals. Cadmium is below detectable limits in all wells. Well No. 3 and 5 are more contaminated than the other wells as contamination is observed even in monsoon season indicating lesser dilution. Well No. 2 does not show any metals contamination indicating its usefulness. The metal contamination is observed more during summer than in monsoon for the wells. The percolation of metals from the leachates of the

- landfill site—north Jordan, *Arid Environ.* 49, 615-630.
- [2] Adefemi OS, Awokunmi EE (2009). The impact of municipal solid waste disposal in Ado Ekiti metropolis, Ekiti State, Nigeria. *Afr. J. Environ. Sci. Tech.* 3(8): 186-189.
- [3] APHA, AWWA & WEF, 20<sup>th</sup> Ed. (1998). Standard Methods for the examination of water and wastewater, American Public Health Association, Washington, D.C.
- [4] Bureau of Indian Standards (BIS) (2012), Indian standard specification for drinking water, IS: 10500, pp. 2-4.
- [5] Campbell DJV (1993). Environmental Management of Landfill Sites. *J.I.W.E.M.* 7(2): 170 - 173.
- [6] Christensen, J. B., D. L. Jensen, C. Gron, Z. Filip and T. H. Christensen, (1998). Characterization of the dissolved organic carbon in landfill leachate-polluted groundwater, *Water Res.*, 32, 125-135.
- [7] D. Dupler, (2001), "Heavy Metal Poisoning," In: J. L. Longe, Ed., *Gale Encyclopedia of Alternative Medicine*, Gale Group, Farmington Hills, pp. 2054-2057.
- [8] DeRosa, E., Rubel, D., Tudino, M., Viale, A., and R.J. Lombardo, (1996). The leachate composition of an old waste dump connected to groundwater: Influence of the reclamation works. *Environ. Monit. Assess.* 40 (3): 239-252.
- [9] Eddy NO (2004a). Physicochemical parameter of water and heavy metal content of water, sediment and fishes from Qua Iboe River Estuary. M.Sc Thesis. Michael. Okpara University of Agriculture, Umudike. Nigeria.
- [10] Fatta D., A Papadopoulos and M., Loizidou, (1999). A study on the landfill leachate and its impact on the groundwater quality of the greater area. *Environ. Geochem. Health* 21 (2): 175-190.
- [11] Federal Environmental Protection Agency (FEPA) (1995). Corporate profile. Metro prints Ltd, Port Harcourt.
- [12] Flyhammar, P. (1995), Leachate quality and environmental effects at active Swedish municipal landfill, in: R. Cossu, H. T. Christensen and R. Stegmann (eds) *Regulations, Environmental Impact and Aftercare. Proceedings Sardinia '95, Fifth International Landfill Symposium. Vol. III, Sardinia, Italy*, pp. 549-557.
- [13] H. Roberts, (2013). "Lead Poisoning," <http://www.setlet.com> IPCS (1991) Nickel. Geneva, World Health Organization, International Programme on Chemical Safety (Environmental Health Criteria 108).
- [14] Looser, M.O., A. Parriaux, and M. Bensimon, (1999). Landfill underground pollution detection and characterization using inorganic traces. *Water Res.* 33, 3609-3616.
- [15] Nwajei PE, Gagophein PO (2000). Distribution of heavy metals in the sediments of Lagos Lagoon. *Pak. J. Sci. Ind. Res.* 43: 338-340.
- [16] Rosen, C.J. (2002). Lead in the home garden and urban soil environment, Communication and Educational Technology Services, University of Minnesota Extension.
- [17] Saarela, J., (2003). Pilot investigations of surface parts of three closed landfills and factors affecting them *Environ. Monit. Assess.* 84,183-192.
- [18] W. H. O (World health organization) (1993). Guidelines for drinking water quality 2nd edition, Vol. 1, Recommendations.

**Table 1.** Concentrations of Metals analyzed from water of the five wells and three sampling points of leachate collected from the Dumpsite.

	Well No.						
		Conc. of Pb	Conc. of Fe	Conc. of Ni	Conc. of Cd	Conc. of Cr	Conc. of Cu
Summer	Well 1	0.78 ± 0.02	3.43 ± 0.026	0.06 ± 0.011	0.0006 ± 0	0.22 ± 0	0.2 ± 0.025
	Well 2	0.004 ± 0.002	0.01 ± 0.002	0.0049 ± 0.0002	0.0006 ± 0	0.002 ± 0.0002	0.002 ± 0.001
	Well 3	0.68 ± 0.03	6.47 ± 0.026	0.06 ± 0.02	0.006±0.001	0.19 ± 0.005	0.13 ± 0.02
	Well 4	0.87 ± 0.02	5.73 ± 0.06	0.1 ± 0.057	0.0006 ± 0	0.25 ± 0.023	0.49 ± 0.02
	Well 5	0.72 ± 0.02	14.64 ± 0.23	0.07 ± 0.02	0.0006 ± 0	0.21 ± 0	0.2 ± 0.1
Monsoon	Well 1	0.004 ± 0.002	0.007 ± 0.002	0.0049 ± 0.0005	0.0006 ± 0.0001	0.002 ± 0.0002	0.002 ± 0.0007
	Well 2	0.004 ± 0.002	0.006 ± 0.002	0.0049 ± 0.0009	0.0006 ± 0	0.002 ± 0.001	0.004 ± 0.002
	Well 3	0.52 ± 0.03	4.79 ± 0.055	0.05 ± 0.02	0.0006 ± 0	0.2 ± 0.057	0.13 ± 0.01
	Well 4	0.004 ± 0.002	0.008 ± 0.002	0.0049 ± 0.0009	0.0006±0.0001	0.002 ± 0.00048	0.03 ± 0
	Well 5	0.75 ± 0.21	3.35 ± 0.158	0.05 ± 0.025	0.0006 ± 0.0002	0.14 ± 0.02	0.15 ± 0.02
Leachate	Point 1	0.49 ± 0.02	9.88 ± 0.79	0.11 ± 0.037	0.0006 ± 0.0001	0.19 ± 0.02	0.17 ± 0.015
	Point 2	0.69 ± 0.09	7.08 ± 0.74	0.12 ± 0.02	0.0006 ± 0	0.23 ± 0.02	0.19 ± 0
	Point 3	0.49 ± 0.05	7.56 ± 0.46	0.1 ± 0.03	0.0006 ± 0.0001	0.2 ± 0	0.17 ± 0.0057

# Application of Spectroscopic Techniques for analysis of interaction between Thermophiles and metal ions

Sonali Zankar Patil\*, Geetha Unnikrishnan

Birla College of Arts, Science and Commerce, Kalyan, Maharashtra, India

## ABSTRACT

The thermophiles are adapted to the environment containing sulfate and other heavy metals, its potential use in bioremediation will be significant. There are various compounds or substances that are responsible for bioremediation. Depending upon the microorganisms, the bioremediation processes can be due to proteins and enzymes that are responsible for carrying out this process or other factors like extracellular polymeric substances (EPS). Quantitative and qualitative determination of biomolecules and microbial assisted phenomena by spectroscopy is a pioneer approach. This research presents the features of protein and EPS from thermophiles with a view to establish their role as central elements in bioremediation of heavy metals. A coordinated physicochemical analysis of water and molecular survey of microbes was conducted for Vajreshwari and Ganeshpuri hot springs. The results of this study expands the current understanding of the microbiology in Vajreshwari and Ganeshpuri hot springs and provide a basis for comparison with other geothermal systems around the world. The study will aid in engineering the extracellular polymeric substances with enhanced characteristics of metal sorption for effective bioremediation of heavy metals of environmental concern.

**Keywords:** Thermophiles, Extracellular Polymeric Substances, Spectroscopic Techniques, Metal Ions.

## I. INTRODUCTION

Microbes are the most fascinating group, with huge diversity devising myriad functional applications in the field of medicine, pharmaceuticals, environmental remediation, and industries. Quantitative and qualitative determination of biomolecules and microbial assisted phenomena by spectroscopy is a pioneer approach. It facilitates the study of atomic and molecular geometries, energy levels, chemical bonds, and interactions between molecules and microbes.

The thermophiles are adapted to the environment containing sulfate and other heavy metals, its potential use in bioremediation will be significant.

There are various compounds or substances that are responsible for bioremediation. This research presents the features Extrapolymeric substances (EPS) from thermophiles with a view to establish their role as central elements in bioremediation of heavy metals. Most of the strains are able to produce extracellular polymeric substances (EPS) mainly of polysaccharidic nature comprising polysaccharides, proteins, nucleic acids, uronicacids, humic substances, lipids, etc (De Philippis & Vincenzini, 2003; Pereira *et al.*, 2009). A coordinated physicochemical analysis of water and molecular survey of microbes was conducted for Vajreshwari and Ganeshpuri hot springs. The study will aid in engineering the extracellular polymeric

substances with enhanced characteristics of metal sorption for effective bioremediation of heavy metals of environmental concern.

## II. METHODS AND MATERIAL

### 1. Sampling and media for isolation of thermophiles:

Water samples were collected from seven different hot springs (from Vajreshwari & Ganeshpuri, Thane) Mumbai. Surface water samples were taken from the Hot Springs using a grab sampler. A 500-ml plastic cup attached to a 2-m pole was dipped into the water twice to rinse it. The sample was then transferred to a clean, new, polyethylene container with a snap-on lid. The temperature of the sample was taken with a laboratory thermometer and recorded. All samples were taken on the same day to prevent discrepancies due to sample date. Samples were kept cool during transport to the laboratory and processed within 12 h of collection (Vieille C. 1996).

Bacillus Medium described by Postgate (1969) was used for routine stock maintenance and all enrichment culture studies.

Bacillus Medium contained (g/ Lit.: Soluble starch – 30.0 g, Agar – 20.0 g, Peptone – 5.0 g, Yeast Extract – 5.0 g, Distilled Water – 1000 ml, pH 7.5 ± 0.2 (45°C). Colonies were isolated from anaerobic roll tubes (Hungate *et. al.* 1969) containing Medium and 4% (w/v) purified agar. Stock cultures of all strains were prepared from single isolated colonies that proliferated on transfer in Media. All stock cultures were incubated at 50°C. Cultures were routinely checked for contamination (Zeikus *et, al.* 1979).

### 2. Screening for Maximum Tolerance capacity for Bioremediation:

All Strains isolated during the course of study were investigated for their maximum tolerance capacity

towards bioremediation. The screening was done by using 500ppm of heavy metals containing 5 specific heavy metals i.e. Cd, Cr, Cu, Fe, Zn (5 heavy metals were chosen as these are common pollutant in industrial wastewater).

### 3. Bioremediation efficiency by Atomic Adsorption Spectroscopy:

100 ml Sterile Nutrient broth containing 500 ppm of Cd<sup>2+</sup>, Cr<sup>2+</sup>, Cu<sup>2+</sup>, Fe<sup>2+</sup> and Zn<sup>2+</sup> were prepared and were inoculated with 24 hour old culture suspensions of all the five bacterial isolates namely SZP 16 and SZP 18. The inoculated flasks were kept at 45°C ± 2°C for 24 hrs. After that, the broths were centrifuged at 6000 rpm for 20 minutes (Sinha and Khare, 2012). The supernatant was analyzed for residual heavy metal by ICP-AES (At SAIF, IIT, Powai, Mumbai, M. S.).

### 4. Strain identification by 16s rRNA Method:

The isolated colonies showing high tolerance to heavy metals were sequenced for its conserved sequences and analysed for partial 16s rRNA by geneOmbio, Pune, Maharashtra. The predicted 16S rRNA sequences from this study were compared with 16S rRNA sequences in a BLASTable database constructed from sequences downloaded from the Ribosomal Database Project (release 8.1; <http://rdp8.cme.msu.edu>). Comparisons were made using the program BLAST (<ftp://ftp.ncbi.nih.gov/BLAST/executables/LATEST/>) and a FASTA-formatted file containing the predicted 16S rRNA sequences. All the sequences were deposited into NCBI database.

### 5. Application of FTIR Spectroscopy for studying mechanism involved in Bioremediation :

The effects of different heavy metals in the growth/survival of the selected isolates leads to production of EPS. The qualitative and quantitative analysis of EPS and their functional group can be easily studied by FTIR.

The thermophiles isolated from hot water springs of Vajreshwari and Ganeshpuri, Thane, Maharashtra, were studied for the effect of heavy metals on the EPS production. And comparison of EPS production from control and treated isolates were studied qualitatively and quantitatively by FTIR analysis.

The protein contents of EPS and total neutral-carbohydrate content were confirmed by FTIR analysis. FT-IR analysis of the bacteria is required to know and to confirm the chemical bonds that played a role in the Bioremediation of metal.

### III. RESULTS AND DISCUSSION

#### 1. Characterization of in situ Bioremediation:

Microbial heavy metal reduction at high temperatures was studied at several sites in Vajreshwari & Ganeshpuri hot springs. Enrichment cultures were initiated with Bacillus Medium. After incubation of all

enrichments for 6 d at *in situ* temperature, the cultures formed a dense colonies (table 1).

#### 2. Bioremediation

The MTC for both the strains for bioremediation of heavy metals were found to be above 1000 ppm (Table 2),

#### 3. Bioremediation efficiency:

The bioremediation of heavy metals were determined by ICP-OES, at SAIF, IIT, Powai, Mumbai, M. S. (Table 3). The data from statistical analysis at 95% confidence limit showed that there is no significant difference in heavy metal ( $Cd^{2+}$ ,  $Cr^{2+}$ ,  $Cu^{2+}$ ,  $Fe^{2+}$  and  $Zn^{2+}$ ) bioremediation potential of all the selected isolates (SZP 16 and SZP 18). Thus, either of the isolate can be used for bioremediation of heavy metals ( $Cd^{2+}$ ,  $Cr^{2+}$ ,  $Cu^{2+}$ ,  $Fe^{2+}$  and  $Zn^{2+}$ ).

**Table 1: Colony characteristics of selected isolates**

Isolate	Size	Shape	Colour	Consistency	Opacity	Gram nature	Motility
SZP 16	Pin point	Irregular	Colourless	Butyrous	opaque	Gram Positive Bacilli	NM
SZP 18	3 mm	Irregular	Dull white	Butyrous	Transparent	Gram Positive Cocci	NM

Isolate	Table 2: Analysis of Maximum Tolerance Capacity for Heavy metals by AAS (concentration in ppm)				
	Cd	Cr	Cu	Fe	Zn
<b>SZP 16</b>	3990	4380	3454	2944	4290
<b>SZP18</b>	2777	3908	3889	2789	4209

**Table 3.** Heavy metal reduction by selected isolates for standard

Metal	Metal removal (%) after 24 hrs.				
	SZP 4	SZP 8	SZP 12	SZP 16	SZP 18
Cd	B66.00 c±1.8	B64.00 c±2.8	A54.00 e±2.6	A59.30 e±2.8	A44.00 d±1.2
Cr	A45.80 d±3.0	A78.20 e±1.8	A41.30 d±2.3	B78.60 e±1.3	B61.60a ±2.9
Cu	C57.40 e±1.5	D51.00 e±2.8	B64.20a ±1.4	A51.00 e±2.6	A52.20 e±2.2
Fe	A50.20 c±1.2	C29.00 b±2.8	B60.80 d±2.4	A58.80 c±1.2	B53.60 c±2.0
Zn	B64.00a ±2.4	A44.60 a±1.4	C32.00 b±2.2	C58.60 a±1.8	A37.40 b±1.2

**Key :** Values are mean ± S. D. (n=3)

#### 4. Identification of selected thermophiles by 16s rRNA :

The selected five strains were sequenced for 16s rRNA (Table 4.4). After comparing the sequence using BLAST database, genus and species were confirmed.

These sequences were deposited in NCBI database and has been given specific strain name (Table 4).

#### 5. FTIR analysis of EPS:

Qualitative and quantitative analysis of protein and carbohydrate was carried out by biochemical method and was confirmed by FTIR (Table 5 and 6, fig. 1, 2, 3 and 4). FT-IR analysis of extracted EPS was carried out and intensity of peaks was compared with that of control spectra (Table 7). The most remarkable difference between the control and test spectra was at intensity of 1600-1700 cm<sup>-1</sup> and 2500 cm<sup>-1</sup> representing hydroxyl (-OH) and amine (-NH<sub>2</sub>) group respectively. This signifies the involvement and changes that occurs during Bioremediation of heavy metals by EPS isolated from the selected isolates (Fig. 5 and 6).

**Table 4:** NCBI Accession Number of identified strains:

Thermophile	Strain name	Accession number
<i>Geobacillus stearothermophilus (SZP 16)</i>	<i>BHALPRAVIN</i>	KM527211
<i>Streptococcus thermophiles (SZP 18)</i>	<i>ROHANMANALI</i>	KM527213

**Table 5:** Protein concentration (µg /ml) Before and after exposure of each heavy metal

Isolate	Contr ol	Cd <sup>2+</sup>	Cr <sup>2+</sup>	Cu <sup>2+</sup>	Fe <sup>2+</sup>	Zn <sup>2+</sup>	Mixed
SZP 16	28±1.5	35±1.6	39±1.3	35±2.0	41±1.9	30±1.0	35±2.0
SZP 18	27±2.8	32±1.1	40±1.8	32±1.5	38±2.1	32±2.6	38±2.1

Isolate	Control	$\text{Cd}^{+2}$	$\text{Cr}^{+2}$	$\text{Cu}^{+2}$	$\text{Fe}^{+2}$	$\text{Zn}^{+2}$	Mixed
SZP 16	25 $\pm$ 2.8	35 $\pm$ 2.8	38 $\pm$ 2.8	35 $\pm$ 2.8	39 $\pm$ 2.8	31 $\pm$ 2.8	31 $\pm$ 2.5
SZP 18	29 $\pm$ 2.8	30 $\pm$ 2.8	38 $\pm$ 2.8	30 $\pm$ 2.8	36 $\pm$ 2.8	30 $\pm$ 2.8	36 $\pm$ 2.8

Isolate	Cd	Cr	Cu	Fe	Zn
SZP 16	Yes	Yes	Yes	Yes	Yes
SZP 18	Yes	Yes	Yes	Yes	Yes

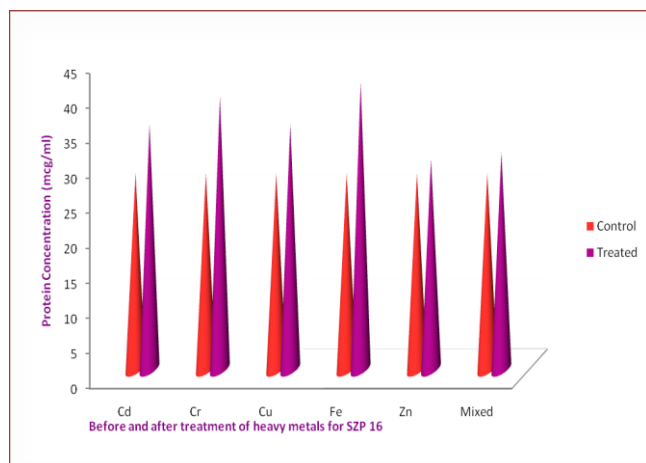


**Figure 1.** Protein Concentration before and after treatment for SZP 16

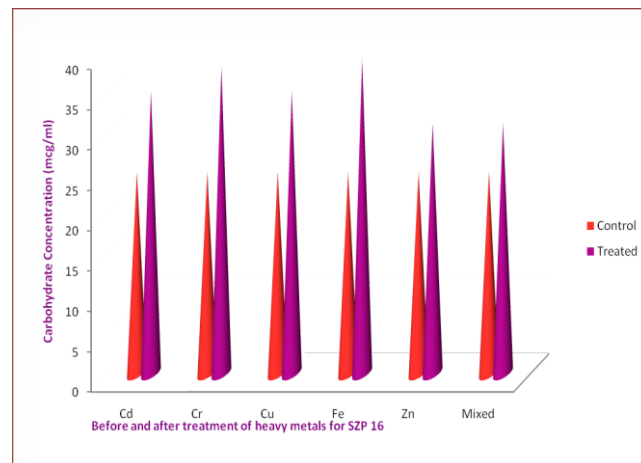


**Figure 2.** Carbohydrate Concentration before and after treatment for SZP 16



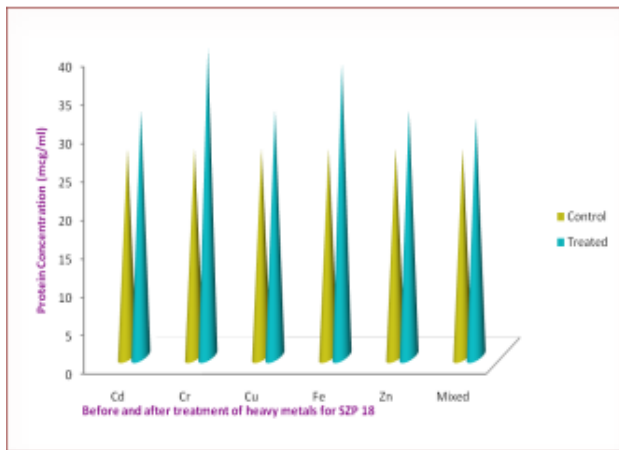


Figure 3. Protein Concentration before and after treatment for SZP 16

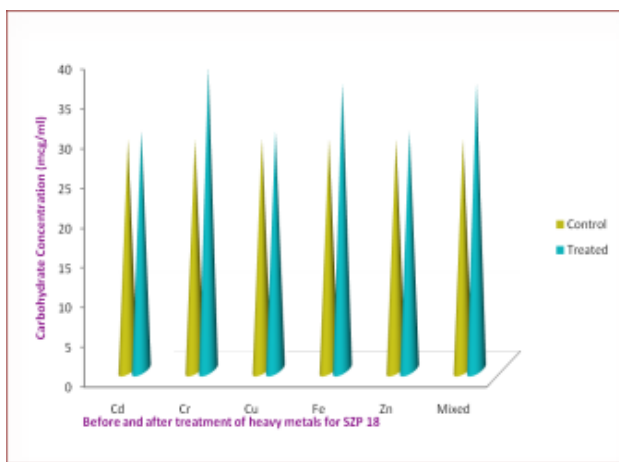


Figure 4. Carbohydrate Concentration before and after treatment for SZP 16

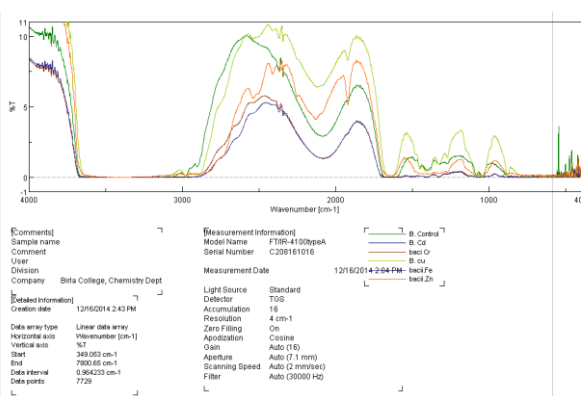


Figure 5. Protein Concentration before and after treatment for SZP 18

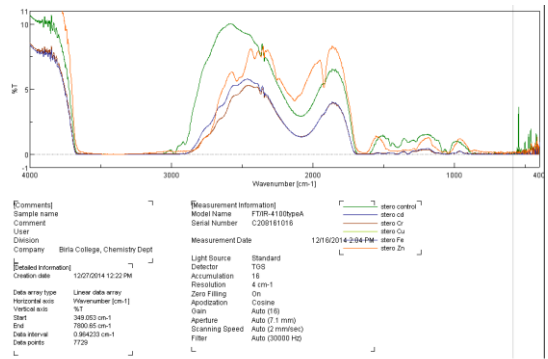


Figure 6. FTIR analysis of EPS production by SZP 18

#### IV. CONCLUSION

Above studies on interactions between metal and EPS produced by selected isolates have established the phenomenon of bioremediation of toxic heavy metal by EPS which plays a central role. Study has developed a simple model system which will provide an insight into the basic mechanism(s) of EPS-metal binding, highlight the specific role of each EPS component including proteins and carbohydrates and justify the interaction(s) amongst the components thereof. The study will aid in engineering the extracellular polymeric substances with enhanced characteristics of metal sorption for effective bioremediation of heavy metals of environmental concern. The research summarizes traditional spectroscopic techniques used for the study of microbes and microbial-assisted products as well as illustrates its application in the field of microbial diversity and remediation.

#### V. REFERENCES

- [1]. **Baptista, M. S., Vasconcelos, M. T.** Cyanobacteria metal interactions: requirements, toxicity, and ecological implications. *Crit. Rev Microbiol*, 2006. 32:127–137.
- [2]. **Buchanan RE, Gibbons N.** Bergey's manual of determinative bacteriology. (Eighth edition), The Williams and Wilkins Co., Baltimore, 1974, 747-842.

- [3]. **Burnat, M., Diestra, E., Esteve, I., Sole, A.** In situ determination of the effects of lead and copper on cyanobacterial populations in microcosms. *PLoS ONE* 4, 2009. e6204.
- [4]. **C. Selle, W. Pohle, H. Fritzsche,** Progress in Fourier Transform Spectroscopy, J. Mink, G. Keresztury, R. Kellner (Eds.), *Mikrochim. Acta*. 1997. 14 449-450 Supplimentary issue.
- [5]. **De Philippis, R., Paperi, R., Sili, C., Vincenzini, M.** Assessment of the metal removal capability of two capsulated cyanobacteria, *Cyanospira capsulata* and *Nostoc PCC7936*. *J. Appl. Phycol.* 2003. 15: 155-161.
- [6]. **Fabienne, F., Carine, L., Jean-Michel, G., Paul, S., Florence Brian-Jaisson, Grégory M., Manon, Daniel G., Anne-Laure M., David, P., Jean, P., Séverine, Z., Sylvie, R.** Isolation and Characterization of Environmental Bacteria Capable of Extracellular Bisorption of Mercury. *Applied and Environmental Microbiology*. 2011. 1097-1106.
- [7]. **Fiore, M. F., Trevors, J. T.** Cell composition and metal tolerance in cyanobacteria. *Biometals*. 1994. 7:83-103.
- [8]. Gadd G M. *Micrbiol.* 2010, 156: 609-643.
- [9]. **Heng, L. Y., Jusoh, K., Ling, C. H. M., Idris, M.** Toxicity of single and combinations of lead and cadmium to the cyanobacteria *Anabaena flos-aquae*. *Bull Environ Contam Toxicol.* 2004. 72:373-379.
- [10]. **Nies, D. H. c.** Microbial heavy-metal resistance in prokaryotes. *FEMS Microbiological Reviews*. 1999, 27: 313-339.
- [11]. **Patil Sonali, Geetha Unnikrishanan.** "Isolation, characterization and identification of heavy metal tolerating thermophiles from hot water spring", *European Journal for Biotechnology and Biosciences*. 2015, Volume: 3, Issue: 7, 17-22.
- [12]. **Patil Sonali.** "Factors responsible for bioremediation in thermophiles". *Photon Journal of Microbiology*, 2017, Photon, 110, 283-286.
- [13]. **Pereira, S., Ernesto, M., Andrea, Z., Arlete, S., Pedro, M., Paula T., De Philippis R.** Using extracellular polymeric substances (EPS) producing cyanobacteria for the bioremediation of heavy metals: do cations compete for the EPS functional groups and also accumulate inside the cell? *Microbiology*, 2011, 157:451-458.
- [14]. **Roy, S., Ghosh, A. N., Thakur, A. R.** Uptake of Pb<sup>2+</sup> by a cyanobacterium belonging to the genus *Synechocystis*, isolated from East Kolkata Wetlands. *Biometals*. 2008. 21:515-524.
- [15]. **W. Babel, A. Steinbuochel (Eds.),** Advances in Biochemical Engineering/Biotechnology Biopolyesters, 2001. Vol. 71, Springer, Berlin, Heidelberg, pp. 51-79 See also pages 81-123, 125-135

# Cauliflower Leaves, an Agro waste : Characterization and its Application for the Biosorption of Copper, Chromium, Lead and Zinc from aqueous solutions

Vandana Gupta<sup>\*1</sup>, Sandesh Jaybhaye<sup>2</sup>, Naresh Chandra<sup>3</sup>

<sup>\*1</sup> Department of Biotechnology, B.K. Birla College of Arts, Science and Commerce, Kalyan, Maharashtra, India

<sup>2</sup> Department of Chemistry, B.K. Birla College of Arts, Science and Commerce, Kalyan, Maharashtra, India

<sup>3</sup> Department of Botany, B.K. Birla College of Arts, Science and Commerce, Kalyan, Maharashtra, India

## ABSTRACT

Cauliflower leaves being non-edible, is frequently discarded from vegetable markets and it forms a part of Municipal Solid Wastes. The present study focuses on using the cauliflower leaves as a biosorbent for the removal of heavy metals Copper, Chromium, Lead and Zinc from spiked solutions of known concentrations as well as from industrial effluents using batch method. The pH, bulk density, ash content, and iodine index of the cauliflower leaves powder were calculated and further characterizations of the leaves like surface morphology and functional groups present on the surface of the biosorbent were carried out using E-SEM and FT-IR respectively. The heavy metal concentrations in the solutions were found out using ICP-AES analysis. After the biosorption process, the removal of heavy metals was found to be 80.43%, 57.26%, 99.39% and 69.91% for Copper, Chromium, Lead and Zinc respectively from spiked solution at pH 7 after adding 1% adsorbent dose at 30°C temperature for 60 minutes. The biosorption was also carried out for effluents collected from industries like powder dusting, chemical, electroplating, paper mill and textile industry and removal of all four metals were found to be in the range of 26% to 100% after biosorption process. Characterization of the biosorbent by FTIR showed the presence of various functional groups like hydroxyl, aliphatic methylene group, aromatic groups, etc. which might have involved in interacting/ binding to metal ions. The SEM images of the material showed distinct changes in the surface morphology after interacting with the metal solutions which may be due to metal stress on the biosorbent.

**Keywords:** Biosorption, pH, bulk density, Ash content, Iodone Index, ICP-AES, FT-IR, SEM

## I. INTRODUCTION

Most of the industries in India are situated along the banks of the river for easy source of water and also for discharge of their effluents. According to Central Pollution Control Board (CPCB) report, Maharashtra state has the largest number of polluted river water stretches in the country. The industries contributing to such pollution include petrochemical industries, sugar mills, distilleries, leather processing industries,

paper mill, agrochemicals and pesticides manufacturing industries and pharmaceutical industries. The wastes often contain a wide range of contaminants such as petroleum hydrocarbons, chlorinated hydrocarbons, toxic metals, various acids, alkalis, dyes and other chemicals. Hence there is a need for extensive monitoring of discharged industrial effluents which has the potential to pollute the nearby water bodies like rivers or creeks [1]. Environmental pollution particularly from heavy metals and minerals

in the wastewater is the most serious problem in India. Due to extensive anthropogenic activities such as industrial operations particularly mining, agricultural processes and disposal of industrial waste materials; their concentration has increased to dangerous levels [2]. In most wastewaters, the concentration of heavy metals present is much larger than the safe permissible limits [3]. The heavy metals from waterbodies may accumulate in the body of flora and fauna and later on may pass through the food chain into the plants, fishes and human beings. These toxic metals enter the human body mostly through food and water. However, it also enter through inhalation of polluted air, use of cosmetics, drugs, poor quality herbal formulations (herbo-mineral preparations) and Unani formulations. In humans, heavy metal toxicity can cause chronic degenerative diseases like mental disorders, pain in muscles and joints, gastro intestinal disorders and vision problems. Genotoxicity and cancer can also occur. Sometimes the symptoms are vague and difficult to diagnose at early stage [4].

Over the decades, several methods have been devised for the treatment and removal of heavy metals. The commonly used procedures for removing metal ions from aqueous streams include chemical precipitation, lime coagulation, ion exchange, reverse osmosis and solvent extraction. But all these methods show disadvantages like incomplete metal removal, high reagent and energy requirements, generation of toxic sludge or other waste products that require careful disposal [5]. The search for new technologies involving the removal of toxic metals from wastewaters has directed attention to biosorption, based on metal binding capacities of various biological materials. Biosorption can be a cost-effective treatment method that is capable of removing heavy metals from aqueous effluents [6]. Several researchers have reported the removal of heavy metal through algae, marine algae, bacteria, yeast and higher plants in immobilized as well as in free state [7][8]. The fins of *Catla catla* fishes were found to be successful in adsorbing copper, chromium, lead and zinc from

different industrial effluents [9]. The present work focusses on using one of the commonly discarded vegetable wastes, cauliflower leaves for the biosorption of heavy metals from industrial effluents.

## II. MATERIALS AND METHODS

### A. Preparation of Biosorbent

The Cauliflower Leaves (CL) was collected from local vegetable market situated in Andheri, Mumbai, M. S. India. The CL was washed with tap water for multiple times followed by thrice washing with distilled water to remove adhering dust particles. The washed leaves were then oven dried at 80°C till crispy. The dried materials were grounded into fine powder using kitchen mixer grinder. The powdered CL was then stored in polythene bags till further use.

### B. Preparation of metal solutions

Stock solutions (1000 mg/l) of heavy metals were prepared by dissolving analytical grade of respective metal salts like  $\text{CuSO}_4 \cdot 5\text{H}_2\text{O}$ ,  $\text{K}_2\text{CrO}_4$ ,  $\text{Pb}(\text{NO}_3)_2$  and  $\text{ZnO}$ , in deionized water. The working standard solution (50 mg/L) was prepared by diluting stock solution to appropriate volumes.

### C. Treatment of metals solutions with CL powder

The biosorption process was carried out for four toxic heavy metals (Copper, Chromium, Lead, Zinc). 100 ml of 50 mg/L solution of each metal concentration were treated with 1% of biosorbent at pH 7 for 60 minutes at 30°C with occasional stirring. The solution was then filtered using Whatmann filter paper No. 1. The metal concentration of the filtrate was then carried out using ICP-AES at SAIF Dept. IIT Bombay.

### D. Treatment of industrial effluents with CL powder

The effluents samples were collected from different industries like paper mill, chemical industry, electroplating industry, powder dusting industry and textile industry situated in the Navi Mumbai MIDC

areas. The effluent samples were stored in polythene bottles till further use. The metal concentration in the industrial effluents was found out using ICP-AES at SAIF Dept. IIT Bombay.

#### E. Calculation of efficiency of biosorption

Percentage of metal removal was calculated as follows:

$$\text{Metal Removal (\%)} = \frac{100 (C_o - C_e)}{C_o}$$

Where  $C_o$  is the initial metal concentration (mg/l),  $C_e$  is the final metal concentration after biosorption (mg/l).

#### F. Characterization of Cauliflower Leaves

The pH, bulk density, ash content and iodine index of cauliflower leaves were calculated as per protocols mentioned in [10].

1) *pH of the biosorbent*: One gram of biosorbent was added to 100ml of deionized water in a conical flask. The mixture was stirred for 15-20 minutes and filtered. The pH of the filtrate was determined using pH meter.

2) *Ash Content*: The ash content was determined by heating one gram of each sample in muffle furnace set at temperature of 500°C for two hours. The materials were allowed to cool in desiccators for several minutes. Then ash content (%) was estimated using following formula:

$$\text{Ash Content} = \frac{W_2 - W_0}{W_1 - W_0} \times 100$$

Where  $W_0$  – Weight of empty crucible (gm)

$W_1$  – Weight of empty crucible + biosorbent (gm)

$W_2$  – Weight of empty crucible + ash (gm)

3) *Bulk Density*: The bulk density was determined by measuring the 10ml capacity of dried cylinder and sample was packed inside the cylinder and weighed. The difference in the weights gave the

mass of the biosorbent. Bulk density of the sample was calculated using the following formula:

$$\text{Bulk density (gm/l)} = \frac{M_2 - M_1}{V}$$

Where  $M_2$  – mass of cylinder + sample

$M_1$  – mass of empty cylinder

$V$  – Volume of cylinder

4) *Iodine number (or iodine index)*: 0.1 g of biosorbent was placed with 25 mL of iodine solution in a 250 mL conical flask and was shaken for 1 min. After that the solution was filtered and 10 mL of the filtrate was taken in a conical flask. The solution was titrated with 0.01 N sodium thiosulfate solution until it become clear. The iodine number of the biosorbent was determined by using the formula as follows.

$$\text{Iodine number} = \frac{V * (T_i - T_f) * C_i * M_i}{T_i * g}$$

Where  $V$ - The volume of iodine solution (25 mL)

$T_i$ -The volume of sodium thiosulfate solution used for the titration of 10 mL iodine solution

$T_f$  -The volume of sodium thiosulfate solution used for the titration of 10 mL filtrate

$g$ - Represents the weight of adsorbent (0.1 g)

$M_i$ - the molar weight of iodine (126.9044 g/mol)

$C_i$  is the concentration of iodine solution (0.01 N)

5) *Fourier Transformed InfraRed (FT-IR) Spectroscopy*: The FTIR study was carried by using potassium bromide (KBr) disc method over the wavelength region 4,000 $\text{cm}^{-1}$  to 400 $\text{cm}^{-1}$  to determine the presence of functional groups present on the biosorbent. The ratio of sample: KBr was maintained as 1:10. The FTIR spectra were recorded on a FTIR spectrophotometer – FT/IR – 4100 type A (C208161016) using a standard light source and TGS detector at Department of Chemistry, Birla College, Kalyan.

6) *Environmental Scanning Electron Microscopy (E-SEM)*: The surface morphology of the biosorbent

before and after heavy metals adsorption were observed using Environmental Scanning electron microscopy (E-SEM) at IIT-Bombay. The powdered samples were placed on the sample stubs. The samples were then dried under IR light for 2-3 minutes followed by platinum coating for 600 seconds using JEOL JFC-1600 Auto fine Coater. Samples were then scanned using FEI QUANTA 200 E-SEM operating at 15 kV. The image analysis of the biosorbents were carried out under 2500x magnification.

### III. RESULTS AND DISCUSSION

The cauliflower leaves (CL) as a biosorbent showed adsorption of all four metals (Cu, Cr, Pb and Zn) under the given conditions. The efficiency of CL for biosorption varied for all four metals which was calculated in the form of percent removal (Table 2). Also, the characteristics of Cauliflower leaves were as follows:

**Table 1.** Characteristics Of Cauliflower Leaves

Characteristics	Cauliflower leaves
pH	7
Ash content (%)	10.5263
Bulk density (gm/ml)	0.2887
Iodine Index (mg/gm)	368.9081

**Table 2.** Percent Removal Of Heavy Metals From Spiked Samples And Industrial Effluents

Industry	% Removal of Heavy Metal			
	Copper	Chromium	Lead	Zinc
Spiked Sample	52.03	47.84	72.08	47.31
Powder Dusting	--	100	18.93	99.29
Electroplating	40.84	31.23	55.82	53.65
Paper Mill	100	--	19.6	84.0

			8	2
Textile	100	97.44	54.12	44.54
Chemical	99.22	59.9	5.77	26.42

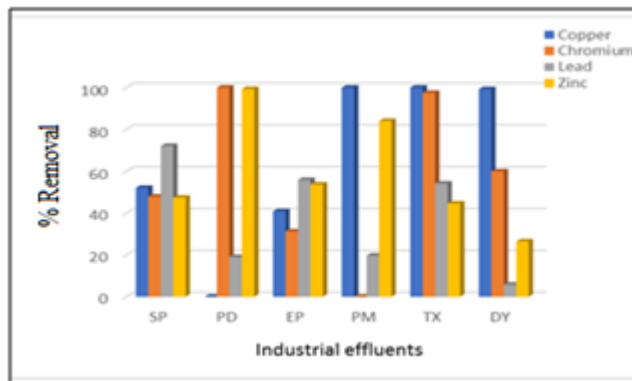


**Figure 1.** Figure showing percent removal of heavy metals from spiked solution and industrial effluents

The functional groups present on the surface of CL were found out using FT-IR (Table 3). Figure 2a shows the FTIR spectrum of biosorbent before the biosorption of heavy metals. The appearance of a broad peak at 3434.6- 3450.99  $\text{cm}^{-1}$  is due to the stretching vibration of free-OH or -NH (str.) on the adsorbent surface. The peaks at 2924.52  $\text{cm}^{-1}$  to 2852.2  $\text{cm}^{-1}$  indicate the C-H stretching mode of aliphatic compounds. Peaks detected at 1639-1640  $\text{cm}^{-1}$ , and 1412-1414  $\text{cm}^{-1}$  correspond to aromatic C=C bending, C-C stretching (in ring) aromatic respectively. The peak at 1020  $\text{cm}^{-1}$  might be due to C-O stretching of alcohols, carboxylic acids, esters, and ethers present on the surface of the biomass. Figure 2b shows the spectra of biosorbent after the adsorption of heavy metals. The spectra of CL did not show considerable changes in the frequencies of functional groups after the adsorption of heavy metals at the surface of biosorbent which indicates that it is due to their involvement in sorption process through physical Vander Waals forces. Hence, shifting in the peaks at was not noticeable. This study indicates that there are functional groups *viz.* carboxyls, hydroxyl, phosphate, amino and amide, present on the biosorbent which may facilitate heavy metal binding on the cell surface.

**Table 3.** Ft-Ir Spectra Of Cauliflower Leaves

Sr · No	Location wave number (cm <sup>-1</sup> )		Vibrati on	Functional group
	Before Biosorpti on	After Biosorpti on		
1	3434.6	3450.99	0-H str.	Bonded and non bonded hydroxyl groups and water
2	2924.52	2924.52	C-H str. asymmetrical	Aliphatic methylene group
3	2853.17	2852.2	C-H str. symmetrical	Aliphatic methylene group
4	2347.91	2336.06	N-H Str.	Ammonium ions
5	1639.2	1640.16	C=O, COO- str.	Amide I, carboxylates aromatic ring modes, alkenes
6	1561.09	1562.06	-NO <sub>2</sub> groups	Nitrogroups
7	1414.53	1412.6	C-C str. (in ring)	aromatic
8	-	1339.32	S=O	sulfone
9	1020.16	1020.12	-C-H plane bending	Aromatic
10	802.242	801.278	=C-H bend	Alkenes
11	644.108	643.144	S-O bending	sulphate

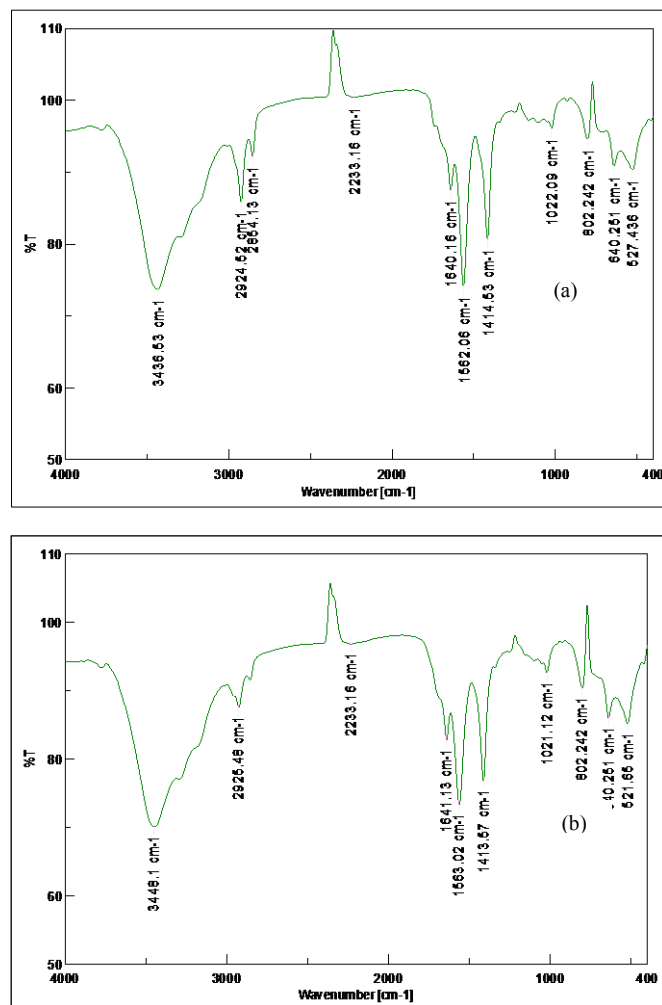


**Figure 2.** FT-IR Spectra of Cauliflower leaves (a)before treatment with heavy metals (b) after treatment with heavy metals

The SEM image of cauliflower leaves before biosorption shows longitudinal filaments which got circular after biosorption process. This may be due to heavy metal stress. Tubular pores and cavities increase the surface area of the biosorbent. Hence, SEM study showed that there is distinct change in surface morphology of the biosorbent after treatment with heavy metals.

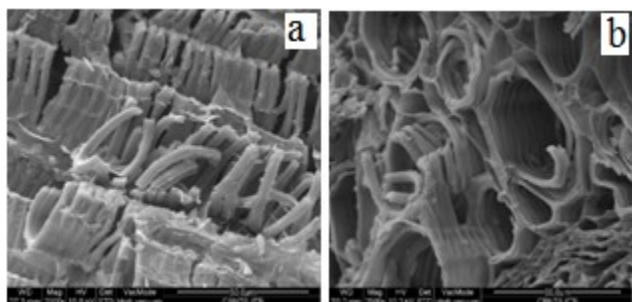


**Figure 3.** SEM Images of Cauliflower leaves (a) before treatment with heavy metals (b) after treatment with heavy metals

### III. CONCLUSION

The cauliflower leaves powder was found to be efficient in adsorbing heavy metals from spiked metal solutions as well as from different industrial effluents. The characteristics of the CL powder like iodine number showed good value (i.e. 368.9081 mg/g) which may lead to its application as a commercial adsorbent of heavy metals. The FTIR spectra of the adsorbent did not show much difference before and after treatment with adsorbent which may indicate that adsorption is mostly physical in nature via Vander Waals force of attraction. This may lead to easy desorption of adsorbed metals and may help in recovery of metals. Hence, the cauliflower leaves which is discarded as wastes from markets can be considered as a good adsorbent for removal of heavy metals from industrial effluents.

### IV. ACKNOWLEDGEMENT

The authors are thankful to at SAIF Dept. IIT Bombay for analysis of heavy metals using ICP-AES and surface morphology study using E-SEM.

### V. REFERENCES

[1] Singare, P., Dhabarde, S. 2014. Toxic metals pollution due to industrial effluents released along Dombivali Industrial Belt of Mumbai, India, *European Journal of Environmental and Safety Sciences* 2(1): 5-11.

- [2] Lakherwal, D. 2014. Adsorption of Heavy Metals: A Review. *International Journal of Environmental Research and Development*. ISSN 2249-3131, 4(1), 41-48.
- [3] Ugwekar, R. Lakhawat, G. 2012. Recovery Of Heavy Metal By Adsorption Using Peanut Hull, *International Journal of Advanced Engineering Technology*, E-ISSN 0976-3945, 3(3) July-Sept, 2012, 39-43.
- [4] Indian National Science Academy (INSA, August 2011). 'Hazardous metals and minerals pollution in India, a position paper'. Angkor Publishers Pvt .Ltd., Noida.
- [5] Ahalya ,N.,. Ramachandra, T.V., Kanamadi, RD. 2003. Biosorption of Heavy Metals, *Research Journal Of Chemistry And Environment*, Vol.7 (4) Dec. (2003), 71-79.
- [6] Monisha, J., Blessy, B. M., Moshami, S. S., Krishnamurthy, T. P. and Sangeeta, K. R. (2014). 'Biosorption of Few Heavy Metal Ions using Agricultural wastes', *Journal of Environment Pollution and Human Health*, Vol. 2 (1), 1-6.
- [7] Davis, Thomas A., Bohumil Volesky and Alfonso Mucci: A review of the biochemistry of heavy metal biosorption by brown algae. *Water Res.*, 37, 4311-4330 (2003).
- [8] Nirmal Kumar, Oommen, C. 2012. Removal of heavy metals by biosorption using freshwater alga *Spirogyra hyaline*, *Journal of Environmental Biology* ISSN: 0254-8704, 33, 27-31.
- [9] Gupta, V.; Jaybhaye, S., Chandra, N. 2017. 'Biosorption Studies of Copper, Chromium, Lead and Zinc Using Fins of Catla Catla Fish', *International Journal for Research in Applied Science & Engineering Technology*, ISSN: 2321-9653, 5(9), 902-909.
- [10] Shrestha, S. 2016. Chemical, Structural and Elemental Characterization of Biosorbents Using FE-SEM, SEM-EDX, XRD/XRPD and ATR-FTIR Techniques, *Journal of Chemical Engineering & Process Technology*, DOI: 10.4172/2157-7048.1000295.



# Comparative Analysis of Antibacterial Properties of Clove and Ginger Extracts Using Gram Negative Bacteria *E.coli*

Vinod S. Narayane\*<sup>1</sup>, Rahat R. Khan<sup>2</sup>, Sumaiya R. Majeed<sup>2</sup>, Nutan B. Kamble<sup>3</sup>.

Department of zoology, Birla College Kalyan (west), Maharashtra, India

## ABSTRACT

Spices are predominantly used for their flavour, and aroma in foods and beverages. Since decades they are known to have diversified uses. The nutritional, anti-oxidant, anti-microbial and medicinal properties of spices have far-reaching implications. Clove is aromatic flower buds of a tree *Syzygium aromaticum* a commonly used spice. All over the world Clove has been used successfully since ages as it is one of the most effective antibacterial agent. Ginger (*Zingiber officinale*) a member of family zingerbeceae is also known for its medicinal use. It is prescribed for treating headache, nausea, rheumatism and cold etc. It also has a capacity to eliminate harmful bacteria responsible for diarrhoea. Growth curve and well diffusion were the methods used for the study. In comparative study of clove and ginger it was found that both are equally effective in inhibiting the growth of *E.coli*. *Escherichia coli* commonly known as *E.coli* are the most common bacteria in human intestine, which helps in preventing the entry of pathogenic microorganisms. Thus it serves as a better experimental model for bacteriological and anti-microbial studies. Growth curve was studied with the help of optical density with the help of Elico CL63 Photometer. Growth curve method indicated that the sterile aqueous extract of clove was more effective than the sterile aqueous extract of ginger, whereas well-diffusion method also indicated that crude extract of clove is more effective than wet ginger extract.

**Keywords :** *Syzygium aromaticum*, *Zingiber officinale*, *Escherichia coli*, Inhibition zone.

## I. INTRODUCTION

Microbiome plays a major role in healthy living of an organism [1]. A healthy, balanced and proper diet is one of the key factors for healthy living. Gut encloses several types of bacteria including *E.coli*. Contaminated food and water are the main sources of this microflora that enters our gut. Few *E.coli* species help in preventing diseases as well as building up the immune response of living organisms, while others can be a causative agent for various diseases [1]. Healthy and proper diet comprises of the food rich in nutritional value as well as taste. Taste being the key factor of raised appetite is brought about by the addition of spices to the food. Spices not only adds flavor to food but also gives it a rich aroma that enhances the craving for food [2]. Spices not only hold a vital place in food industry but also in pharmacology. Spices such as cardamom, cinnamon, black pepper, asafoetida, bay leaves, clove, cumin seeds garlic, ginger, onions etc are been used in every kitchen since ages. Apart from its use in kitchen they are been widely used for various medicinal properties [7,8].

Clove is aromatic flower buds of a tree *Syzygium aromaticum* has been used for its antiseptic and analgesic effects and has been studied for use as an anticoagulant and anti-inflammatory effects [6]. Clove has a long history of culinary and medicinal use. The oil was used as an expectorant and antiemetic with inconsistent clinical results [7,8]. Clove tea was used to relieve nausea. Use of the oil in dentistry as an analgesic and local antiseptic continues today.

Clove buds yield approximately 15% to 20% of a volatile oil that is responsible for the characteristic smell and flavor. The bud also contains a tannin complex, a gum and resin, and a number of glucosides of sterols. The principal constituent of distilled clove bud oil (60% to 90%) is eugenol (4-

allyl-2-methoxyphenol). Clove oil is applied for the symptomatic treatment of toothaches and is used for the treatment of dry socket (post extraction alveolitis) [7,8,9]. Clove oil is reported to have antihistaminic and antispasmodic properties, most likely due to the presence of eugenyl acetate. Cloves are also said to have a positive effect on healing stomach ulcers. A 15% tincture of cloves is effective in treating topical fungal, ringworm infections. As with many other volatile oils, clove oil inhibits gram-positive and gram-negative bacteria [10].

Ginger scientifically known as *Zingiber officinale*) a flowering plant, is widely used as a spice or a folk medicine. It has been used for its antibacterial, antifungal, pain-relieving, anti-ulcer, anti-tumor and other properties. Ginger is originated in the tropical rainforests from the Indian subcontinent to southern Asia where ginger plants show considerable genetic variation. It is well advised to use as it is cheap and have large effective cure [15].

## II. METHODS AND MATERIAL

**Collection of Sample:** clove was collected from the local grocery shop and fresh ginger was also collected from local market Kalyan.

### **Preparation of Extracts:**

#### **Aqueous soxhlet extract:**

The powdered form of clove was used for the experiment. The aqueous extract of clove was prepared using the soxhlet apparatus. 25 Gms of clove powder was used for preparing 100 ml of extract using distilled water. This extract was further concentrated to 25 ml by evaporation. The extract was then autoclaved and stored in sterile condition at 4°C.

The ginger were washed and divided in two parts. One part of the ginger was used for the aqueous

extract preparation and the other part was kept at 40°C for drying. The aqueous extract of fresh as well as dried ginger was prepared using the soxhlet apparatus. 25 Gms of fresh ginger and dried ginger powder was used for preparing 100 ml of extract separately using distilled water. The extract was then autoclaved and stored in sterile condition at 4°C.

#### Crude extract preparation:

Crude extract was prepared using 25 gms of clove in 50 ml of distilled water and was further evaporated to 25 ml separately cooled and preserved at 4°C till further use.

Crude extract of ginger was prepared using 25gms of wet ginger and dried ginger in 50ml distilled water separately and was evaporated to 25ml, cooled and preserved at 4°C till further use.

#### Preparation of bacterial suspension:

Pure isolated colonies of the *E.coli* were obtained from the Department of Microbiology Birla College Kalyan. Colonies of *E.coli* were sub-cultured on a nutrient agar slant and was further preserved in refrigerator.

#### Preparation of nutrient broth:

25 ml of nutrient broth was prepared using distilled water, autoclaved and stored at 4°C.

#### Preparation of nutrient agar plates:

20 ml of nutrient agar was poured on sterile plates

### ANTIMICROBIAL ASSAY BY GROWTH CURVE METHOD:

#### Growth curve analysis using sterile aqueous extract:

24 ml of sterile autoclaved nutrient broth was inoculated with 1ml of soxhleted clove extract and 1ml of *E.coli* culture. It was then incubated in shaker incubator at 37°C for 11 hrs. , and the growth was analyzed at regular intervals of 1 hr. similarly growth analysis of *E.coli* was studied using ginger extract.

All the studies were performed in triplicates. Control was also maintained similarly using sterile distilled water.

#### Growth curve analysis using crude extract:

24 ml of sterile autoclaved nutrient broth was inoculated 1ml of *E.coli* culture and 1ml of crude clove extract separately and was incubated in shaker incubator at 37°C for 3hrs. , and the growth was analyzed at regular intervals of 10 min. similarly growth curve analysis of *E.coli* was studied using 1ml of *E.coli* culture and 24 ml of clove and ginger extract individually, was also All the studies were performed in triplicates. Control was also maintained similarly using sterile distilled water.

### ANTIMICROBIAL ASSAY BY WELL DIFFUSION ASSAY:

Nutrient agar plates were used as medium for screening antibacterial activity. 100µl of *E.coli* culture was spread on culture plates uniformly using a sterile spreader. Wells of 1cm were dug out using a sterile cork borer in solidified agar medium. The plates were divided into three quadrants I, II, III. Dilutions of 1%, 10% and 100% solutions of crude extracts were used. The plates were incubated at 37°C for 24hrs and observed for inhibition zone of growth around the wells.

## III. RESULTS AND DISCUSSION

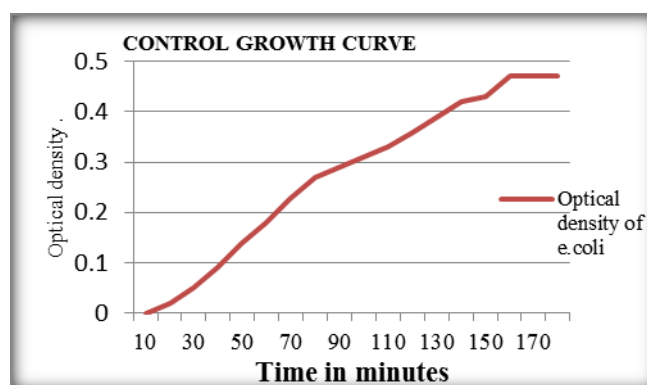
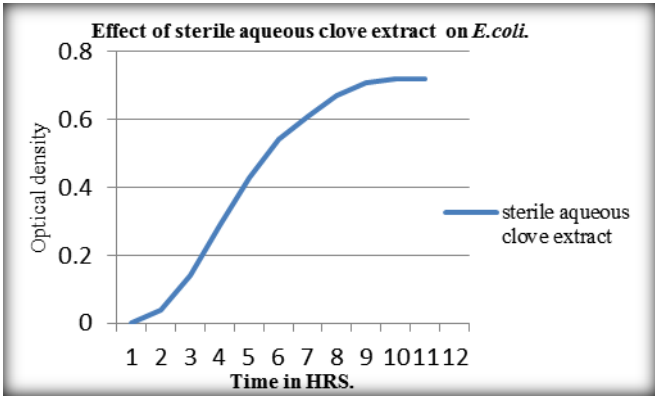
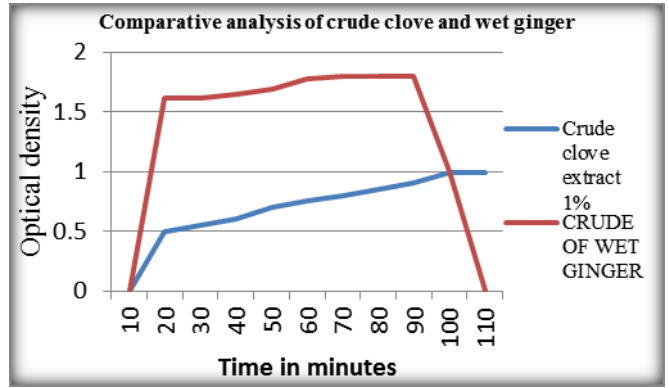


Figure 1



**Figure 2**



**Figure 5**

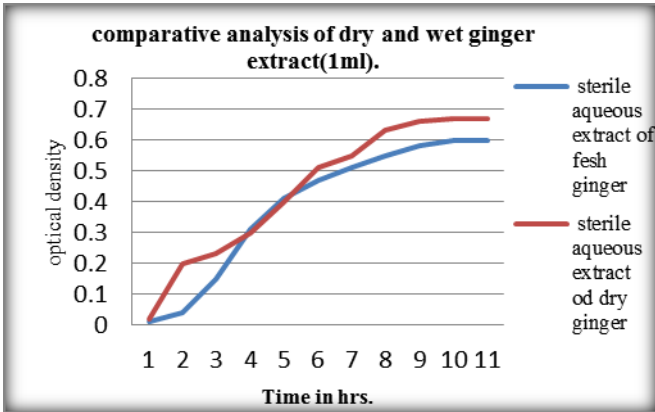


**Figure 3**



**Figure 6.** Inhibition zone of control sample.

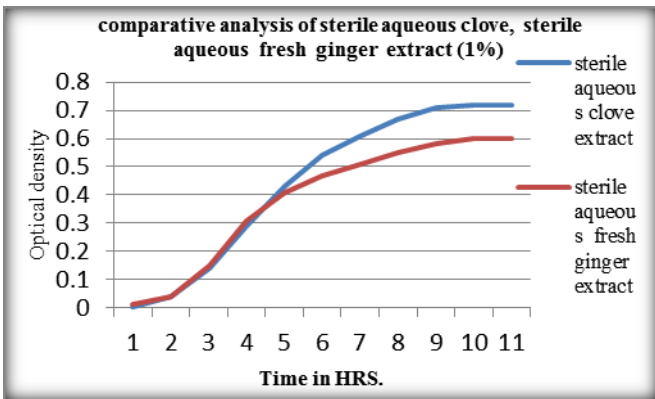


**Figure 4**



**Figure 7.** Inhibition zone of crude clove extract at different concentrations.



**Figure 8.** Inhibition zone of crude fresh ginger extract at different concentrations.

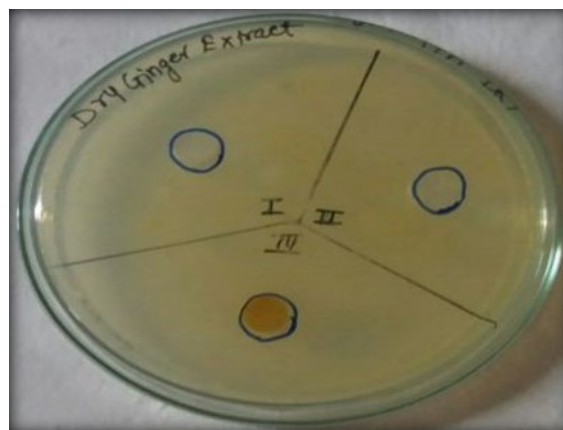


**Figure 9.** Inhibition zone of crude dry ginger extract at different concentrations.

**Table 1.** Showing the inhibition zone of crude extract of clove, crude extract of fresh ginger and crude extract of dry ginger at three different concentrations.

	Crude extract of clove.			Crude extract of fresh ginger.			Crude extract of dry ginger			Control
<b>Concentration.</b>	1%	10%	100%	1%	10%	100%	1%	10%	100%	100µl <i>E.coli</i> .
<b>Inhibition zone.(cm)</b>	1.6cm	1.8cm	2.2cm	1.2cm	1.4cm	1.6cm	1.2cm	1.4cm	1.4cm	0 cm

Figure 1 represents the growth curve of control sample which was not exposed to any herbal extract while the Figure 2 represents the growth curve of *E. coli* where the sterile aqueous extract of clove was incorporated with the culture medium at the concentration of 1 ml/25 ml of nutrient broth. It was found that sterile aqueous extract of clove was more effective in inhibiting the growth of *E.coli* as compared to control. Figure 3 represents the comparative analysis of sterile aqueous extract of dry and fresh ginger which proved that fresh ginger was more effective than dry ginger extract. Fig 4 represents that in comparative analysis of sterile aqueous extract of clove, 1ml extract / 25 ml of nutrient broth is more effective than fresh ginger extract. From Fig 5 it is evident that crude aqueous extract of clove is effective than fresh ginger extract.

Figure 6 indicates the control growth of *E.coli* on nutrient agar plate.

The agar ditch method primarily focus on the inhibition zones formed using three different concentrations of crude extracts of clove and ginger extracts respectively, as seen in fig .7,8, and 9. no inhibition zone is seen in control agar ditch filled with sterile distilled water. Whereas the inhibition zones formed around the crude extracts of clove and ginger increases with an increase in concentration used (fig 7, 8, 9, table 1).

Clove also well known as *Syzygium aromaticum* has various phytochemicals identified and extracted using various extraction solvents. Sixteen volatile compounds were identified from the n-hexane extract of the buds of *Syzygium aromaticum* by using gas chromatography-mass spectroscopy (GC-MS).

The major components were eugenol (71.56 %) and eugenol acetate (8.99 %). The dichloromethane extract of the buds yielded limonin and ferulic aldehyde, along with eugenol. The flavonoids tamarixetin 3-O- $\beta$ -D-glucopyranoside, ombuin 3-O- $\beta$ -D-glucopyranoside and quercetin were isolated from the ethanol extract [4]. In past the antimicrobial properties of these compounds are been studied using various extraction solvents [4]. As stated above in this investigation water was used as a solvent. When compared with the earlier literature it was found that clove possess antibacterial properties and thus was able to inhibit the growth of *E.coli*. [5]

Ginger, the rhizome of the *Zingiber officinale*, plays an important role in prevention of diseases. Numerous active ingredients are present in ginger including terpenes and oleoresin which called ginger oil. Ginger also constitutes volatile oils approximately 1% to 3% and non-volatile pungent components oleoresin [18]. The major identified components from terpene are sesquiterpene hydrocarbons and phenolic compounds which are

gingerol and shogaol [18] and lipophilic rhizome extracts, yielded potentially active gingerols, which can be converted to shogaols, zingerone, and paradol. It is reported that ginger extract has antimicrobial properties these extracts are been prepared using numerous extraction solvents. The current investigation primarily focuses on the detection of antibacterial properties using aqueous extracts. It was found that fresh ginger extracts were more effective in inhibiting the *E.coli* growth than dry ginger extracts but in comparison to clove, clove was found to be more effective.

#### IV. CONCLUSION

The antimicrobial studies on Clove and fresh Ginger indicated that fresh Ginger was more effective than the dry Ginger. Whereas in further investigation using sterile aqueous extracts it was observed that fresh Ginger was more effective than Clove. In agar ditch method it was observed that crude extract of clove was more effective than Ginger in inhibiting the growth of *E.coli*.

#### V. REFERENCES

- [1]. Clark J.A., Coopersmith C.M. Intestinal crosstalk: A new paradigm for understanding the gut as the “motor” of critical illness. *Shock*. 2007;28:384–393. Doi: 10.1097/shk.0b013e31805569df.
- [2]. Tapsell LC, Hemphill I, et.al, Health benefits of herbs and spices: the past, the present, the future, *Med J Aust*. 2006 Aug 21;185(4Suppl):S4-24.
- [3]. R. A. Mashelkar, “Second world Ayurveda congress (theme: Ayurveda for the future) inaugural address: part III,” (2008), Evidence-Based Complementary and Alternative Medicine, vol.5, no. 4, pp. 367–369.
- [4]. Mahmoud I. Nassar<sup>1</sup> et.al (2007) Chemical Constituents of Clove (*Syzygium aromaticum*, Fam. Myrtaceae) and their Antioxidant Activity.
- [5]. Jerusha Santa Packyanathan, et al, (2017), *J. Pharm. Sci. & Res.* Vol. 9(7), 1203-1204.
- [6]. Alma MH, Ertas M, et.al, Chemical composition and content of essential oil from the bud of cultivated Turkish clove (*Syzygium aromaticum* L.). *BioResources* 2, no. 2, 2007, 265-269.
- [7]. Tepe B, Daferera D, et, al. In vitro antimicrobial and antioxidant activities of the essential oils and various extracts of *Thymus eigi* M.Zohary et P.H. Davis. *J Agric Food Chem*, 52, 2004, 1132–1137.
- [8]. Chaieb K., Hajlaoui H. et.al., The chemical composition and biological activity of clove essential oil, *Eugenia caryophyllata* (*Syzygium aromaticum* L. Myrtaceae): a short review. *Phytother. Res.*, 21, 2007, 501–506.
- [9]. Sundar S, Jayasree T, et. al., antimicrobial activity of aminoglycoside antibiotics combined with clove and ginger, *World Journal of Pharmacy and Pharmaceutical Sciences*, 4(6), 2015, 1515-1524.
- [10]. B C Nzeako,\* Zahra S N Al-Kharousi et.al, Antimicrobial Activities of Clove and Thyme Extracts *Sultan Qaboos Univ Med J*. 2006 Jun; 6(1): 33-39. PMID: PMC3074903
- [11]. Arora D, Kaur J. Antimicrobial activity of

- spices. *International journal of Antimicrobial Agents*. 1999;12:257–262.
- [12]. Gislene GF, Paulo C, Giuliana L. Antibacterial Activity of Plant Extracts and Phytochemicals on Antibiotic Resistant Bacteria. *Braz J Microbiol*. 2000;31:314–325.
- [13]. Iram Gull, 1 Mariam Saeed,1et.al,( 2012) Inhibitory effect of *Allium sativum* and *Zingiber officinale* extracts on clinically important drug resistant pathogenic bacteria *Ann Clin Microbiol Antimicrob.*; 11: 8., Published online 2012 Apr 27. Doi: 10.1186/1476-0711-11-8.
- [14]. Fu YJ, Zu YG, et.al,. Antimicrobial Activity of clove and rosemary essential oils alone and in combination. *Phytother Res*. 2007;21:989–999.
- [15]. Gupta S1, Ravishankar S. A comparison of the antimicrobial activity of garlic, ginger, carrot, and turmeric pastes against *Escherichia coli* O157:H7 in laboratory buffer and ground beef. *Foodborne Pathog Dis*. 2005 Winter; 2(4):330-40.
- [16]. Marsunn Ortiz, Antimicrobial Activity of Onion and Ginger against two Food Borne Pathogens *Escherichia Coli* and *Staphylococcus Aureus*, Volume 1 Issue 4 – 2015.
- [17]. Fei-Fei Qin, HUI-LIAN XU , Active components in ginger and their therapeutic use in complementary medicines., *medicinal and plant science biotechnology*.
- [18]. Arshad H Rahmani,1 Fahad M Al shabrmi, Active ingredients of ginger as potential candidates in the prevention and treatment of diseases via modulation of biological activities *Int J Physiol Pathophysiol Pharmacol*. 2014; 6(2): 125–136.
- [19]. Zick SM, Djuric Z, et.al, Pharmacokinetics of 6-gingerol, 8-gingerol, 10-gingerol, and 6-shogaol and conjugate metabolites in healthy human subjects. *Cancer Epidemiol Biomarkers Prev*. 2008;17:1930–1936.
- [20]. Hasan HA, Rasheed Raauf AM,et.al,(2012). Pharmaceut Chemical Composition and Antimicrobial Activity of the Crude Extracts Isolated from *Zingiber Officinale* by Different Solvents. *Pharmaceute Anat Acta*. 2012;3:184.
- [21]. Govindarajan VS. Ginger - chemistry, technology, and quality evaluation: part 2. *Crit Rev Food Sci Nutr*. 1982;17:189–258.

# Bio-Electricity Generation Using Kitchen Waste And Molasses Powered MFC

Yash Manjerkar<sup>1</sup>, Shivani Kakkar<sup>2</sup>, Annika Durve-Gupta\*<sup>3</sup>

<sup>1</sup>Department of Biotechnology, Birla College of Arts, Science and Commerce, Kalyan, Thane, Maharashtra, India

<sup>2</sup>Department of Biotechnology, Birla College of Arts, Science and Commerce, Kalyan, Thane, Maharashtra, India

<sup>3</sup>Department of Biotechnology, Birla College of Arts, Science and Commerce, Kalyan, Thane, Maharashtra, India

## ABSTRACT

With the energy demands all over the world, resulting in energy crises and environmental pollution, the need for alternative sources of energy has arisen. The dependence on fossil fuel is unsustainable because of its exhausting supplies and impact on environment. As a result focus is on alternative, renewable and carbon neutral energy sources which are necessary for environmental and economic sustainability. Microbial Fuel Cells (MFCs) are bioreactors that convert chemical energy present in the organic or inorganic compound substrates to electrical energy through catalytic reactions of microorganisms. Electricity generation from MFC using sugarcane molasses and kitchen waste as fuel was investigated in this study. A dual chambered MFC was made using readily available and cheap material. The electrodes used in the MFC were made up of aluminium mesh having a thickness of 2mm. The bacteria present intrinsically in the molasses and kitchen waste were used for the MFC operation. Samples were subjected to BOD and organic matter content analysis to determine the efficiency of the MFC with respect to waste treatment. It was observed that as the time increased, the BOD and organic matter content decreased. The nature of the microbial population seen in the waste also changed. The maximum potential established was 365 mV in the case of molasses and 260 mV in the case of kitchen waste. The MFCs using the kitchen garbage has proved to be a good way to green electricity generation as well as the recycle of organic waste to maintain a healthy and pollution free environment.

**Keywords:** Microbial fuel cells, kitchen waste, molasses, organic matter, BOD

## I. INTRODUCTION

Every year the global energy demand increases. Approximately 86% of the world energy production comes from fossil fuels. Fossil fuels especially petroleum. Coals are being exhausted, leading to an energy crisis in the near future [1-4]. Furthermore the combustion of the fossil fuels adds CO<sub>2</sub> to the atmosphere and causes global warming. Consequently there is a need to develop a new type of energy source as alternative to fossil fuels [5-7].

To overcome this energy requirement mankind has been exploring the possibility of alternative sources of energy and has been trying tapping the energy resources of all origin; solar power, nuclear power, water power, wind power, geothermal power, tidal power, wave and ocean currents etc. One of the emerging technologies of interest in this regard is microbial fuel cells (MFCs).

Bioelectricity production is production of electricity by organisms. This is due to release of



electrons during their metabolism. These electrons produced can be captured so as to maintain a stable or continuous source of energy production. Bacterial cells when provided a suitable substrate can metabolize the components producing electrons which can be harvested and utilized by connecting them through a circuit. These components can be packed into an assembly called a 'microbial fuel cell' (MFC) proving to be a source of energy [8].

A MFC consists of several components primarily divided into two chambers- anodic and cathodic chamber containing the anode and cathode, respectively. These chambers are separated by a proton exchange membrane (PEM) (Figure 1). The microbes present in the anodic chamber are provided with a favourable substrate which is anaerobically degraded to release electrons which are transported from the anode to the cathode via external circuit and the protons generated are selectively passed through the exchange membrane. Both these products produced due to the action of the microbes in the anodic compartment travel to the cathode and react with oxygen to produce water [9]

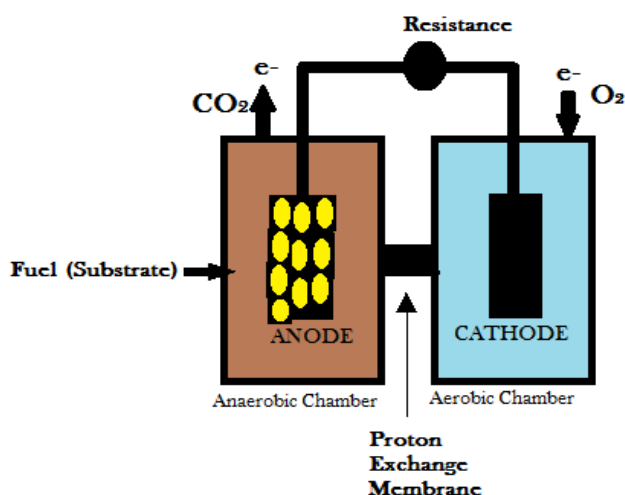


**Figure 1.** Schematic of a dual chamber microbial fuel cell

Massive attention is being given to this technology as a novel approach aimed at bioelectricity production along with simultaneous wastewater treatment [10,11]. MFC may be best described as a bioreactor, where microbes act as biocatalyst in metabolizing the organic substances containing the organic carbon to generate electricity [12, 13].

The aim of this research is to take the inward assents of waste materials, like molasses and kitchen household waste using double chamber MFC for electricity generation and thus help in waste disposal. The gains to be made from doing this are that MFCs are a very clean and efficient method of energy production.

## II. MATERIALS AND METHODS

### Setting up the MFC

The dual chambered MFC was setup using readily available materials, two transparent polyacrylic plastic containers with lid having a capacity of one litre, two PVC pipes with coupler, Aluminium mesh, Paper clips, Copper wire, Electrical tape, Duct tape, Milli voltmeter and Egg shell membrane as a proton exchange membrane (PEM) [14].

A hole was drilled for copper wire on the lids of containers. In the anode chamber, holes were drilled for the sampling to be done at intervals and one small hole for ventilation on the cathode chamber. One hole precisely of the size of a PVC pipe was drilled on one side of both containers for the salt bridge. Electrodes were prepared by folding aluminum mesh a few times over and bound with large paper clips. Ends of the copper wire were stripped and attached to both electrodes. Copper wire was inserted into the drilled holes on lids and the holes were sealed with electrical tape. The copper wires were attached to a millivoltmeter to

detect the potential difference that will be established in the MFC (Figure 2).

To prepare the salt bridge, two PVC segments were fed through the holes in the sides of the chambers and secured using tape and a bonding material like Bondtite to form a watertight seal. The egg shell membrane (PEM) was stretched over one end of the PVC segment and then both segments were attached to each other using the coupler, thus locking the PEM in place.



**Figure 2.** The Chambers Connected with the Salt Bridge

#### **Organic raw material**

The organic waste matter used for this work was molasses which was obtained from a local sugarcane juice centres in Kalyan and kitchen waste (orange peels, banana peels, vegetable peels, leftover vegetables etc.) which was obtained from a number of households.

The organic waste was blended properly in a mixer by adding water. A slurry was formed of proper consistency and poured into the anode chamber. The chamber was filled with the slurry till the brim. The pH of the slurry was checked. Samples were taken for organic matter content [15] and BOD [16]. The electrodes were submerged in the respective chambers and the lids were closed. The anode chamber was made airtight. The bacteria in the anode chamber were exposed to as little oxygen as possible. The bacteria present intrinsically in the organic waste were used for this MFC operation, thus no external inoculum was added. The collected samples were subjected to BOD and organic matter content analysis to

calculate the performance of the MFC with respect to waste treatment. This analysis also estimated the effect of the different waste content, as molasses largely contains sucrose as its substrate whereas kitchen waste will contain a more diverse nature of organic matter.

### **III. RESULT AND DISCUSSION**

#### **Performance of MFC**

The performance of the MFC was analyzed by observing the readings on the millivoltmeter which showed the potential difference established between the two electrodes and thus, the current established. The anode chamber was maintained in anaerobic conditions.

As it can be observed from the readings, the electricity output of the MFC increased with time for 4 days after the beginning of the operation of MFC. But after 4 days, the electricity output decreased until the 7<sup>th</sup> day (Figure 3, Figure 5). In their research, Moqsud *et al.*, (2013) [8] have gone on record and have had similar results regarding the current output in their MFC using organic waste. In their research, the current output increased for the first week, reached a peak and then it gradually decreased.

This decrease in current output maybe attributed to the decrease in organic matter, as the organic matter gets used up by the microbes present in the waste. As the organic matter serves as the food for the microbes in the MFC, their respiration rate will decrease as the organic matter decreases. This will in turn cause less electrons and protons to be produced and thus less current output.

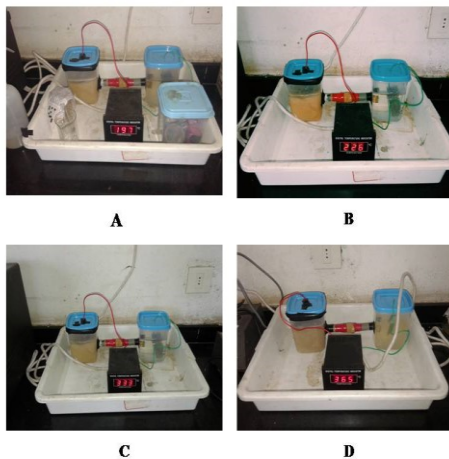


**Figure 3.** Milli voltmeter readings at different time intervals. (Molasses)

#### Kitchen Waste:

The kitchen waste (orange peels, banana peels, vegetable peels, leftover vegetables etc.) was taken for the MFC operation and blended well to form a slurry and poured into the anode chamber. The milli voltmeter readings were taken over a period of 7 days. The conditions were maintained identical as when the MFC was operated using molasses. The kitchen waste also has a large amount of organic matter.

The electricity output increased gradually until the 4<sup>th</sup> day, similar to the case when the MFC was operated with molasses. But the peak of the electricity output was not as high as molasses. After the 4<sup>th</sup> day, the electricity output gradually decreased until the 7<sup>th</sup> day (Figure 4, Figure 5). Moqsud *et al.*, (2013) [8] work on a MFC operated using kitchen garbage had similar results with respect to the trends of the electricity output. In their research they have reported that the organic waste of can be recycled as Bio-electricity generation. The MFCs by using the kitchen garbage is proved to be a good way to green electricity generation as well as the recycle of organic waste to maintain the healthy and pollution free environment. The by-product of the electricity

generation in MFC by composting method can be used as soil conditioner after further treatment which is another way to serve agricultural based countries.

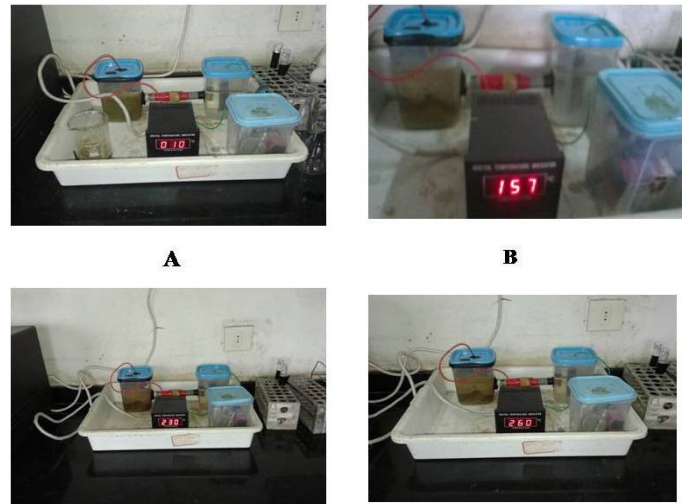


**Figure 5.** Millivoltmeter readings over the period of 7 days for MFC with kitchen waste

BOD analysis [16] of molasses and kitchen waste showed that the BOD of the sample decreased from day 1 to day 7 (Figure 6). A decrease of 54.55% was observed in molasses while only 5.7% decrease was seen in kitchen waste. It has been observed that the BOD of the sample decreases over a period of time with MFC operation. Ghangrekar and Shinde (2003) [17] have reported in their research that the MFC demonstrated its effectiveness for the treatment of wastewater with BOD removal of about 90%. Most pristine rivers have BOD of less than 2ppm. Although, such low BOD is almost impossible to achieve in wastewaters, it is of a very high significance that we are able to lower the BOD using MFCs. The BOD of untreated sewage varies, but averages around 600 ppm [18]. Thus, the results that have been achieved in this work are promising as the BOD of the waste water was almost halved. Although the BOD removal was low in the kitchen waste, it is a promising aspect as the MFC worked on kitchen waste from homes with no externally added components.

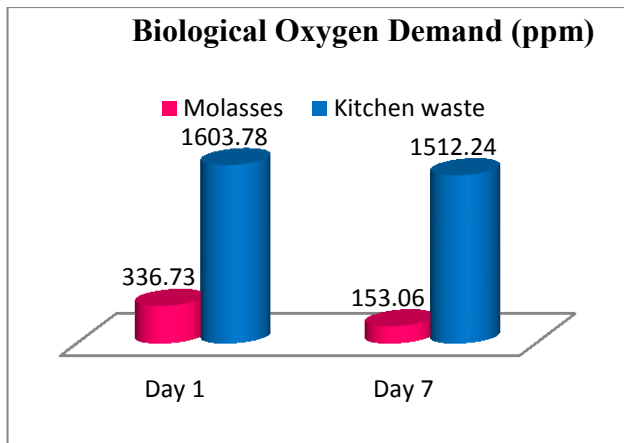


**Figure 6.** Comparison of BOD levels of molasses and kitchen waste after using in MFC

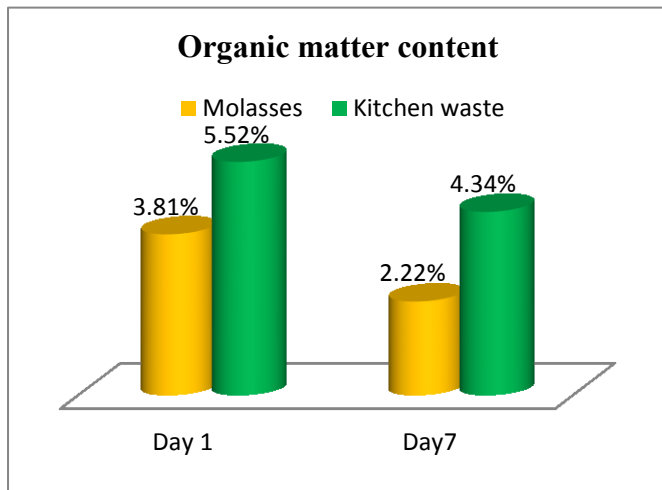


**Figure 7.** Comparison of organic matter content of molasses and kitchen waste after using in MFC

The organic matter content [15] of the sample decreased over the period of 7 days of the MFC operation. The percent decrease was 41.67% for molasses whereas for kitchen waste, the decrease was 21.31% (Figure 7). This was expected as the organic matter was being utilized by the microorganisms for their metabolism. This decrease in organic matter content also justifies the decrease in the current output. The depletion of organic matter proves that the MFC technology may be the potential answer for the wastewater treatment problem as it produces electricity simultaneously. As observed from the results, the kitchen waste

powered microbial fuel cell did not show much decrease (21.31%) in the percent of organic matter. It might be the case that the microorganisms present intrinsically in the kitchen waste were not able to utilize the organic matter present in the kitchen waste.

The MFCs were considered to be used for treating waste water early in 1991 [19]. Municipal wastewaters, containing a multitude of organic compounds, could be used to fuel MFCs. The amount of power generated by MFCs in the wastewater treatment process can potentially halve the electricity needed in a conventional treatment process that consumes a lot of electric power aerating activated sludges. Furthermore, organic molecules such as acetate, propionate, butyrate can be thoroughly broken down to CO<sub>2</sub> and H<sub>2</sub>O. MFCs using certain microorganisms have a special ability to remove sulfides as required in wastewater treatment [20].

The available sources of organic matter and substrate probably change the type of microbial population in the organic matter after the working of MFC. Gram's staining before and after the MFC operation showed an overview of the microbial population in the organic matter. Gram staining of the molasses samples revealed that before the MFC operation the overall microbial population in molasses had Gram positive as well as Gram negative bacteria along with yeast. After 7 days of MFC operation, the Gram stain showed majority of Gram negative bacteria and the formation of biofilms. Similar case was seen in kitchen waste. On 7<sup>th</sup> day, Gram negative bacteria were the majority. The bacterial community at the anode is mainly affected by the type of substrates used and ultimately influences the current generation [21]. Also, it is important to know that there are a number of bacteria in MFCs which may not be

directly involved in the current production. Instead, they are involved in the degradation of complex organic substrates to simpler ones which are then used by exoelectrogens [22].

#### IV. CONCLUSION

The organic waste can be recycled as Bio-electricity generation. The MFCs by using the kitchen garbage has proved to be a good way to green electricity generation as well as the recycle of organic waste to maintain a healthy and pollution free environment. Many works in this field have reported that the by-product of the electricity generation in MFC by composting method can be used as soil conditioner after further treatment which is another way to serve the agricultural based country.

The maximum potential established was 365 mV in the case of molasses and 260mV in the case of kitchen waste. It is a common belief that the electricity output of a MFC depends upon the amount of organic matter present. But as observed in this work, the organic matter content was seen to be more in the case of kitchen waste with respect to molasses, but even then the electricity output was more in molasses powered MFC. As it is known that molasses contains a large amount of sucrose which forms the major part of its organic matter. Also, sucrose is utilized by many microbes readily. On the other hand, the organic matter in kitchen waste is not necessarily of one type, and it may have many different constituents which may hinder the growth of some bacteria. Overall, the performance of the kitchen waste powered MFC was not as good as molasses powered MFC. The BOD removal was minimal and so was the organic matter content lowering. The molasses powered MFC is a promising aspect as molasses is also a waste and is readily available. The kitchen waste MFC has to be further looked into as to find out what other factors might be affecting it. Parameters such as distance

between the electrodes, surface area of the electrodes, catholytic composition, etc. need to be studied further to check the efficiency of the same.

#### V. REFERENCES

1. Chang I.S., Kim B.H., Lovitt R.W., Bang J.S. (2001) Effect of CO partial pressure on cell-recycled continuous CO fermentation by *Eubacterium limosum* KIST612. *Process Biochem* 37: 411-421.
2. Chang I.S., Jang J.K., Gil G.C., Kim M., Kim H.J., Cho B.W., Kim B.H. (2004) Continuous determination of biochemical oxygen demand using microbial fuel cell type biosensor. *Biosens Bioelectron* 19: 607-613.
3. Chang I.S., Moon H., Jang J.K., Kim B.H. (2005) Improvement of a microbial fuel cell performance as a BOD sensor using respiratory inhibitors. *Biosens Bioelectron* 20: 1856-1859.
4. Cheng X., Shi Z., Glass N., Zhang L., Zhang J, Song, D., Liu, Z.-S., Wang, H., Shen, J. (2004) A review of PEM hydrogen fuel cell contamination: Impacts, mechanisms, and mitigation. *J Power Sources* 165: 739-765.
5. Gong M., Liu X., Tremblay J., Johnson C. (2007) Sulfur-tolerant anode materials for solid oxide fuel cell application. *J Power Sources* 168: 289-298
6. Kim I.S., Chae K.J., Choi M.J., Verstraete W. (2008) Microbial fuel cells: recent advances, bacterial communities and application beyond electricity generation. *Environ Eng Res* 13: 51-65.
7. Kim J.R., Min B., Logan B.E. (2005) Evaluation of procedures to acclimate a microbial fuel cell for electricity production. *Appl Microbiol Biotechnol* 68: 23-30.
8. Moqsud A.M., Omine K., Yasufuku N., Hyodo M., Nakata Y. (2013). Microbial fuel cell (MFC)

- for bioelectricity generation from organic wastes. *Waste Manage.* 33:2465–2469.
9. Sharma Y, Li B. (2010). The variation of power generation with organic substrates in single-chamber microbial fuel cells (SCMFCs). *Bioresour Technol.* 101:1844–1850.
  10. Sevda, S., Dominguez-Benetton, X., Vanbroekhoven, K., De Wever, H., Sreekrishnan, T.R., Pant, D. (2013). High strength wastewater treatment accompanied by power generation using air cathode microbial fuel cell. *Appl. Energy* 105, 194–206 doi:10.1016/j.apenergy.2012.12.037
  11. Watanabe, K., (2008). Recent Developments in microbial fuel cell technologies for sustainable Bioenergy. *Journal of Bioscience and Bioengineering*, 106: 528-536.
  12. Gil G.C., Chang I.S., Kim B.H., Kim M., Jang J.K., Park, H.S., Kim, H.J., (2003) Operational parameters affecting the performance of a mediator-less microbial fuel cell. *Biosens Bioelectron* 18: 327-334.
  13. Song C. (2008) Fuel processing for low-temperature and high-temperature fuel cells: Challenges and opportunities for sustainable development in the 21 st century. *Catal Today* 77: 17-49.
  14. Du Z., Li H., Gu T., (2007) A state of the art review on microbial fuel cells: A promising technology for wastewater treatment and bioenergy, *Biotechnology Advances* 25: 464–482
  15. Walkley, A., 1947. A critical examination of a rapid method for determination of organic carbon in soils - effect of variations in digestion conditions and of inorganic soil constituents. *Soil Sci.* 63: 251-257.
  16. Winkler, L.W. (1888). Die Bestimmung des in Wasser gelösten Sauerstoffes. *Berichte der Deutschen Chemischen Gesellschaft*, 21: 2843–2855.
  17. Ghangrekar M. M. and Shinde V. B. (2008) Microbial fuel cell for electricity generation and sewage treatment *Water Science & Technology—WST* 58.1
  18. Shukla, A., Suresh, P., Berchmans, S. and Rajendran, A. (2004). Biological fuel cells and their applications. *Current Science*
  19. Habermann, W. and Pommer, E.H. (1991) Biological Fuel Cells with Sulphide Storage Capacity. *Applied Microbiology and Biotechnology*, 35, 128-133. <https://doi.org/10.1007/BF00180650>
  20. Rabaey K. and Verstraete W. (2005) “Microbial fuel cells: novel biotechnology for energy generation,” *Trends Biotechnology*
  21. Zhang Y., Min B., Huang L., Angelidaki I. (2011) Electricity generation and microbial community response to substrate changes in microbial fuel cell. *Bioresour Technol* 102:1166–1173
  22. Patil S.A., Surakasi V.P., Koul S., Ijmulwar S., Vivek A., Shouche Y.S., Kapadnis B.P. (2009) Electricity generation using chocolate industry wastewater and its treatment in activated sludge based microbial fuel cell and analysis of developed microbial community in the anode chamber. *Bioresour Technol* 100:5132–5139.

# Ferroelectric SbSI-Crystals Exhibiting Dual Electrical Nature

Harish K. Dubey<sup>\*1</sup>, Dattatray E. Kshirsagar<sup>1</sup>, K. D. Barhate<sup>2</sup>, Maheshwar Sharon<sup>3</sup>

<sup>1</sup>Nanotech Lab., Department of Physics, B. K. Birla College, Kalyan (W), Maharashtra, India

<sup>2</sup>Department of Chemistry, B. K. Birla College, Kalyan (W), Maharashtra, India

<sup>3</sup>Walchnad Centre for Nanotechnology and Bionanotechnology, Walchand College of Arts and Science, Solapur, Maharashtra, India

## ABSTRACT

We report synthesis and characterization of rod shaped SbSI crystals that exhibit semiconducting and metallic properties as well. The shiny crystals of SbSI were synthesized using powders of antimony, sulphur and iodine as the precursors by an indigenously developed chemical vapour deposition (CVD) technique. The as-obtained crystals were characterized through the SEM, EDS, XRD, micro Raman analysis and electrical conductivity techniques. The crystal composition was determined by an EDS technique and is found to be very nearly stoichiometric. Surface morphology by SEM showed needle shaped crystallites of 50-100  $\mu\text{m}$  in size. The X-ray diffraction studies gave crystalline nature with a good match of interplaner distances ( $d$ ), reflected intensities ( $I/I_{\text{max}}$ ) and lattice constants revealing orthorhombic phase structure of SbSI. Micro- Raman analysis showed characteristics peaks at 12  $\text{cm}^{-1}$ , 70  $\text{cm}^{-1}$ , 81  $\text{cm}^{-1}$ , 90  $\text{cm}^{-1}$ , 118  $\text{cm}^{-1}$ , 151  $\text{cm}^{-1}$ , 226  $\text{cm}^{-1}$  and 331  $\text{cm}^{-1}$  confirming the crystal to be SbSI. SbSI showed semiconducting behaviour in the range of temperature from 300K to 525K whereas it behaves as Metallic in the 300K to 4K temperature range.

**Keywords:** Orthorhombic, SbSI, CVD, electrical conductivity, semiconductor to superconductivity transition.

## I. INTRODUCTION

SbSI is a ferroelectric material with the Curie point at about 20°C and has the highest Curie temperature in the class of compounds of V-VI-VII series. It crystallizes in orthorhombic rod like structure with the lattice constants:  $a = 8.49 \text{ \AA}$ ,  $b = 10.1 \text{ \AA}$  and  $c = 4.16 \text{ \AA}$  [1,2]. The typical crystal structure of SbSI is shown in fig. 1.

Its rod shaped crystals are composed of double chains of  $(\text{Sb}_2\text{S}_2\text{I}_2)_n$  (fig. 1A) having covalent bonds and weak Vander Waals forces between the neighbouring chains. These rods are usually grown in bunches along  $c$ - axis coinciding with the ferroelectric (polar)  $c$ -axis (fig. 1B) [2].

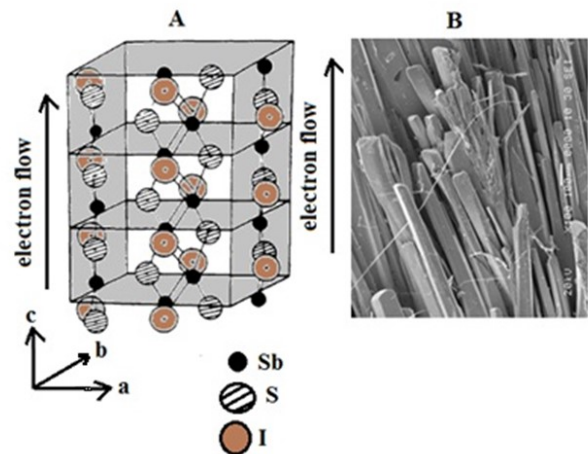


Fig. 1 (A) Orthorhombic structure of SbSI showing the proposed direction of flow of electron in  $c$ -

direction and (B) SEM Image of SbSI obtained by a CVD method.

This structure has some similarity with bismuth and thallium based superconductors. SbSI is a ferroelectric semiconductor [3-6] and has attracted the attention of physicists for its large number of interesting properties such as pyroelectric [7-9], photoconductive [10-11], piezoelectric [12-14], electro-optic [15] and other nonlinear dielectric effects [16-17]. However, to the best of our knowledge no study has been reported with SbSI for its electrical conductivity properties in the temperature range below 300K. In the present paper, we report our efforts on the synthesis of SbSI by an indigenously developed chemical vapor deposition method and its characteristic properties thorough the XRD, SEM, micro Raman analysis and electrical conductivity measurements in the 4K to 550K temperature range.

## II. METHODS AND MATERIAL

### II.1 Synthesis of SbSI by a chemical vapour deposition technique

In a CVD setup, vapours of the three constituent elements (antimony, sulphur and iodine) are to be produced at some suitable temperature and transported to one place where recombination reaction takes place to form SbSI. This requirement needs a provision to interconnect three furnaces such that, from each furnace, the vapours of the individual element are transported to one common place for reaction to take place. A CVD unit consisting of three furnaces each controlled with a separate temperature controller, three quartz tubes containing three constituents (i.e. Sb, S and I), Ar gas to carry the vapours of elements into the quartz tube containing Sb and a gas flow controller was developed in our laboratory [18]. Fig. 2 shows its block diagram .

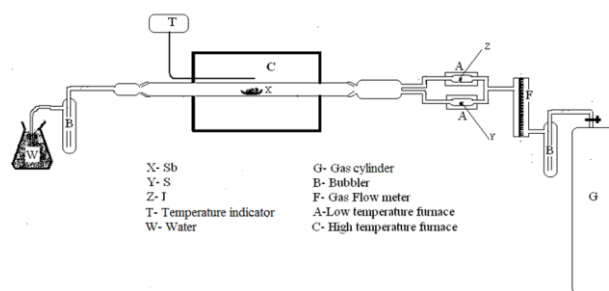


Fig. 2. Block diagram of a CVD unit

Known quantity of powdered Sb (2 gm) was kept in a quartz boat (X) and was placed inside the quartz tube having two inlets and one outlet openings. Powders of other two elements were placed in the two interconnected quartz tubes having two openings placed in two furnaces (A). The known quantities of sulfur (Y) (2 gm) and iodine (Z) (2 gm) were kept in the respective quartz tubes. To carry the vapours of sulfur and iodine, Ar gas was allowed to carry the vapours from two quartz tubes (A) to quartz tube (X) which contains Sb. Flow rate (0.5 cc/min) of carrier gas was controlled by a flow meter (F). Care was taken to allow equal flow rate of carrier gas into the two quartz tubes (A). A gas bubbler (B) was also introduced at the outlet of the quartz tube. The gas coming out of the reaction tube was bubbled into flask (W) containing water. Initially the quartz tube was flushed with Ar to make entire tube free of oxygen. Thereafter, the furnace (C) was switched ON to attain the set temperature. Two quartz tubes containing Sulfur and iodine were heated to attain the melting points of the respective elements. Care was taken so that the carrier gas from furnace (A) could flow to furnace (C) only when the temperatures of the furnaces (A) and (C) had attained the melting point of the respective materials kept in each furnace. Thus, vapours of S and I were transported by the Ar gas to the quartz tube containing molten Sb. The reaction time of the process was optimized to 6 hrs. The reaction amongst these three elements takes place in the quartz tube (X) at its set temperature. We tried three temperatures typically, 650°C, 750°C and 850°C. It was observed that crystals were grown



nically at 650°C. At the end of the experiment, rod shaped SbSI was taken out and characterized by the XRD, Raman, surface morphology and electrical conductivity measurement techniques.

Known quantity of powdered Sb (2 gm) was kept in a quartz boat (X) and was placed inside the quartz tube having two inlets and one outlet openings. Powders of other two elements were placed in the two interconnected quartz tubes having two openings placed in two furnaces (A). The known quantities of Sulfur (Y) (2 gm) and iodine (Z) (2 gm) were kept in the respective quartz tubes. To carry the vapours of Sulfur and Iodine, Ar gas was allowed to carry the vapours from two quartz tubes (A) to quartz tube (X) which contains Sb. Flow rate (0.5 cc/min) of carrier gas was controlled by a flow meter (F). Care was taken to allow equal flow rate of carrier gas into the two quartz tubes (A). A gas bubbler (B) was also introduced at the outlet of the quartz tube. The gas coming out of the reaction tube was bubbled into flask (W) containing water. Initially the quartz tube was flushed with Ar to make entire tube free of oxygen. Thereafter, the furnace (C) was switched ON to attain the set temperature. Two quartz tubes containing sulfur and iodine were heated to attain the melting points of the respective elements. Care was taken so that the carrier gas from furnace (A) could flow to furnace (C) only when the temperatures of the furnaces (A) and (C) had attained the melting point of the respective materials kept in each furnace. Thus, vapours of S and I were transported by the Ar gas to the quartz tube containing molten Sb. The reaction time of the process was optimized to 6 hrs. The reaction amongst these three elements takes place in the quartz tube (X) at its set temperature. We tried three temperatures typically, 650°C, 750°C and 850°C. It was observed that crystals were grown nicely at 650°C. At the end of the experiment, rod shaped SbSI was taken out and characterized by the XRD, Raman, surface morphology and electrical conductivity measurement techniques.

## II.2. Characterization of SbSI crystals

The SbSI crystals were analysed compositionally by an EDAX attached to the SEM. A JEOL-6360 SEM with a probe current of 1 nA was used for this purpose. The SEM images were also obtained by this machine. The energy range for sample scanning was 0-20 KeV. The XRD was recorded for a good quality sample by Phillips PW 3710 X-ray diffractometer using  $\text{CuK}\alpha$  line. The range of  $2\theta$  values was from  $10^\circ$  to  $80^\circ$ . The Raman spectrum was also obtained using Horiba Jobin-Yvon Lab Raman spectrophotometer for the powdered sample. He-Ne laser source (632.88 nm wavelength) was used for this purpose. The electrical conductivity was measured for a pallet sample in the temperature range from 4K to 300K by a four probe method and a two probe method was also used to measure the resistivity in the 300K to 550K temperature range.

## III. RESULTS AND DISCUSSION

The chemical composition of the as-synthesized SbSI crystal was determined by the EDAX technique. The as-grown crystal had 1:1.04:1.5 stoichiometry. Iodine was found to be in little higher percentage compared to other two elements. This may be because the quantity of vapours of iodine carried by the Ar gas was in slightly excess due to its high vapour pressure. The X-ray diffraction pattern was obtained for this powdered sample in the  $2\theta$  range from  $10^\circ$  to  $80^\circ$  and is shown in fig. 3. It appears that the sample is crystalline with sharp and highly intense peaks. All the reflections matched with the orthorhombic phase for SbSI and the cell constants are found to be:  $a=0.851$  nm,  $b=1.015$  nm and  $c=0.424$  nm.

Figure 3. X-ray diffractogram of SbSI powder

The micro Raman spectrum of powdered SbSI was obtained in the 0 to 500  $\text{cm}^{-1}$  range [19]. The measurements were performed using a 50X objective lens, D 0.3 filter and randomly at 10 different positions. The spectrum was taken at room

temperature (27°C) i.e. in paraelectric phase and is shown in fig. 4. SbSI is known to undergo phase transition from ferroelectric to paraelectric at 200°C. The characteristic peaks (fig. 4) obtained at 12 cm<sup>-1</sup>, 70 cm<sup>-1</sup>, 81 cm<sup>-1</sup>, 90 cm<sup>-1</sup>, 118 cm<sup>-1</sup>, 151 cm<sup>-1</sup>, 226 cm<sup>-1</sup> and 331 cm<sup>-1</sup> are in good consonance with the results reported by Agrawal (1971) [20] and Gommonai (2003) [21] confirming the crystal to be SbSI. Since no peaks have been reported beyond 500 cm<sup>-1</sup>, no spectrum was taken for higher wave numbers.

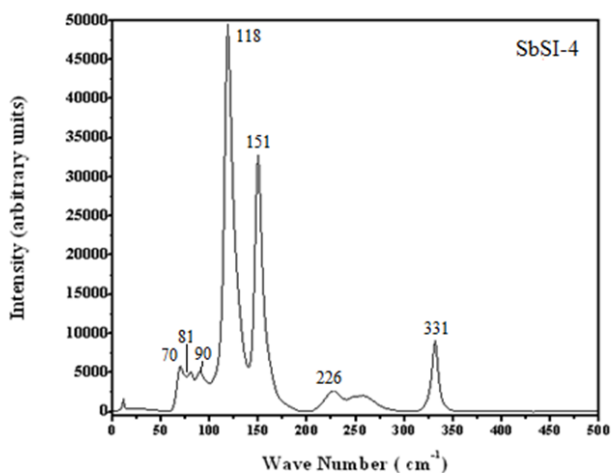


**Figure 4.** Raman spectrum of the SbSI crystal (at R.T.)

The electrical conductivity was measured for the pellets of this crystal by a four probe method. The range of temperature was from 4K to 300K. Figure 5 shows variation of electrical resistance as a function of temperature.

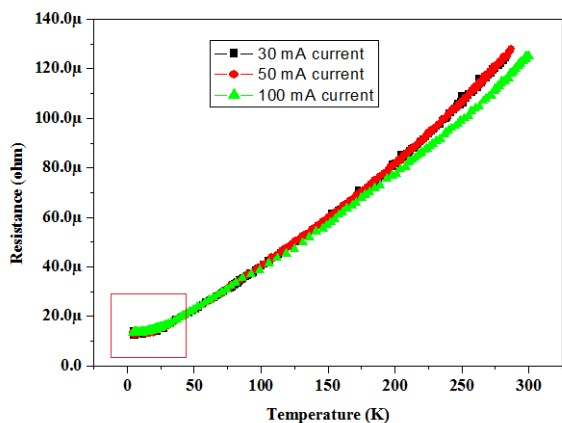


**Figure 5 (A).** Resistivity of SbSI versus temperature in the temperature range of 0K to 300K [19]

SbSI shows a transition temperature at 20K where its resistance falls down to almost zero i.e.  $1.3 \times 10^{-4} \Omega$ . The resistance remains constant thereafter. To the best of our knowledge no efforts have been made till today to study the resistivity of this material below 300K. Resistance of this pellet sample was also measured by a two probe technique in the 300K-525K temperature range. This is shown in fig. 6 .

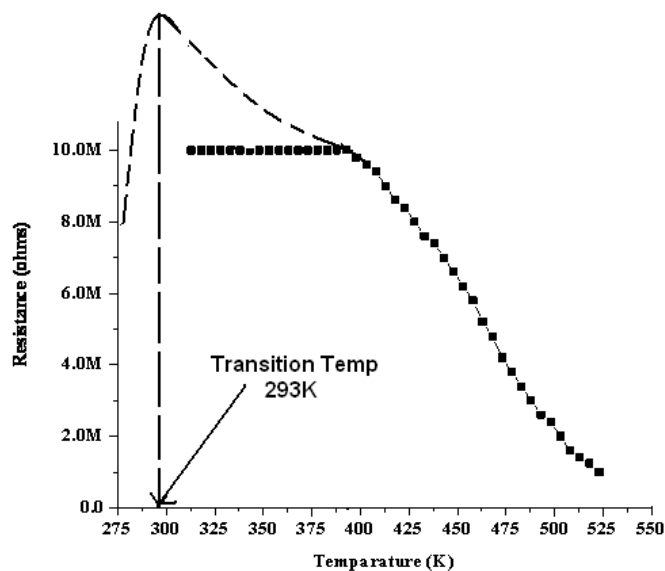


**Figure 6** Electrical resistance of SbSI in the 300K to 525K temperature range.

When the nature of plots of electrical resistivity vs temperature in the 4K to 300K and 300K to 550 K temperature ranges are examined, it suggests that the ferroelectric phase of SbSI is metallic below 300K whereas paraelectric phase is semiconducting in 300K to 525K temperature range, because it is reported that below 220°C it shows ferroelectric and above this temperature it is pyroelectric [22-24].

To the best of our knowledge, we have not come across any report on SbSI showing phase transition from metallic to semiconducting behaviour. Such behaviour needs in-depth studies as to why transition from metallic to semiconducting behaviour occurs in SbSI crystals.

We believe that there may be structural changes occurring in SbSI at different temperatures those need to be examined below 20K, above 50K, below 293K and around 500K and clarified. The structural changes at this temperature may be able to throw

some light on its special behaviour at 20K, phase transition at 293K and reasons for transition from metallic to semiconducting behaviour.

#### IV. CONCLUSION

SbSI crystals were grown by utilizing elemental components of the compound and using a simple chemical vapour deposition technique designed and developed in our laboratory. The material is characterized to be of the composition equal to 1:1.04:1.5. Iodine content is observed to be slightly higher in the material. The material was characterized by the XRD, Raman and surface morphology and has been observed to be rod shaped. Electrical conductivity was measured by the four probe technique in the temperature range of 4K to 300K and by the two probe technique in the temperature range of 300K to 525K. SbSI crystals exhibit metallic properties in 4K to 300K range and semiconducting 300K to 525K range, that is a dual electrical nature. The transition of metallic to semiconducting behaviour takes place at around room temperature.

#### V. REFERENCES

- [1]. Atsushi Kikuchi, Yoshio Oka, Etsuro Sawaguchi, Journal of the Physical Society of Japan 23(2) (1967) 337-354
- [2]. S. Narayanan, R. K. Pandey, IEEE 95(1995) 309-311.
- [3]. Hui Ye, Yuhuan Xu., John. D, Mackenzie, Proceeding of SPIE 3943(2000) 95-101.
- [4]. Hui Ye, Ligong Yang, Peifu, Proceeding of SPIE, 4918 (2002) 99-104.
- [5]. L. Palaniappan, M. Shanmugham, F. D. Gnanam and P. Ramasamy, Journal of Crystal Growth 79 (1986) 159-521.
- [6]. Padmakar Kichambare, Maheshwar Sharon, Solid State Ionics 62 (1993) 21-26
- [7]. A Bhalla, R. E. Newnham. and. L. E. Cross, 33 (1981) 3-7.
- [8]. S. Ozdemir, T. Firat, A. M. Mamedov, Material Research Bulletin 39 (2004) 1065-1073
- [9]. Kiyoyasu Imai, Shuji Kidawa, Mitsuo Ida, Journal of the Physical Society of Japan 21(10) (1966) 1855-1860.
- [10]. R Nitsche and W.J. Merz, Journal of Phys and Chem solids, Pergamon Press 13 (1960), 154-155.
- [11]. W.J Merz, R. Nitsche, W. J. "Photoconduction in Ternary V-VI-VII Compounds, J. Phys. Chem. Solids 13 (1960) 154-155.
- [12]. V. M. Fridkin, I. I. Groshik, V. A. Lakhovizkaya, M. P. Mikhailov and V. N. Nosov. Applied Physics Letters 10(12) (1967) 354-356.
- [13]. D. Berlincourt, Hans Jaffe, W. J Merz and R. Nitsche, Applied Physics Letters 4-3 (1964) 61-63.
- [14]. G. A. Samara, Ferroelectrics 9 (1975) 209-219.
- [15]. Andrzej Kidawa, Material Science and Engineering 52 (1982) 263-266.
- [16]. M. Nowak M. , P. Szperlich, A. Kidawa, M. Kepinska, P. Gorczycki and B. Kauch, Proceedings of SPIE 5136 (2003) 172-177.
- [17]. A. Babaev, I. K. Kamilov, C. N. Kallaev, S. B. Sultanov, A. A. Amirova and A. M. Dzhabrailov, 5(3) (2003) 791-794
- [18]. Abhai Mansingh, K. N. Srivastava, Bachchan Singh, Applied Physics, 10 (1977) 2117-2126.
- [19]. Harish K. Dubey, L. P. Deshmukh, Madhuri Sharon, Maheshwar Sharon, and D. E. Kshirsagar. Advanced Science, Engineering and Medicine 6 (2014) 1-5
- [20]. Harish K. Dubey, L.P. Deshmukh, D.E. Kshirsagar, Madhuri Sharon, Maheshwar Sharon, 40 (2013) 2-8
- [21]. Agrawal D.K. and C. H. Perry, Physical Review B, 4 (6) (1971) 1893-1902
- [22]. V. Gomonnai, I. M. Voynarovych, A. M. Solomon, Yu. M. Azhniuk, A. A. Kikineshi, V.P. Pinzenik , M. Kis-Varga, L . Daroczy, V. V. Lopushansky, Material Research Bulletin 38 (2003) 1767-1772.
- [23]. A. Fatuzzo, G Harbeke, W. J. Merz, R. Nitsche, H. Roetschi and W. Ruppei, Physical Review 127(6) (1962) 2036-2037.
- [24]. A. Audzijonis, J. Grigas, A. Kajokas, S. Kvederavicius and V. Paulikas 219 (1998) 37-45.
- [25]. A. Audzijonis, V. Paulikas, L. Zigas and S. Kvederavicius, Phase Transitions, 67(1997) 437-446.

# Surface Area measurement of Carbon Nanomaterials obtained from Castor oil

Vinod Lohakane<sup>\*1</sup> Ratnakar Hole<sup>1</sup>, Sandesh Jaybhaye<sup>2</sup>, Achyut Munde<sup>1</sup>

<sup>\*1</sup>Department of Chemistry, Milind College of Science Aurangabad, Maharashtra, India

<sup>2</sup>Department of Chemistry, Nanotechnology Research Lab., Birla College, Kalyan, Maharashtra, India

## ABSTRACT

This document Carbon nanomaterials (CNM's) synthesized from castor oil by direct pyrolysis at 750°C in an inert atmosphere. CNMs was then characterized by (XRD) X-ray diffraction, SEM (Scanning Electron Microscope) and FTIR (Fourier Transform Infra-Red Spectroscopy)The specific surface area measurement of CNMs was done by using adsorption of methylene blue dye(MB). In this method a fixed concentration of aqueous methylene blue solution was allowed to adsorb on fixed quantity of carbon nanomaterial. The amount of adsorbed methylene blue dye was determined by UV spectrophotometer. It was found that the concentration of adsorbed methylene blue corresponds to the surface area of test sample. The surface area of CNM was found to be 32m<sup>2</sup>/g. The obtained data was correlated with that of BET surface area measurement and found to be comparable.

**Keywords :** Castor Oil, Surface Area, Carbon Nanomaterial.

## I. INTRODUCTION

A carbon nanotubes discovery in 1991 [1] was a microscopic wonder, due to the porosity with nanometer size and large surface area. The synthesis of carbon nanomaterials from natural precursors receiving the interest because of its unique characteristics of utilization of waste material in different applications via synthesis of different CNM's. from it. Most of the researchers are using petroleum products for the preparation of carbon nano materials; sandesh Jaybhaye et al [2] at NTRC is able to produce these materials from plant derived precursors. There are various physical and chemical properties of CNM has been studied for different applications like hydrogen storage [3] super capacitor [4] solar cell applications [5] micro wave absorption

for lithium ion battery [6] etc. has been carried out. Specific surface area is one of the important property of carbon nanomaterials that can be related to their physical or chemical behaviour. The most commonly used methods to evaluate the specific surface area of carbon nanomaterials are based on adsorption of nitrogen [7], water vapour [8], ethylene glycol mono ethyl ether [9] or colour dye [10]. A very simple adsorption of methylene blue hereafter will be called as MB is used in lab to determine the specific surface area of the carbon nanomaterials which is synthesized in laboratory using a castor seed oil. In this method MB is used to adsorb on CNM and is then evaluated by using a UV-Vis spectrophotometer.

## II. METHODS AND MATERIAL

### PREPARATION OF CATALYST

The catalyst is necessary for the synthesis of Carbon nanomaterials. The diameter of the catalyst particles should be in nano range  $\sim 40$  to  $60$  nm. Particles of such size can be produced by the urea decomposition method [11].

A mixture of Nickel nitrate and urea; 5g and 10g each respectively was taken in a beaker and kept on heater with continuous stirring. A homogeneous liquid mixture was formed then this mixture was kept in muffle furnace in presence of air at  $300^{\circ}\text{C}$  till completely dry. As a result, urea gets decomposed and burned off, nickel was oxidized to form nickel oxides which was left in the form of residue.

Then this residue of Nickel oxide was collected and reduced in Hydrogen atmosphere at  $650^{\circ}\text{C}$  for 2 hours. This gave Nickel catalyst of nano size.

### SYNTHESIS OF CNM

The CNM was synthesized from castor oil using a Nickel catalyst by chemical vapour deposition method (CVD). In this CVD synthesis method two electric furnaces A and B (vaporizing Furnace A and Pyrolyzing Furnace B) and one meter long quartz tube kept inside both the furnaces was used. The schematic representation of arrangement of all the apparatus was as represented in fig-1. Weighed 4 g of castor oil in quartz boat (C) and 200 mg of Nickel catalyst in other quartz boat (D) and kept both the boats in furnace A and B respectively.

The Hydrogen gas was allowed to pass through a quartz tube (Q) for five minutes with constant flow rate so as to remove the oxygen from tube. The temperature of pyrolysis furnace (B) was set to  $750^{\circ}\text{C}$ . Once the furnace B reaches a desired temperature. The furnace A was turned on and the temperature was set to the boiling point of castor oil (i.e.  $\sim 350^{\circ}\text{C}$ ). The heating of furnace A was continued till all oil gets vaporized. The heating of furnace B

was continued for one Hour. The furnace B was allowed to cool at room temperature and the material was collected from boat D.

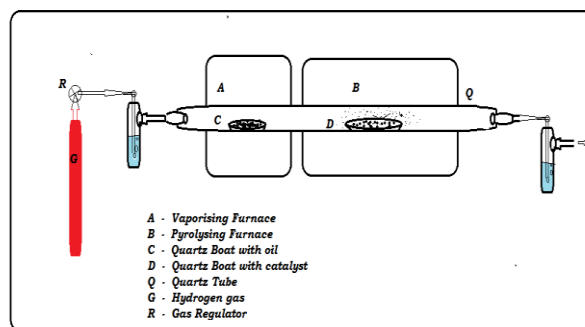


Fig 1. Schematic representation of CVD furnace

### PURIFICATION OF CNM

The obtained CNM was treated with  $\text{HNO}_3$  and  $\text{HCl}$  so as to dissolve the traces of metal impurities and amorphous carbon. The purified CNM was then dried in furnace at  $200^{\circ}\text{C}$  for 1Hr.

## III. RESULT AND DISCUSSION

The purified CNM was characterized by using a SEM, FTIR and powder XRD.

### SEM STUDY

Scanning Electron Microscopy study of CNM represents the morphology of CNM as shown in fig below

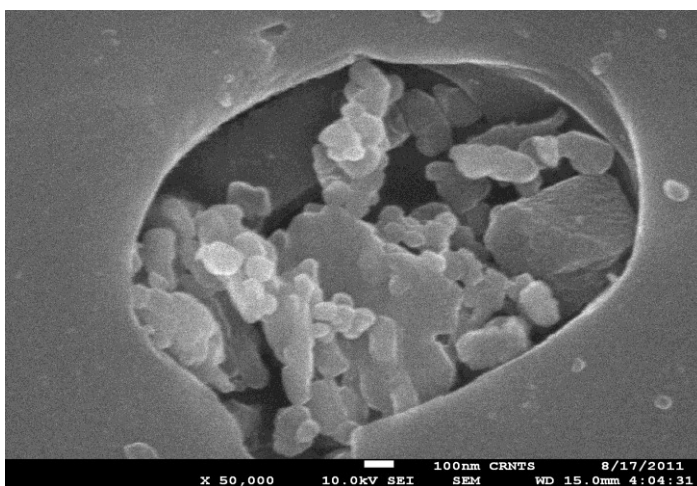


Fig.2 SEM image of CNM obtained from castor oil

## FTIR STUDY

FTIR spectrum of CNM is as shown below. It shows a characteristic band of carbon at 1218 cm<sup>-1</sup> which represents the presence of carbon only and the absence of any other impurities.

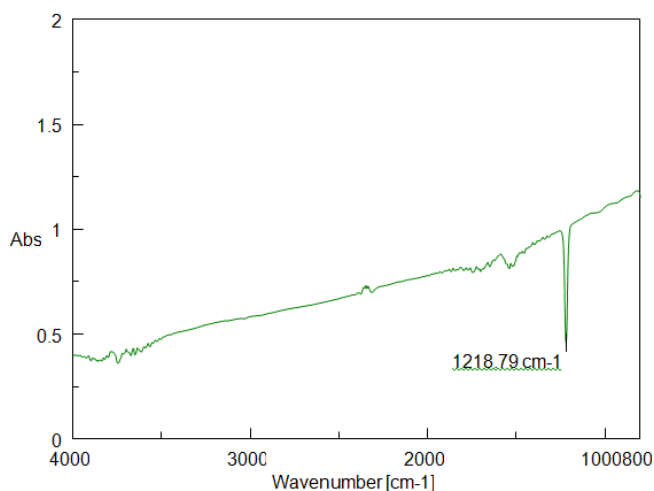


Fig.3: FTIR spectra of CNM obtained from castor oil

## XRD STUDY

The diffractogram of CNM shows two peaks one at 26.46° and another at 44.38° which are the characteristic peaks of CNM.

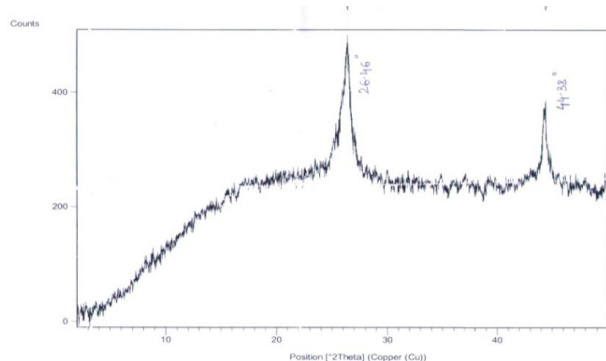


Fig.4.XRD diffractogram of CNM obtained from castor oil

## SURFACE AREA MEASUREMENT OF CNM BY METHYLENE BLUE

CNM prepared by pyrolysis of castor oil is directly used for this experiment. Surface area of this CNM is measured using methylene blue adsorption method. Methylene blue solution was prepared in distilled water and the concentration of methylene blue solutions was analyzed by measuring its absorbance at 662 nm on UV/Vis spectrophotometer. This

wavelength corresponds to the maximum absorption peak of the Methylene blue. First of all a calibration curve of O.D. of methylene blue against its standard concentration (1 to 5 ppm) is plotted and is shown in fig.5. The regression factor is found to be 0.99

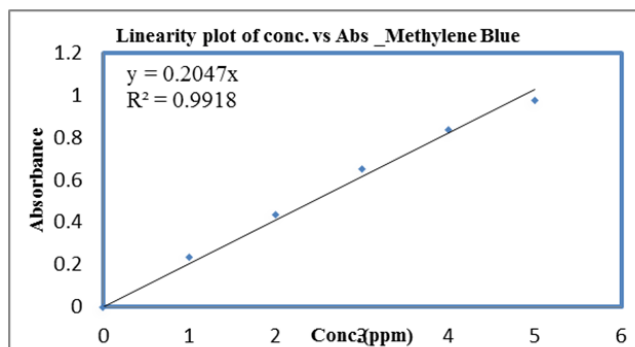


Fig.5. Calibration Curve of Absorbance Vs conc.

0.050 g of CNM is taken in 50ml conical flask containing 5 ppm solution of methylene blue. The mixture is stirred until all the CNM gets submerged into the solution. This mixture is kept at room temperature and shaken periodically for 10 mins and allowed to settle the small particulates. After 10mins, the methylene blue uptake onto carbon was calculated from the difference between the methylene blue concentration before and after adsorption onto the carbon and difference corresponds directly to the active surface area of carbon.

The Specific surface area measured by using this technique is found to be 30.03M<sup>2</sup>/g

## IV. CONCLUSIONS

Adsorption of methylene blue allows the determination of the specific surface area of Carbon Nanomaterial. This work has shown that the method was simple and requires less elaborate apparatus and time than other methods. Using this technique, we have shown that the CNM obtained from castor oil have different specific surface areas. Consequently, this finding makes it possible to use specific surface area measurements directly as a characteristic in quality control, much like other mechanical properties of CNMs. This method was found to be comparable to that of existing BET surface area measurement technique.

Table 1 : Surface Area Results

Sr.No.	Sample Details	Surface Area m <sup>2</sup> /g	
		BY BET	Methylene blue
1	CNM from Castor Oil	30.69	32.0

## V. REFERENCES

- [1]. "Ijimas. Nature (London) 1991; 354 (56)."
- [2]. Vilas Khairnar, Sandesh Jaybhaye, Chi- Chang Hu, Rakesh Afre, T. Soga and Maheshwar Sharon, Carbon Letters, Vol. 9(3), (2008) 188-194.
- [3]. C Dillon, K. M. Jones, T. A. Bekkedahl, C. H. Kiang, D. S. Bethune, M. J. Heben, (1997), Nature 386, 377-379.
- [4]. Vilas Khairnar, Maheshwar Sharon, Sandesh Jaybhaye, Michael Neumann, SRINMC Vol. 36(2), (2006)171-173.
- [5]. Sandesh V. Jaybhaye, Maheshwar Sharon, Dattatray E. Kshirsagar Carbon materials for energy application 2005; 171-178
- [6]. Sunil Bhardwaj, Maheshwar Sharon, T. Ishihara, Sandesh Jaybhaye, Rakesh Afre, T. Soga and Madhuri Sharon, Carbon Letters Vol. 8(4),(2007) 1-7.
- [7]. Brunauer S, Emmett P.H. and Teller E. J.Am.Chem.Soc.,60,309,(1938)
- [8]. Quirk J.P. Soil sci.8, 423,(1955)
- [9]. Dechnik I. and Stawinski J. Soil Sci.,3,15(1970)
- [10]. Maheshwar Sharon, Sandesh Jaybhaye, D. Sathiyamoorthy and Sunil Bhardwaj, Proceedings of the International Conference on Molecules to Materials at Longowal, Punjab, March 3-4, 2006 pp. 50-52.
- [11]. "A. K. Chattarjee, Maheshwar Sharon, Ranjan Bannerjee, Michael Neumann Spallart - Electrochemical Acta 48 2003; 3439-3446."

# Effluent Treatment by Multi Walled Carbon Nano Tubes

Archana Singh<sup>1</sup>, Sandesh Jaybhaye<sup>1</sup>, Harish K. Dubey<sup>2</sup>, Siddhesh Kalambe<sup>1</sup> and Brijesh Gaud<sup>1</sup>

<sup>1</sup>Department of Chemistry, B. K. Birla College, Kalyan (W), MS, India

<sup>2</sup>Department of Physics, B. K. Birla College, Kalyan (W), MS, India

## ABSTRACT

The Industries which are using hazardous chemicals have the potential to pollute water resources through the discharge of the effluent to rivers and other water bodies. Thus the demand for developing technologies leading to an effective removal of this effluent has become a great challenge. Advancements in nanoscience and engineering are giving new opportunities to develop more cost-effective and environmentally acceptable water treatment technologies. Carbon nanotubes (CNTs) are emerging as potential adsorbents because of its well defined cylindrical hollow structure, large surface area, high aspect ratios, hydrophobic wall and easily modified surfaces. Large scale and Low cost synthesis of CNTs using Acacia Concinna (mimosaceae) at 700°C in an inert atmosphere using chemical oil vapour deposition method (COVD) is reported. The morphology of CNTs was studied using SEM, XRD, FTIR etc and are used for the effluent treatment.

**Keyword:** Multi Walled Carbon nanotubes, Acacia Concinna, Effluent treatment, Chemical Vapour Deposition

## I. INTRODUCTION

Now days, due to stringent environmental rules [1] and regulations, most of the Mineral processing and Metal finishing industries are facing severe problems in the disposal of waste water produced at large scale. There is a possibility of formation of complex ions with waste waters containing ammonia, fluoride, or cyanide ions along with heavy metals. Carbon nanotubes (CNT) adsorption technology has potential to remove the bacterial pathogens, natural organic matters (NOM), and cyanobacterial toxins from water systems [2]. By using filters made of carbon nanotubes, pollutants could be removed more effectively from contaminated water as compared to common charcoal filters. CNTs have a very large surface area [3] that gives them a high capacity to retain pollutants such as water-soluble drugs. A team

at the University of Vienna found that at concentrations likely to occur in the environment, the tubes removed 13 tested Polycyclic Aromatic Hydrocarbons (PAHs) from contaminated water. It is very useful in Environmental Science Technology [4].

Plant based oils are an important source for large scale [5] and low cost synthesis of Multi walled carbon Nanotubes (MWCNTs) using Chemical Oil Vaporization technique. The present study is aimed to synthesize low cost bio-adsorbent materials [6,7] in the form of MWCNTs and study its ability to purify wastewater.

## II. METHODS AND MATERIAL

**Preparation of MWCNTs:**



The low cost production of MWCNTs was obtained by heating *Acacia Concinna* (mimosaceae) at 700°C for about 4 hrs in an inert atmosphere of nitrogen by using Chemical Oil Vapour Deposition (COVD) method. The schematic diagram of indigenously developed apparatus to synthesize the desired material is shown in Fig.1

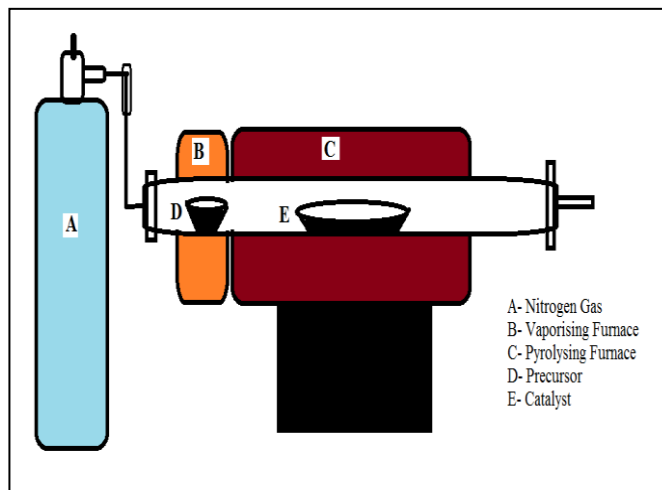


Fig. 1 Schematic diagram of CVD furnace used for synthesis of CNT

The catalyst plays an important role in the synthesis and has a large impact on the diameter of MWCNTs. Iron nano particles obtained by urea decomposition method using Ferric Nitrate are used as catalyst for the synthesis of MWCNTs.

**Purification:**

As grown MWCNTs was purified using dilute Hydrochloric acid and Nitric acid by reflux method. The purified MWCNTs are used for effluent treatment.

**Characterizations:**

The obtained materials were analysed compositionally by SEM. A JEOL-6360 SEM with a probe current of 1 nA was used for this purpose. The energy range for sample scanning was 0-20 KeV. The XRD was recorded for a good quality sample by Phillips PW 3710 X-ray diffractometer using CuK $\alpha$  line. The range of 2 $\theta$  values was from 10°-80°. To confirm the nature of the synthesized nanoparticles and their purity Fourier Transform Infrared

spectroscopy (FTIR) studies were performed. FTIR analysis was done on Jasco 4100.

**Effluent treatment:**

The column has been packed with MWCNTs. The packing materials consists of a height of 15cm and diameter 4 cm of the Pyrex glass tube (column) with a length of 46 cm (Fig. 2). The different parameters such as pH, Conductivity and TSA have been studied. The parameters which affect the rate of adsorption such as MWCNTs, temperature, pH, ionic strength, metal ion concentration etc, were also studied and optimized.



Fig 2 Experimental column packed with MWCNTs

**III. RESULTS AND DISCUSSION**

The SEM image shows an existence of Carbon nano tube which is Multi walled in nature [8, 9]. The effective diameter of the tube appears to be 36.6 nm as seen in the following image [Fig. 3].

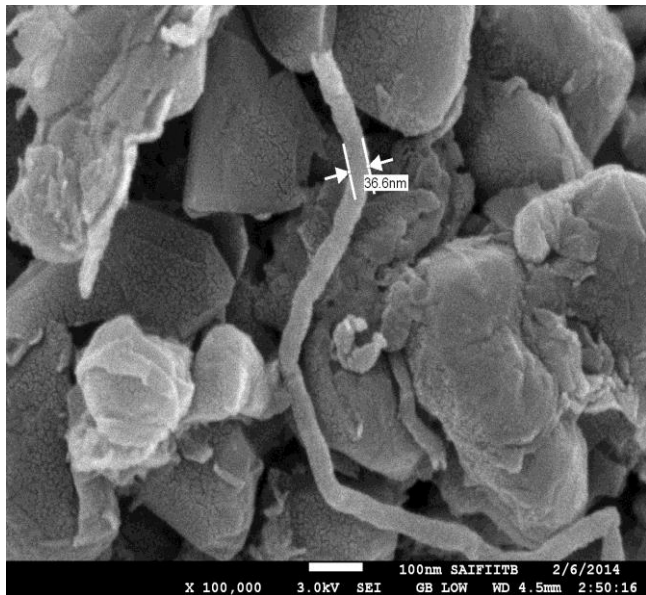


Fig 3 SEM Image of MWCNT obtained from Acacia Concinna oil by CVD method

The Characteristic peaks in the XRD plot correspond to the Crystalline Caron material. The obtained plot matches with the plots reported by the researchers for the Multi Walled Carbon nano Tubes.

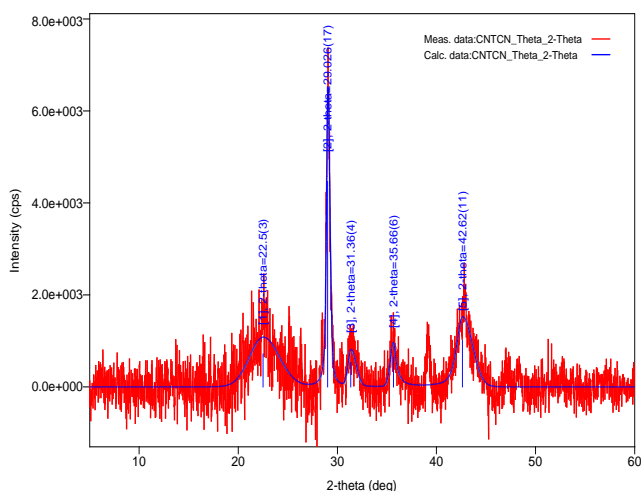


Fig 4 XRD Image of CNT obtained from Acacia Concinna by CVD method

From FTIR analysis it is evident that MWCNTs obtained from oil shows that wave numbers ranging between 3551-1021cm<sup>-1</sup>, it indicates presence of several functional groups such as Hydroxide (3428 cm<sup>-1</sup>), Carbonyl (1573 cm<sup>-1</sup>), C-N str (1420 cm<sup>-1</sup>) C-H str. (2921 cm<sup>-1</sup>) . 1420 cm<sup>-1</sup> is also attributed to MWCNTs vibration mode. (Fig.5)

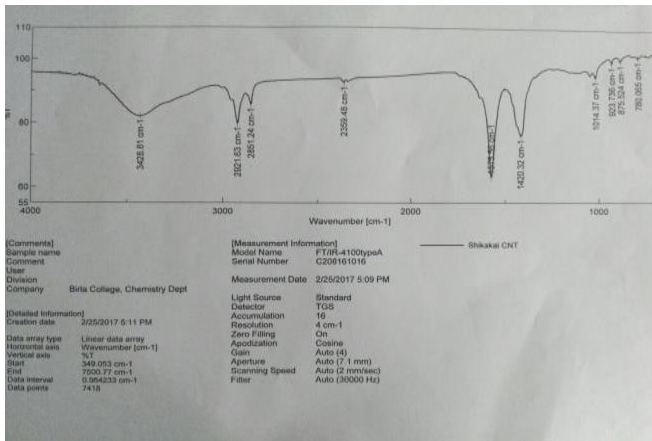


Fig. 5 FTIR Spectra of the obtained MWCNT

The pH of effluent is found to 5.9, Therefore, it is not potable for drinking purposes (as per the BIS – 10500 (2004-2005) 6. 5 to 8.5 desirable limit for drinking water) [10]. The pH of CNTs treated effluent water sample was found to be 7.35 which are within the limits of the expected pH for the drinking water.

According to BIS 10500 (2004-2005), desirable limit the dissolved solids in drinking water is 500 mg/l. The amount of dissolved solids in the sample before filtration was found to be 0.028 mg/l whereas after dissolving the Carbon nano materials in the water and subsequent filtration the amount of dissolved solids in the sample was found to be 0.012 mg/l. Hence, it can be said that the purified water sample can be used for drinking purpose and does not require further treatment. Conductivity of waste water sample is 0.170 ms/cm and CNTs treated effluent water sample is found to be 0.164 ms/cm. The table 1 shows a comparison of several parameters of effluent before and after CNTs treated.

Table 1 Comparison of parameters of effluent before and after treatment

Parameter studied	Effluent sample	CNTs treated effluent sample
PH	5.9	7.35
Conductivity	0.170ms/cm.	0.164 ms/cm.
Total Solids	0.028 mg/l	0.012 mg/l



Fig 6 Colour comparison of the effluent before and after treatment

#### IV. CONCLUSION

The low cost production of multi walled carbon Nano tubes (MWCNTs) using plant based oil is an important source for large scale synthesis. MWCNTs using Acacia Concinna oil were pyrolysed at 700°C in an inert atmosphere of nitrogen by using Chemical Vapour Deposition method (CVD). The catalyst used in this large scale production plays an important role in the diameter of MWCNTs. Fe catalyst obtained by co precipitation method gave the uniform diameter of MWCNTs. The MWCNTs as prepared by can be used as the adsorbent for the treatment of effluents from water sample.

The pH of CNTs treated effluent was found to be within the limits of the expected pH for the drinking water. The amount of dissolved solids in the sample was found to be 0.012 mg/l and the Conductivity of CNTs treated effluent sample was found to be 0.164 ms/cm. From the above results we conclude that MWCNTs are can be most suitable material for the effluent treatment.

#### V. REFERENCES

- [1]. Xuemei, R.; Changlun, C.; Masaaki, N.; Xiangke, W.: Carbon nanotubes as adsorbents in environmental pollution management: a review. *Chem. Eng. J.* 170, 395–410 (2011).
- [2]. Qu, X.; Alvarez, P.J.J.; Li, Q.: Applications of nanotechnology in water and wastewater treatment. *Water Res.* 47, 3931–3946 (2013)
- [3]. Sandesh Jaybhaye, Pandurang Satpute and Mandar Medhi, Carboxylation of Multi-walled Carbon Nanotubes by Ultra sonication, *Int. Journal of Chemistry*, Vol 3 (2) (2014) pp 224 – 228. (ISSN 2249 –2119).
- [4]. Alvarez, P. J. : Nanotechnology in the environment: the good, the bad and the ugly. *J. Environment. Eng.* 132(10), 1233 (2006).
- [5]. Rinkesh Kurkure, Sandesh Jaybhaye, Abhijeet Sangale, Synthesis of copper/copper oxide nanoparticles in ecofriendly and nontoxic manner from floral extract of *Caesalpinia pulcherrima* *Int. J. on Recent and Innovation Trends in Computing and Communication (IJRITCC)* Vol. 4 (4),2016, pp 363-366 ISSN: 2321-8169.
- [6]. Yang, R.T.: *Adsorbents: Fundamentals and Applications*. Wiley, Hoboken (2003).
- [7]. Vandana Gupta, Sandesh Jaybhaye, Naresh Chandra, Biosorption Studies of Copper, Chromium, Lead and Zinc Using Fins of Catla Catla Fish, *International Journal for Research in Applied Science & Engineering Technology (IJRASET)* Vol. 5(9), 2017, pp 902-909,
- [8]. S Jaybhaye, M. Sharon, L. Singh, A. Ansaldo, D. Ricci, E. Di Zitti, “Taguchi Methodology to Grow Single-Walled Carbon Nanotubes on Silicon Wafer”, *Int. Journal, IEEE- Xplore Digital Library* (2009) 838-841.
- [9]. Dattatraya E. Kshirsagar, Vijaya Puri, Madhuri Sharon, Sandesh Jaybhaye, Rakesh A. Afre, Prakash Somani, and Maheshwar Sharon., “Carbon Nanobeads from Brassica Nigra Oil: Synthesis and Characterization”, *Int. Journal, Adv. Sci. Lett.* 2, (2009), 388–390.
- [10]. Rasel Das , Sharifah Bee Abd Hamid, Md. Eaqub Ali , Ahmad Fauzi Ismail , M.S.M. Annuar , Seeram Ramakrishna, Multifunctional carbon nanotubes in water treatment: The present, past and future, *Int. Journal of Desalination* 354 (2014) 160–179.



## Organised by

Department of Chemistry,  
Birla College, Kalyan, Maharashtra, India

## Publisher

Technoscience Academy

Website : [www.technoscienceacademy.com](http://www.technoscienceacademy.com)

Email: [info@technoscienceacademy.com](mailto:info@technoscienceacademy.com)

